論文 / 著書情報
Article / Book Information

題目(和文)	
Title(English)	Hydrocarbon-based Polymer Electrolyte Membranes for Fuel Cell Applications
著者(和文)	SHENGLI
Author(English)	Li Sheng
出典(和文)	学位:博士(工学), 学位授与機関:東京工業大学, 報告番号:甲第9282号, 授与年月日:2013年9月25日, 学位の種別:課程博士, 審査員:早川 晃鏡,高田 十志和,芹澤 武,石曽根 隆,松本 英俊
Citation(English)	Degree:Doctor (Engineering), Conferring organization: Tokyo Institute of Technology, Report number:甲第9282号, Conferred date:2013/9/25, Degree Type:Course doctor, Examiner:,,,,
学位種別(和文)	博士論文
Type(English)	Doctoral Thesis

Hydrocarbon-based Polymer Electrolyte Membranes for Fuel Cell Applications

Department of Organic and Polymeric Materials

Li Sheng

Ph.D. Dissertation

Hydrocarbon-based Polymer Electrolyte Membranes for Fuel Cell Applications

燃料電池用炭化水素系高分子電解質膜の開発

2013. 7

Li Sheng

11D07188

Department of Organic and Polymeric Materials,

Graduate School of Science and Engineering,

Tokyo Institute of Technology

Contents

Chapter 1 General Introduction..... 1
1-1. Polymer electrolyte membrane fuel cell (PEMFC) 1
1-2. Polymer electrolyte membrane (PEM) 2
1-3. PEM based on sulfonated perfluoropolymers..... 3
1-4. PEM based on sulfonated polystyrene and its derivatives..... 5
1-5. PEM based on sulfonated wholly aromatic hydrocarbon polymers 7
1-5-1. Sulfonated polyimides 7
1-5-2. Sulfonated poly(arylene ether)s 9
1-5-3. Sulfonated polyphenylenes 11
1-5-4. Polybenzimidazoles 14
1-6. PEM based on phosphonated polymers..... 17
1-7. Recent challenges for PEMs..... 19
1-8. Purpose of this study..... 21
1-9. References..... 22

Chapter 2 Phosphoric Acid-doped Polybenzimidazole / Sulfonated Polybenzimidazole for Polymer Electrolyte Membranes..... 28
2-1. Introduction..... 29
2-2. Results and Discussion 32
2-2-1. OPBI membrane 32
2-2-1-1. Mechanical analysis and proton conductivity..... 32
2-2-1-2. Components in the catalyst layers of MEAs..... 33
2-2-1-3. Effect of temperature on the performances of MEAs 36
2-2-2. SPBI membrane 38
2-2-2-1. Synthesis of BCPOBDS-Na..... 38
2-2-2-2. Synthesis, solubility and viscosity of SPBIs..... 39
2-2-2-3. Thermal stability and dynamic mechanical properties..... 42
2-2-2-4. PA doping, tensile properties and proton conductivity 45

2-2-2-5. Single-cell fuel cell performance 47
2-3. Conclusions 48
2-4. Experimental 49
2-5. References 55

Chapter 3 Polystyrenes with Phosphonic Acid via Long Alkyl Side Chains for Polymer Electrolyte Membranes 58
3-1. Introduction 59
3-2. Results and Discussion 61
3-2-1. Synthesis of monomer 61
3-2-2. Synthesis of polymers 62
3-2-3. Thermal properties 63
3-2-4. Ion exchange capacity (IEC) and oxidative stability 64
3-2-5. Water uptake and hydration number 65
3-2-6. Proton conductivity 67
3-2-7. Atomic force microscope (AFM) observation 68
3-3. Conclusions 69
3-4. Experimental 70
3-5. References 73

Chapter 4 Random Copolystyrene Derivatives Containing Pendant Alkyl Sulfonic Acid for Polymer Electrolyte Membranes 75
4-1. Introduction 76
4-2. Results and Discussion 78
4-2-1. Synthesis of PVA 78
4-2-2. Synthesis of $PBOS_x$-*r*-PVP_y and $PBOS_x$-*r*-$PSBOS_y$ 78
4-2-3. Preparation of cross-linked $PBOS_x$-*r*-$PSBOS_y$ membranes 80
4-2-4. Thermal stability and oxidative stability 80
4-2-5. Dynamic mechanical properties 83
4-2-6. IEC, water uptake and dimensional change 84
4-2-7. Proton conductivity 85
4-2-8. Transmission electron microscope (TEM) observation 86
4-3. Conclusions 88
4-4. Experimental 89
4-5. References 93

Contents

Chapter 5 Block Copolystyrene Derivatives Containing Pendant Alkyl Sulfonic Acid for Polymer Electrolyte Membranes 96
5-1. Introduction 97
5-2. Results and Discussion 99
5-2-1. Synthesis of PHS_x-*b*-P*n*BOS_y and $PSBOS_x$-*b*-P*n*BOS_y 99
5-2-2. Preparation of cross-linked $PSBOS_x$-*b*-P*n*BOS_y membranes 101
5-2-3. Thermal stability and mechanical properties 101
5-2-4. Oxidative stability 102
5-2-5. IEC, water uptake and dimensional change 103
5-2-6. Proton conductivity 104
5-2-7. TEM and small angle X-ray scattering (SAXS) 107
5-3. Conclusions 109
5-4. Experimental 110
5-5. References 115

Chapter 6 Poly(*m*-phenylene)s Containing Pendant Alkyl Sulfonic Acid for Polymer Electrolyte Membranes 117
6-1. Introduction 118
6-2. Results and Discussion 120
6-2-1. Synthesis of monomers and polymers 120
6-2-2. Cross-linked SPMPs 123
6-2-3. Thermal stability 123
6-2-4. Oxidative stability 124
6-2-5. Mechanical properties 125
6-2-6. IEC, water uptake and dimensional change 125
6-2-7. Proton conductivity 128
6-3. Conclusions 129
6-4. Experimental 130
6-5. References 134

Chapter 7 Poly(phenylene ether)s Containing Pendant Alkyl Sulfonic Acid for Polymer Electrolyte Membranes 137
7-1. Introduction 138
7-2. Results and Discussion 140
7-2-1. Synthesis of monomers and polymers 140
7-2-2. Thermal properties and oxidative stability 144

7-2-3. Mechanical property 145
7-2-4. IEC, water uptake and dimensional change 146
7-2-5. Proton conductivity 147
7-2-6. Morphology 148
7-3. Conclusions 150
7-4. Experimental 151
7-5. References 156

Chapter 8 Poly(arylene ether ether nitrile)s Containing Different length of Pendant Alkyl Sulfonic Acid for Polymer Electrolyte Membranes 158
8-1. Introduction 159
8-2. Results and Discussion 161
8-2-1. Synthesis of sodium bromoalkylsulfonates and polymers 161
8-2-2. Thermal stability 164
8-2-3. IEC, water uptake and dimensional change 165
8-2-4. Oxidative stability and mechanical properties 166
8-2-5. Proton conductivity 168
8-2-6. Morphology 169
8-3. Conclusions 171
8-4. Experimental 172
8-5. References 176

Chapter 9 General Conclusion 178
General Conclusion 178
Appendix 182
Acknowledgements 184

Chapter 1

General Introduction

With the rapid development of technology and economy, we humans also have to pay a heavy price for the limited fossil fuel resources. Scientists of all countries had made certain progress after many years' hard research works. Fuel cell is an energy conversion device which directly transforms the chemical energy of fuels such as hydrogen and methanol into electrical energy without producing any pollutants. This technology receives great attention especially since the 1960s. It is an intrinsically energy-efficient and environment-friendly device; the characteristic of system is the energy conversion efficiency is not restricted by "Carnot Cycle" because the reaction process doesn't involve in combustion. For example, the efficiency could be achieved in electric power plants as high as 70-80% by using solid oxide fuel cells as compared to the current efficiency of 30-37% with combustion. With combined advantages of low environment impact, high energy density and good conversion efficiency, fuel cells have been considered one of the next-generation power technologies for automotive, stationary, and portable application.

1-1. Polymer electrolyte membrane fuel cell (PEMFC)

Fuel cells can be classified into five types according to the kinds of electrolyte: (1) an alkaline fuel cell (AFC) with an alkaline solution electrolyte (such as potassium hydroxide KOH); (2) a phosphoric acid fuel cell (PAFC) with an acidic solution electrolyte; (3) a molten carbonate fuel cell (MCFC) with a molten carbonate salt electrolyte; (4) a solid oxide fuel cell (SOFC) that have a ceramic ion/solid oxide conducting electrolyte; and (5) a polymer electrolyte membrane fuel cell (PEMFC), which is also termed as a proton exchange membrane fuel cell. PEMFC employs a solid polymer electrolyte to separate the fuel from the oxidant. It has certain potential advantages, such as portable application, high efficiency, high energy density, quiet

operation, and environmental friendliness, attracting increasing attention in the past decade.

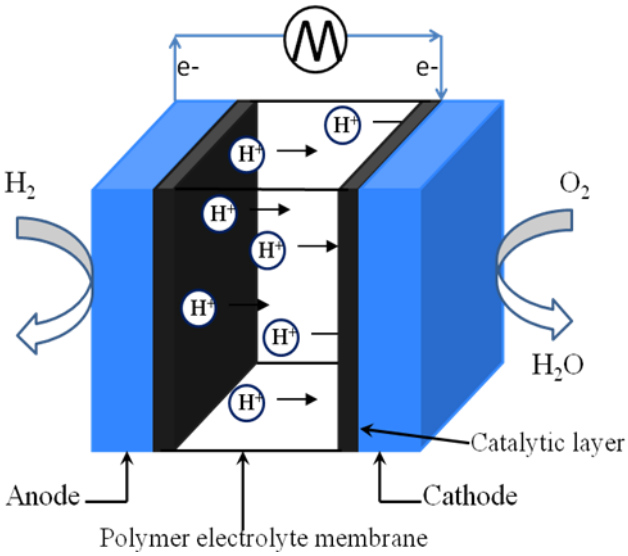

Anode: $H_2 \longrightarrow 2H^+ + 2e^-$

Cathode: $1/2O_2 + 2H^+ + 2e^- \longrightarrow H_2O$

Overall: $H_2 + 1/2O_2 \longrightarrow H_2O$ + Electrial Energy + Heat Energy

Figure 1-1. The operating principle and electrode reactions of PEMFC.

Figure 1-1 shows the operating principle and electrode reactions of PEMFC. On the anode side, hydrogen is oxidized to form two protons and two electrons. The protons are transferred from the anode to the cathode through the polymer electrolyte membrane (PEM), which is also termed the proton exchange membrane, while the electrons travel outside the cell to drive a load. On the cathode side, the protons and electrons combine with oxygen to form water.

1-2. Polymer electrolyte membrane (PEM)

In the PEMFC system, the PEM is a crucial component. It has three main functions: (1) be an anode/cathode separator to prevent the mixing of fuel and oxidant (typically hydrogen and air), (2) be a good electrical insulator to prevent cell from short-circuiting between the electrodes, and (3) be a medium for proton transport from the anode to the

cathode.[1]

Therefore, the PEM itself has the following requirements: (1) high mechanical strength in both the dry and hydrated states. Generally, the maximum stress of the membrane in both the dry and hydrated states should be higher than 20 MPa. High mechanical strength membrane cannot be broken when prepared membrane electrode assembly (MEA); (2) high proton conductivity, no less than 0.1 S/cm at relative humidity (RH) between 25-50 % in the temperature range of 80-120 ^{o}C is required; (3) high oxidative stability, which is very important for the lifetime of PEMFC. The HOO• and HO• radicals can attack the polymer main chain easily to induce the polymer degradation; (4) low electronic conductivity; (5) low permeability of fuel gas or liquid, it helps to achieve a high open circuit voltage (OCV). The fuel and oxidant would react to each other directly if the permeability is high, which leads to low or no electric potential difference of both electrodes. This study is focused on the development of PEM.

1-3. PEM based on sulfonated perfluoropolymers

Perfluorosulfonic acid (PFSA) polymer membranes have been received the most attention in recent years due to excellent performance, such as high proton conductivity, high thermal and oxidative stability. They have become one of most promising candidate for PEMs. The first PFSA was DuPont's Nafion®, synthesized in 1966[2] and then used as PEM. Another PFSA to be developed for membrane applications are the polymers with little shorter side-chain when compared with Nafion, developed by Dow Chemical and Asahi Chemical, respectively. Their chemical structures are shown in Figure 1-2. It can be seen that the electronegative fluorine atoms on the carbons are connected with the sulfonic acid groups, leading low pKa value about -5.5, which is thought to be one reason why the conductivity of PFSAs is high even at low RH.

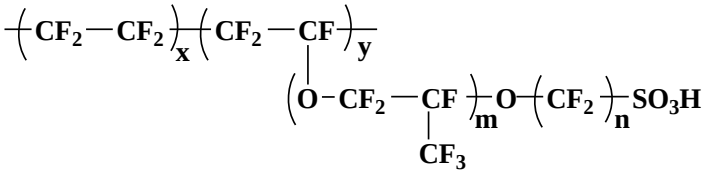

Nafion 117 m>1，n=2，x = 5-13.5 y = 1000； Flemion m = 0 or 1，n = 1-5；

Aciplex m = 0-3，n = 2-5，x = 1.5-14； Dow m = 0，n = 2，x = 3-10，y = 1

Figure 1-2. Chemical structure of perfluorosulfonic acid polymer (PFSA).

Table 1-1. The properties of the perfluorosulfonic acid PEMs.

Membrane	Equivalent weight ($g\ mol^{-1}$)	Proton Conductivity ($S\ cm^{-1}$)	Water content (%)	Lifetime (h)
Nafion	1000-1200	0.05-0.20	34-37	> 50000
Dow	800-850	0.12-0.20	56	> 10000
Flemion	800-1500	0.05-0.20	35	> 50000
Aciplex	800-1500	0.05-0.20	43	> 50000

Table 1-1 displays the results of properties such as proton conductivity, water uptake and lifetime of these PFSA membranes.[3] These polymers contain the hydrophobic polymer backbones (fully fluorinated) and very strong hydrophilic side chain (acid side chain), which resulted in well-developed phase separation. The schematic microstructure of Nafion is shown in Figure 1-3.[4] The well-connected hydrophilic morphology is thought to be another reason to obtain high proton conductivity at low RH.

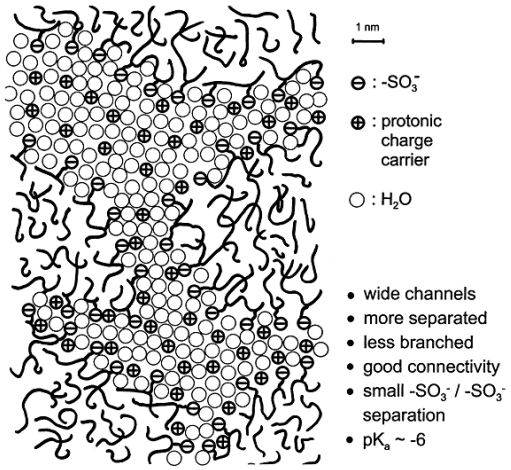

Figure 1-3. Schematic representation of the microstructure of Nafion (derived from SAXS experiments[5])

Although the PFSA membranes have many advantages, as described above, their chemical synthesis is challenging due to the safety concerns of tetrafluoroethylene and the cost/availability of the perfluoroether comonomers. Several other drawbacks such as high methanol permeability, and limited operation temperature (< 100 ^{o}C) due to their low glass transition temperature (T_g is around 110-130 ^{o}C under dry conditions and

lower than that under wet conditions) are also limited their industry applications.

1-4. PEM based on sulfonated polystyrene and its derivatives

In order to solve the above problems, numerous approaches have been made so far to develop alternative membranes. One alternative to the PFSA-based backbones is polystyrene. The styrenic monomers are widely available and easy to modify. Polystyrene is easily synthesized via conventional free radical and other polymerization techniques. The sulfonated polystyrene (SPS)-based PEM was first developed for Gemini space program in the early 1960s. This material is particularly interesting because of the structural differences between this material and the widely studied PFSA (e.g., Nafion-like) materials. The differences are manifested in both the chemical composition of the backbone (hydrocarbon vs fluorocarbon), which affect the association characteristics of the polymer chains in an aqueous environment, and the nature of the sulfonate group, that is, SPS bears a phenylsulfonic acid as opposed to the more acidic fluorosulfonic acid found in Nafion. However, the SPS membrane is readily degraded by a radical attack that takes place during PEMFC operation. The low chemical stability has been found to be due to tertiary hydrogen (α-H), which is particularly susceptible to an oxidative attack.[6-7] For this reason, improving the oxidative stability of the SPS membrane is strongly required.

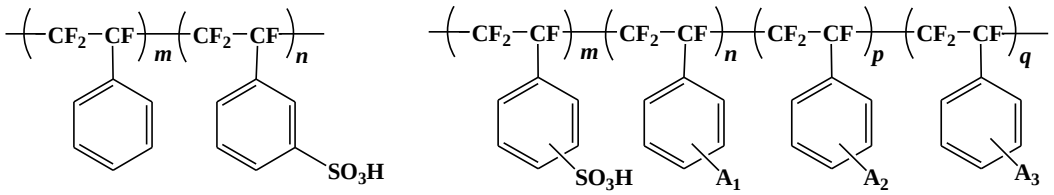

Figure 1-4. Chemical structure of sulfonated poly(trifluorostyrene) (L) and BAM PEMs (R).

The sulfonated poly(trifluorostyrene) (Figure 1-4, (L)), the main chain of these membranes consists of C-F also studied in early time, however it still cannot meet the requirement of longtime use in fuel cell due to its low mechanical property and chemical stability. Presently, there are two commercial PEMs are based on styrene or styrene-like monomers, one is the BAM from Ballard.[8] Ballard Advanved Materials Corporation modified the sulfonated poly(trifluorostyrene) (Figure 1-4 (R)). They show good thermal and chemical stability, excellent mechanical property. It has been reported

that this generation of BAM membranes exhibited some superior performance to perfluorinated membranes, such as Nafion 117, at current densities greater than 0.6 A/cm,[9,10] the lifetime in fuel cell can be achieved as high as 15000 h. However, the cost of this type of SPS is still high.

The other commercial styrene-like PEM is Dais Analytic's sulfonated styrene/ethylene-butylene/styrene (S-SEBS) block copolymers. The chemical structures as shown in Figure 1-5. The S-SEBS was sulfonated with sulfur trioxide/triethyl phosphate in dichloroethane/cyclohexane solvent mixture at -5~0 ^{o}C. The resulting membranes show high proton conductivity (0.07~0.1 S/cm) when fully hydrated.[11-13] The Dais Analytic' PEM is much less expensive to produce than that of Nafion and Ballard's fluorinated SPS. This kind of block copolymers exhibited a rich array of microphase-separated morphologies because of the ability to tailor the block length and composition of the nonsulfonated starting polymer.[14] Another SPS, partially sulfonated styrene-ethylene interpolymer (S-SE) (Figure 1-6), is also widely studied due to its simple synthesis process and low cost. The ion exchange capacity (IEC) can be controlled by the molar ratio of polystyrene unit. However, the drawback of employing hydrocarbon-based SPS is their poor oxidative stability. For this reason, Dais membranes are aimed at portable fuel cell power sources of 1 kW or less, for which operating temperatures are less than 60 ^{o}C.

More recently, Lee et al. have synthesized sulfonated block copolystyrene containing

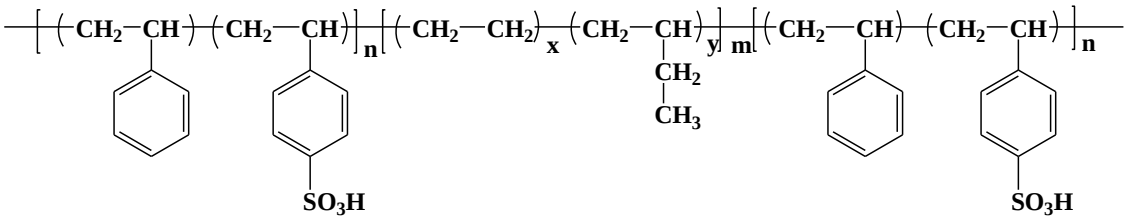

Figure 1-5. Structure of sulfonated styrene/ethylene-butylene/styrene (S-SEBS) block copolymer.

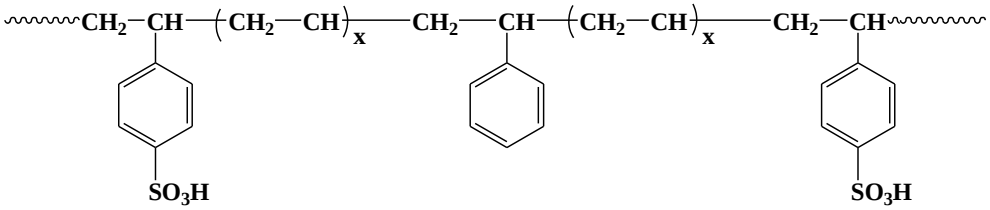

Figure 1-6. Structure of partially sulfonated styrene-ethylene interpolymer (S-SE).

pendant alkylsulfonic acid.[82] As shown in Figure 1-7, incorporation of flexible alkyl spacers between the sulfonic acids and the polymer backbone, instead of the direct attachment of $–SO_3H$ to the polymer backbone, provides the $–SO_3H$ more freedom in movement and thus enhances the relay motion of proton to improve the proton conductivity at low RH. The proton conductivity of this membrane was 0.06 S/cm at 60% RH and 80 ^oC, which was two times higher than that of Nafion 117 at the same conditions.

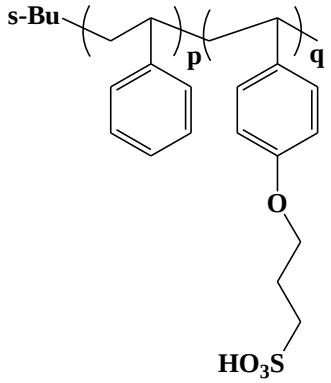

Figure 1-7. Structure of sulfonated block copolystyrene containing pendant alkylsulfonic acid.

1-5. PEM based on sulfonated wholly aromatic hydrocarbon polymers

Wholly aromatic polymers are thought to be one of the most promising alternatives for high performance PEMs because of their availability, processability, wide variety of chemical compositions, and anticipated stability in fuel cell environment. The sulfonated wholly aromatic polymers such as poly(arylene ether sulfone)s (PAES),[15-17] poly(phenylene)s (PP),[18-20] polyimide (PI),[21-24] poly(ether ether ketone)s (PEEK),[25-28] polybenzimidazoles (PBI),[29,30] polybenzoxazoles (PBO)[31,32] and polybenzothiazoles (PBT) [33,34] receive great attention in recent years.

1-5-1. Sulfonated polyimides

It is well-known that aromatic polyimides have found wide application in many industrial fields due to their excellent thermal stability, high mechanical strength, good film forming ability, and superior chemical resistance. These merits are just what are required for the polyelectrolyte membrane materials used in fuel cell systems. However, common five-membered ring polyimides are generally unstable toward acid due to the

ease of hydrolysis of imide rings, and sulfonated polyimides are expected to be more unstable than the nonsulfonated ones. Six-membered ring polyimides have been found to be fairly stable toward both acid and pure water.[35-36]

Mercier and coworkers first synthesized various sulfonated copolyimides from naphthalene-1,4,5,8-tetracaboxylic dianhydride (NTDA), 2,2'-bendizine sulfonic acid (BDSA, a kind of commercially available sulfonated diamine), and common nonsulfonated diamine monomers.[37] Faure and his workers also studied the difference between the oxydiphthalic dianhydride (ODPA)-based polyimides and NTDA-based polyimides. Their results indicated that ODPA-based polyimides were not stable enough in fuel cell conditions, whereas NTDA-based ones were fairly stable as long as the sulfonation degree was controlled to an appropriate level. Figure 1-8 shows the structure of NTDA-based polyimides. Most sulfonated polyimides (SPIs) showed higher proton conductivity (> 0.1 S/cm) than that of Nafion have been reported under fully hydrated state.[38-40] In spite of improved hydrolytic stability by introducing six-membered imide rings, hydrolytic stability is still the most critical issue for SPIs. Okamoto et al.[41-42] synthesized several kinds of SPIs and studied their hydrolytic stability. They found that sulfonated diamines affected the hydrolytic stability. Electron-rich and flexible sulfonated diamines could increase the hydrolytic stability of SPIs. Watanabe et al.[43] introduced aliphatic segments both in the main and in the side chains. The resulting membranes dramatically enhanced the hydrolytic stability of SPIs compared with the fully aromatic SPIs because this structure can increase the electron density of imide groups as well as reduce the possibility of nucleophilic attack by water, and this kind of partially alkylated SPIs enabled 5000 h fuel cell operation at 80 ^{o}C. They also investigated the effect of the length of the side chains on the hydrolytic stability to find that longer pendant chains were distanced from the imide rings, which could reduced the possibility of nucleophilic attack by water molecules onto the main chains.

Another interesting feature of SPIs is anisotropic water swelling. Most SPI membranes showed higher through-plane (thickness direction) water swelling than in-plane (surface direction) regardless of the kind of sulfonic acid groups and the chemical components. Typical SPIs showed through-plane proton conductivity 25% lower than the in-plane one. The detailed mechanical has not been understood.

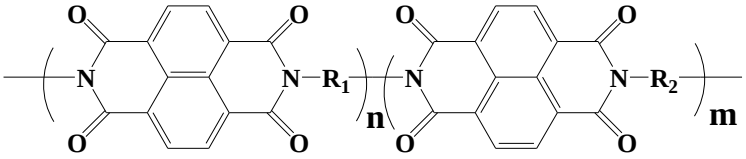

R_1: Sulfonated diamines

Main-chain-type

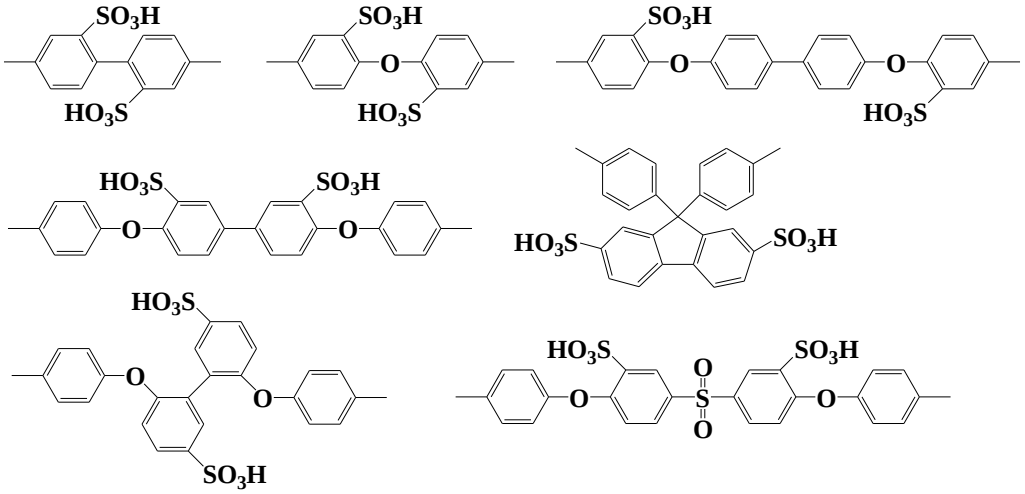

Side-chain-type

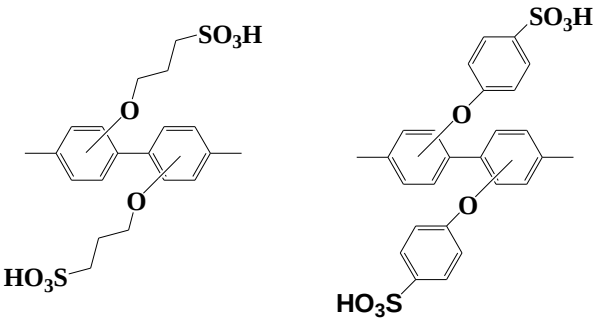

R_2: Nonsulfonated diamines

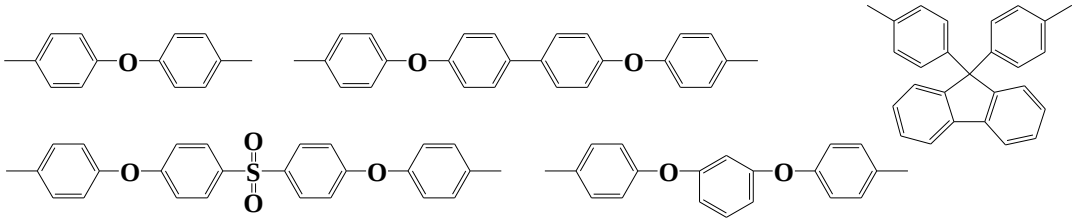

Figure 1-8. Chemical structure of NTDA-based polyimides.

1-5-2. Sulfonated poly(arylene ether)s

Poly(arylene ether)s (PAEs) are one of the most studied polymers as a PEMFC membrane because of their well-known oxidative and hydrolytic stability under harsh conditions. And these polymers offer many advantages, such as simple synthesis and

fabrication, good thermal stability, and low manufacturing costs. Because of the polycondensation mechanism, the synthesis requires high purity monomers with a precise functional group stoichiometry to obtain high molecular weight polymers. Excessive water swelling and reduced selectivity in the high ion exchange capacity (IEC) sulfonated PAEs has prompted ample research activity by controlling its microstructures, including the introduction of some nonsulfonated monomer units. Typical PAEs are poly(phenylene oxide) (PPO), poly(arylene ether ketone) (PAEK), and poly(arylene ether sulfone) (PAES), poly(arylene ether ether ketone) (PEEK). Figure 1-9 shows many different chemical structures of PAEs, including partially fluorinated materials. Sulfonated PPO was synthesized from poly(2,6-dimethyl-phenylene oxide), which was available as a commercial product and chlorosulfonic acid by Fox et al. of General Electric Co. in 1960s.[44] There are two methods to introduce the active proton exchange sites to PAEs, postmodification approach and direct copolymerization of sulfonated monomers.[7] Genova-Dimitrova et al. have compared several sulfonating agents (*e.g.* chlorosulfonic acid), they found the strong sulfonating agents yielded an inhomogeneous reaction while the mild sulfonating agents (*e.g.* trimethylsiylchlorosulfonate) were homogeneous reaction. However, there are several major drawbacks of postsulfonation reaction including the lack of control over the degree and location of functionalization, which is usually a problem when dealing with macromolecules. Polymer degradation or crosslinking was also observed during postsulfonation reaction. Robeson and Matzner, who first reported the sulfonated monomer,[45] directly synthesized the sulfonated PAE. More recently, Ueda et al. synthesized the sulfonated 4,4'-dichlorodiphenyl sulfone.[46] The directly copolymerized sulfonated materials were produced under very similar reaction conditions employed for many years for the synthesis of nonsulfonated PAEs using the weak base route. The conductivity and water uptake of this series of copolymers also increased with increasing IEC. However, once the degree of disulfonation reached 60 mol%, the membranes swelled dramatically, and would not be useful as PEMs.[7] To achieve high proton conductivity with moderate IEC values, many researchers focused on the study of the morphology of the membranes. An ideal morphology has been pursued by microphase separation of segmented block copolymers in which hydrophilic sulfonated polymer segments form an interconnected three-dimensional network responsible for efficient proton transport, while a complementary network of hydrophobic nonsulfonated segments imparts a reinforcing effect, preventing excessive swelling in water and enhancing the mechanical properties.[47] Our group reported several sulfonated

random and alternating multiblock PAES,[48-50] and by changing the hydrophilic/hydrophobic block lengths to investigate the influence of each length on the membrane properties. The results indicated that the membranes possessing the longest block lengths showed good proton conductivity (0.007 S/cm, 50% RH and 80 ^{o}C) due to the large hydrophilic domains and better connected to each other. The alternating multiblock copolymers showed higher proton conductivity (0.0086 S/cm, 50% RH and 80 ^{o}C) than the random multiblcok copolymers (0.0061 S/cm, 50% RH and 80 ^{o}C) with the similar IEC value (~ 2 mequiv/g).

On the other hand, the locally and densely sulfonated PAEs are also widely studied, in which the concentrated sulfonic acid units in a membrane allow for the creation of hydrophilic domains to improve the proton conductivity at low RH. More recently, Hay and coworkers reported the synthesis of end-functionalized poly(sulfide ketone)s with six sulfonic acid moieties at the α,ω-chain ends for PEMs.[51] The synthesized polymers achieved relatively high proton conductivity (0.0037-0.0069 S/cm) at 100% RH with a very low IEC (0.47-0.48 mequiv/g). And they also synthesized SPEKs bearing six or eight sulfonated groups at each of the chain ends by a similar approach to prepare membranes with the IEC of 1.25 mequiv/g. These membranes showed much better proton conductivity. Our group also synthesized the sulfonated block copolymers with locally and densely hydrophilic units (Figure 1-10),[52] these membranes (IEC=2.03 mequiv/g) showed high proton conductivity comparable to Nafion in a wide range of RH (30-95% RH and 80 ^{o}C).

Recently, researchers were interested in SPAEs with benzonitrile groups from the presulfonated monomers.[93-97] Introduction of the polar nitrile groups is to increase the interpolymer interaction and to decrease water uptake compared with other SPAEs. The author reported the relatively low water uptake without sacrificing proton conductivity, and the direct methanol fuel cell (DMFC) performance with the membrane outperformed the other SPAEs and Nafion.[94]

1-5-3. Sulfonated polyphenylenes

Polyphenylene (PP) provides advantages as a fuel cell membrane due to the lack of hetero linkages in its polymer backbone. The wholly aromatic polymer main chains are highly stable to hydrolysis and oxidation. Therefore, polyphenylene and especially their derivatives received much attention. One disadvantage is its low solubility in most organic solvents, which limits the formation of high molecular weight polymers due to the growing rigid rod chains during polymerization. There are mainly two methods to

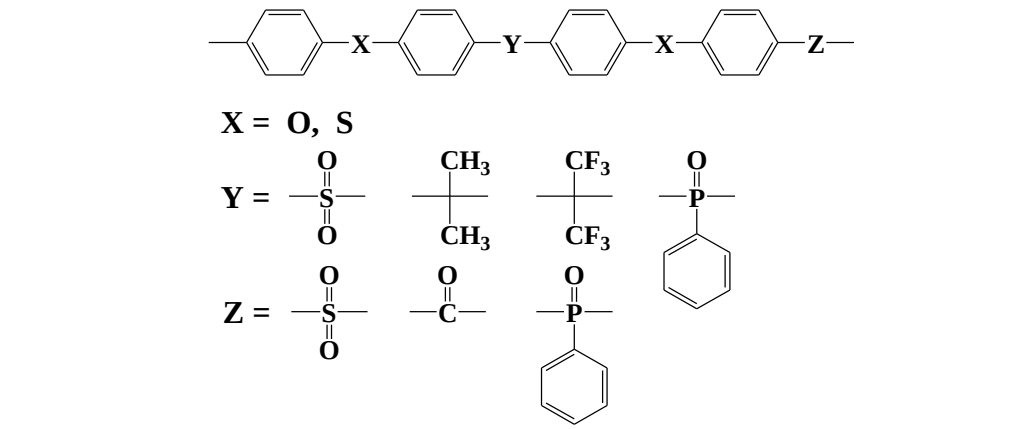

Figure 1-9. General chemical structure for poly(arylene ether)s.

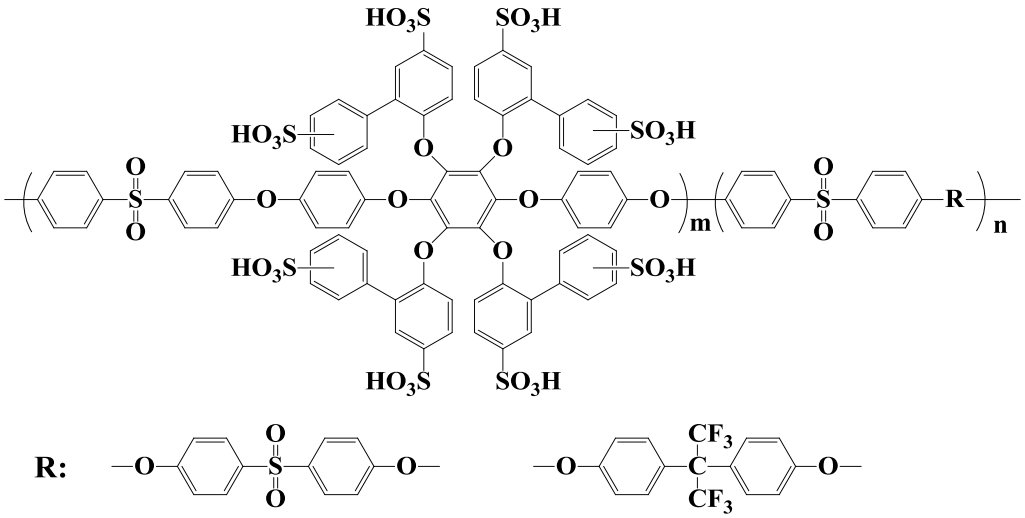

Figure 1-10. Chemical structure of sulfonated poly(arylene ether)s with dense and locally sulfonic acid groups.

overcome this problem. One is introducing pendent groups to the phenyl rings, which improve the solubility of polyphenylene as well as retaining many of the useful characteristics. Sulfonated substituted poly(2,5-benzophenone), usually, synthesized from 2,5-dichlorobenzophenone via nickel(0)-catalyzed coupling polymerization (Figure 1-11),[9] followed by sulfonation with sulfuric acid or by etherification with monomer, which containing sulfonic acid group. However, these sulfonated polyphenylenes and their derivatives formed non-flexible films probably due to the rigid rod backbone, even amorphous and high molecular weight polymers formed brittle membranes. The inability of these polymers to form flexible membranes was a barrier in their testing as a PEM. Some researcher groups prepared polymer blends with

sulfonated polypenylene and other desirable blends, such as poly(arylene ether phosphine oxide) (PPO), which have a compatibility with each other.[9,53,54] A research group in Sandia National Laboratories synthesized a novel polyphenylene by Diels-Alder polymerization followed by sulfonation.[55] The sulfonated polyphenylenes (SPPs) showed a little lower proton conductivity than that of poly(ether sulfone) and SPI with the similar IEC values and water uptake. This is maybe the rigid structure of SPPs restrict ionic groups to aggregate and form ionic clusters. Zhang et al. synthesized SPP directly from sulfonated monomer, sodium 3-(2,5-dichlorobenzoyl)benzenesulfonate, and 2,5-dichlorobenzophenone (Figure 1-12).[56] This method has been proven to be more advantageous than that of post-sulfonation, in terms of improved control of the position, number, and distribution of the sulfonic acid group along the polymer backbone. These side-chain type SPP membranes have a microphase-seperated structure composed of hydrophilic side-chain domains and hydrophobic polyphenylene main chain domains shown by transmission electron microscopic (TEM), and the proton conductivity of membranes reached values above 3.4 $\times$ 10^{-1} S/cm at 120 ^{o}C, which is almost 2-3 times higher than that of Nafion 117 at the same measurement conditions.

The other method to improve the solubility of SPP is block copolymerization with more flexible oligomers. Ghassemi et al. have synthesized oligo SPP, which was block-copolymerized with oligo PAES.[9]

Ohira et al. introduced different lengths of alkyl side chains and compared their effect on the membrane properties (Figure 1-13).[57] The length of alkyl side chains did not affect the proton conductivity and water uptake, however, the gas permeability under wet conditions varied with the length of the side chains.

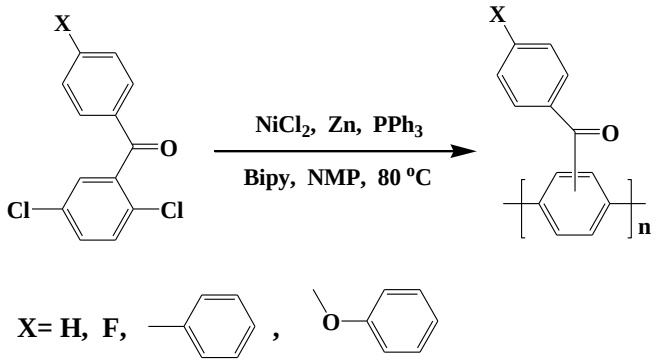

Figure 1-11. Polymerization technique of poly(2,5-benzophenone).

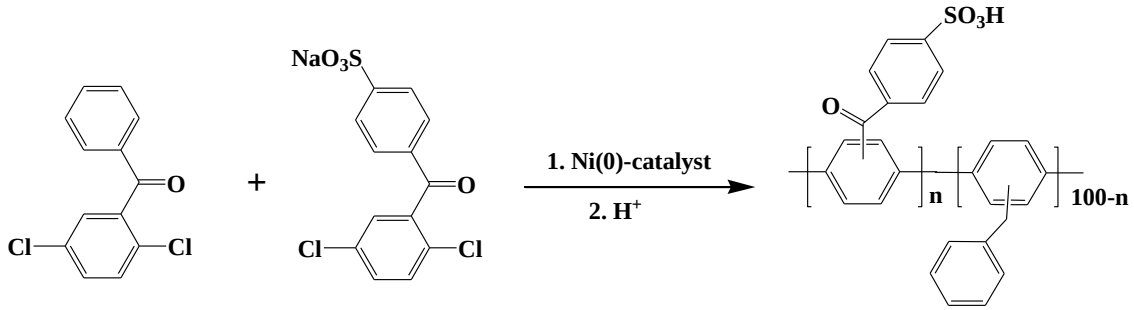

Figure 1-12. Polymerization technique of sulfonated poly(2,5-benzophenone)s (SPPs).

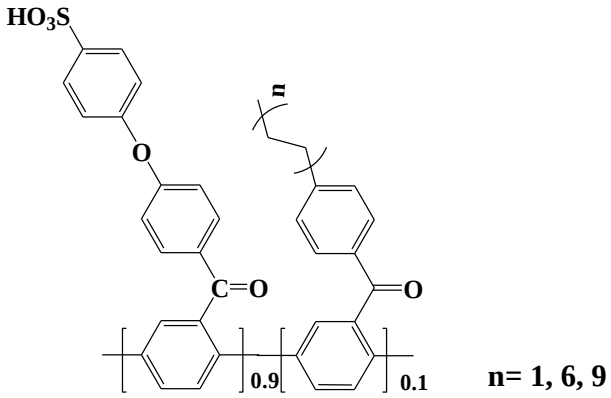

Figure 1-13. Structure of sulfonated copolyphenylene.

1-5-4. Polybenzimidazoles

Polybenzimidazoles (PBIs) containing basic imdazole groups in the main chains show excellent thermally stability (T_g = 425-426 ^oC), high mechanical property and low cost, which are another attractive candidates for PEMs. The term PBI is used in two ways: in a wide definition PBI refers to a large family of aromatic heterocyclic polymers containing benzimidazole units; in a specific way PBI refers to the commercial product, poly 2,2'-*m*-(phenylene)-5,5'-bibenzimidazole) (Figure 1-14). The drawbacks of the PBI are their poor solubility in common organic solvents and infusibility due to the hydrogen bonding and fully aromatic structure. To overcome these shortcomings and for fuel cell uses, more efforts have been made to modify the polymer structure. One is sulfonation of the polymers, however, PBI is difficult to sulfonate directly by using sulfuric or sulfonic acids, the resultant sulfonation degree is low and the polymer is brittle.[72] Therefore, an alternative two-step method was developed, (1) activation of PBI by deprotonating the nitrogen in the benzimidazole rings of the polymer backbone with an alkali metal hydride (LiH or NaH), followed by (2) reaction with arylsulfonates or alkylsulfonates.[73-76] The introduction of arylsulfonic

or alkylsulfonic acids was found to create proton conductivity with better thermal, chemical, and mechanical stabilities compared to those of sulfonic acid groups directly on the main chain. The other method is directly casting membranes from an acidic solution, such as polyphosphoric acid (PPA), a mixture of phosphoric acid (PA) and trifluoroacetic acid. Many researchers also synthesized the sulfonated PBI directly from sulfoanted monomers.

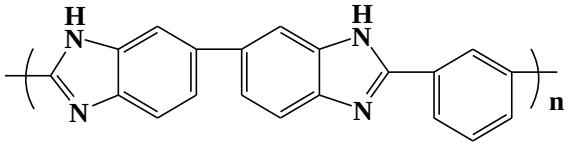

Figure 1-14. Structure of commercial PBI.

Figure 1-15 shows the structure of the sulfonated PBIs. However, compared with common sulfonated polymer membranes containing no basic units in their chemical structures, sulfonated PBIs generally show rather low proton conductivity because the proton transport becomes relatively difficult resulting from the strong acid-base interactions between the sulfonic acid groups and basic imidazole rings.[58] One mole imidazole ring can react with one mole sulfonic acid group to form ionic cross-linking. As the mole number of sulfonic acid groups is less than that of imidazole ring, the proton conductivity is generally at the level of 10^{-4}-10^{-3} S/cm even at 100% RH which is too low to meet the lowest requirement (10^{-2} S/cm) for practical use.

Sacinell and coworkers are the first group to use the acid-doped PBIs to fuel cell.[59,60] Recent years, many kinds of acid doped PBIs have been prepared, the PA-doped PBIs

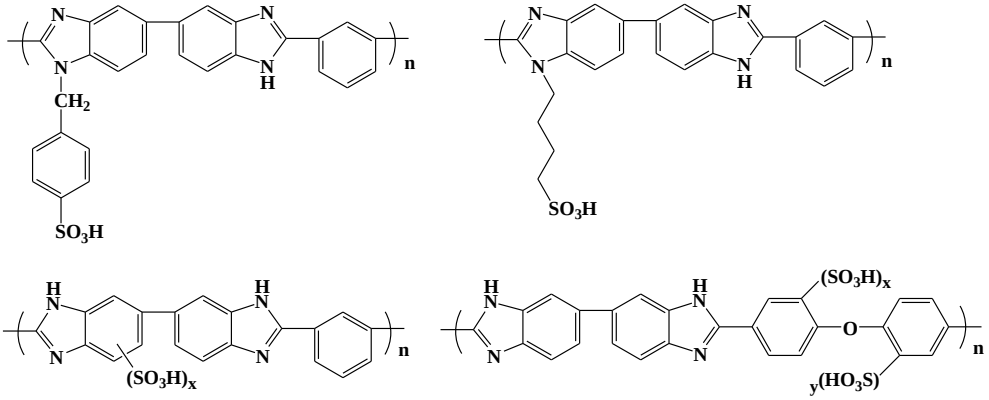

Figure 1-15. Structure of sulfonated PBI.

displayed high proton conductivities even under anhydrous condition, and which makes

them very suitable for use in high temperature (120-200 ^{o}C) fuel cell.[61-70] There are many advantages by developing alternative membranes operational at higher temperatures than 100 ^{o}C, for example, (1) the kinetics for both electrode reactions will be enhanced; (2) above the boiling point of water, operation of PEMFCs involves only a single phase of water, therefore can be simplified; (3) the required cooling system will be simple and practically possible due to the increased temperature gradient between the fuel cell stack and the coolant; (4) the CO tolerance will be dramatically enhanced, from 10-20 ppm of CO at 80 ^{o}C, to 1000 ppm at 130 ^{o}C, and up to 30000 ppm at 200 ^{o}C.[71] However, the big problem associated with common PBIs is the poor mechanical strength at high PA-doping levels (defined as the averaged mole number of PA per mole of PBI repeat unit), which is essential for achieving high-proton conductivity. When phosphoric acid is introduced into the polymer structure at low acid-doping level range (< 2), the molecular cohesion between the PBI chains is decreased. However, the hydrogen bonding between nitrogen atoms and the phosphoric acid increases the cohesion. As a result of these opposite effects, no significant change of modulus or tensile strength of the PBI membranes was observed.[77] When acid-doping levels is higher than 2, i. e. the number of acid molecules surpasses the number of the basic sites, free acid will be present. The free acid would increase the separation for PBI backbones and therefore decrease the intermolecular forces. Consequently the membrane strength is decreased dramatically, more at higher temperature. The commercial PBI, for example, becomes too weak at high-doping levels of 13-16 to fabricate into membrane electrode assemblies (MEAs), and it is suggested that doping levels should be controlled at 5-6 to balance the proton conductivity and the mechanical strength of the membranes.[62,64] More recently, there have been a few reports on the crosslinked PBIs. It is well known that crosslinking is a common method to suppress membrane swelling and improve the mechanical properties. Li et al. have reported that the commercial PBI could be crosslinked by thermal treatment at 160-300 ^{o}C in the presence of a crosslinker (α,α'-dibromo-*p*-xylene) and the resulting crosslinked membranes displayed high tensile strength of 21-23 MPa at the doping level of 8.5, corresponds to the PA uptake of around 250 wt%.[65] Xu et al. have also reported that crosslinked hyperbranced PBI membranes could maintain reasonably high mechanical strength at high PA-doping level, which is superior to the commercial PBI membranes.[78,79] For practical use as a high temperature PEM, many research groups have studied the fuel cell performance and lifetime of PA-doped PBI fuel cell. Wang et al. investigated the PA-doped commercial PBI for use in a H_2/O_2 fuel cell in 1996, the results showed that the

PA-doped PBI fuel cell worked well at 150 ^{o}C with atmospheric pressure hydrogen and oxygen which were humidified at room temperature. No membrane dehydration was observed over 200 h operating.[80] Li et al. also reported many datas about the fuel cell performance of the PA-doped PBI.[81] Figure 1-16 shows a set of polarization curves at 200 ^{o}C under different pressures. A maximum power output of over 1.0 W/cm has been achieved with H_2/O_2 under a pressure of 3/3 bar at 200 ^{o}C without gas humidification. However, the eventual loss of the doping acid and the oxidative degradation of the polymer have been the major concern with respect to the lifetime of the acid-doped PBI membranes under fuel cell operation.

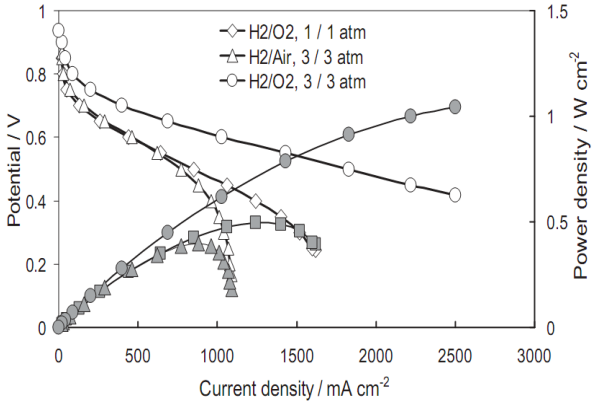

Figure 1-15. Fuel cell performance based on PA-doped PBI membranes at 200 ^{o}C under different pressures. The open symbols are for the potential axis (left) and the solid symbols are for the power density axis (right).

Li et al. also showed that a lifetime of 5000 h at 150 ^{o}C has been achieved at a constant cell voltage of 0.5 V and continuous H_2/O_2 operation (Figure 1-17). A similar result was obtained by Celanese, i.e., 6000 h at 160 ^{o}C with a small voltage decay rate. This continuous operation at temperatures above 100 ^{o}C involves no liquid water formation and therefore minimizes the possible acid leakage. Figure 1-18 showed the result of the thermal cycling test with a daily shutdown and restart. A slight decrease in current density at a cell voltage of 0.5 V was observed over a time period of 1400 h.

1-6. PEM based on phosphonated polymers

Polymer membranes containing phosphonic acid groups are one of the promising candidate for PEMs, which show high thermal stability and oxidative resistivity,[83,84]

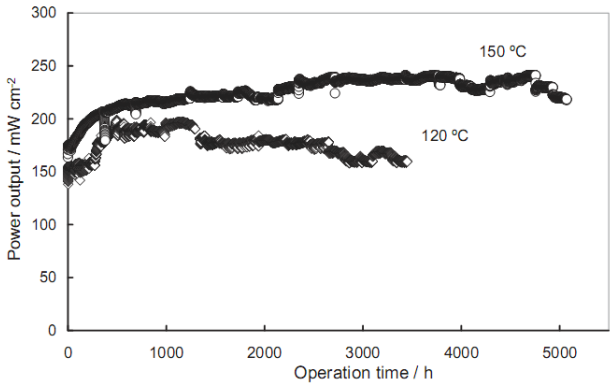

Figure 1-17. Lifetime test of PA-doped PBI cell under continuous operation at 120 ^{o}C and 150 ^{o}C.

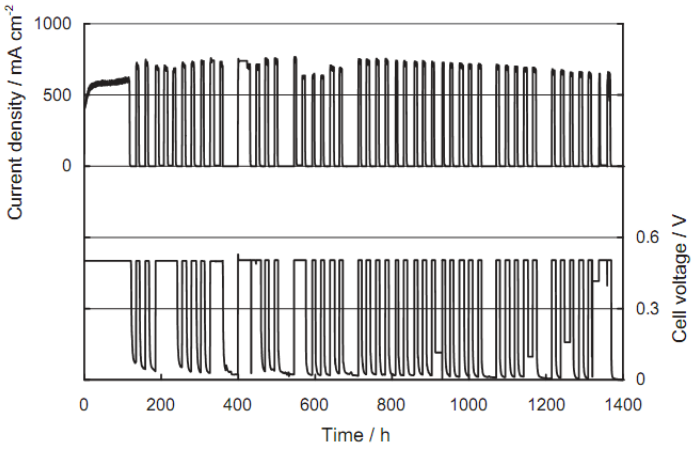

Figure 1-18. Lifetime test with shut down-restart cycling of a PA-doped PBI cell at 150 ^{o}C

have drawn considerable attention in past years. They have the specific ability of facilitating proton conductivity at a low RH or even under anhydrous conditions [20-23] because the phosphonic acid provides amphoteric properties, and shows a high degree of self-dissociation and hydrogen bonding, and the proton is transported through structure diffusion (the Grotthus mechanism[85,86]). For example, the PA-doped PBIs (we also introduced in this chapter) exhibit relatively high proton conductivity (0.03 S/cm) at approximately 150 ^{o}C.[87,88] In addition, phosphoric acid has comparatively better electrochemical and thermo-oxidative stability and allows higher reaction rates for hydrogen oxidation and oxygen reduction on Pt electrode surfaces. However, the main disadvantage of PA-doped membranes is that the H_3PO_4 small molecules can diffuse out of the membrane over time. Therefore, many reseachers focus on the study of phosphonated polymers, which tethering phosphonic acid groups to a polymer backbone.

It is well known that the acidity of phosphonic acids is lower than that of sulfonic acids, thus higher ionic contents are necessary to attain high conductivies. Poly(vinylphosphonic acid) (PVPA) with very simple structure and extremely high concentration of phosphonic acid which is directly attached to flexible polymer chain has emerged as an interesting candidate. Phosphonic acid is considered to form a strong hydrogen-bonding network involving both P＝O and P－OH as proton acceptor and proton donor groups.[89] The chemical structure of PVPA including a possible hydrogen-bond chain is shown in Figure 1-19. Their proton conductivity in the norminally dry state was on the order of 1×10^{-4} to 1×10^{-3} S/cm at approximately 150 ^{o}C. However, PVPA has poor mechanical properties for use in a fuel cell in large part due to its low T_g around -23 ^{o}C.[90]

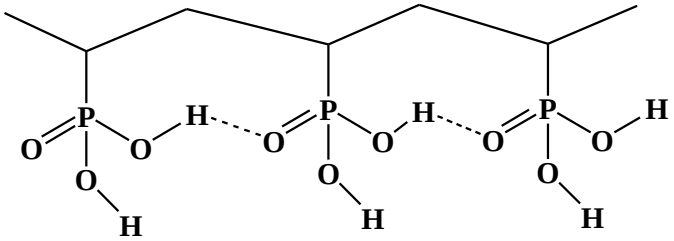

Figure 1-19. Chemical structure of PVPA showing a possible hydrogen-bonding scheme for the phosphonic acid groups.

One method to solve this problem is incorporating aromatic groups into the polymer structure. Quite recently, our group reported that PEMs (PDPAA) based on polyacrylates with phosphonic acid via long alkyl side chains (Figure 1-20) exhibited a very high proton conductivity comparable to that of the Nafion 117 membrane in the range of 30–80% RH at 80 ^{o}C, regardless of the significant low water uptake behavior.[91] Yoon et al. reported that the poly(vinylbenzyloxy-alkyl-phosphonic acid)s (Figure 1-21) showed the proton conductivity of 3×10^{-4} S/cm at 140 ^{o}C under nominally anhydrous conditions. They concluded that the high proton conductivity may be attributed to the highly aggregated proton conducting acid channels with mobile hydrogen bond networks. The flexible side chains may have a positive effect on the aggregation of the protongenic group and hydrogen bond formation.[92]

1-7. Recent challenges for PEMs

As discussed above, there are many kinds of PEMs have been investigated as alternatives for perfluonated polymers in last 20 years. For preparation of these PEMs,

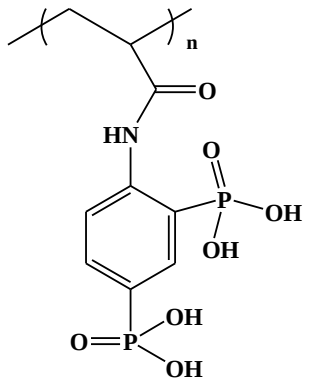

Figure 1-20. Structure of phosphonated poly(N-phenylacrylamide) (PDPAA).

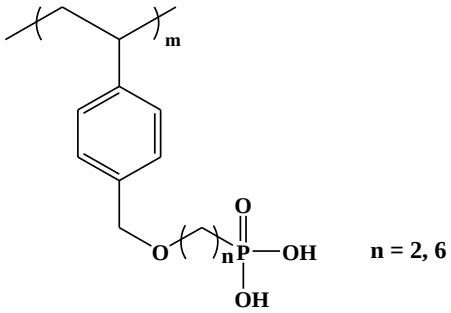

Figure 1-21. Structure of phosphonated poly(vinylbenzyloxy-alkyl-phosphonic acid)s.

generally, there are two approaches: (1) prepare PA-doped PBIs and phosphonated polymers, the PA shows high degree of self-dissociation and hydrogen bonding, so protons are transported through hydrogen bonding between phosphoric/phosphonic acids. This kind of PEM would show high proton conductivity even under anhydrous condition, and can be used at high temperature (120-200 ^{o}C); (2) synthesize the sulfonated polymers, such as SPS, SPI, SPPO, SPAE. The protons are carried by water (Vehicle mechanism) or transported through hydrogen bonding between water (Grotthuss-type mechanism), therefore, for this kind of PEM, water is essential for proton transport, and can be used at temperature < 120 ^{o}C. Although significant advancement has been achieved in the development of these membranes, there are still remaining unresolved application issues when they used as PEMs:

(1) For sulfonated membranes, the water uptake of the membranes is significantly related to the proton conductivity. However, the excessively high water uptake causes serious swelling and therefore the membrane is mechanically too weak to be used as PEMs. Crosslinking is an effective way to suppress the swelling, however, the proton conductivity decreased with increased crosslinker, and also the membranes become

brittle, so controlled the crosslinker amount is very important.

(2) These membranes show very low proton conductivity at low RH. In order to simplify the fuel cell system, a membrane with a proton conductivity of no less than 0.1 S/cm at 25-50% RH and 80-120 ^{o}C is required. To improve the proton conductivity at low RH deserves the most attention in future membrane development.

(3) Durability including the oxidative stability and mechanical stability would be a more serious issue for hydrocarbon-based membranes. It is well known that poor oxidative stability of the membranes may cause failure during long-term fuel cell operation. The oxidative stability of SPS, SPAE and SPI should be improved.

(4) For phosphonated polymers, they show lower proton conductivity than the sulfonated polymers at similar IEC values due to the much lower acidity of the phosphonic acid.

(5) For PA-doped PBI membrane, the disadvantages are poor solubility of PBI and mechanical strength decreased dramatically after absorbed PA, and the absorbed PA are easily leaked from membranes.

1-8. Purpose of this study

In this study, we want to solve these problems, we focus on the development of novel hydrocarbon-based PEMs for alternatives of perfluorinated PEMs. We prepared PA-doped PBIs, we modified the structures of PBIs to increase their solubility in aprotic solvents and improve mechanical strength after doped with PA. We also synthesized the phosphonated and sulfonated hydrocarbon-based PEMs with high proton conductivity at low RH (RH < 50%) and high oxidative stability. The details are summarized into 9 chapters as follows:

In chapter 1, the general introduction about the background of this study is described.

In chapter 2, the first section, the ether containing PBI poly[2,2’-(*p*-oxydiphenylene)-5,5’-bibenzimidazole] (OPBI) was synthesized to improve the solubility of PBI and PA-doped OPBI was prepared as PEM. The moderate molecular weight poly[2,2’-(m-phenylene)-5,5’-bibenzimidazole] (*m*PBI) used as the binder in catalyst layers for the first time to improve the fuel cell performance. A detailed study of fuel cell performance at different temperature was carried out. In the second setion, for further improvement of the fuel cell performance, sulfonated polybenzimidazoles (SPBIs) have been studied. The mechanical properties and fuel cell performance of PA-doped SPBIs were also investigated.

In chapter 3, a series of polystyrenes with phosphonic acids via 4, 6, and 8 methylene

spacers have been synthesized. Moreover, the relationship between the length of the alkyl chain and the properties of the membranes, such as water uptake, proton conductivity and morphology were also investigated.

In chapter 4, the cross-linked membranes of random copolystyrene derivatives based on a hydrophobic alkoxystyrene unit and a hydrophilic styrene unit containing a pendant alkyl sulfonic acid with the IEC of 2.57-3.03 mequiv/g were prepared by using 4,4'-methylene-bis[2,6-bis(hydroxyethyl)phenol] (MBHP) as the crosslinker in the presence of acid agent. The oxidative stability and proton conductivity at different RH were evaluated.

In chapter 5, for further improvement of the proton conductivity at low RH, especially at 30% RH, the cross-linked membranes of block copolystyrene derivatives, which have the similar structure with the random copolysytene (chapter 4), have been synthesized based on living anionic polymerization. The performance of these crosslinked block copolymers was described.

Furthermore, to improve the thermal and mechanical properties, the polymer aromatic main chain was chosen in place of polystyrene. The poly(*m*-phenylene)s and poly(phenylene ether)s with sulfonic acid via alkyl side chains were prepared in chapter 6 and 7, respectively. The membrane properties were investigated in detail.

In chapter 8, to clarify the detailed structure-property relationship for the design of future PEM, the poly(arylene ether ether nitrile)s with ether group on the main chain and different length of alkylsulfonated side chains were synthesized. The nitrile groups are also introduced into the polymer main chain to decrease the swelling of the membrane. The effects of the length of the side chains on the properties of membranes were investigated.

In chapter 9, the conclusion of this study and the prospection was also discussed.

1-9. References

(1) Polymer science: a comprehensive reference, polymers for a sustainable environment and green energy, volume 10.
(2) GB Patent 1034197, **1966.**
(3) Kreuer, K.D. *J. Membr. Sci.* **2001,** *185,* 29-39.
(4) Mauritz, K. A.; Moore, R. B. *Chem. Rev.* **2004,** *104,* 4535-4586.
(5) Ise, M. Polymer Elektrolyt Membranen: Untersuchungen zur Mikrostruktur und zu den Transporteigenschaften für Protonen und Wasser, Ph.D. Thesis, University of Stuttgart, **2000.**

(6) Assink, R. A.; Arnold, C.; Hollandsworth, R. P. *J. Membr. Sci.* **1991,** *56,* 143-151.

(7) Hickner, M. A.; Ghassemi, H.; Kim, Y. S.; Einsla, B. R.; McGrath, J. E. *Chem. Rev.* **2004,** *104,* 4587-4612.

(8) Wei, J.; Stone, C.; Steck, A. E. *U.S. Patent* 5422411, **1995.**

(9) Steck, A. E. Proceedings of the first international symposium of new materials for fuel cell systems: 1'Ecole polytechnique de Montreal: Montreal, **1995,** p74

(10) Steck, A. E.; Stone, C. Proceedings of the 2nd international symposium on new materials for fuel cell and modern battery system, 1'Ecole polytechnique de Montreal: Montreal, **1997,** p792.

(11) Wnek G. Abstract of papers, 222nd ACS National Meeting, Chicago, IL, United States, August 26-30, **2001.**

(12) Kim, J.; Kim, B.; Jung, B. *J. Membr. Sci.* **2002,** *207,* 129-137.

(13) Serpico, J. M.; Ehrenberg, S. G.; Fontanella, J. J.; Jiao, X.; Perahia, D.; McGrady, K. A.; Sanders, E. H.; Kellogg, G. E.; Wnek, G. E. *Macromolecules* **2002,** *35,* 5916-5921.

(14) Wnek, G. E.; Rider, J. N.; Serpico, J. M.; Einset, A. G. Electrochem. Soc. Proc. **1995,** *23,* 247.

(15) Bae, B.; Hoshi, T.; Miyatake, K.; Watanabe, M. *Macromolecules* **2011,** *44,* 3884-3892.

(16) Miyatake, K.; Chikashige, Y.; Higuchi, E.; Watanabe, M. *J. Am. Chem. Soc.* **2007,** *129,* 3879-3887.

(17) Zhang, Y.; Wan, Y.; Zhao, C.; Shao, K.; Zhang, G.; Li, H.; Lin, H.; Na, H. *Polymer* **2009,** *50,* 4471-4478.

(18) Ghassemi, H. McGrath, J. E. *Polymer* **2004,** *45,* 5847-5854.

(19) Kobayashi, T.; Rikukawa, M.; Sanui, K.; Ogata, N. *Solid State Ionics* **1998,** *106,* 219-225.

(20) Hickner, M. A.; Fujimoto, C. H.; Cornelius, C. J. *Polymer* **2006,** *47,* 4238-4244.

(21) Genies, C.; Mercier, R.; Sillion, B.; Cornet, N.; Gebel, G.; Pineri, M. *Polymer* **2001,** *42,* 359-373.

(22) Fang, J. H.; Guo, X. X.; Harada, S.; Watari, T.; Tanaka, K.; Kita, H.; Okamoto, K. *Macromolecules* **2002,** *35,* 9022-9028.

(23) Yin, Y.; Fang, J.; Watari, T.; Tanaka, K.; Kita, H.; Okamoto, K. *J. Mater. Chem.***2004,** *14,* 1062-1070.

(24) Saito, J.; Miyatake, K.; Watanabe, M. *Macromolecules* **2008,** *41,* 2415-2420.

(25) Kobayashi, T.; Rikukawa, M.; Sanui, K.; Ogata, N. *Solid State Ionics* **1998,** *106,*

219-225.

(26) Xing, P.; Robertson, G. P.; Guiver, M. D.; Mikhailenko, S.; Kaliaguine, S. *Macromolecules* **2004,** 37, 7960-7967.

(27) Mikhailenko, S. D.; Robertson, G. P.; Guiver, M. D.; Kaliaguine, S. *J. Membr. Sci*. **2006,** *285,* 306-316.

(28) Li, X.; Liu, C.; Lu, H.; Zhao, C.; Wang, Z.; Xing, W.; Na, H. *J. Membr. Sci.* **2005,** *255,* 149-155.

(29) Jouanneau, J.; Mercier, R.; Gonon, L.; Gebel, G. *Macromolecules* **2007,** *40,* 983-990.

(30) Mader, J. A.; Benicewicz, B. C. *Macromolecules* **2010,** *43,* 6706-6715.

(31) Li, J.; Lee, C. H.; Park, H. B.; Lee, Y. M. *Macromol. Res.* **2006,** *14,* 438-442.

(32) Tan, N.; Xiao, G. Y.; Yan, D. Y. *Polym. Bull.* **2009,** *62,* 593-604.

(33) Tan, N.; Chen, Y.; Xiao, G. Y.; Yan, D. Y. *J. Membr. Sci.* **2010,** *356,* 70-77.

(34) Tan, N.; Xiao, G. Y.; Yan, D. Y. *Chem. Mater.* **2010,** *22,* 1022-1031.

(35) Vallejo, E.; Pourcelly, G.; Gavach, C.; Mercier, R.; Pineri, M. *J. Membr. Sci.* **1999,** *160,* 127-137.

(36) Genies, C.; Mercier, R.; Sillion, B.; Cornet, N.; Gebel, G.; Pineri, M. *Polymer* **2001,** 42, 359-373.

(37) Faure, S.; Mercier, R.; Aldebert, P.; Pineri, M.; Sillion, B. *French Pat. 9605707,* **1996.**

(38) Yin, Y.; Fang, J.; Cui, Y.; Tanaka, K.; Kita, H.; Okamoto, K.-I. *Polymer* **2003,** *44,* 4509-4518.

(39) Miyatake, K.; Asano, N.; Watanabe, M. *J. Polym. Sci., Part A: Polym. Chem.* **2003,** *41,* 3901-3907.

(40) Einsla, B. R.; Kim, Y. S.; Hickner, M. A.; Hong, Y.-T.; Hill, M. L.; Pivovar, B. S.; McGrath, J. E. *J. Membr. Sci.* **2005,** *255,* 141-148.

(41) Okamoto, K.-I.; Yin, Y.; Yamada, O.; Islam, M. N.; Honda, T.; Mishima, T.; Suto, Y.; Tanaka, K.; Kita, H. *J. Membr. Sci.* **2005,** *258,* 115-122.

(42) Hu, Z.; Yin, Y.; Yaguchi, K.; Endo, N.; Higa, M.; Okamoto, K.-I. *Polymer* **2009,** *50,* 2933-2943.

(43) Asano, N.; Aoki, M.; Suzuki, S.; Miyatake, K.; Uchida, H.; Watanabe, M. *J. Am. Chem. Soc.* **2006,** *128,* 1762-1769.

(44) Fox, D. W.; Shenian, P. *U. S. Pat. 3709841,* **1973.**

(45) Robeson, L. M.; Matzner, M. *U. S. Pat. 4380598,* **1983.**

(46) Ueda, M.; Toyota, H.; Ochi, T.; Sugiyama, J.; Yonetake, K.; Masuko, T.; Teramoto,

T. *J. Polym. Sci. Polym. Chem. Ed.* **1993,** *31,* 853-858.

(47) Higashihara, T.; Matsumoto, K.; Ueda, M. *Polymer* **2009,** 50, 5341-5357.

(48) Nakabayashi, K.; Matsumoto, K.; Ueda, M. *J. Polym. Sci. Part: A, Polym. Chem.* **2008,** *46,* 3947-3957.

(49) Nakabayashi, K.; Matsumoto, K.; Ueda, M. *J. Polym. Sci. Part: A, Polym. Chem.* **2008,** *46,* 7332-7341.

(50) Nakabayashi, K.; Matsumoto, K.; Ueda, M. *Polymer J.* **2009,** 41, 332-337.

(51) Matsumura, S.; Hlil, A. R.; Lepiller, C.; Gaudet, J. Guay, D.; Shi, Z. *Macromolecules* **2008,** *41,* 281-284.

(52) Mastumoto, K.; Higashihara, T.; Ueda, M. *Macromolecules* **2009,** *42,* 1161-1166.

(53) Smith, C. D.; Grubbs, H.; Webster, H. F.; Gungor, A.; Wightman, J. P.; McGrath, J. E. *High Perform. Polym.* **1991,** *3*, 211-229.

(54) Wang, S.; Zhuang, H.; Shobha, H. K.; Glass, T. E.; Sankarapandian, M. ; Ji, Q.; Shultz, A. R.; McGrath, J. E. *Macromolecules* **2001,** *34,* 8051-8063.

(55) Fujimoto, C. H.; Hickner, M. A.; Cornelius, C. J.; Loy, D. A. *Macromolecules* **2005,** *38,* 5010-5016.

(56) Wu, S.; Qiu, Z.; Zhang, S.; Yang, X.; Li, Z. *Polymer* **2006,** *47,* 6993-7000.

(57) Seesukphronrarak, S.; Ohira, K.; Kidena, K.; Takimoto, N.; Kuroda, C. S.; Ohira, A. *Polymer* **2010,** *51,* 623-631.

(58) Jouanneau, J.; Mercier, R.; Gonon, L.; Gebel, G. *Macromolecules* **2007,** *40,* 983-990.

(59) Samms, S. R.; Wasmus, S.; Savinell, R. F. *J. Electrochem. Soc.* **1996,** *143,* 1498-1504.

(60) Samms, S. R.; Wasmus, S.; Savinell, R. F. *J. Electrochem. Soc.* **1996,** *143,* 1225-1232.

(61) Wainright, J. S.; Wang, J.-T.; Weng, D.; Savinell, R. F.; Litt, M. *J. Electrochem. Soc.* **1995,** *142,* 121-123.

(62) Li, Q.; He, R.; Jensen, J. O.; Bjerrum, N. J. *Fuel Cells* **2004,** *4,* 147-159.

(63) Yu, S.; Xiao, L.; Benicewicz, B. C. *Fuel Cells* **2008,** *8,* 165-174.

(64) Xiao, L.; Zhang, H.; Scanlon, E.; Ramananthan, L. S.; Choe, E.-W.; Rogers, D.; Apple, T.; Benicewicz, B. C. *Chem. Mater.* **2005,** *17*, 5238-5333.

(65) Li, Q.; Pan, C.; Jensen, J. O.; Noye, P.; Bjerrum, N. J. *Chem. Mater.* **2007,** *19,* 350-352.

(66) Lin, H. L.; Hsieh, Y. S.; Chiu, C.W.; Yu, T. L.; Chen, L. C. *J. Power Sources* **2009,** *193*,170-174.

(67) Kim, T.-H.; Kim, S.-K.; Lim, T.-W.; Lee, J.-C. *J. Membr. Sci.* **2008,** *323,* 362-370.

(68) Carollo, A.; Quartarone, E.; Tomasi, C.; Mustarelli, P.; Belotti, F.; Magistris, A.; Maestroni, F.; Parachini, M.; Garlaschelli, L.; Righetti, P. P. *J. Power Sources* **2006,** *160,* 175-180.

(69) Xiao, L.; Zhang, H.; Jana, T.; Scanlon, E.; Chen, R.; Choe, E.-W.; Ramanathan, L. S.; Yu, S.; Benicewicz, B. C. *Fuel Cells* **2005,** *5,* 287-295.

(70) Lobato, J.; Canizares, P.; Rodrigo, M.A.; Linares, J. J.; Aguilar, J. A. *J. Membr. Sci.* **2007,** *306,* 47-55.

(71) Li, Q.; He, R.; Gao, J.; Jensen, J. Q.; Bjerrum, N. J. *J. Electrochem. Soc.* **2003,** 150, 1599-1605.

(72) Linkous, C. A.; Anderson, H. R.; Kopitzke, R. W.; Nelson, G. L. *Int. J. Hydrogen Energy,* **1998,** *23,* 525-630.

(73) Glipa, X.; Haddad, M. E.; Jones, D. J.; Roziere, J. *Solid State Ionics* **1997,** *97,* 323-331.

(74) Gieselman, M.; Reynolds, J. R. *Macromolecules* **1992,** *25,* 4832-4834.

(75) Tsuruhara, K.; Hara, K.; Kawahara, M.; Rikukawa, M.; Sanui, K.; Ogata, N. *Electrochim. Acta.* **2000,** *45,* 1223-1226.

(76) Kawahara, M.; Rikukawa, M.; Sanui, K. *Polym. Adv. Technol.* **2000,** *11,* 1-5.

(77) Litt, M.; Ameri, R.; Wang, Y.; Savinell, R.; Wainwright J. *Mater. Res. Soc. Symp. Proc.* **1999,** *548,* 313-323.

(78) Xu, H.; Chen, K.; Guo, X.; Fang, J.; Yin, J. *J. Membr. Sci.* **2007,** *288,* 255-260.

(79) Xu, H.; Chen, K.; Guo, X.; Fang, J.; Yin, J. *J. Polym. Sci., Part A: Polym. Chem.* **2007,** *45,* 1150-1158.

(80) Wang, J. T.; Savinell, R. F.; Wainright, J.; Litt, M.; Yu, H. *Electrochem. Acta.* **1996,** *41,* 193-197.

(81) Li, Q. F.; He, R .H.; Jensen, J. O.; Bjerrum, N. J. *Fuel Cells* **2004,** *4,* 147-159.

(82) Lee, H.-C.; Lim, H.; Su, W.; Chao, C.-Y. *J. Polym. Sci. Part A: Polym. Chem.* **2011,** *49,* 2325-2338.

(83) Jiang, D. D.; Yao, Q.; Mckinney, M. A.; Wilkie, C. A. *Polym. Degrad. Stab.* **1999,** *63,* 423-434.

(84) Schuster, M.; Rager, T.; Noda, K. D.; Maier, J. *Fuel Cells* **2005,** *5,* 355-365.

(85) Kordesch, K.; Simader, G. Fuel Cells and Their Applications; VCH: Weinheim, Germany, **1996.**

(86) Kreuer, K.-D.; Rabenau, A.; Weppner, W. *Angew Chem. Int. Ed.* **1982,** *94,* 224-225.

(87) Wainright, J. S.; Wang, J, T.; Weng, D.; Savinell, R. f.; Litt, M. *J. Electrochem. Soc.*

1995, *142,* L121-L123.

(88) Kerres, J. A. *J. Membr. Sci.* **2001,** *185,* 3-27.

(89) Lee, Y. J.; Bingol, B.; Murakhtina, T.; Sebastiani, D.; Meyer, W. H.; Wegner, G.; Spiess, H. W. *J. Phys. Chem. B* **2007,** *111,* 9711-9721.

(90) Sevil, F.; Bozkurt, A. *J. Phys. Chem. Solid* **2004,** *65,* 1659-1662.

(91) Fukuzaki, N.; Tamura, Y.; Kazuhiro Nakabayashi, Nakazawa, S.; Murata, S.; Higashihara, T.; Ueda, M. *Polym. Prepr. Jpn.* **2011,** *60,* 1582.

(92) Lee, S.-II.; Yoon, K.-H.; Yoon, D. Y. *Chem. Mater.* **2012,** *24,* 115-122.

(93) Jutemar, E. P.; Jannasch, P. *J. Polym. Sci.: Part A: Polym. Chem.* **2011,** *49,* 734-745.

(94) Kim, Y. S.; Kim, D. S.; Liu, B.; Guiver, M. D.; Pivovar, B. *J. Electrochem. Soc.* **2008,** *155,* B21-B26.

(95) Kim, D. S.; Kim, Y. S.; Guiver, M. D.; Pivovar, B. S. *J. Membr. Sci.* **2008,** *321,* 199-208.

(96) Gao, Y.; Robertson, G. P.; Guiver, M. D.; Mikhailenko, S. D.; Li, X.; Kaliaguine, S. *Polymer* **2006,** *47,* 808-816.

(97) Gao, Y.; Robertson, G. P.; Guiver, M. D.; Mikhailenko, S. D.; Li, X.; Kaliaguine, S. *Macromolecules* **2005,** *38,* 3237-3245.

Chapter 2

Phosphoric Acid-doped Polybenzimidazole / Sulfonated Polybenzimidazole for Polymer Electrolyte Membranes

ABSTRACT: The ether containing PBI (OPBI), poly[2,2'-(*p*-oxydiphenylene)-5,5'-bibenzimidazole] was synthesized to increase the solubility of PBI. Phosphoric acid (PA)-doped OPBI membrane was prepared into membrane electrode assemblies (MEAs) for the high temperature polymer electrolyte membrane fuel cells, and the moderate molecular weight poly[2,2'-(*m*-phenylene)-5,5'-bibenzimidazole] (*m*PBI) with good solubility in aprotic solvents was synthesized and utilized as the binder in catalyst layers for the first time. The optimized MEA exhibited the maximum output power density of 366 mW/cm^2 at 160 ^{o}C with H_2-O_2 gases without external humidification. Moreover, a series of sulfonated polybenzimidazoles (SPBIs) with varied ion exchange capacities (IECs) were also synthesized by random condensation copolymerization of a new sulfonated dicarboxylic acid monomer 4,6-bis(4-carboxyphenoxy)benzene-1,3-disulfonate, 4,4'-dicarboxydiphenyl ether and 3,3'-diaminobenzidine. Most of the SPBIs showed good solubility in polar aprotic organic solvents such as dimethylsulfoxide (DMSO) and *N*,*N*-dimethylacetamide (DMAc). Thermogravimetric analysis (TGA) revealed that the SPBIs have excellent thermal stability (desulfonation temperatures (on-set) > 370 ℃).The SPBI membranes exhibited phosphoric acid (PA) uptake in the range 180-240 wt% (8-13 molecules of PA per polymer repeating unit) in 85 wt% PA at 50 ℃, while high mechanical properties (13-20 MPa) are maintained. The fuel cell fabricated with the PA-doped SPBI membrane displayed better performance with the highest output power density of 580 mW/cm^2 at 170 ℃ than that of PA-doped OPBI.

2-1. Introduction

Polymer electrolyte membrane fuel cells (PEMFCs) are one of the most promising power sources for both mobile and stationary applications.[1,2] A proton exchange membrane (PEM) is one of the key components of a PEMFC system, which functions as the anode/cathode separator as well as the medium for proton transport from the anode to the cathode. Up to date, the state-of-the-art PEMs and binders in the catalyst layers of gas diffusion electrodes[3,4] are sulfonated perfluoropolymers, typically, Dupont's Nafion because of its excellent chemical and electrochemical stability and high proton conductivity. However, some disadvantages such as high cost, high fuel crossover and low operating temperatures (< 100 ℃) seriously limited their industrial application. In addition, at the low working temperatures condition, platinum-based catalysts tend to be poisoned by impurities from the reforming processes. Thus intensive efforts have been devoted to the development of low-cost proton-conducting electrolytes used at elevated temperatures to reduce the impurities poisoning.[5-9]

Aromatic polybenzimidazoles (PBIs), known for their excellent thermal and thermoxidative stability, high mechanical strength and storage modulus, outstanding chemical resistance, have found important industrial applications. The phosphoric acid (PA)-doped polybenzimidazoles,[7-9] are one of the promising candidates, which can function at higher temperatures and low relative humidity (RH), even under non-humidification conditions,[10-12] as well as promote the fuel impurities tolerance,[13,14] increase the electrode kinetics,[15] and facilitate the heat recovery.[16,17] The widely used polybenzimidazole was the commercially available poly[2,2'-(*m*-phenylene)-5,5'-biben-zimidazole] (*m*PBI).[18,19] However, the *m*PBI shows poor solubility due to its rigid-rod structure and strong hydrogen bonding. For example, to cast membranes or prepare the catalyst layers of electrodes, *m*PBI has to be dissolved at high temperature (near the boiling point of aprotic solvents), preferably under an elevated pressure and oxygen-free atmosphere.[13, 20-22] For the long time storage, 1.5-2 wt% lithium salt needs to be added into the solution as stabilizer.[22, 23] At the end of preparation, the prepared membranes or electrodes need to be washed with hot water to remove the solvent and stabilizer.[13,22,24,25] One of the methods to improve the solubility of PBI is to introduce the flexible units to the main chain.[29,30] Such as poly[2,2'-(*p*-oxydiphenylene)-5,5'-bi-benzimidazole] (OPBI), which contains flexible ether linkages between aromatic units in the main chain.[31-34] The OPBI shows good solubility in aprotic solvents,[31,35,36] high thermal stability,[31-38] and excellent mechanical properties.[34,35,38,39] However, the fuel cell performance of the PA-doped OPBI has not been reported yet.[38,40]

The viscosity of the binder in catalyst layers also plays important role in MEAs. The fabrication process of the catalyst layers can be facilitated by using a well soluble and less viscous binder. It is well known that the solubility and viscosity of a polymer are related to its molecular weight. The lower molecular weight polymer tends to present higher solubility and lower viscosity, and vice versa.[41] Therefore, the *m*PBI with moderate molecular weight is expected to present good solubility and medium viscosity. Its utilization could overcome both the poor solubility of higher molecular weight *m*PBI and the inadequate binding capability of low molecular weight *m*PBI, and thus facilitate the preparation of catalyst layers in MEAs. Nafion[22,40,42] and high molecular weight *m*PBI[21,22,24] have dominantly been used as the binders in catalyst layers. However, the preparation and the use of moderate molecular weight *m*PBI as the binder in catalyst layers and the performances of the prepared MEAs have not been reported yet.

On the other hand, the sulfonated PBI membranes also have been synthesized and studied for possible use in fuel cells. However, compared with common sulfonated polymer membranes containing no basic units in their chemical structures SPBIs generally show rather low proton conductivity because the proton transport becomes relatively difficult resulting from the strong acid-base interactions between the sulfonic acid groups and basic imidazole rings.[43] One mole imidazole ring can react with one mole sulfonic acid group to form ionic cross-linking. As the mole number of sulfonic acid groups is less than that of imidazole ring, the proton conductivity is generally at the level of 10^{-4}-10^{-3} S/cm even at 100% RH which is too low to meet the lowest requirement (10^{-2} S/cm) for practical use.[44] Recently Gomez-Romero et al. reported an interesting phenomenon that the PA-doped SPBI derived from 5-sulfoisophthalic acid mono-sodium salt and 1,2,4,5-tetraaminobenzene displayed higher proton conductivity than the PA-doped non-sulfonated PBIs even at the same doping levels (number of PA molecules per imidazole ring). This should be favorable for achieving high fuel cell performance. However, the structure-property relationship of SPBIs and in particular, the fuel cell performance have far less been investigated yet.

In the first section of this chapter, the PA-doped OPBI membrane with good solubility was chosen as the electrolyte membrane, and the moderate molecular weight *m*PBI was synthesized as the binder in catalyst layers. The preparation of MEAs was simplified. A detailed study of MEAs preparation and the performances of corresponding H_2-O_2 single cells were reported. In the second section, a series of SPBIs with varied ion exchange capacities (IECs) were prepared, the thermal stability, mechanical properties, radical oxidative stability, PA-doping, proton conductivity and

fuel cell performance of the SPBI membranes were also investigated.

2-2. Results and Discussion

2-2-1. OPBI membrane

High molecular weight OPBI (Scheme 2-1) with good solubility and mechanical property was synthesized and used to dope PA. The obtained OPBI displayed high inherent viscosity (η_{inh}=1.05 dL/g which was measured at 0.5 g/dL OPBI solution in DMSO at 30 ℃), indicating that high molecule weight OPBI has been successfully synthesized.[35]

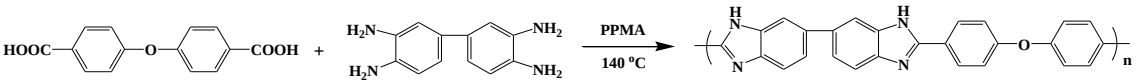

Scheme 2-1. Synthesis of OPBI

2-2-1-1. Mechanical analysis and proton conductivity

Mechanical property plays an important role for the real PEMFCs application. Mechanical properties of the OPBI membrane and the corresponding PA-doped OPBI membrane were evaluated by the tensile tests. The maximum stress (MS) for the undoped OPBI membrane was 116 MPa at 25 ℃ at 32 % relative humidity (Table 2-1). The doping of PA led to a significant reduction in tensile strength of the membrane, and the PA-doped OPBI membrane exhibited MS of 44 MPa. However, the elongation at break was enhanced from 27% to 57%. This was attributed to the plasticization effect of PA in the membrane. When the temperature was raised to 150 ℃ (the corresponding relative humidity was 0.2 %), the tensile strength decreased and the elongation at break increased for both the undoped OPBI membrane and the PA-doped OPBI membrane, and the changes were more significant for the PA-doped OPBI membrane. The PA-doped OPBI membranes displayed higher MS than the PA-doped *m*PBI membranes with the same doping level reported in the literature,[7,45] which was strong enough for preparation of MEAs.

Proton conductivity was measured using a two-probe electrochemical impedance spectroscopy technique over the frequency range from 100 Hz to 100 kHz. A strip of PA-doped OPBI membrane and two platinum electrodes were set in a Teflon cell. The cell was placed in a thermo-controlled chamber, which had an inlet and an outlet for the continuous dry N_2 flow. The chamber was heated at 150 ℃ for 10 h to remove water vapor thoroughly (the 0% relative humidity). And then, the temperature of chamber was kept constant for 1 h at each desired temperature point from 90 to 170 ℃. It was found that the proton conductivity increased with temperature (Figure 2-1). PA-doped OPBI

Table 2-1. Maximum stress (MS) and elongation at break (EB) of OPBI and PA-doped OPBI membranes.

Membrane	Temperature [a] (℃)	MS (MPa)	EB (%)
OPBI	25	116	27
	150	101	31
PA-doped OPBI	25	44	57
	150	17	84

[a]At 25 °C and 32 % relative humidity, and 150 °C and 0.2 % relative humidity.

showed the highest proton conductivity of 4.0 mS/cm at 170 ℃. To check if there was the hysteresis of the conductivity, the corresponding proton conductivities in both the cooling run (from 170 to 90 ℃) and the subsequent heating run (from 90 to 170 ℃) were measured and compared (Figure 2-1). The proton conductivities obtained at reverse runs were quite similar at each temperature point, indicating that the hysteresis phenomenon was negligible.

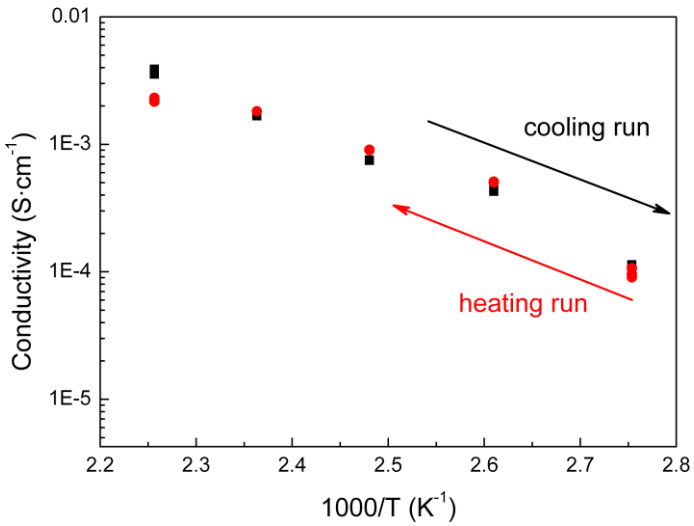

Figure 2-1. Variation of proton conductivity of the PA-doped OPBI membrane as a function of temperature at 0% relative humidity measured first in the cooling run (from 170 °C to 90 °C) and subsequently in the heating runs (from 90 °C to 170 °C).

2-2-1-2. Components in the catalyst layers of MEAs

The synthesized moderate molecular weight *m*PBI (Scheme 2-2) was easily dissolved in DMAc at room temperature and a clear solution up to 4.0 wt% was obtained in the

absence of any stabilizer. The inherent viscosity of the moderate molecular weight *m*PBI was 0.21 dL/g, which was measured in DMAc at a concentration of 0.5 g/dL with an Ubbe-lohde viscometer at 30 ℃. The good solubility and medium viscosity of moderate molecular weight *m*PBI could facilitate the preparation of MEAs.

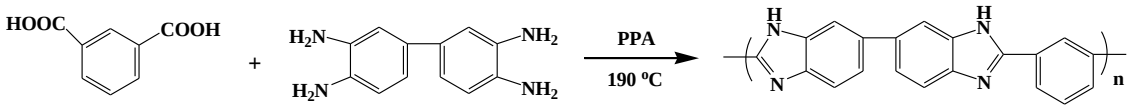

Scheme 2-2. Synthesis of *m*PBI

The *m*PBI and OPBI, which synthesized in this chapter, were used as a binder in the catalyst layers, respectively, and the performance of each other was discussed in detail. The 20 wt% Pt/C catalyst ink which contained 78 wt% catalyst and 22 wt% moderate molecular weight *m*PBI (dry weight) was selected as reported.[13,23,25] It was found that without external humidification the maximum power output 155 mW/cm^2 was achieved at 160 ℃ (Figure 2-2, a'). The lower maximum power densities were obtained if the PA-doped OPBI membranes didn't dry to remove the PA on the surface before preparing MEA (Figure 2-2, b'). It was proposed that the PA on the surface of doped OPBI membranes could absorb water rapidly from the ambient moisture before the hot press. Thus the PA-doped OPBI membranes needed to be wiped off with filter papers. At the same time, the hot air needed to be blown onto the catalyst layers if the acid droplets were visible on the catalyst layers before the hot press. Figure 2-2, c' showed that a littler higher power density of 189 mW/cm^2 was achieved when OPBI used as binder in gas diffusion electrodes. Although PA-doped electrodes containing OPBI displayed higher power density, the OPBI as the binder presented high viscosity, and accurate measurement of the catalyst ink components was inconvenient. Thus the PA-doped electrodes containing moderate molecular weight *m*PBI were mainly studied in this chapter.

Then, the 40 wt% Pt/C catalyst ink which contained 95 wt% catalyst and 5 wt% moderate molecular weight *m*PBI (dry weight) was selected. A much enhanced cell performance was obtained when the 40 wt% Pt/C catalyst was used, and the maximum power density was 303 mW/cm^2 (Figure 2-3, a'). The quantity of the catalyst ink was decreased when the content of platinum in catalysts increased. Thus, the differences of performances in single cells were derived from the reduction of catalyst layer thickness

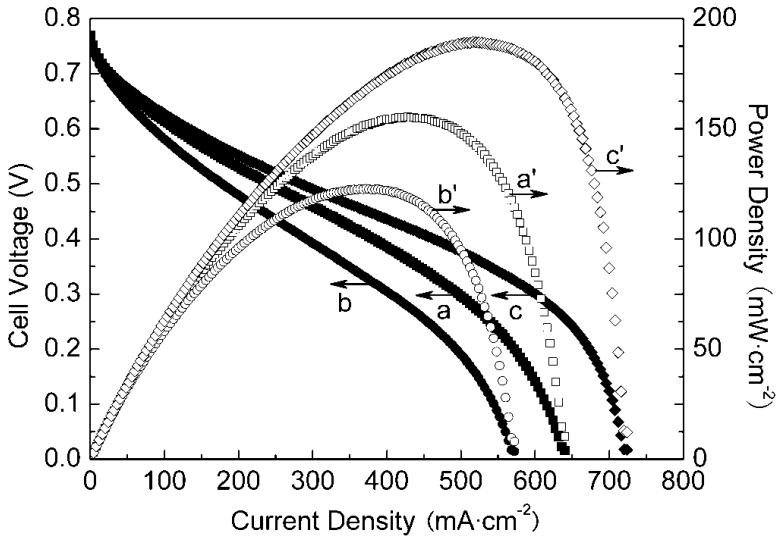

Figure 2-2. Performances of H_2-O_2 single cells based on PA-doped OPBI membranes at 160 ℃. Gases were fed without humidification and hot press at 150 ℃ and 1.2 MPa for 10 min. (a, a') PA-doped electrodes containing moderate molecular weight *m*PBI; (b, b') PA-doped electrodes containing moderate molecular weight *m*PBI, without sufficient drying; (c, c') PA-doped electrodes containing OPBI.

and the concomitant enhancement of mass transfer rate. In the controlled experiments, the polyvinylidene difluoride (PVDF) was added into the catalyst ink to replace part of the moderate molecular weight *m*PBI. The hydrophobicity of PVDF resulted in the lower water uptake in the electrodes and the enhancement of mass transfer rate. The weight ratio of PVDF/moderate molecular weight *m*PBI was chosen as 1/2.[10,53] Consequently the 40 wt% Pt/C catalyst ink contained 95 wt% catalyst, 1.7 wt% PVDF (dry weight) and 3.3 wt% moderate molecular weight *m*PBI (dry weight). It was found that the highest output power density 366 mW/cm^2 was obtained by the addition of PVDF (Figure 2-3, b'). When H_2 and air were introduced into the single cell using this MEA, the open circuit voltage was reduced from 0.79 V to 0.75 V due to the reduction of oxygen partial pressure and the corresponding maximum power density was 225 mW/cm^2 (Figure 2-3, c').

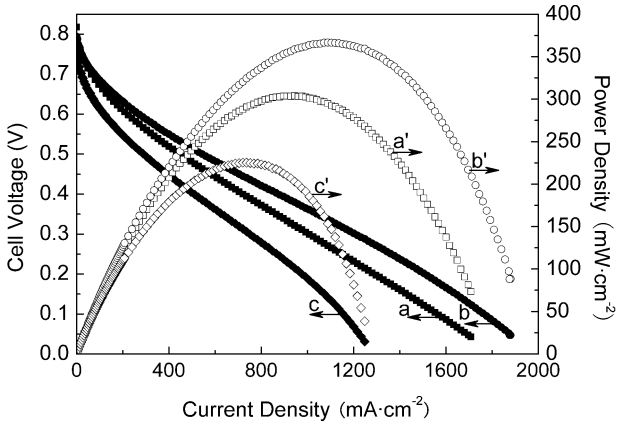

Figure 2-3. Performances of single cells based on PA-doped OPBI membranes at 160 ℃. Gases were fed without humidification and hot press at 150 ℃ and 1.2 MPa for 10 min. (a, a') H_2-O_2 single cell using the PA-doped electrodes containing moderate molecular weight *m*PBI; (b, b') H_2-O_2 single cell using the PA-doped electrodes containing moderate molecular weight *m*PBI and PVDF; (c, c') H_2-air single cell of MEA in (b, b').

2-2-1-3. Effect of temperature on the performances of MEAs

The effect of temperature on the performances of single cells was also investigated. The performance was increased significantly when increased the temperature from 80 to 160 ℃ (Figure 2-4). Figure 2-5 shows the electrochemical impedance spectrometry (EIS) curves with PA-doped OPBI measured at different temperatures under ambient pressure without external humidification. It can be seen that both the membrane resistance and the reaction resistance at electrode/electrolyte interfaces were decreased with increased temperatures which indicated that the electrode kinetics was enhanced as temperature increased. When the temperature was 160 ℃, the membrane resistance was about 0.07 Ω (Figure 2-5, e), and the corresponding through-plane conductivity of PA-doped OPBI membrane in the real single cell was estimated as 0.016 S/cm (the membrane thickness was 55 μm). This through-plane conductivity was consistent with the through-plane conductivity (0.025-0.04 S/cm) of PA-doped OPBI membranes reported in the literature,[36,39] and was close to those through-plane conductivities (0.02-0.05 S/cm) of typical PA-doped *m*PBI membranes with the similar doping level in the literature.[8,46]

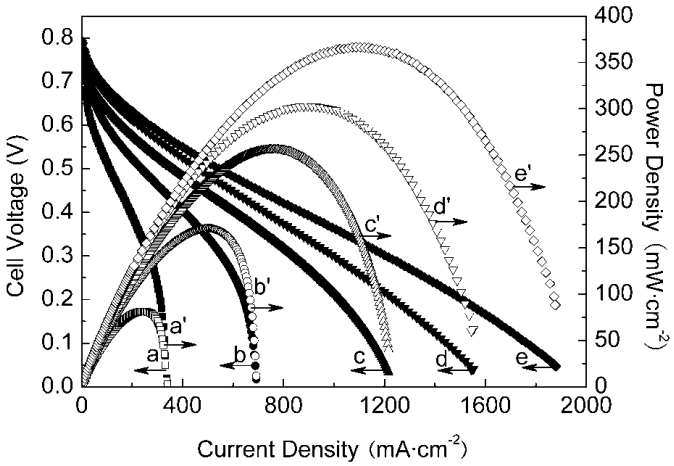

Figure 2-4. Effect of temperature on the performances of H_2-O_2 single cells based on PA-doped OPBI membranes. Electrodes contained moderate molecular weight *m*PBI and PVDF. Gases were fed without humidification. Hot press at 150 ℃ and 1.2 MPa for 10 min. Cell temperature was: (a, a') 80 ℃; (b, b') 100 ℃; (c, c') 120 ℃; (d, d') 140 ℃; (e, e') 160 ℃.

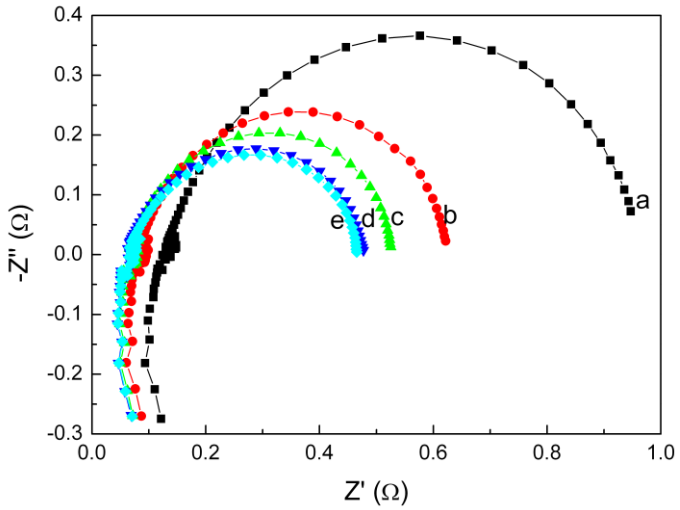

Figure 2-5. Electrochemical impedance spectrometry (EIS) curves with PA-doped OPBI membrane measured at different temperatures with H_2-O_2 gases under ambient pressure without external humidification. Electrodes contained moderate molecular weight *m*PBI and PVDF. Hot press at 150 ℃ and 1.2 MPa for 10 min. Cell temperature was: (a) 80 ℃; (b) 100 ℃; (c) 120 ℃; (d) 140 ℃; (e) 160 ℃.

2-2-2. SPBI membrane

2-2-2-1. Synthesis of BCPOBDS-Na

As shown in Scheme 2-3, a novel sulfonated dicarboxylic acid monomer, BCPOBDS-Na, was synthesized via three-step reactions. In the first step, 4-fluorobenzonitrile reacted with 1,3-dihydroxybenzene to form the intermediate product *m*BCNPOB at a high yield of 93%. Next, *m*BCNPOB was hydrolyzed under basic condition in glycol to give the dicarboxylic acid product *m*BCPOB at a yield of 83%. Finally, *m*BCPOB was sulfonated to produce the sulfonated dicarboxylic acid monomer, BCPOBDS-Na, using 95% sulfuric acid as the sulfonating reagent. The chemical structures of the synthesized sulfonated dicarboxylic acid monomer as well as the intermediate products were characterized by FT-IR, ^{1}H NMR and ^{13}C NMR spectra.

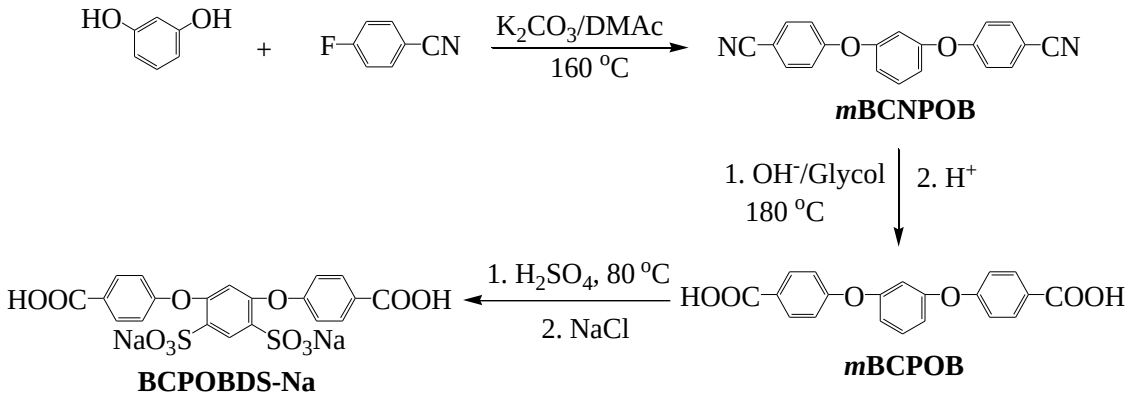

Scheme 2-3. Synthesis of BCPOBDS-Na.

Figure 2-6 shows the FT-IR spectra of *m*BCNPOB, *m*BCPOB and DSBCPOB-Na. In Figure 2-6(a), the absorption band at 2230 cm^{-1} is assigned to -C≡N stretching vibration of *m*BCNPOB. This band completely disappeared in Figure 2-6(b) and a new absorption band at 1694 cm^{-1} which is attributed to the carboxyl carbonyl groups appeared. This indicates that the -C≡N groups have been completely hydrolyzed to carboxyl groups. In Figure 2-6(c), the absorption bands at 1072 and 1034 cm^{-1} are assigned to the symmetric and asymmetric stretching of the sulfonic acid groups indicating that success of the sulfonation reaction. The extremely broad absorption bands in the range 3500-2500 cm^{-1} in Figure 2-6(b) and (c) are the characteristic bands of the hydroxyl groups of carboxyl or sulfonic acid groups and the water absorbed in the samples. The ^{1}H NMR and ^{13}C NMR spectra of DSBCPOB-Na are shown in Figure 2-7 and 2-8, respectively. The peak

assignments are just consistent with the chemical structure indicating that BCPOBDS-Na has been successfully synthesized.

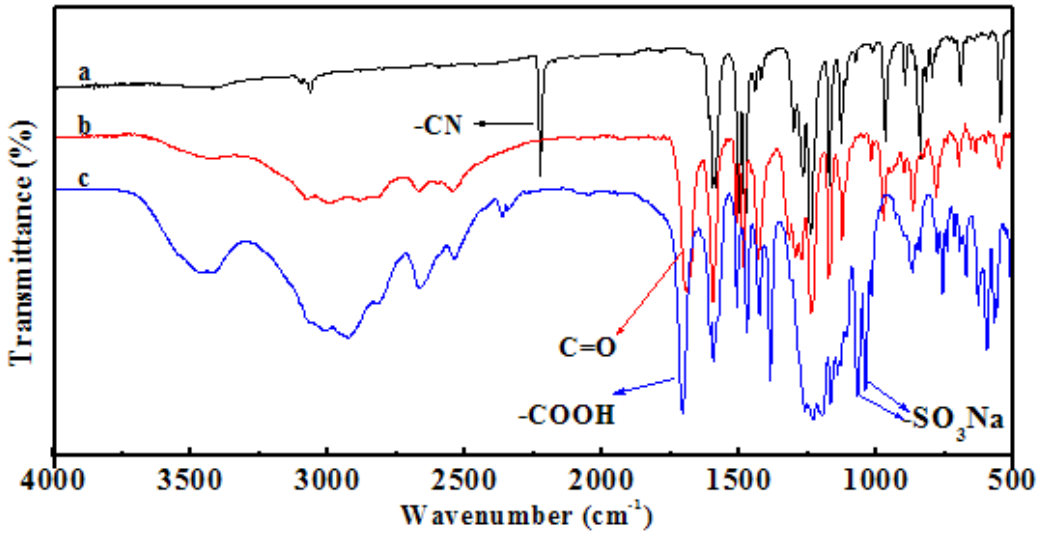

Figure 2-6. FT-IR spectra of (a) *m*BCNPOB, (b) *m*BCPOB and (c) DSBCPOB-Na.

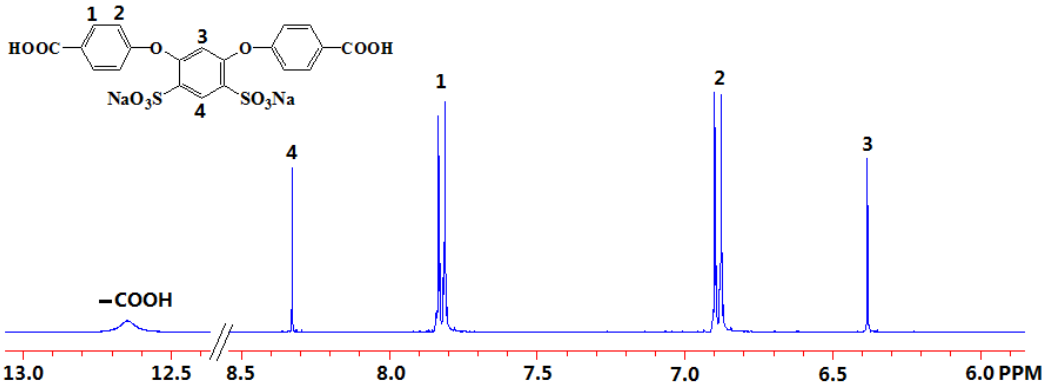

Figure 2-7. ^{1}H NMR spectrum of BCPOBDS-Na.

2-2-2-2. Synthesis, solubility and viscosity of SPBIs

A series of sulfonated copolybenzimidazoles with varied IECs were prepared by random copolymerization of BCPOBDS-Na, DCDPE and DAB in PPMA at 140 ℃ for 45 min (Scheme 2-4). The IECs were controlled by controlling the molar ratio between BCPOBDS-Na and DCDPE. The high molecular weight homopolymer could not be prepared from BCPOBDS-Na and DAB because of its poor solubility in the reaction medium (gel-like product formed during the polymerization process).

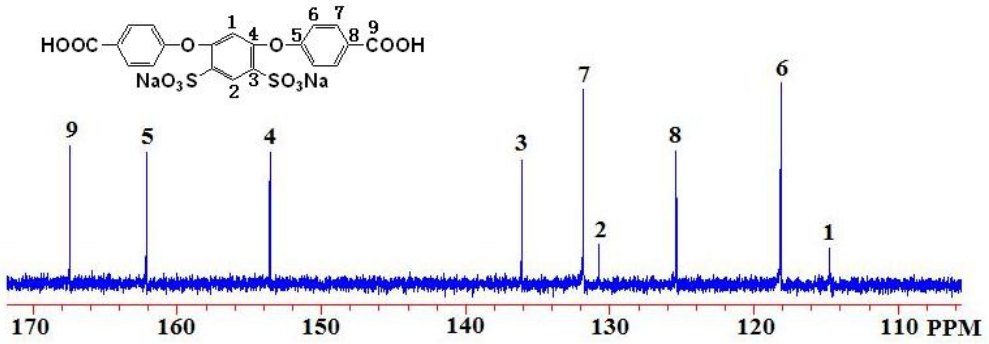

Figure 2-8. ^{13}C NMR spectrum of BCPOBDS-Na.

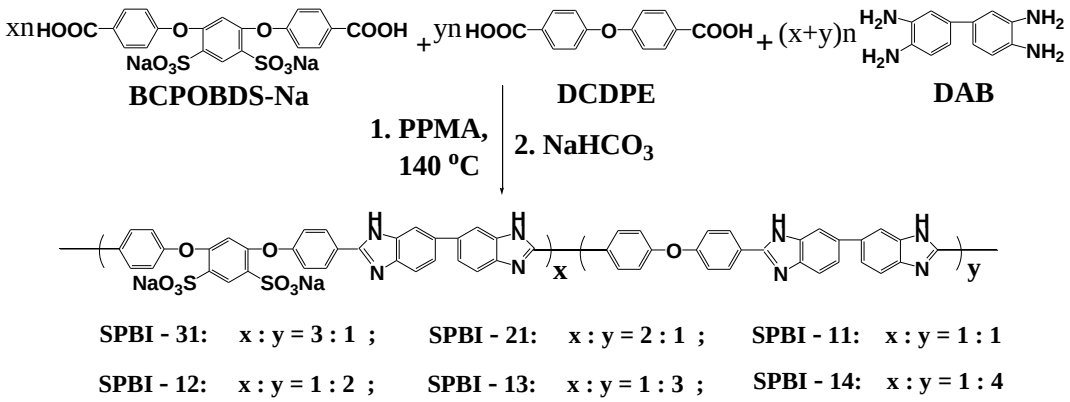

Scheme 2-4. Synthesis of SPBIs.

The FT-IR spectra of the synthesized SPBIs in their sodium salt form are shown in Figure 2-9. The characteristic absorption bands of imidazole rings at 3440 cm^{-1} (stretching of non-hydrogen-bonded N-H), 3220 cm^{-1} (stretching of hydrogen-bonded N-H), 1634 cm^{-1} (C=N stretching) and 1480 cm^{-1} (in-plane deformation of imidazole rings) are clearly observed, while the characteristic absorption band of carboxyl carbonyl groups of the dicarboxylic acid monomers at 1694 cm^{-1} completely disappeared. This indicated the complete formation of imidazole rings.[47] The chemical structure of the synthesized SPBIs was also confirmed by ^{1}H NMR spectra (Figure 2-10). The peak assignments are in good agreement with the proposed chemical structures.

The solubility behaviors and the inherent viscosities of the synthesized SPBIs (in their sodium salt form) were summarized in Table 2-2. It can be seen that the solubility in aprotic organic solvents is dependent on the IECs of the SPBIs, and the higher IEC, the poorer solubility. For example, the SPBI-31 having the highest IEC among the copolymers of this chapter is only partially soluble in aprotic organic solvents (DMSO,

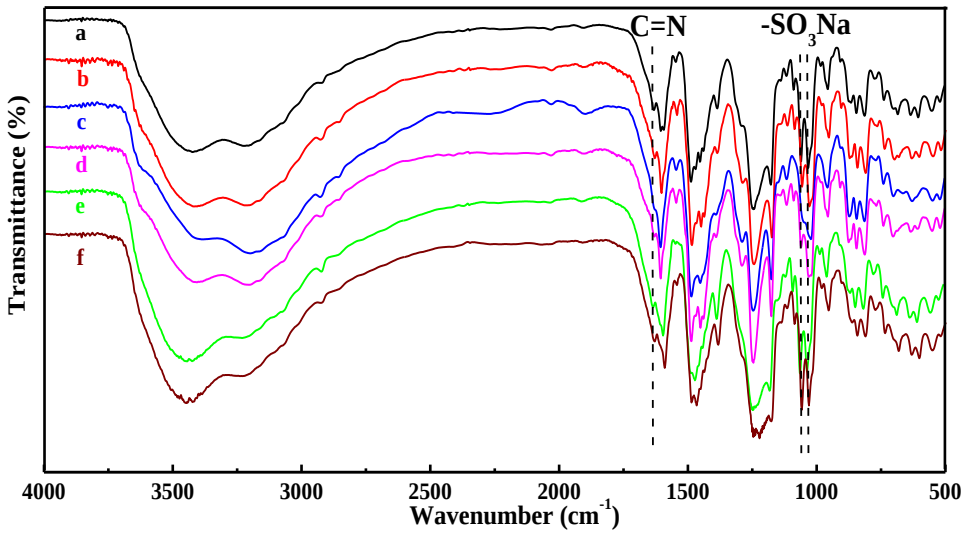

Figure 2-9. FT-IR spectra of the synthesized SPBIs a: SPBI-11; b: SPBI-12; c: SPBI-13; d: SPBI-14; e: SPBI-21; f: SPBI-31).

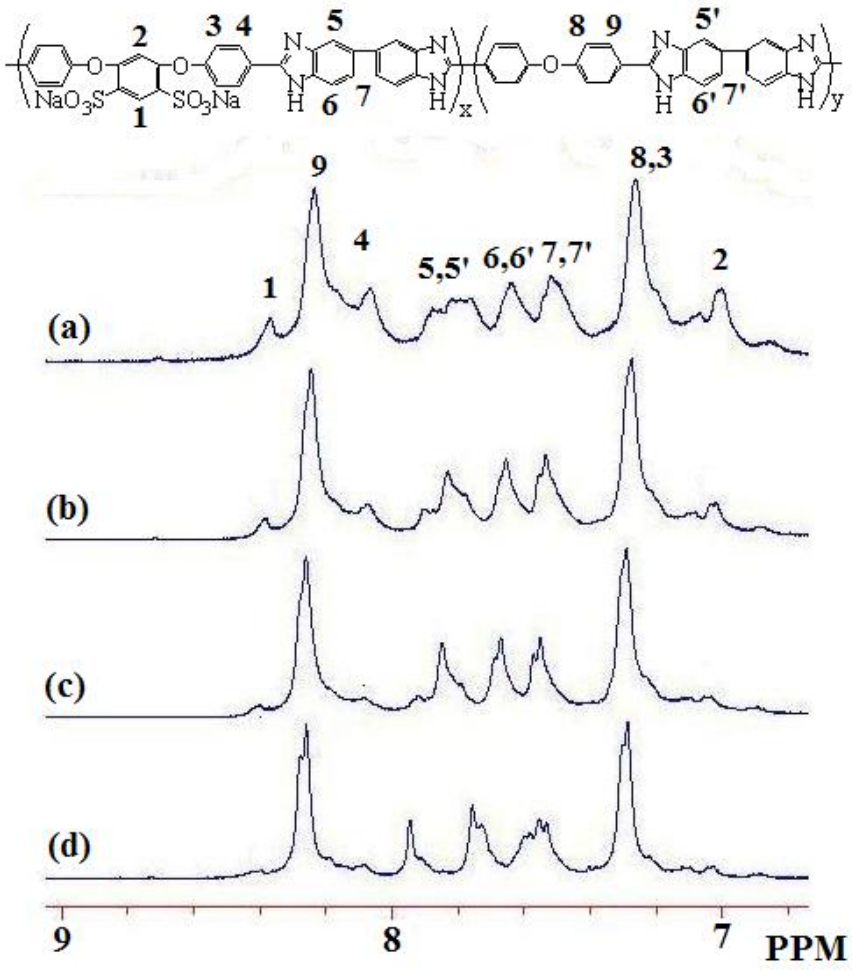

Figure 2-10. ^{1}H NMR spectra of SPBIs (a: SPBI-11; b: SPBI-12; c: SPBI-13; d: SPBI-14).

DMF, DMAc and NMP) and strong acids on heating, whereas the SPBI-14 is soluble in all the aprotic solvents and strong acids at room temperature. In addition, all the SPBIs are completely insoluble in methanol.

The inherent viscosities of the SPBIs except SPBI-31 and SPBI-21 were measured at a concentration of 0.5 g/dL in DMSO at 30 ℃. As shown in Table 2-2, all the SPBIs displayed very high inherent viscosities (> 1.2 dL/g). Moreover, transparent and tough membranes were prepared by solution cast method indicating that high molecular weight copolymers have been successfully synthesized.

Table 2-2. Solubility and inherent viscosities (η_{inh}) of the synthesized SPBIs

Polymer	η_{inh}[a]	Solubility						
	(dL/g)	DMSO	DMF	DMAc	NMP	H_2SO_4	$MeSO_3H$	Methanol
SPBI-31	NM	+-	+-	+-	+-	+-	+-	--
SPBI-21	NM	+-	+-	+-	+-	+-	+-	--
SPBI-11	1.29	+	+-	+	+-	++	++	--
SPBI-12	1.42	++	+	+	+	++	++	--
SPBI-13	1.37	++	++	++	+	++	++	--
SPBI-14	1.26	++	++	++	+	++	++	--

[a]Measured in DMSO at 0.5 g/dL and 30 ℃.

Keys: "++": soluble at room temperature; "+": soluble on heating; "+-": partially soluble on heating; "-": insoluble on heating.

NM: not measured because of poor solubility of the polymers in DMSO.

2-2-2-3. Thermal stability and dynamic mechanical properties

The thermal stability of the SPBIs in their proton form was evaluated by TGA in air. Prior to measurement the samples were preheated at 150 ℃ for 0.5 h to remove the absorbed moisture. As shown in Figure 2-11, all the samples displayed a two-stage weight loss behavior. The first stage weight loss approximately in the range 370-480 ℃ is ascribed to the desulfonation reaction.[35,44] The values of weight loss in this stage are close to the theoretical values of sulfonic acid group contents in the polymers. The SPBI-11, for example, had a first stage weight loss 14.5% which is close to the calculated value (15.3%). The second-stage weight loss starting from ~480 ℃ is attributed to the decomposition of the polymer main chain. The TGA results indicated that the prepared SPBIs have fairly high thermal stability which well meets the

requirement for use in fuel cells.

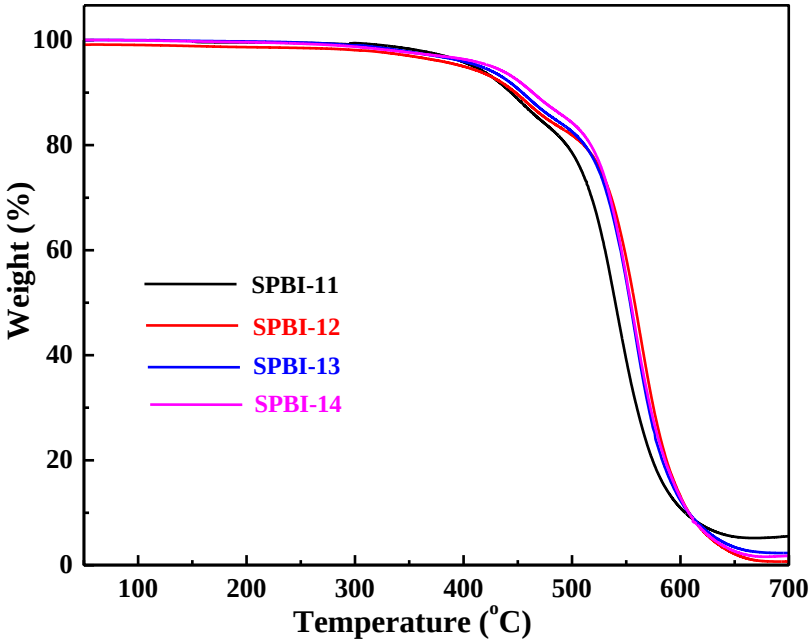

Figure 2-11. TGA curves of the SPBIs (in their proton form) in air.

The dynamic mechanical properties of the SPBIs membranes were investigated by DMA and the curves are shown in Figure 2-12. For all the membranes the storage modulus primarily increased with an increase in temperature up to ~150 ℃ due to the evaporation of the absorbed water which functioned as plasticizer in the membranes. The maximum storage molduli of the SPBI membranes are in the order: SPBI-11 > SPBI-12 > SPBI-13 > SPBI-14, which are just consistent with the order of IEC. The strong acid-base interactions (ionic cross-linking) restricted polymer chain movement. Higher IECs resulted in larger cross-linking densities of the membranes and therefore higher storage moduli were obtained. The glass transition temperature (T_g) was estimated from the peaks of tangent delta and the results are listed in Table 3-2. All the SPBIs displayed very high T_g (299-312 ℃) due to ionic cross-linking as well as the rigid polymer backbones. Moreover, the SPBIs with higher IECs tend to have higher T_g due to the larger cross-linking densities.

The radical oxidative stability of the SPBIs was evaluated by the remaining weight after they were soaked in Fenton's reagent (3% H_2O_2 containing 3 ppm $FeSO_4$) at 80 ℃

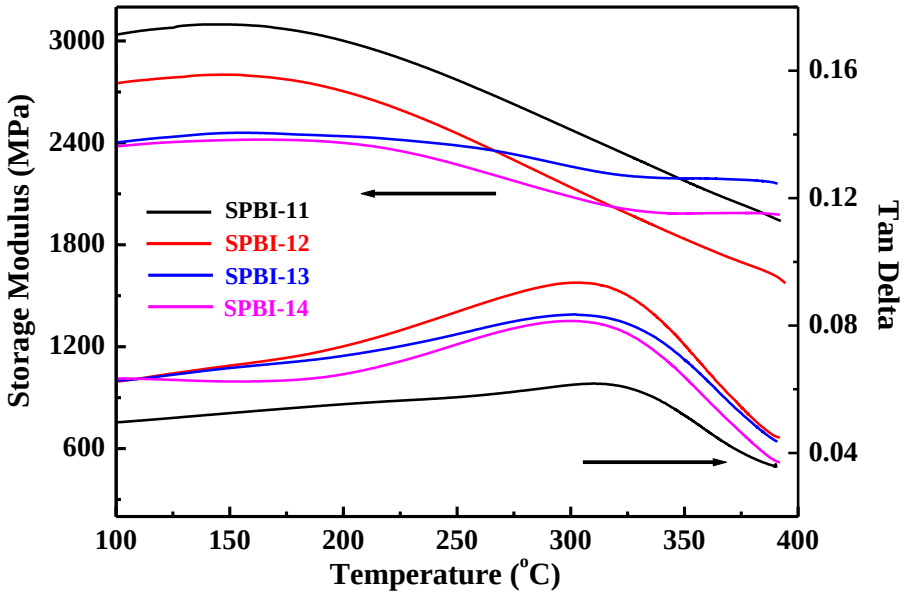

Figure 2-12. DMA curves of the SPBI membranes in nitrogen.

for 12 h and the results are listed in Table 2-3. The SPBI-12, SPBI-13 and SPBI-14 showed more than 80 % remaining weight after the Fenton's test. The SPBI-11 membrane showed significantly lower remaining weight (58 %) than the others but could still keep membrane form. It should be noted that common sulfonated hydrocarbon polymers have been reported to completely dissolve in the Fenton's reagent in a very short period of time (a few hours) at the same temperature.[50-52] The results of the Fenton's test in this chapter indicated that the synthesized SPBIs have excellent radical oxidative stability.

Table 2-3 Ion exchange capacities (IECs), glass transition temperature (T_g), maximum storage moduli (E's) and remaining weight (RW) after Fenton's test of the SPBI membranes

Polymer	IEC (mequiv/g)		T_g (℃)	E' (MPa)	RW[b] (%)
	Theoretical	Measured[a]			
SPBI-11	1.90	1.62	312	3100	58
SPBI-12	1.37	1.07	303	2800	84
SPBI-13	1.08	0.91	301	2500	85
SPBI-14	0.89	0.76	299	2400	86

[a] By titration method; [b] Measured by soaking the membranes in Fenton's reagent (3% H_2O_2 containing 3 ppm $FeSO_4$) at 80 ℃ for 12 h.

2-2-2-4. PA doping, tensile properties and proton conductivity

The PA doping was performed by immersing the SPBI membranes (acid form) in 85% PA solution at 50 ℃ for four days and the PA uptake results are listed in Table 2-3. The SPBI membranes showed PA uptake in the range 180-240 wt% corresponding to the doping levels φ (defined as the number of PA molecules per repeat unit) of 8.1-13. The PA uptake is also related to the IECs and the membranes with higher IECs tend to have higher PA uptake as has been observed with the sulfonated poly(2,5-benzimidazole) (ABPBI).[49]

The tensile properties of the SPBI membranes with and without PA-doping were measured and the results are listed in Table 2-4. It can be seen that after PA-doping the SPBI membranes showed largely decreased stress at break but greatly increased elongation at break due to the plasticization effect of PA. It's well known that the mechanical strength of PA-doped polybenzimidazole membranes is mainly dependent on the PA uptake (doping level) and the higher PA uptake, the lower mechanical strength. Polymer molecular weight is another factor which affects the mechanical strength. At the same doping level, the high molecular weight (105.1 kDa) PBI has been reported to have higher mechanical strength than the lower molecular weight (38.4 kDa) PBI.[48] In this chapter, the undoped SPBI-11, SPBI-12, SPBI-13 and SPBI-14 membranes showed close stress at break (89-96 MPa). Since they are structurally similar to each other, these SPBIs might have similar molecular weights. However, the PA-doped SPBI-11, SPBI-12 and SPBI-13 displayed even higher stress at break than SPBI-14 despite the larger PA uptake values of the former. The SPBI-11 membrane having the highest PA uptake (240 wt%) displayed the largest stress at break (20 MPa). This is likely related to the differences in ionic cross-linking density of the SPBI membranes. Because sulfonic acid is more acidic than phosphoric acid the sulfonic acid groups of the SPBIs should preferentially react with the basic benzimidazole groups to form ionic cross-linking. The SPBI membranes with higher IECs have higher ionic cross-linking densities which may contribute to the improvements in mechanical strength of the PA-doped SPBI membranes. It should be noted that the values of stress at break of the PA-doped SPBI membranes except SPBI-14 were comparable or higher than that of the PA-doped high molecular weight PBI membrane with similar PA uptake.[48] The PA-doped SPBI-11 membrane displayed comparable tensile strength and significantly larger elongation at break than the cross-linked commercial PBI membrane[27] despite the higher PA doping level.

Table 2-4. Phosphoric acid (PA) uptake, maximum stress (MS), elongation at break (EB) and proton conductivity (σ) of PA-doped membrane at 170 ℃ at 0% relative humidity

Membrane	PA Uptake (wt%)	φ	MS[a] (MPa)	EB[a] (%)	σ (mS/cm)	Ref.
SPBI-11	240	13	96(20)	17(92)	37.3	This chapter
SPBI-12	220	11	96(15)	12(144)	18.8	This chapter
SPBI-13	190	9.1	93(17)	22(129)	10.7	This chapter
SPBI-14	180	8.1	89(13)	29(90)	3.63	This chapter
PBI	190-210	6.0-6.6	(13-14)	(-)	18-22	48
CrL-PBI	-	8.5	(21-23)	(20-28)	-	27

[a] Measured at room temperature and 40% relative humidity. The data in parentheses refer to the phosphoric acid-doped membranes; -: Not available from the literature.

The proton conductivities of the PA-doped SPBI membranes were measured at 0% RH and different temperatures (90-170 ℃) and the results are shown in Figure 2-13. It can be seen that for all the SPBI membranes the proton conductivity increased with increasing temperature. Moreover, the membranes with higher PA-doping levels tend to have higher proton conductivities in the whole temperature range. The SPBI-11 membrane showed the highest proton conductivity (37.3 mS/cm at 170 ℃) due to the highest doping level.

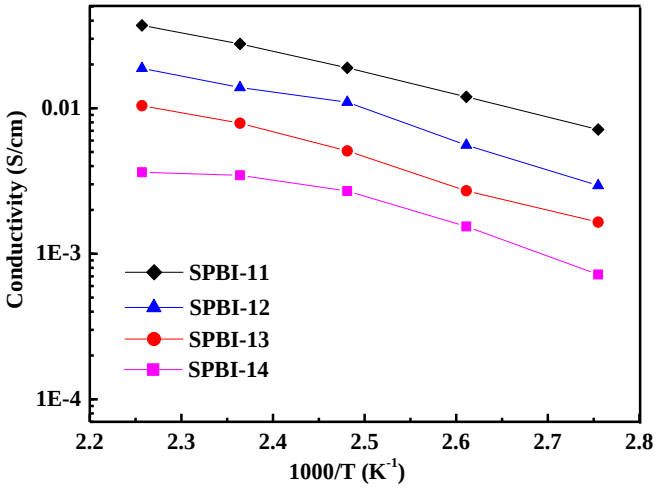

Figure 2-13. Variation of proton conductivity of the SPBI membranes as a function of temperature at 0% relative humidity in cooling run.

2-2-2-5. Single-cell fuel cell performance

The PA-doped SPBI-11 membrane with the PA uptake of 240 wt% and membrane thickness of 50 μm was used as the proton exchange membrane. 40% Pt/C and *m*PBI were used as the catalyst and binder, respectively. The Pt loading in both the anode and the cathode was 0.5 mg/cm^2. Preliminary fuel cell performance was evaluated with hydrogen-oxygen gases under ambient pressure without external humidification. Figure 2-14 showed the variation of fuel cell performance as a function of temperature. It can be seen that with an increase in temperature the maximum output power density of the fuel cell increased. This is consistent with the temperature dependence of proton conductivity as shown in Figure 2-13. The fast electrochemical reaction kinetics is another factor responsible for the improved fuel cell performance at elevated temperatures. The highest output power density of 580 mW/cm^2 was obtained at the current density of 1.68 A/cm^2 at 170 ℃ with hydrogen-oxygen gases indicating good performance of the fuel cell. It should be noted that the fuel cell performance in this chapter is comparable or significantly higher than those using other PA-doped PBI membranes as the proton exchange membranes at similar Pt-loading level as reported in the literature (maximum output power densities: 600 mW/cm^2 at 180 ℃ with 1.0 mg/cm^2 Pt loading,[26] 280 mW/cm^2 at 160 ℃ with 0.5 mg/cm^2 Pt loading,[54] 600 mW/cm^2 at 160 ℃ with 1.0 mg/cm^2 Pt loading,[28] 320 mW/cm^2 at 125 ℃ with 0.5 mg/cm^2 Pt loading[48]).

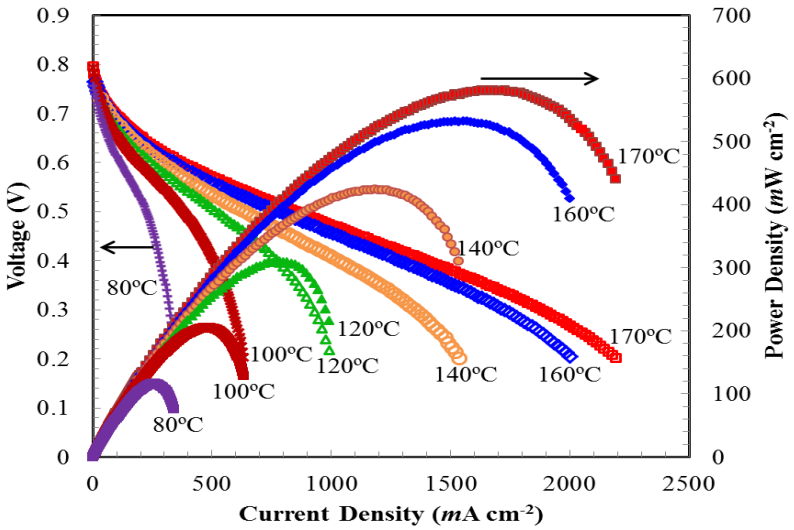

Figure 2-14. Performance of the fuel cell fabricated with the PA-doped SPBI-11 membrane (PA uptake = 240 wt%) at varied temperatures with hydrogen-oxygen gases under ambient pressure without external humidification.

2-3. Conclusions

In the first section of this chapter, the ether containing PBI (OPBI) was synthesized to increase the solubility of PBI. PA-doped OPBI membrane was prepared as PEM and the moderate molecular weight *m*PBI binders was synthesized used as a catalyst binder in the catalyst layers. The optimized MEAs exhibited desirable performances in the electrochemical tests up to 160 ℃, which the output power density was 366 mW/cm^2. This investigation opened up a new way to develop the practical proton-conducting fuel cell systems working at elevated temperatures.

In the second section of this chapter, a new sulfonated dicarboxylic acid monomer DSBCOP-Na has been successfully synthesized via three-step reactions and a series of high molecular weight SPBIs with varied IECs have been prepared by random copolymerization of DSBCOP-Na, DCDPE and DAB in PPMA at 140 ℃.

1) The prepared SPBIs except the SPBI-31 and SPBI-21 showed good solubility in aprotic solvents such as DMSO and DMAc.
2) The SPBI membranes showed moderate PA uptake (180-240 wt%) corresponding to the doping levels (defined as the number of PA molecules per repeat SPBI unit) of 8.1-13 in 85 wt% PA solution at 50 ℃ and the membranes with higher IECs tended to have larger PA uptake.
3) Ionic cross-linking is favorable for improving the mechanical strength of the PA-doped SPBI membranes. The PA-doped SPBI-11 membrane displayed the highest mechanical strength despite its highest PA uptake.
4) High proton conductivity up to 37.3 mS/cm was achieved with the PA-doped SPBI-11 membrane at 170 ℃ at 0% relative humidity.
5) The fuel cell fabricated with the PA-doped SPBI-11 membrane displayed good performance at high temperatures with hydrogen-oxygen gases under ambient pressure without external humidification, and the highest output power density of 580 mW/cm^2 was obtained at 170 ℃.

2-4. Experimental

Materials

3,3'-Diaminobenzidine (DAB), 4-fluorobenzonitrile, 1,3-dihydroxybenzene and 4,4'-dicarboxydiphenyl ether (DCDPE) was purchased from Acros Organics. Polyvinylidene difluoride (PVDF) was purchased from 3M. Methanesulfonic acid (MSA), phosphorus pentoxide (P_2O_5), isophthalic acid (IPA), polyphosphoric acid (PPA), phosphoric acid (PA), dimethyl sulfoxide (DMSO), 1-methyl-2-pyrrolidone (NMP), *N*,*N*-dimethylacetamide (DMAc), sodium bicarbonate ($NaHCO_3$), ammonia solution and ethanol were purchased from Sinopharm Chemical Reagent Co. Ltd. (SCRC). DMSO was distilled under reduced pressure and dried by 4A molecular sieves before use. DAB, MSA, P_2O_5, IPA, PPA, PA, NMP, DMAc, $NaHCO_3$, ammonia solution, ethanol, and PVDF were used as received.

Polymerization

OPBI was synthesized by condensation polymerization of DAB and DCDPE in the PPMA solution (P_2O_5/MSA in a weight ratio of 1:10) at 140 ℃ with around 10 wt% total monomer concentration.[32] 2.0 g P_2O_5 and 20.0 g MSA were added into a 100 ml dry three-neck flask under N_2 atmosphere. The reaction mixture was magnetically stirred and heated at 100 ℃ under N_2 atmosphere until a homogeneous solution was formed. After cooling to room temperature, DCDPE (1.2912 g, 5.0 mmol) and DAB (1.0714 g, 5.0 mmol) were added into the solution, and the reaction mixture was stirred and heated at 140 ℃ for 160 min. Then the mixture was slowly transferred into ice water with stirring. The brown solid product was filtered and soaked in 5 wt% $NaHCO_3$ solution under 60 ℃ for 36 h, then filtered and thoroughly washed with the deionized water, and finally dried in a vacuum oven at 120 ℃ for 10 h. At room temperature, OPBI was easily dissolved in DMAc under sonication for 15 min to obtain a transparent solution up to 10 wt%, and the stabilizer is not needed for the long time storage. The moderate molecular weight *m*PBI was synthesized as follows: 8.4 g P_2O_5 and 41.9 g PPA were added into a 100 mL dry three-neck flask under N_2 atmosphere. The reaction mixture was mechanically stirred and heated at 100 ℃ under N_2 atmosphere until a homogeneous solution was formed. After cooling to room temperature, IPA (2.4916 g, 15.0 mmol) and DAB (3.1030g, 14.5 mmol) were added into the solution and the reaction mixture was stirred and heated at 150 ℃ for 2 h and subsequently at 190 ℃ for 10 h. Then the mixture was slowly transferred into ice water with stirring. The yellow solid product was filtered and soaked in diluted ammonia solution (1:1 v/v ammonia

solution and deionized water) under N_2 atmosphere at 40 ℃ for 48 h, then filtered and thoroughly washed with deionized water, and finally dried in a vacuum oven at 120 ℃ for 24 h.

Synthesis of 1,3-bis(4-cyanophenoxy)benzene (mBCNPOB)

To a 150 mL dry three-necked flask equipped with a nitrogen inlet and an outlet, a dropping funnel, a Dean-Stark trap and a condenser were added 5.51 g (50 mmol) of 1,3-dihydroxybenzene, 13.81 g (100 mmol) of K_2CO_3 and 60 mL DMAc. The reaction mixture was magnetically stirred at room temperature for 2 h and then heated at 140 ℃ for 5 h. 20 mL toluene in the dropping funnel was added to remove any water by forming toluene-water azeotrope which was collected in the Dean-Stark trap. The reaction mixture was allowed to cool to room temperature and then 12.11 g (100 mmol) of 4-fluorobenzonitrile was introduced, and the mixture was further heated at 160 ℃ for 24 h. After cooling to room temperature, the reaction mixture was poured into deionized water with stirring. The resulting brown precipitate was filtered off, washed with deionized water and dried at 70 ℃ for 20 h in vacuum. 14.51 g (yield: 93%) of brownish product was obtained, mp (by differential scanning calorimetry (DSC)): 122 ℃. ^{1}H NMR (DMSO-d6, ppm): 6.79 (s, 1H), 6.92 (d, 2H), 7.05 (d, 4H), 7.42 (t, 1H), 7.64 (d, 4H). ^{13}C NMR (DMSO-d6, ppm): 106.24, 112.81, 117.18, 119.12, 119.31, 132.56, 135.38, 156.69 and 161.20.

Synthesis of 1,3-bis(4-carboxyphenoxy)benzene (mBCPOB)

To a 500 mL dry three-neck flask equipped with a nitrogen inlet and an outlet and a condenser were added 8.11 g (26 mmol) of *m*BCNPOB, 7.28 g (130 mmol) of KOH and 195 mL glycol. The reaction mixture was magnetically stirred and heated at 180 ℃ for 24 h followed by vacuum distillation to remove the solvent glycol. The solid product was dissolved in deionized water and then acidified with concentrated hydrochloric acid till the pH = 1. The white precipitate was collected by filtration, thoroughly washed with deionized water and dried in vacuum at 120 ℃ for 20 h. 7.55 g (yield : 83%) of white product was obtained, mp (by DSC): 300 ℃. ^{1}H NMR (DMSO-d6, ppm): 6.85 (s, 1H), 6.94 (d, 2H), 7.08 (d, 4H), 7.48 (t, 1H), 7.94 (d, 4H), 12.80 (s, 1H). ^{13}C NMR (DMSO-d6, ppm): 112.01, 116.24, 118.32, 126.38, 132.29, 132.27, 157.34, 161.01 and 167.35.

Synthesis of disodium 4,6-bis(4-carboxyphenoxy)benzene-1,3-disulfonate (BCPOBDS-Na)

To a 150 mL dry flask were added 7.00 g (20 mmol) *m*BCPOB and 80 mL concentrated sulfuric acid. The reaction mixture was magnetically stirred and heated at 80 ℃ for 24 h. After cooling to room temperature, the mixture was carefully poured into 300 g crushed ice, and then 62 g of sodium chloride was added to salt out the product. The resulting precipitate was filtered off, washed with saturated sodium chloride solution and dried at 100 ^{o}C for 20 h in vacuum. The crude product was added to 200 mL DMSO and the mixture was magnetically stirred at room temperature for 2 h. The insoluble part was filtered off and the filtrate was distilled under reduced pressure. The solid product was thoroughly washed with acetone and then dried at 120 ℃ for 20 h in vacuum. 7.09 g (yield: 64%) white product was obtained. MS: m/z = 553.0 (M - H^+), 531.0 (M - Na^+), 418.9 (M -2Na^+ -2COO ·).

Preparation of sulfonated copolybenzimidazoles (SPBI-xy, x and y refer to the molar ratio of BCPOBDS-Na to DCDPE)

A typical procedure is described as follows using the copolymer SPBI-11 as an example.

To a 150 mL dry three-neck flask were added 0.8561 g (4 mmol) DAB, 0.5162 g (2 mmol) DCDPE, 1.1088 g (2 mmol) *BCPOBDS-Na* and 20 mL PPMA under nitrogen flow. The reaction mixture was magnetically stirred and heated at 80 ℃ for 2 h and 140 ℃ for 45 min. After cooling to ~80 ℃, the highly viscous solution mixture was poured into ice water with stirring. The resulting yellowish fiber-like polymer was filtered off and soaked in 5 wt% $NaHCO_3$ solution at room temperature for 48 h. The solid polymer was collected by filtration, thoroughly washed with deionized water and dried at 120 ℃ for 24 h under vacuum.

Membranes formation, proton exchange and PA-doping

The prepared OPBI and SPBIs in their sodium salt form were dissolved in DMSO. The solutions were cast onto glass plates and dried at 80 ℃ for 20 h in an air oven. The as-cast membranes were peeled off and subsequently immersed into hot methanol for 5 h to remove any residual solvent.

Proton exchange treatment was performed by immersing the SPBI membranes in 1 M sulfuric acid solution at 60 ℃ for two days. The membranes were take out, thoroughly rinsed with deionized water till the rinsed water became neutral, and dried in a vacuum

oven at 120 ℃ for 20 h.

The PA-doped OPBI and SPBI membranes were prepared by immersing the films in 85 wt% PA for 4 days at room temperature and 50 ℃, respectively.

Preparation of MEAs.

MEAs were prepared with moderate molecular weight *m*PBI in the catalyst layer by the typical optimized procedures.[55] The Pt/C catalyst and the binder solution (4 wt% in DMAc) were added into DMAc. The weight ratio of catalyst/binder (dry weight)/DMAc was 78/22/7800 for the 20 wt% Pt/C catalyst (BASF fuel cell, Inc.) and 95/5/9500 for the 40 wt% Pt/C catalyst (Johnson Matthey, Inc.). The mixture was stirred for 24 h, and was treated in an ultrasonic bath for 5 min. And then the homogeneous slurry was sprayed (using airbrush) onto 2.5 cm × 2.5 cm carbon cloth-based gas diffusion layers (LT 1200-W, 370 μm thickness, 27 wt% polytetrafluoroethylene, BASF fuel cell, Inc.) to obtain gas diffusion electrodes. Both gas diffusion electrodes with 0.5 mg/cm^2. Pt loading was dried at 190 ℃ in a vacuum oven for 3 h to remove the remaining DMAc. Afterwards they were soaked with a 15 wt% PA/ethanol solution for 10 min at room temperature in order to soften the ionic contact between the membrane and the electrodes, and then dried at 60 ℃ for 1 h. The PA-doped OPBI and SPBI-11 membrane was wiped off with filter papers to remove the bled acid, and were sandwiched between two pieces of dry gas diffusion electrodes. The electrodes and the membrane were hot-pressed under a pressure of 1.2 MPa at 150 ℃ for 10 min.

Measurements

FT-IR spectra were recorded on a Perkin-Elmer Paragon 1000PC spectrometer. ^{1}H NMR and ^{13}C NMR spectra were recorded on a Varian Mercury Plus 400 MHz instrument. Mass spectrum (MS) were recorded with an Agilent 1100 LC/MSD instrument. Reduced viscosity (η) was measured in DMSO at a polymer concentration of 0.5 g/dL with an Ubbelohde viscometer at 30 ℃. Differential scanning calorimetry (DSC) was measured in N_2 on a DSC 6200 instrument at a heating rate of 10 ℃/min from room temperature to 400 ℃. Thermogravimetric analysis (TGA) was performed in air with a TGA2050 instrument. Prior to measurement, all the samples were preheated at 150 ℃ for half an hour to remove the absorbed moisture. Subsequently the samples were cooled to 50 ℃ and then reheated to 800 ℃ at a heating rate of 10 ℃/min. Tensile measurements were carried out with an Instron 4456 instrument at room temperature and 25% relative humidity at a crosshead speed of 5 mm/min. For each kind of

membrane, three samples were used for the measurements and the tensile stress and the elongation at break was estimated by the averaged values of the three samples. Dynamic mechanical analysis (DMA) was measured on a Q800 DMA apparatus (TA instruments, USA) in tension mode under nitrogen atmosphere at a frequency of 1.0 HZ in temperature range 50-400 ℃ at a heating rate of 10 ℃/min. The samples were 30 mm long, 8 mm wide and 30-40 μm thick.

Ion exchange capacity (IEC) was measured by titration method. The samples were immersed in 1.0 M NaCl solution at 40 ℃ for 3 days. After that, the samples were not taken out and the NaCl solution was directly titrated with 0.01 M NaOH using phenolphthalein as pH indicator.

The radical oxidation stability of the membranes was determined by Fenton's test. The completely dried samples were soaked in the Fenton's reagent (3% H_2O_2 containing 3 ppm $FeSO_4$) at 80 ℃ for 12 h. The remaining weight (RW) of the samples after Fenton's test was used to evaluate the radical oxidation stability of the membranes.

Phosphoric acid uptake (S_{PA}) of the SPBI membranes was measured by immersing the dry membranes in 85% phosphoric acid solution at 50 ℃ for four days. Then the membranes were taken out, wiped with tissue paper, and dried at 110 ℃ for 24 h in vacuum. S_{PA} was calculated according to the following equation:

$$S_{PA} = \frac{W_1 - W_0}{W_0} \times 100 \qquad (1)$$

where W_0 and W_1 refer to the weight of the dry undoped membrane and the dry doped membrane, respectively.

Proton conductivity was measured using a two-probe electrochemical impedance spectroscopy technique over the frequency range from 100 to 100 kHz. A sheet of PA-doped membrane and a pair of platinum electrode was set in a Teflon cell. The cell was placed in a thermo-controlled chamber, which had an inlet and an outlet for continuous nitrogen flow. Before starting the conductivity measurement, the chamber was heated at 150 ℃ for one day to remove any water vapor so that the relative humidity could reach 0%. After that, the temperatures of chamber was set at desired values and kept constant for 1 h at each point. The resistance value was determined from high-frequency intercept of the impedance with the real axis. Proton conductivity was calculated from the following equation:

$$\sigma = d \big/ (twR) \qquad (2)$$

where d is the distance between the two electrodes, t and w are the thickness and width

of the membrane, and *R* is the resistance measured.

Single cell test and electrochemical characterization

The MEAs were installed in the standard testing fixture (FC05-MP, the active geometrical area of 5 cm^2, ElectroChem, Inc.). The assembly torque was 5N·m. The performances of single cells were tested at different temperatures using a homemade fuel cell test system. Gases without humidification were fed to the single cell at the flow rates of 100, 150 and 750 mL/min for H_2, O_2 and air, respectively for PA-doped OPBI membrane, and 100 mL/min for H_2, 300 mL/min for O_2 for PA-doped SPBI-11 membrane, (the oxygen stoichometry was 8 at a current density of 1 A/cm^2). The working pressure of the single cell was atmospheric pressure. Current-voltage curves were measured using a DC electronic load (IT8514F) and recorded by the constant current mode at a scan rate of 400 mA/min. Electrochemical impedance measurements were performed at the open circuit. The frequency ranged from 100 KHz to 100 MHz, with a potential amplitude of 10 mV. Datas were collected using a computer controlled CHI 604B electrochemical analyzer (Chenhua, Shanghai).

2-5. References

(1) Savadogo, J. *New Mater. Electrochem. Syst.* **1998,** *1,* 47-66.

(2) Rikukawa, M.; Sanui, K. *Prog. Polym. Sci.* **2000,** *25,* 1463-1502.

(3) Costamagna, P.; Srinivasan, S. *J. Power Sources* **2001,** *102,* 242-252.

(4) Steele, B. C. H.; Heinzel, A. *Nature* **2001,** *414,* 345-352.

(5) Rikukawa, M.; Sanui, K. *Prog. Polym. Sci.***2000,** *25,* 1463-1502.

(6) Roziè re, J.; Jones, D. J.; *Ann. Rev. Mater. Res.* **2003,** *33,* 503-555.

(7) Li, Q.; He, R.; Jensen, J. O.; Bjerrum, N. J. *Fuel Cells* **2004,** *4,* 147-159.

(8) Li, Q. F.; Jensen, J. O.; Savinell, R. F.; Bjerrum, N. J. *Prog. Polym. Sci.* **2009,** *34,* 449-477.

(9) Asensio, J. A.; Sánchez, E. M.; Gómez-Romero, P. *Chem. Soc. Rev.* **2010,** *39,* 3210-3239.

(10) Liu, G.; Zhang, H. M.; Hu, J. W.; Zhai, Y. F.; Xu, D. Y.; Shao, Z. G. *J. Power Sources* **2006,** *162,* 547-552.

(11) Zhai, Y. F.; Zhang, H. M.; Liu, G.; Hu, J. W.; Yi, B. L. *J. Electrochem. Soc.* **2007,** *154,* B72-B76.

(12) Kwon, K.; Kim, T. Y.; Yoo, D. Y.; Hong, S. G.; Park, J. O. *J. Power Sources* **2009,** *188,* 463-467.

(13) Li, Q. F.; He, R. H.; Gao, J. A.; Jensen, J. O.; Bjerrum, N. J. *J. Electrochem. Soc.* **2003,** *150,* A1599-A1605.

(14) Pan, C.; He, R. H.; Li, Q. F.; Jensen, J. O.; Bjerrum, N. J.; Hjulmand, H. A.; Jensen, A. B. *J. Power Sources* **2005,** *145,* 392-398.

(15) Lobato, J.; Cañizares, P.; Rodrigo, M. A. Linares, J. J. *Electrochim. Acta,* **2007,** *52,* 3910-3920.

(16) Jensen, J. O.; Li, Q.; He, R.; Pan, C.; Bjerrum, N. J. *J. Alloy. Compd.* **2005,** *404,* 653-656.

(17) Jensen, J. O.; Li, Q. F.; Pan, C.; Vestbø, A. P.; Mortensen, K.; Petersen, H. N.; Sørensen, C. L.; Clausen, T. N.; Schramm, J.; Bjerrum, N. J. *Int. J. Hydrog. Energy* **2007,** *32,* 1567-1571.

(18) Neuse, E. W. *Adv. Polym. Sci.* **1982,** *47,* 1-42.

(19) Chung, T. S. *Polym. Rev.* **1997,** *37,* 277-301.

(20) Li, Q. F.; Hjuler, H. A.; Bjerrum, N. J. *Electrochim. Acta* **2000,** *45,* 4219-4226.

(21) Cheng, C. K.; Luo, J. L.; Chuang, K. T.; Sanger, A. R. *J. Phys. Chem. B* **2005,** *109,* 13036-13042.

(22) Lobato, J.; Cañizares, P.; Rodrigo, M. A.; Linares, J. J.; Manja-vacas, G. *J. Membr.*

Sci. **2006,** *280,* 351-362.

(23) Li, Q. F.; Hjuler, H. A.; Bjerrum, N. J. *J. Appl. Electrochem.* **2001,** *31,* 773-779.

(24) Wang, J. T.; Savinell, R. F.; Wainright, J.; Litt, M.; Yu, H. *Electrochim. Acta* **1996,** *41,* 193-197.

(25) Pan, C.; Li, Q. F.; Jensen, J. O.; He, R. H.; Cleemann, L. N.; Nilsson, M. S.; Bjerrum, N. J.; Zeng, Q. X. *J. Power Sources* **2007,** *172,* 278-286.

(26) Mader, J. A.; Benicewicz, B. C. *Macromolecules* **2010,** *43,* 6706-6715.

(27) Li, Q.; Pan, C.; Jensen, J. O.; Noye, P.; Bjerrum, N. J. *Chem. Mater.* **2007,** *19,* 350-352.

(28) Xiao, L.; Zhang, H.; Jana, T.; Scanlon, E.; Chen, R.; Choe, E.-W.; Ramanathan, L. S.; Yu, S.; Benicewicz, B. C. *Fuel Cells* **2005,** *5,* 287-295.

(29) Qian, G. Q.; Smith, D. W.; Benicewicz, B. C. *Polymer* **2009,** *50,* 3911-3916.

(30) Qian, G. Q.; Benicewicz, B. C. *J. Polym. Sci. Pol. Chem.* **2009,** *47,* 4064-4073.

(31) Foster, R. T.; Marvel, C. S. *J. Polym. Sci.* **1965,** *3,* A417-A421.

(32) Ueda, M.; Sato, M.; Mochizuki, A. *Macromolecules* **1985,** *18,* 2723-2726.

(33) Özaytekin, İ.; Karataş, İ. *J. Appl. Polym. Sci.* **2008,** *109,* 1861-1870.

(34) Sannigrahi, A.; Ghosh, S.; Lalnuntluanga, J.; Jana, T. *J. Appl. Polym. Sci.* **2009,** *111,* 2194-2203.

(35) Xu, H. J.; Chen, K. C.; Guo, X. X.; Fang, J. H.; Yin, J. *Polymer* **2007,** *48,* 5556-5564.

(36) Kim, T. H.; Kim, S. K.; Lim, T. W.; Lee, J. C. *J. Membr. Sci.* **2008,** *323,* 362-370.

(37) Wrasidlo, W.; Empey, R. *J. Polym. Sci. Pol. Chem.* **1967,** *5,* 1513-1526.

(38) Dai, H.; Zhang, H.; Zhong, H.; Jin, H.; Li, X.; Xiao, S.; Mai, Z. *Fuel Cells* **2010,** *10,* 754-761.

(39) Leykin, A. Y.; Askadskii, A. A.; Vasilev, V. G.; Rusanov, A. L. *J. Membr. Sci.* **2010,** *347,* 69-74.

(40) Modestov, A. D.; Tarasevich, M. R.; Filimonov, V. Y.; Leykin, A. Y. *J. Electrochem. Soc.* **2009,** *156,* B650-B656.

(41) Wainright, J. S.; Litt, M. H.; Savinell, R. F. in "Handbook of Fuel Cells - Fundamentals, Technology and Applications", Ed., Vielstich, W.; Gasteiger, H. A.; Lamm, A. *John Wiley & Sons Ltd.* **2003,** p436.

(42) Kim, H. J.; An, S. J.; Kim, J. Y.; Moon, J. K.; Cho, S. Y.; Eun, Y. C.; Yoon, H. K.; Park, Y.; Kweon, H. J.; Shin, E. M. *Macromol. Rapid Commun.* **2004,** *25,* 1410-1413.

(43) Asensio, J. A.; Borros, S.; Gomez-Romero, P. *J. Polym. Sci., Part A: Polym. Chem.*

2002, *40,* 3703-3710.

(44) Jouanneau, J.; Mercier, R.; Gonon, L.; Gebel, G. *Macromolecules* **2007,** *40,* 983-990.

(45) Lobato, J.; Cañizares, P.; Rodrigo, M. A.; Linares, J. J.; Aguilar, J. A. *J. Membr. Sci.* **2007,** *306,* 47-55.

(46) Seel, D. C.; Benicewicz, B. C.; Xiao, L.; Schmidt, T. J. in "Handbook of Fuel Cells - Fundamentals, Technology and Applications", Ed., Vielstich, W.; Yokokawa, H.; Gasteiger, H. A. *John Wiley & Sons Ltd.* **2009,** p300.

(47) Bouchet, R.; Siebert, E. *Solid State Ionics* **1999,** *118,* 287-299.

(48) Lobato, J.; Canizares, P.; Rodrigo, M. A.; Linares, J. J.; Aguilar, J. A. *J. Membr. Sci.* **2007,** *306,* 47–55.

(49) Asensio, J. A.; Gomez-Romero, P. *Fuel cells* **2005,** *5,* 336-343.

(50) Nakabayashi, K.; Higashihara, T.; Ueda, M. *Macromolecules* **2010,** *43,* 5756-5761.

(51) Xing, P.; Robertson, G. P.; Guiver, M. D.; Mikhailenko, S.; Kaliaguine, S. *Macromolecules* **2004,** *37,* 7960-7967.

(52) Saito, J.; Miyatake, K.; Watanabe, M. *Macromolecules* **2008,** *41,* 2415-2420.

(53) Li, M. Q.; Shao, Z. G.; Scott, K. *J. Power Sources* **2008,** *183,* 69-75.

(54) Lin, H. L.; Hsieh, Y. S.; Chiu. C. W.; Yu, T. L.; Chen, L. C. *J. Power Sources* **2009,** *193,* 170-174.

(55) Fang, L.; Fang, J. H.; Ma, Z. F.; Guo, X. X. CN. 201010181022.4

Chapter 3

Polystyrenes with Phosphonic Acid via Long Alkyl Side Chains for Polymer Electrolyte Membranes

ABSTRACT: A series of polystyrenes with phosphonic acid (**5**) via long alkyl side chains (4, 6, and 8 methylene units) were prepared by the radical polymerization of the corresponding diethyl ω-(4-vinylphenoxy)alkylphosphonates, followed by the hydrolysis with trimethylsilyl bromide. The resulting phosphonated polystyrene membranes had a high oxidative stability against Fenton's reagent at room temperature. The membranes prepared from **5** exhibited a very low water uptake, similar to that of Nafion 117 over the wide range of 30-80% relative humidity (RH). The proton conductivities of these membranes are lower than that of Nafion 117 in the range of 30-90% RH, but comparable or higher than those of the reported phosphonated polymers with higher IEC values, such as the phosphonated poly(*N*-phenylacrylamide) (PDPAA, IEC: 6.72 mequiv/g) and fluorinated polymers with pendant phosphonic acids (M47, IEC: 8.5 mequiv/g), at low RH conditions despite the much lower IEC values (3.0-3.8 mequiv/g) of these membranes. These results suggest that the flexible pendant side chains of **5** would contribute to the formation of hydrogen-bonding networks by considering the very low water uptake of these polymers.

3-1. Introduction

Proton exchange membrane fuel cells (PEMFCs) are considered one of the most promising power sources for both mobile and stationary applications due to their high energy conversion efficiency and low pollution.[1-3] The proton exchange membrane (PEM) is an indispensable component of a PEMFC to transport protons from the anode to the cathode. Currently, the state-of-the-art PEMs are sulfonated perfluoropolymers (*e.g.*, Nafion® and Flemion®) , which show high proton conductivities over a wide range of relative humidities at a moderate operating temperature due to the well-defined phase separation between the hydrophobic main chains and the hydrophilic side chains. However, several drawbacks, such as high cost, high methanol permeability and limited operating temperature (< 100 ^{o}C), restrict their practical use in PEMFCs. Thus, the development of well-balanced alternatives, which should meet several requirements (*e.g.*, high proton conductivity, high membrane stability, low fabrication cost, etc.), is essential today for the realization of PEMFCs. In recent years, the hydrocarbon-based polymer exchange membranes have been proposed for PEMs due to their flexibility in molecular design, synthesis, and cost-performance. Many efforts have been made to study a wide variety of sulfonated hydrocarbon-based polymers, such as sulfonated poly (ether ether ketone)s (SPEEKs),[4,5] sulfonated polyphenylenes,[6,7] sulfonated polysulfones (SPSFs),[8,9] sulfonated polyimides (SPIs),[10,11] and some of them show comparable or even higher proton conductivities than that of Nafion in water or under a high relative humidity (RH). However, the proton conductivity significantly decreased when the RH decreased, which is too low to meet the requirement for practical use. On the other hand, the PEMFC operation under reduced RH can increase the efficiency of the system and provide a greatly simplified water management. The development of PEMs having a high proton conductivity at a low RH is currently in strong demand for PEMFCs.

Studies of the phosphonated polymers have drawn considerable attention in past years. The phosphonated polymers are recognized as one of the materials for PEMs which may potentially show some crucial advantages over the sulfonated membranes.[12-19] They have the specific ability of facilitating proton conductivity at a low RH or even under anhydrous conditions [20-23] because the phosphonic acid provides amphoteric properties, and shows a high degree of self-dissociation and hydrogen bonding, and the proton is transported through structure diffusion (the Grotthus mechanism[24,25]). Recently, Yoon et al. reported that the poly(vinylbenzyloxy -alkylphosphonic acid)s showed the proton conductivity of 3 $\times$ 10^{-4} S/cm at 140 ^{o}C

under nominally anhydrous conditions. They concluded that the high proton conductivity may be attributed to the highly aggregated proton conducting acid channels with mobile hydrogen bond networks. The flexible side chains may have a positive effect on the aggregation of the protongenic group and hydrogen bond formation.[26] Quite recently, we reported that PEMs based on polyacrylates with phosphonic acid via long alkyl side chains exhibited a very high proton conductivity comparable to that of the Nafion 117 membrane in the range of 30-80% RH at 80 ^{o}C, regardless of the significant low water uptake behavior. [27] However, an ester linkage may have a problem regarding hydrolytic stability, thus other robust linkages are preferable. To remedy this issue, alkylphosphonic acids were introduced to the polystyrenes through the more stable ether linkages than the ester ones.

In this chapter, we synthesized a series of polystyrenes with phosphonic acids via 4, 6, and 8 methylene spacers. Moreover, the relationship between the length of the alkyl chain and the properties of the membranes, such as water uptake, proton conductivity and morphology, were also investigated.

3-2. Results and Discussion

3-2-1. Synthesis of monomer

As shown in Scheme 3-1, three phosphonated monomers, **3a**, **3c** and **3c**, were easily prepared by the solid state phase transfer catalyst reaction of **1** and corresponding diethyl ω-bromoalkylphosphonates **(2)**. Their chemical structures were characterized by FT-IR**,** ^{1}H NMR**,** and ^{13}C NMR spectroscopies. Figure 3-1 shows the ^{1}H NMR spectra of the three monomers **3**, and the typical ^{13}C NMR spectrum of **3a** is shown in Figure 3-2. All peaks could be assigned to the expected structure of the monomers **3**, indicating that the monomers were successfully synthesized.

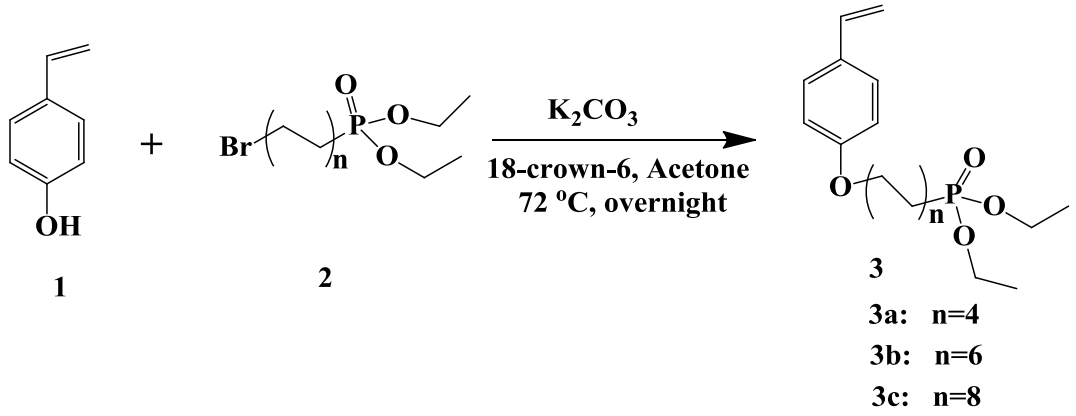

Scheme 3-1. Synthesis of phosphonated monomers **3a**, **3b** and **3c**.

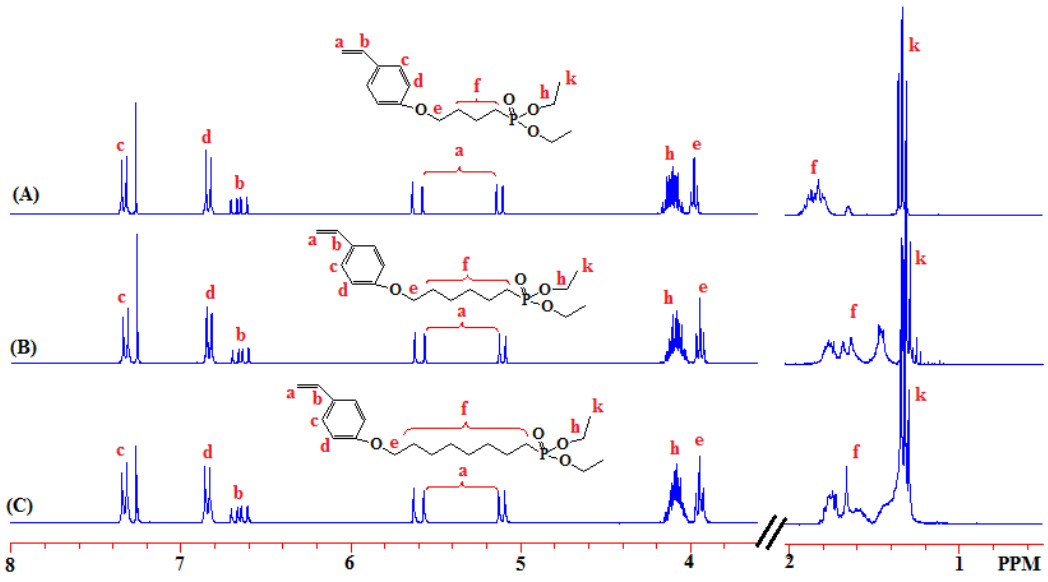

Figure 3-1. ^{1}H NMR spectra of phosphonated monomers: (A) 3a, (B) 3b and (C) 3c**.**

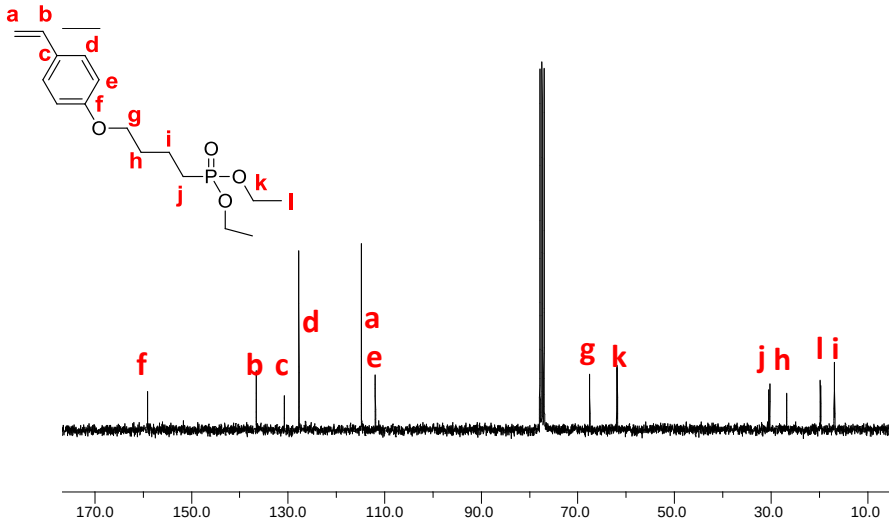

Figure 3-2. ^{13}C NMR spectrum of **3a.**

3-2-2. Synthesis of polymers

The polymer synthesis were done by the radical polymerization of the monomers **3** using AIBN as the initiator in DMF, followed by hydrolysis of the phosphonic acid ester using trimethysilyl bromide (Scheme 3-2). The polymerization smoothly proceeded and produced the corresponding poly(diethyl ω-(4-vinylphenoxy)alkylphosphonate)s (**4**). The number-average and weight-average molecular weights of **4** estimated by GPC based on the polystyrene standards are listed in Table 3-1. The results indicated that high molecular weight polymers were successfully prepared.

The chemical structures of **4** were confirmed by FT-IR and ^{1}H NMR spectroscopies. In the FT-IR spectra of **4a** and **5a** (Figure 3-3), the disappearance of the absorption at around 1608 cm^{-1} due to the vinyl group was confirmed and the characteristic absorption at 1033 cm^{-1} corresponding to the phosphonic ester disappeared after the hydrolysis, while the absorption at 2333 cm^{-1} corresponding to the phosphonic acids appeared. The ^{1}H NMR spectra of **4a** and **5a** are shown in Figure 3-4. The signals of the characteristic vinyl group (δ = 5.07-6.72) disappeared in the ^{1}H-NMR spectrum of **4a**, and the signals corresponding to the phosphonic ethyl ester group are observed at 4.17-4.02 and 1.39-1.27 ppm. This result suggested that the vinyl polymerization completely proceeded without the decomposition of the monomer. On the other hand, the signals of the phosphonic ethyl ester at 4.17-4.02 and 1.39-1.27 ppm completely disappeared in the ^{1}H-NMR spectrum of **5a** after the hydrolysis, which also supports the

fact that the hydrolysis proceeded without any decomposition or side reaction to give the desired **5a**.

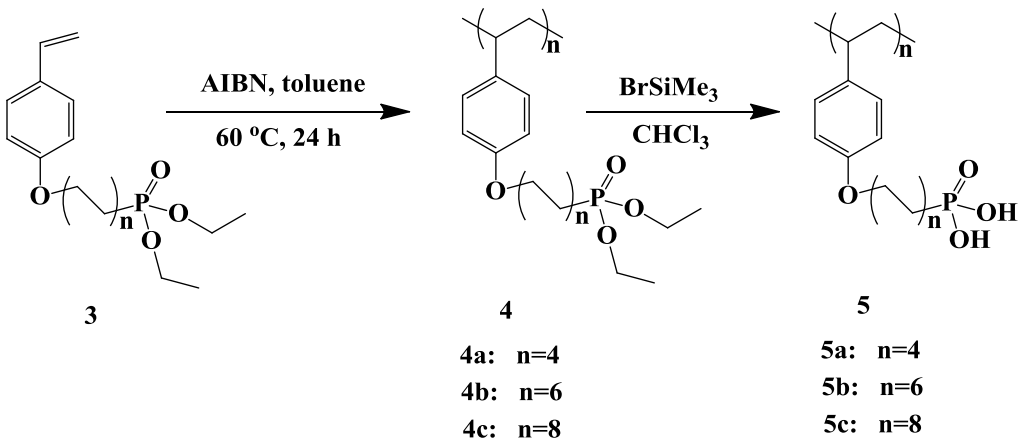

Scheme 3-2. Synthesis of **5a**, **5b** and **5c**.

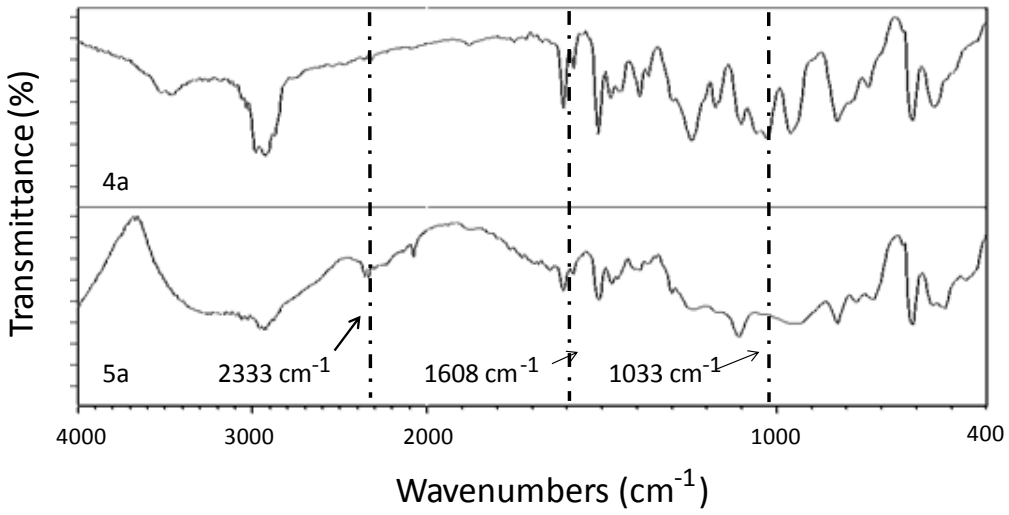

Figure 3-3. FT-IR spectra of **4a** and **5a**.

3-2-3. Thermal properties

The thermal stability of the polymers 5 was investigated by TGA under nitrogen. Prior to the measurement, the samples were preheated at 100 ℃ for 30 min to remove the absorbed moisture. As shown in Figure 3-5, all the samples displayed a two-stage weight loss behavior. The first stage weight loss in the approximate range of 200-310 ℃ is ascribed to the elimination of the phosphonic acid groups. The second-stage weight loss starting from ~400 ℃ is attributed to the decomposition of the

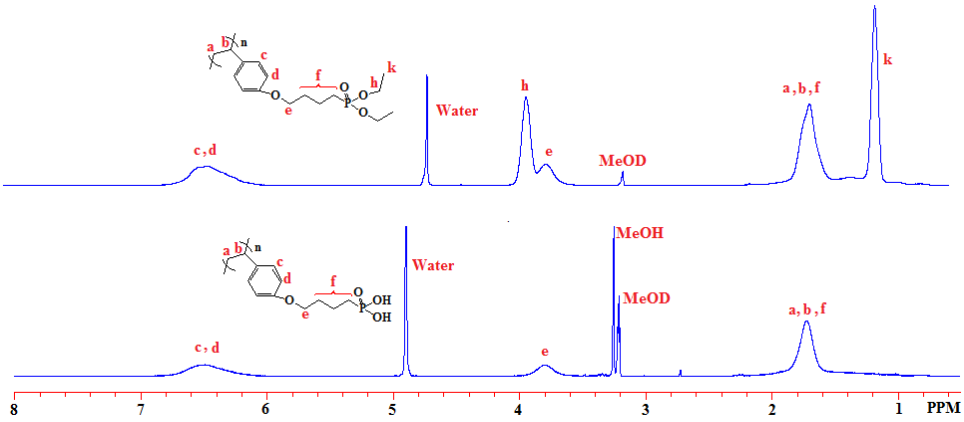

Figure 3-4. ^{1}H NMR spectra of the **4a** and **5a**.

polymer main chain. The TGA results indicated that the polymers **5** have a sufficient thermal stability which well meets the requirement for use in fuel cells. The mechanical property of **5b** was representatively measured by thermo mechanical analysis (TMA) at room temperature showing a tensile strength of 10 MPa at break, which is inferior to that of Nafion 117 (~30 MPa).

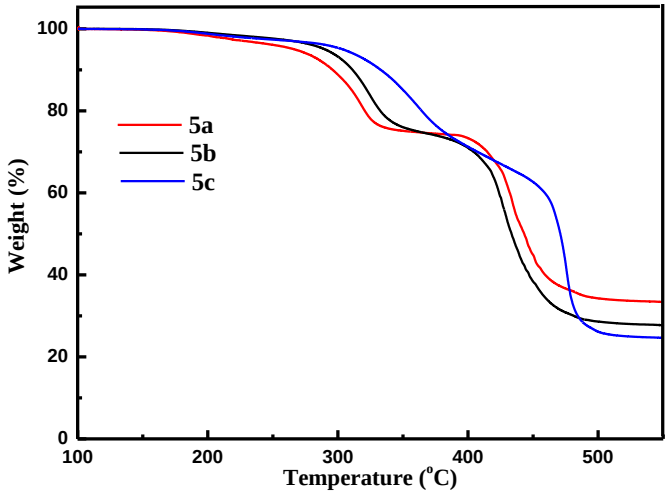

Figure 3-5. TGA curves of **5a**, **5b**, and **5c**.

3-2-4. Ion exchange capacity (IEC) and oxidative stability

The IEC was measured based on the acid-base titration method. The samples were immersed in a saturated NaCl solution at room temperature for two days. The samples were then removed and the NaCl solution was titrated with 0.02 M NaOH until *p*H=7.

The IEC values (Table 3-1) decreased in the order **5a**, **5b**, and **5c** because of the different lengths of the side chain.

The radical oxidative stability of the polymers **5** was evaluated by the remaining weight after they were soaked in Fenton's reagent at room temperature for 24 h and at 80 ^{o}C for 1 h, the results of which are listed in Table 3-1. All the membranes showed more than 94% remaining weights after Fenton's test. Generally, polystyrene is not considered an ideal material for sulfonated PEM application due to its poor oxidative stability of the benzylic C-H bond,[29] and many common sulfonated hydrocarbon-based polymers have been reported to completely dissolve in Fenton's reagent within a few hours.[30,31] The results of Fenton's test in this chapter indicated that the polymers **5** have an excellent oxidative stability, probably due to their quite low water uptake as will be discussed later.

Table 3-1. Ion exchange capacities (IECs), molecular weight (M_n and M_w) and remaining weight (RW) after Fenton's test of membranes prepared from polymers **5**

Polymer	IEC (mequiv/g)		M_n[b]	M_w[b]	M_w/M_n[b]	RW[c]	RW[d]
	Theoretical	Measured[a]	(KDa)	(KDa)		(%)	(%)
5a	3.90	3.80	50.2	90.0	1.79	98.3	94.2
5b	3.52	3.42	45.8	86.8	1.90	98.5	95.5
5c	3.20	3.00	48.0	79.0	1.65	98.4	96.3

[a] By titration method; [b] Determined by GPC based on polystyrene standards;
[c] Measured by soaking the membranes in Fenton's reagent (3% H_2O_2 containing 20 ppm $FeSO_4$) at room temperature for 24 h; [d] Measured by soaking the membranes in Fenton's reagent (3% H_2O_2 containing 2 ppm $FeSO_4$) at 80 ^{o}C for 1 h.

3-2-5. Water uptake and hydration number

The water uptake properties of the PEMs have a strong influence on their proton conductivity because water molecules play an important role as a proton transportation carrier in membranes. The water uptakes of **5a**, **5b** and **5c** are shown in Figure 3-6(A), and compared to that of Nafion 117. All the membranes show lower water uptakes (< 25 %) even at 90 % RH, leading to an excellent dimensional stability. The water uptake of **5c** is comparable to that of Nafion 117 even at 90% RH. Moreover, their water uptakes are similar to that of Nafion 117 in the wide range of 30-80% RH. In our previous report,[32] the phosphonated poly(*N*-phenylacrylamide) (PDPAA) showed a higher water uptake which was almost two times higher than that of **5** over the entire

range of RH due to the higher IEC value (IEC=6.72 mequiv/g).

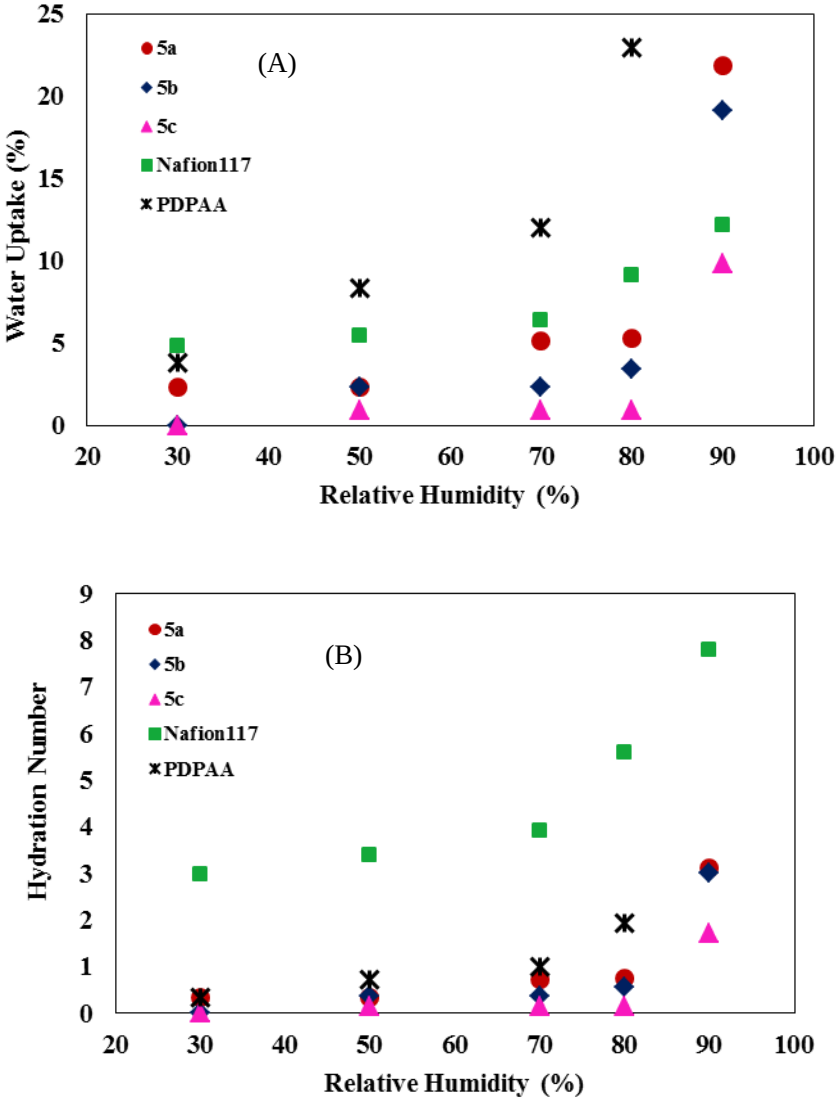

Figure 3-6. (A) Water uptake and (B) hydration numbers (λ) of three membranes **5** under different RH.

Furthermore, the λ value, which is the number of water molecules per an acid group, is plotted versus RH (Figure 3-6(B)). The values decrease with the increasing alkyl chain length of alkylphosphonic acids. Compared to the Nafion 117 membrane, significantly lower λ values are observed in all the membranes over the entire range of RH, probably due to the low acidity of phosphonic acid. The high degree of hydrogen bonding and the lower acidity of the phosphonic acid groups can limit the water uptake behavior of the membrane in the phosphonated polymers.

3-2-6. Proton conductivity

Proton conductivity is the primary property that determines the PEM performance. The proton conductivity of three membranes with different side chain lengths was measured at 80 °C under different RH (30-95%) conditions and the results are shown in Figure 3-7. It can be seen that for all the membranes, the proton conductivity increases with the increasing RH. The **5a** membrane with four methylene spacer units showed slightly higher proton conductivity due to its higher IEC value than the other two membranes. The proton conductivity of **5** is lower than that of Nafion 117, which is likely related to the differences in the acidity between the sulfonic acid and phosphonic acid. For comparison, the proton conductivities of the reported phosphonated polymers with much higher IEC values, such as PDPAA[32] (IEC: 6.72 mequiv/g) and M47[33] (IEC: 8.4 mequiv/g), and their chemical structures are shown in Figure 3-7. It should be noted that the proton conductivities of **5** are higher than that of M47 in the range of 50-95 % RH, even though they do not possess fluorinated segments as does M47 and have twice the lower IEC value. The high proton conductivity of **5** may be attributed to a higher degree of hydrophilic/hydrophobic microphase separation assisted by long spacer units. On the other hand, although PDPAA showed a high proton conductivity at 70-95% RH comparable to Nafion 117, its conductivity sharply dropped when the RH decreased

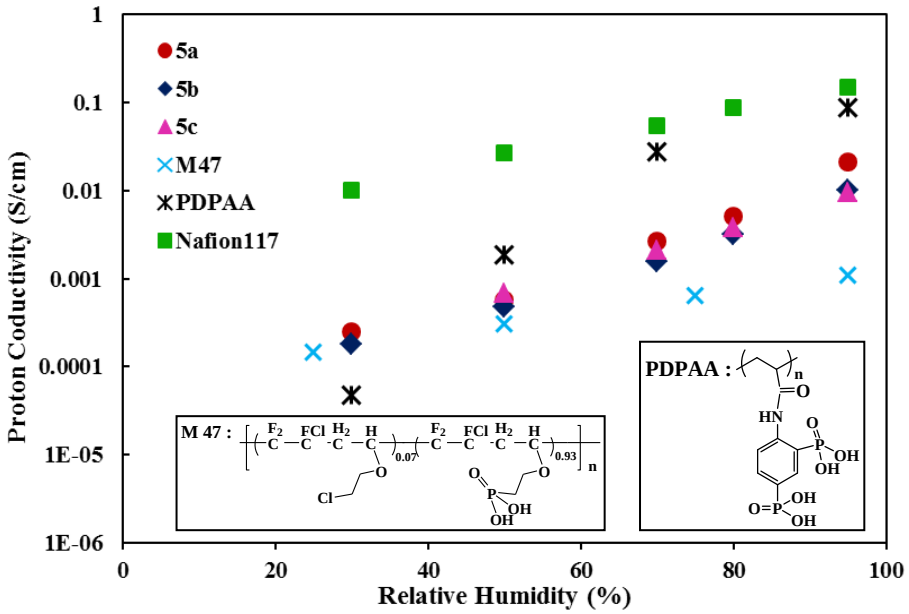

Figure 3-7. Proton conductivity as a function of relative humidity of membranes **5,** Nafion 117, PDPAA[32] at 80 °C and M47[33] at 90 °C.

regardless of the high IEC values (6.72 mequiv/g), which means the water-assisted mechanism works in proton conduction. However, the membranes **5** exhibit a much higher proton conductivity than that of PDPAA at 30% RH, although they exhibit a lower proton conductivity than that of Nafion 117. These results suggest that the flexible pendant side chains of **5** would contribute to the formation of hydrogen-bonding networks by taking into consideration of a very low water uptake of these polymers. On the other hand, compared to the proton conductivity of PEMs based on polyacrylates with phosphonic acid via long alkyl side chains, the membranes **5** showed lower proton conductivity probably due to lower IECs (3.0-3.80 mequiv/g) than that (4.1-5.44 mequiv/g) of PEMs based on polyacrylates[27]. Thus, the membranes **5** with the IEC values over 4.5 mequiv/g would be prepared to form well connected hydrogen-bonding networks.

3-2-7. Atomic force microscope (AFM) observation

The tapping mode phase image of the surface of the **5b** membrane was recorded as a representative example under ambient conditions on the 500 × 500 nm scale to investigate its morphological characteristics. The dark and bright regions were assigned to the flexible structure corresponding to the hydrophilic domains with phosphonic acid groups containing water and the rigid structure corresponding to the hydrophobic domains, respectively. As can be seen in Figure 3-8, continuous hydrophilic domains are clearly observed, implying that the long and flexible hydrophilic side chains induce the aggregation to form wide hydrophilic channels.

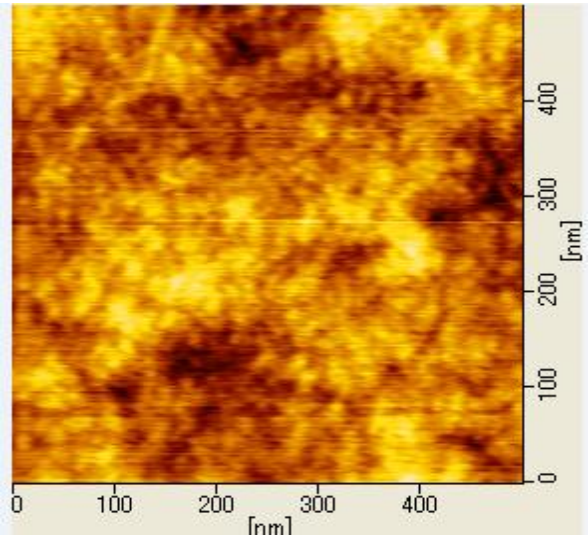

Figure 3-8. Morphology of **5b** studied by AFM.

3-3. Conclusions

Polystyrenes with phosphonic acid via long alkyl side chains were developed for PEMs. These membranes showed a very low water uptake, similar to that of Nafion 117 in the wide range of 30-80% RH, and high oxidative stability against Fenton's reagent. Moreover, the proton conductivities of these membranes were comparable or higher than those of the reported phosphonated polymers under low RH conditions, **PDPAA** and **M47**, even though the IEC values of these membranes are much lower than those of **PDPAA** and **M47**. These results proved that the flexible pendant side chains induced the self-assembly of the hydrophilic domains (i.e., the formation of hydrogen-bonding networks) to achieve good proton transportation.

3-4. Experimental

Materials

Diethyl 4-bromobutylphosphonate (**2a**), diethyl 6-bromohexylphosphonate (**2b**), and diethyl 8-bromooctylphosphonate (**2c**) were prepared according to a previous report[28]. Other solvents and reagents were used as received.

Synthesis of diethyl 4-(4-vinylphenoxy)alkylphosphonate (3)

The monomer, diethyl 4-(4-vinylphenoxy)butylphosphonate (**3a**), was prepared as follows: **2a** (1.53 g, 5.1 mmol), 4-vinylphenol (**1**) (0.674 g, 5.6 mmol), potassium carbonate (1.41 g, 10.2 mmol) and 18-crown-6 (0.03 g, 0.11 mmol) were dispersed in dry acetone (10.0 mL). Then the mixture was refluxed for 17 h. After evaporation the solvent, distilled water was added. The aqueous layer was extracted two times with toluene. The organic layer was washed with water, dried over anhydrous magnesium sulphate, and filtered. The organic layer was concentrated under reduced pressure. The product was isolated by column chromatography on silica gel (ethyl acetate/n-hexane = 2/1 v/v). Yield: 1.34 g (77%). FT-IR (Si, cm^{-1}): 2981, 1735, 1608, 1511, 1473, 1392, 1245, 1176, 1025, 960. ^{1}H NMR ($CDCl_3$, δ, ppm): 7.30-7.38 (2H, d), 6.80-6.87 (2H, d), 6.60-6.72 (1H, q), 5.55-5.65 (1H, d), 5.08-5.16 (1H, d), 4.02-4.17 (4H, m), 3.93-4.01 (2H, t), 1.71-1.95 (6H, m), 1.27-1.39 (6H, t).

Other monomers, diethyl 6-(4-vinylphenoxy)hexylphosphonate (**3b**) and diethyl 8-(4-vinylphenoxy)octylphosphonate (**3c**) were obtained by the similar procedure described above.

3b: FT-IR (Si, cm^{-1}):2947, 1735, 1608, 1508, 1473, 1389, 1238, 1107, 933, 825, 771, 725. ^{1}H NMR ($CDCl_3$, δ, ppm): 7.29-7.39 (2H, d), 6.79-6.90 (2H, d), 6.60-6.72 (1H, q), 5.55-5.66 (1H, d), 5.07-5.16 (1H, d), 4.01-4.17 (4H, m), 3.91-4.00 (2H, t), 1.40-1.85 (8H, m), 1.28-1.38 (6H, t).

3c: FT-IR (Si, cm^{-1}): 2927, 1608, 1511, 1469, 1388, 1254, 1176, 1041, 957. ^{1}H NMR ($CDCl_3$, δ, ppm): 7.28-7.38 (2H, d), 6.79-6.88 (2H, d), 6.58-6.72 (1H, q), 5.54-5.65 (1H, d), 5.06-5.15 (1H, d), 4.00-4.17 (4H, m), 3.89-3.99 (2H, t), 1.25-1.83 (20H, m).

Synthesis of poly(diethyl 4-(4-vinylphenoxy)alkylphosphonate) (4)

A typical procedure for the synthesis of poly(diethyl 4-(4-vinylphenoxy) butyl -phosphonate) (**4a**) is as follows.

The monomer **3a** (1.00 g, 3.22 mmol), 2,2'-azobis(isobutyronitrile) (AIBN) (0.0211 g, 0.129 mmol), and dry toluene (1.30 mL) were placed in a sealed glass tube after

standard freeze-evacuate-thaw procedures. The mixture was stirred at 60 ^{o}C for 24 h. After cooling to room temperature, the mixture was diluted with toluene and then poured in hexane. The precipitate was collected and dried in vacuo at 40 ^{o}C for 10 h to give **4a** (0.88 g, 88%).

Synthesis of poly(4-(4-vinylphenoxy)alkylphosphonic acid) (5)

A typical procedure for the synthesis of poly(4-(4-vinylphenoxy)butylphosphonic acid) (**5a**) is as follows.

To the chloroform solution (8.3 mL) of **4a** (0.52 g, 1.66 mmol) was added dropwise trimethylsilyl bromide (1.29 mL, 9.95 mmol) at 0 ^{o}C, and the mixture was stirred at 40 ^{o}C for 24 h. After evaporation, the residue was dissolved in methanol and the solution was stirred at room temperature for 6 h. Then methanol was evaporated and the obtained product was then dried in vacuo at 40 ^{o}C for 24 h to produce **5a** (0.42 g, 98%). FT-IR (Si, cm^{-1}): 2946, 2333, 1612, 1508, 1238, 1106, 933, 825. ^{1}H NMR (MeOD, δ, ppm): 4.36 (2H, broad), 2.54–1.50 (5H, m).

Membrane preparation and ion exchange capacity (IEC)

Methanol solutions of **5** were cast onto flat Teflon sheets. Drying the solution at 80 ^{o}C for 12 h gave transparent membranes. IEC values of **5** were determined by titration with 0.02 M NaOH aq.

Measurements

^{1}H NMR (300 MHz) and ^{13}C NMR (75 MHz) spectra were recorded on a Bruker DPX300S spectrometer using $CDCl_3$ or MeOD-d_4 as solvent and tetramethylsilane as reference. Fourier transform infrared (FT-IR) spectra were obtained with a Horiba FT-120 Fourier transform spectrophotometer. Number- and weight-average molecular weights (M_n and M_w) were measured by gel permeation chromatography (GPC) on a Hitachi LC-7000 system equipped with polystyrene gel columns (TSKgel GMHHR-M) eluted with *N*,*N*-dimethylformamide (DMF) containing 0.01 M LiBr at a flow rate of 1.0 mL/min calibrated by standard polystyrene samples. Thermogravimetric analysis (TGA) was measured in N_2 on a Seiko EXSTAR 6000 TG/DTA 6300 thermal analyzer at a heating rate of 10 °C/min.

Water uptake

The humidity dependence of water uptake was measured by placing the membrane in

a thermo-controlled humid chamber for 4 h. Then the membrane was taken out, and quickly weighed on a microbalance. Water uptake (*WU*) was calculated according to the following eqution:

$$WU = (W_s - W_d)/W_d \times 100 \text{ wt \%}$$

where, W_s and W_d are the weights of wet and dried membranes, respectively.

Proton conductivity

Proton conductivity in plane direction of the membrane was determined using an electrochemical impedance spectroscopy technique over the frequency from 5 Hz to 1 MHz (Hioki 3532-80). A two-point-probe conductivity cell with two platinum plate electrodes was fabricated. The cell was placed in a thermo-controlled humid chamber at 80 ^{o}C for 4 h before the measurement. Proton conductivity (σ) was calculated from the following equation:

$$\sigma = d/(t_s w_s R)$$

where d is the distance between the two electrodes, t_s and w_s are the thickness and width of the membrane, and R is the resistance measured.

Oxidative stability

The oxidative stability of the membranes was tested by immersing the films into Fenton's reagent (3% H_2O_2 aqueous solution containing 20 ppm $FeSO_4$) at room temperature. The remaining weight after they were soaked in Fenton's reagent at room temperature for 24 h was used to evaluate the oxidative stability of the membranes.

3-5. References

(1) Savadoga, O. *J. New. Mater. Electrochem. Syst.* **1998,** *1,* 47-66.

(2) Mauritz, K. A.; Moore, R. B. *Chem. Rev.* **2004,** *104,* 4535-4586.

(3) Rikukawa, M.; Sanui, K. *Prog. Polym. Sci.* **2000,** *25,* 1463-1502.

(4) Zaidi, S. M. J.; Mikhailenko, S. D.; Robertson, G. P.; Guiver, M. D.; Kaliaguine, S. *J. Membr. Sci.* **2000,** *173,* 17-34.

(5) Matsumoto, K.; Higashihara, T.; Ueda, M. *Macromolecules* **2008,** *41,* 7560-7565.

(6) Ghassemi, H.; McGrath, J. E. *Polymer* **2004,** *45,* 5847-5854.

(7) Wu, S.; Qiu, Z.; Zhang, S.; Yang, X.; Yang, F.; Li, Z. Polymer 2006, 47, 6993-7000.

(8) Schuster, M.; Kreuer, K.-D.; Andersen, H. T.; Maier, J. *Macromolecules* **2007,** *40,* 598-607.

(9) Nakabayashi, K.; Higashihara, T.; Ueda, M. *Macromolecules* **2010,** *43,* 5756-5761.

(10) Genies, C.; Mercier, R.; Sillion, B.; Cornet, N.; Gebel, G.; Pineri, M. *Polymer* **2001,** *42,* 359-373.

(11) Fang, J. H.; Guo, X. X.; Harada, S.; Watari, T.; Tanaka, K.; Kita, H.; Okamoto, K. *Macromolecules* **2002,** *35,* 9022-9028.

(12) Parvole, J.; Jannasch, P. *Macromolecules* **2008,** *41,* 3893-3903.

(13) Parvole, J.; Jannasch, P. *J. Mater. Chem.* **2008,** *18,* 5547-5556.

(14) Perrin, R.; Elomaa, M.; Jannasch, P. *Macromolecules* **2009,** *42,* 5146-5154.

(15) Papadimitriou, K. D.; Andreopoulou, A. K.; Kallitsis, J. K. *J. Polym. Sci. Part A: Polym. Chem.* **2010,** *48,* 2817-2827.

(16) Tayouo, R.; David, G.; Améduri, B.; Roziè re, J.; Roualdè s, S. *Macromolecules* **2010,** *43,* 5269-5276.

(17) Ingratta, M.; Elomaa, M.; Jannasch, P. *Polym. Chem.* **2010,** *1,* 739-746.

(18) Abu-Thabit, N. Y.; Ali, S. A.; Zaidi, S. M. J. *J. Membr. Sci.* **2010,** *360,* 26-33.

(19) Itoh, T.; Hirai, K.; Tamura, M.; Uno, T.; Kubo, M.; Aihara, Y. *J. Solid State Electrochem.* **2010,** *14,* 2127-2189.

(20) Schuster, M.; Rager, T.; Noda, A.; Kreuer, K. D.; Maier, J. *Fuel Cells* **2005,** *5,* 355-365.

(21) Steininger, H.; Schuster, M.; Kreuer, K. D.; Kaltbeitzel, A.; Bingö l, B.; Meyer, W. H.; Schauff, S.; Brunklaus, G.; Maier, J.; Spiess, H. W. *Phys. Chem. Chem. Phys.* **2007,** *9,* 1764-1773.

(22) Parvole, J.; Jannasch, P. "Advances in Fuel Cells" Ed by Zhao, T. S.; Kreuer, K-D.; Nguyen, T. V. New York, **2007,** 120-185.

(23) Parvole, J.; Jannasch, P. *Macromolecules* **2008,** *41,* 3893-3903.

(24) Kordesch, K.; Simader, G. Fuel Cells and Their Applications; VCH: Weinheim, Germany, **1996.**

(25) Kreuer, K.-D.; Rabenau, A.; Weppner, W. *Angew Chem. Int. Ed.* **1982,** *94,* 224-225.

(26) Lee, S.-Il.; Yoon, K.-H.; Yoon, D. Y. *Chem. Mater.* **2012,** *24,* 115-122.

(27) Fukuzaki, N.; Tamura, Y.; Kazuhiro Nakabayashi, Nakazawa, S.; Murata, S.; Higashihara, T.; Ueda, M. *Polym. Prepr. Jpn.* **2011,** *60,* 1582.

(28) Catel, Y.; Degrange, M.; Pluart, L. L.; Madec, P.-J.; Pham, T.-N.; Picton, L. *J. Polym. Sci. Part A: Polym. Chem.* **2008,** *46,* 7074-7090.

(29) Hickner, M. A.; Ghassemi, H.; Kim, Y. S.; Einsla, B. R.; McGrath, J. E. *Chem. Rev.* **2004,** *104,* 4587-4612.

(30) Xing, P.; Robertson, G. P.; Guiver, M. D.; Mikhailenko S.; Kaliaguine, S. *Macromolecules* **2004,** *37,* 7960-7967.

(31) Saito, J.; Miyatake, K.; Watanabe, M.; *Macromolecules* **2008,** *41,* 2415-2420.

(32) Fukuzaki, N.; Nakabayashi, K.; Nakazawa, S.; Murata, S.; Higashihara, T.; Ueda, M. *J. Polym. Sci. Part A: Polym. Chem.* **2011,** *49,* 93-100.

(33) Tayouo, R.; David, G.; Ameduri, B.; Roziere, J.; Roualdes, S. *Macromolecules* **2010,** *43,* 5269-5276.

Chapter 4

Random Copolystyrene Derivatives Containing Pendant Alkyl Sulfonic Acid for Polymer Electrolyte Membranes

ABSTRACT: Polymer electrolyte membranes (PEMs) of cross-linked polystyrene derivatives, poly{(4-butoxystyrene)$_x$-*random*-[4-(4-sulfobutyloxy)styrene]$_y$} (PBOS$_x$-*r*-PSBOS$_y$), based on a hydrophobic alkoxystyrene unit and a hydrophilic styrene unit containing a pendant alkyl sulfonic acid with the ion exchange capacity (IEC) of 2.57-3.03 mequiv/g were prepared by the reaction of PBOS$_x$-*r*-PSBOS$_y$ with 4,4'-methylene-bis[2,6-bis(hydroxyethyl)phenol] (MBHP) as the cross-linker in the presence of methanesulfonic acid. The cross-linked PBOS$_2$-*r*-PSBOS$_8$ membrane with the IEC of 3.03 showed a high proton conductivity compared to that of Nafion 117 over the entire range of 30-95% RH. Furthermore, the cross-linked membranes had a good mechanical strength even in the dry state as shown by DMA and a high oxidative stability against Fenton's reagent regardless of their high IECs. These results indicated that the introduction of flexible alkylsulfonated side chains to the polystyrene main chains improved the oxidative stability probably due to preventing or reducing the hydroxyl radical attack on the polymer main chain, and also increased the water uptake and the proton conductivity at a low relative humidity due to the well-developed phase separation, which was supported by TEM observations.

4-1. Introduction

Polymer electrolyte membrane fuel cells (PEMFCs) have attracted considerable attention as candidates for power sources because of their high fuel utilization efficiency and environmentally clean operation.[1-3] The polymer electrolyte membrane (PEM), which separates two electrodes and transports protons, is the key component of a PEMFC.[4] In the past decade, much effort has been made on the development of aromatic hydrocarbon polymers as alternative PEM materials to Nafion, because some drawbacks of Nafion, such as high cost and high methanol permeability seriously limit its industrial application.[5-8] In chapter 2, we prepared PA-doped PBIs for high temperature PEMs, and the proton conductivity of PA-doped SPBI-11 membrane was 37.3 mS/cm at 170 ^{o}C and 0% RH. However, the PA is easily leaked from the membranes during long time operation. Therefore, from this chapter, we synthesized PEMs by the other approach, that is, PEMs containing the sulfonic acid group. However, most of the sulfonated aromatic polymers, such as sulfonated poly(arylene ether sulfone),[9-17] sulfonated polyimides,[18-21] sulfonated poly(arylene ether ketone)[22] and sulfonated polyphenylene,[23,24] showed much lower proton conductivities at a low relative humidity (RH), even though at a high RH, the proton conductivity was comparable or higher than that of Nafion. This may be attributed to the lower acidity of the aryl or alkyl sulfonic acid and less effective phase separation of the sulfonated aromatic polymers. Recently, Chao et al.[25] reported an interesting phenomenon that pendant alkylsulfonated side chains on the block copolystyrene are distributed in well-organized domains and thus improved the proton conduction at a low RH (0.06 S/cm at 80 ^{o}C, 60% RH), twice than that of Nafion 117 (0.03 S/cm at 80 ^{o}C, 60% RH). However, the relationship between the structure and properties, in particular, the oxidative stability and mechanical strength have been far less investigated in that paper, because polystyrene is not considered as an ideal material for PEM application due to its poor oxidative stability of the benzylic C-H bond.[26] On the other hand, Okamoto et al.[27-29] and Watanabe et al.[30-32] reported a series of side-chain-type sulfonated polyimides with a pendent sulfonated group and found that introducing aliphatic segments both into the main chain and into the side chains could significantly reduce the chances of nucleophilic attack by water on the imide linkage and improve the hydrolytic stability and proton conductivity of the sulfonated polyimide. Therefore, introducing a flexible side chain into the polystyrene main chain may improve the oxidative stability because of the decreased chance of a hydroxyl radical attacking the polymer main chain, and may also improve the proton conductivity at a low RH due to

the well-developed phase separation.

In this chapter, a series of copolystyrenes containing a hydrophobic main chain and flexible pendent aliphatic sulfonic acid groups with varying ion exchange capacities (IECs) have been synthesized. The thermal stability, dynamic mechanical properties, oxidative stability, water uptake and proton conductivity of the membranes were also investigated.

4-2. Results and Discussion

4-2-1. Synthesis of PVA

As shown in Scheme 4-1, PVP was prepared via a two-step reaction, that is, radical polymerization of 4-vinylphenyl acetate using 2,2'-azobis(isobutyronitrile) (AIBN) as a radical initiator, followed by hydrolysis of the acetate group of PVPA.[34] The number- and weight-average molecular weights of the PVPA were estimated to be M_n = 577,600 and M_w = 1,242,000, respectively.

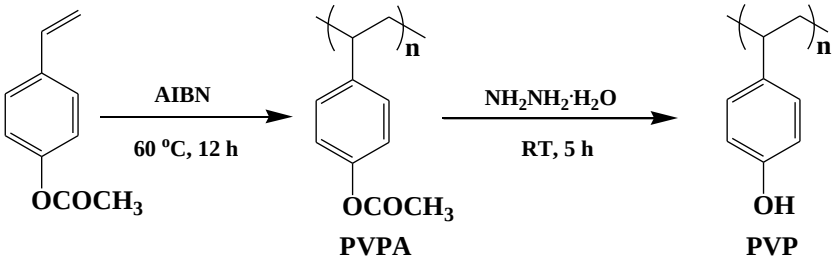

Scheme 4-1. Synthesis of poly (vinyl phenol) (PVP).

4-2-2. Synthesis of $PBOS_x$-*r*-PVP_y and $PBOS_x$-*r*-$PSBOS_y$

A series of polystyrene derivatives, $PBOS_x$-*r*-$PSBOS_y$ based on a hydrophobic alkoxystyrene unit and a hydrophilic styrene unit containing a pendant alkyl sulfonic acid, were prepared by the *O*-butylation of PVP, followed by the reaction with the 1,4-butanesultone of $PBOS_x$-*r*-PVP_y as shown in Scheme 4-2. The IEC values were controlled by controlling the molar ratio between 1-bromobutane and 1,4-butanesultone.

The chemical structure of the synthesized $PBOS_x$-*r*-$PSBOS_y$ as well as the intermediate polymers, $PBOS_x$-*r*-PVP_y, were also confirmed by ^{1}H NMR. Figure 5-1 shows the ^{1}H NMR spectrum of $PBOS_x$-*r*-PVP_y. The characteristic peaks of the methyl protons at δ = 0.91 and methylene protons next to the ether group at δ = 3.86 were observed in $PBOS_x$-*r*-PVP_y. The other peaks were in good agreement with the proposed chemical structures. The ^{1}H NMR spectrum of $PBOS_x$-*r*-$PSBOS_y$ shows characteristic methyl protons next to the sodium sulfonate at δ = 2.59 and the hydroxyl protons completely disappeared (Figure 4-2). The IR spectrum of $PBOS_x$-*r*-$PSBOS_y$ exhibited two characteristic absorptions at 1238 and 1045 cm^{-1} corresponding to the symmetric and asymmetric stretching of the sodium sulfonate groups, respectively (Figure 4-3). These results clearly indicated the formation of the desired $PBOS_x$-*r*-$PSBOS_y$.

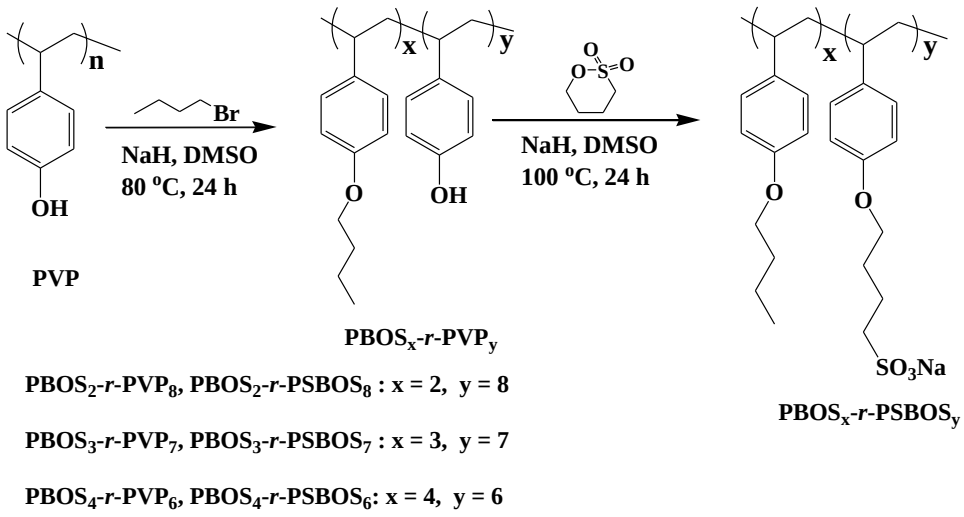

Scheme 4-2. Synthesis of PBOS$_x$-*r*-PSBOS$_y$ and intermediate product PBOS$_x$-*r* PVP$_y$.

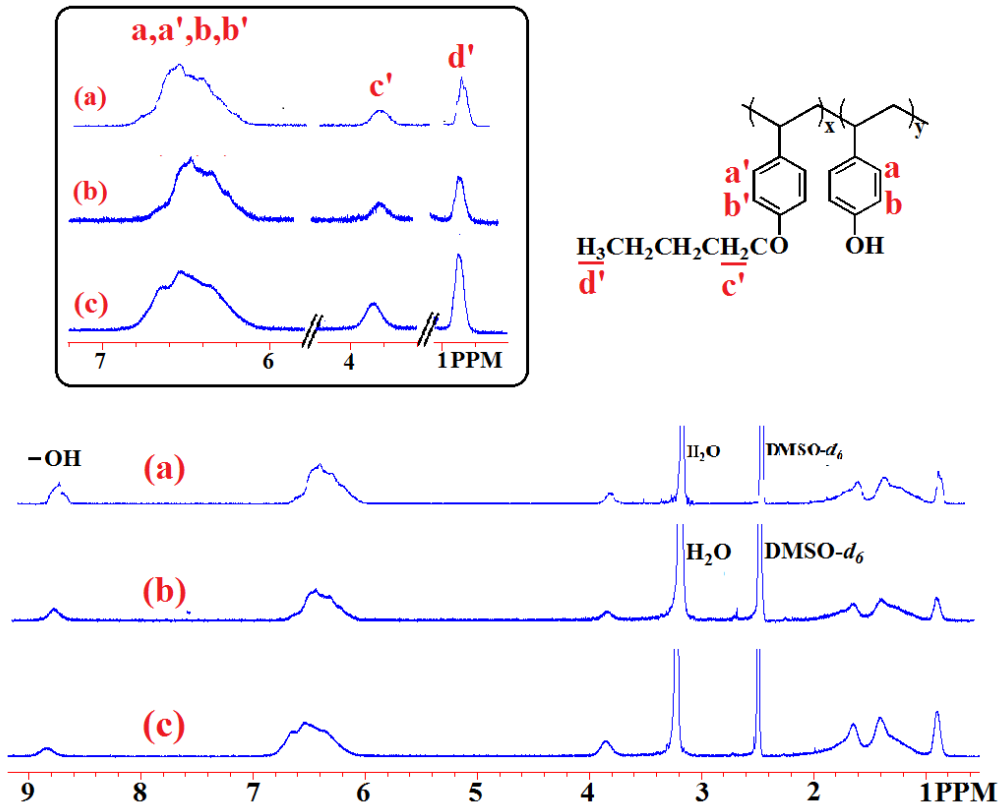

Figiure 4-1. ^{1}H NMR spectra of intermediate product PBOS$_x$-*r*-PVP$_y$: (a) PBOS$_2$-*r*-PVP$_8$, (b) PBOS$_3$-*r*-PVP$_7$ and (c) and PBOS$_4$-*r*-PVP$_6$.

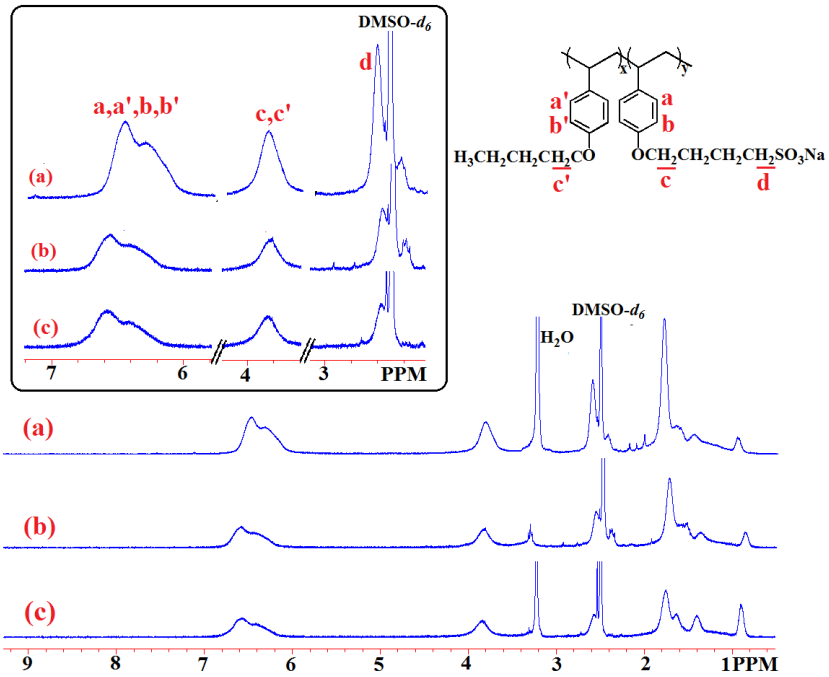

Figure 4-2. ^{1}H NMR spectra of $PBOS_x$-*r*-$PSBOS_y$: (a) $PBOS_2$-*r*-$PSBOS_8$, (b) $PBOS_3$-*r*-$PSBOS_7$ and (c) $PBOS_4$-*r*-$PSBOS_6$.

4-2-3. Preparation of cross-linked $PBOS_x$-*r*-$PSBOS_y$ membranes

As $PBOS_x$-*r*-$PSBOS_y$ were soluble in water, the cross-linked $PBOS_x$-*r*-$PSBOS_y$ were prepared by the electrophilic substitution reaction between the aromatic rings of $PBOS_x$-*r*-$PSBOS_y$ and the carbocation formed from MBHP as the cross-linker in the presence of methanesulfonic acid (Scheme 4-3).[35-37] The cross-linked $PBOS_x$-*r*-$PSBOS_y$ membranes were prepared as follows: a DMSO solution of $PBOS_x$-*r*-$PSBOS_y$, 5 wt% of MBHP and a catalytic amount of methanesulfonic acid was cast onto a glass plate. The film was dried at 120 ℃ for 1 h, and 80 ℃ for 20 h in an ambient atmosphere, and the obtained membrane was then immersed in water. After the cross-linking reaction, the film became insoluble in water, NMP, and DMSO, which indicated that the cross-linking reaction had occurred successfully.

4-2-4. Thermal stability and oxidative stability

The thermal stability of the cross-linked $PBOS_x$-*r*-$PSBOS_y$ membranes in their proton form was evaluated by TGA under nitrogen. Prior to the measurement, the samples were preheated at 100 ℃ for 30 min to remove any absorbed moisture. As shown in Figure 4-4, all the samples displayed a three-stage weight loss behavior. The approximate first stage weight loss in the range of 150-250 ℃ is ascribed to the dehydration between the

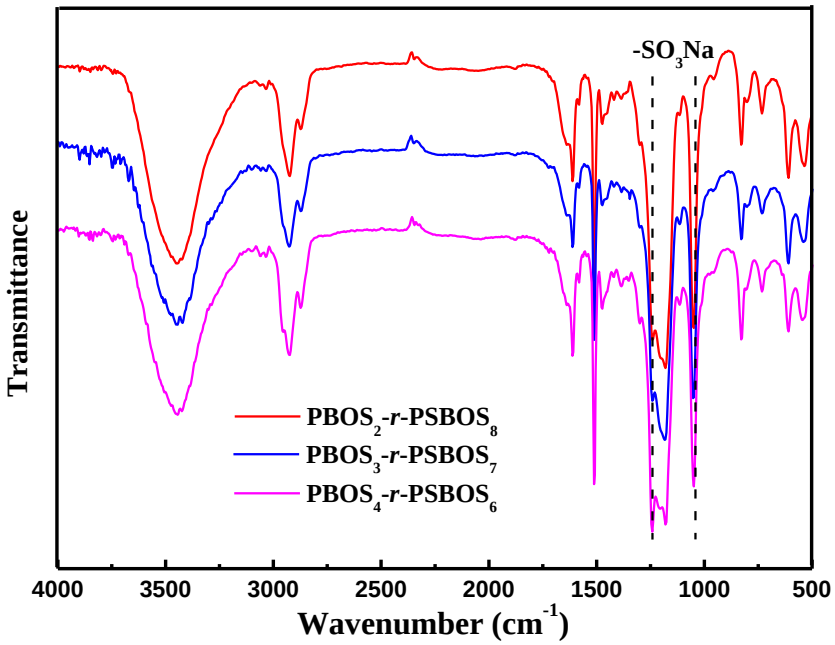

Figure 4-3. FT-IR spectra of $PBOS_x$-*r*-$PSBOS_y$ (in sodium form).

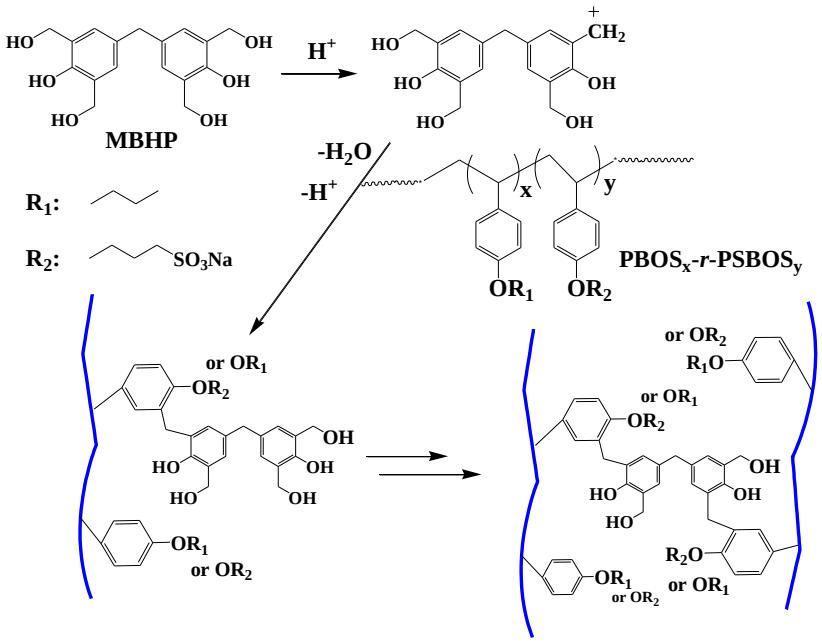

Scheme 4-3. Preparation of the cross-linked $PBOS_x$-*r*-$PSBOS_y$ membranes

sulfonic acids and desulfonation reaction.[30-32] The weight loss values in this stage were close to the theoretical value of the sulfonic acid group contents in the polymers. For example, the $PBOS_2$-*r*-$PSBOS_8$ had a first stage weight loss of 26.7% which was close to the calculated value (27%). The second and third-stage weight losses starting from

~250 ℃ and ~350 ℃ are attributed to the decomposition of the polymer side chains and main chains, respectively.

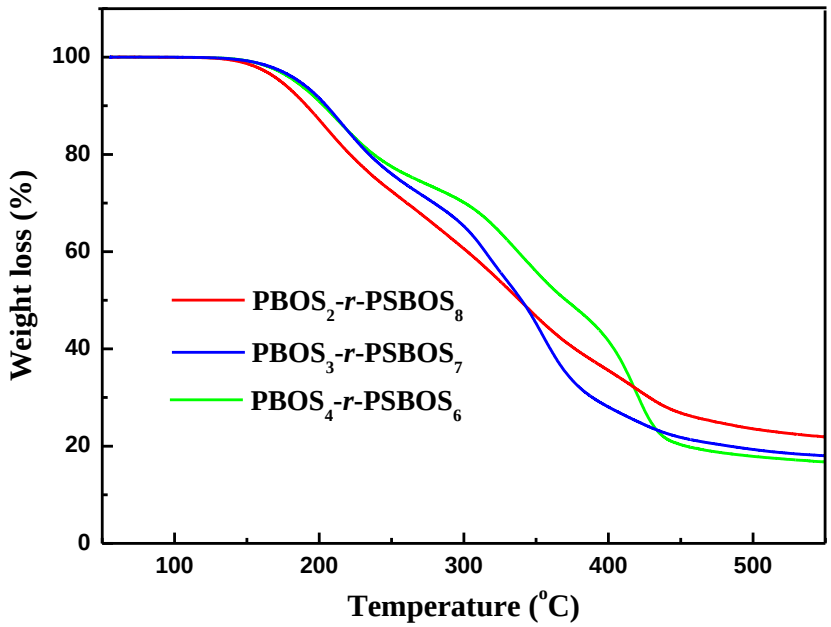

Figure 4-4. TGA curves of the cross-linked $PBOS_x$-*r*-$PSBOS_y$ (in proton form) in N_2.

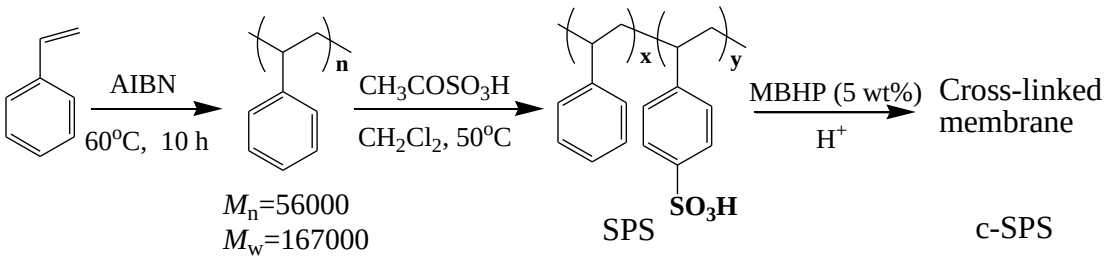

Scheme 4-4. Preparation of the cross-linked SPS membranes.

The membrane stability, in particular, the oxidative stability, is one of the important properties for membrane life when used in fuel cells. The oxidative stability of the cross-linked $PBOS_x$-*r*-$PSBOS_y$ membranes was evaluated by the disappearance time of membranes after they were soaked in Fenton's reagent (3% H_2O_2 containing 20 ppm $FeSO_4$) at room temperature, and their results are summarized in Table 4-1. Sulfonated polymers with high IEC values have been generally known to demonstrate a low oxidative stability against Fenton's reagent.[38-40] The cross-linked $PBOS_2$-*r*-$PSBOS_8$ membrane with the highest IEC value resisted soaking in Fenton's reagent for more than 24 h. For comparasion, we also synthesized the sulfonated polystyrene and then prepared cross-linked membrane (c-SPS) by using same cross-linker MBHP (Scheme

4-4). The IEC value measured by titration method was 2.63 mequiv/g. The disappearance time of c-SPS membrane after soaked in Fenton's reagent was only 4 h. Although the sulfonated polystyrene membrane was cross-linked, it still showed very poor oxidative stability due to the benzylic C-H bond. The $PBOS_x$-*r*-$PSBOS_y$ membranes have a better oxidative stability against Fenton's reagent compared to c-SPS and the other sulfonated polymers with similar IEC values such as the poly(ether sulfone)s,[37] which indicated that the introduction of flexible side chains can effectively improve the oxidative stability. One of the reasons for the high oxidative stability is probably that the main chains with the benzylic C-H bonds are well separated from the sulfonic acids, by which the hydroxy radical attack on the membrane could be significantly suppressed.

Table 4-1. Ion exchange capacities (IECs), disappearance time after Fenton's test, maximum stress (MS), elongation at break (EB) and maximum storage moduli (*E*'s) of the cross-linked $PBOS_x$-*r*-$PSBOS_y$ membranes

polymer	IEC (mequiv/g)		disappearance	*E*'	MS[c]	EB[c]
	Theoretical	Measured[a]	time[b] (h)	(10^9Pa)	(MPa)	(%)
$PBOS_2$-*r*-$PSBOS_8$	3.33	3.03	25	1.10	14	6
$PBOS_3$-*r*-$PSBOS_7$	3.01	2.68	26	1.66	15	10
$PBOS_4$-*r*-$PSBOS_6$	2.85	2.57	45	1.56	18	9
Nafion 117[d]	0.91	-[e]	-	0.4-0.5	26	200

[a] By titration method; [b] Measured by soaking the membranes in Fenton's reagent (3% H_2O_2 containing 20 ppm $FeSO_4$) at room temperature; [c]Measured at room temperature and 60% RH; [d]Cited from reference 42; [e]No data in this reference.

4-2-5. Dynamic mechanical properties

The dynamic mechanical properties of the cross-linked $PBOS_x$-*r*-$PSBOS_y$ membranes were investigated by DMA and the curves are shown in Figure 4-5. The maximum storage moduli (*E*') values of the cross-linked $PBOS_x$-*r*-$PSBOS_y$ membranes are listed in Table 4-1. The *E*' values of around 248 MPa maintained up to 180 ^oC. Although membranes with high IEC values can be generally brittle in the dry state, the E' values of the cross-linked $PBOS_x$-*r*-$PSBOS_y$ membranes indicate that the membranes have a good mechanical strength even in the dry state regardless of their high IEC values. The maximum stress (MS) and elongation at break were measured by TMA at room temperature and 60% RH. The results are listed in Table 4-1. The $PBOS_4$-*r*-$PSBOS_6$ membrane displayed a slightly higher MS than those of the other two membranes,

which was a slightly lower when compared to Nafion 117 (Table 4-1) and Nafion 112 (37 MPa at 50% RH and 20 ^{o}C).[41]

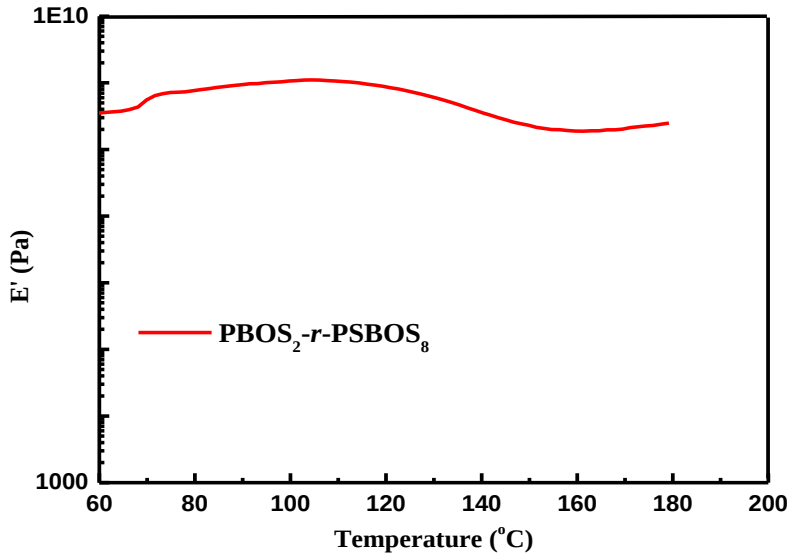

Figure 4-5. DMA curve of the cross-linked PBOS$_2$-*r*-PSBOS$_8$ membrane (in proton form) in nitrogen.

4-2-6. IEC, water uptake and dimensional change

The ion exchange capacity (IEC) is defined as the mequiv. of sulfonic acid per gram of polymer, which plays a crucial role in the water uptake and proton conductivity of the membranes. The IEC values were determined by a titration method, and the measured IEC values of the cross-linked PBOS$_x$-*r*-PSBOS$_y$ membranes were in the range of 2.57-3.03 mequiv/g (Table 4-1). For most sulfonated PEMs, the water uptake of the membranes is significantly related to the proton conductivity because water within the membrane acts as a carrier of the protons. However, the excessively high water uptake causes serious swelling and is mechanically too weak to be used as PEMs. Cross-linking is an effective way to depress the swelling. The water uptake and dimensional changes of the cross-linked PBOS$_x$-*r*-PSBOS$_y$ membranes are shown in Figure 4-6 and Figure 4-7, respectively. As shown in Figure 4-6, all the cross-linked PBOS$_x$-*r*-PSBOS$_y$ membranes show an acceptable water uptake (< 103 wt%) even though they have higher IEC values (> 2.5 mequiv/g). Among these membranes, the cross-linked PBOS$_2$-*r*-PSBOS$_8$ membrane shows a higher water uptake than the other two membranes over the entire range of RH because of its higher IEC value (3.03 mequiv/g). Moreover, the water uptake of the cross-linked PBOS$_2$-*r*-PSBOS$_8$ membrane

is 21 wt% even at 30% RH, which can be expected to effectively work for proton conduction. The large dimensional change may cause difficulty in fabricating fuel cell devices. Thus, the dimensional change of the cross-linked membranes was measured in both the length and thickness directions. Although it increases with the increasing IEC values, all the cross-linked membranes exhibit an isotropic swelling and a dimensional change lower than 25% (Figures 4-7) over the entire range of RH, which is the same behavior as the other sulfonated membranes.[17,39] These water uptake and dimensional changes are acceptable values, indicating that the cross-linking structure suppresses the unacceptable swelling.

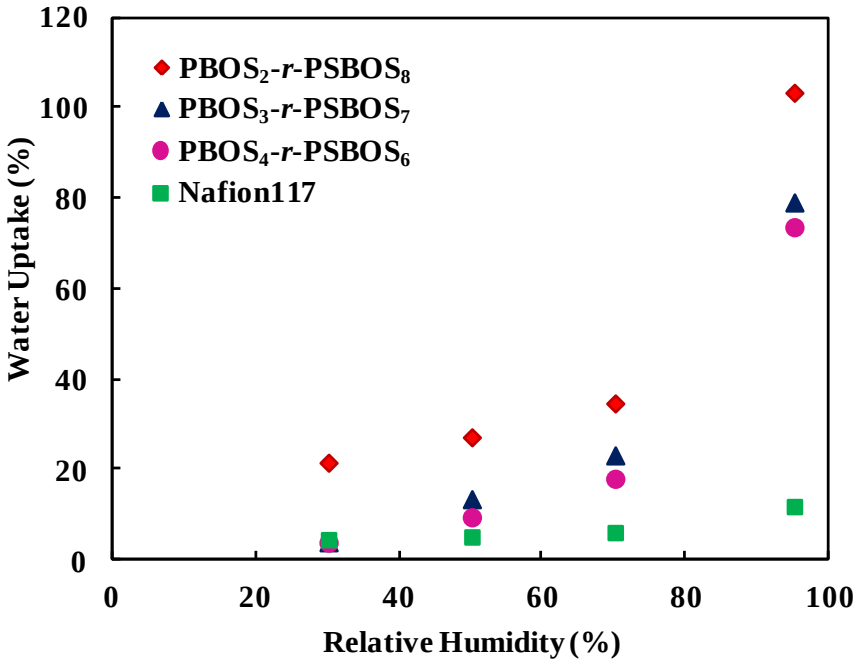

Figure 4-6. Water uptake of cross-linked $PBOS_x$-*r*-$PSBOS_y$ membranes and Nafion 117 at different RH and 80 ^{o}C.

4-2-7. Proton conductivity

The proton conductivities of the cross-linked $PBOS_x$-*r*-$PSBOS_y$ and Nafion 117 were measured at different RH and 80 ^{o}C (Figure 4-8). As shown in Figure 4-8, the proton conductivities of the cross-linked $PBOS_3$-*r*-$PSBOS_7$ and $PBOS_4$-*r*-$PSBOS_6$ membranes comparable to that of Nafion 117 at 95% RH, but decrease a lot when decreasing the RH. On the other hand, the cross-linked $PBOS_2$-*r*-$PSBOS_8$ membrane exhibits quite higher proton conductivities (0.24-0.26 S/cm) than that of Nafion 117 (0.1 S/cm) at 95%

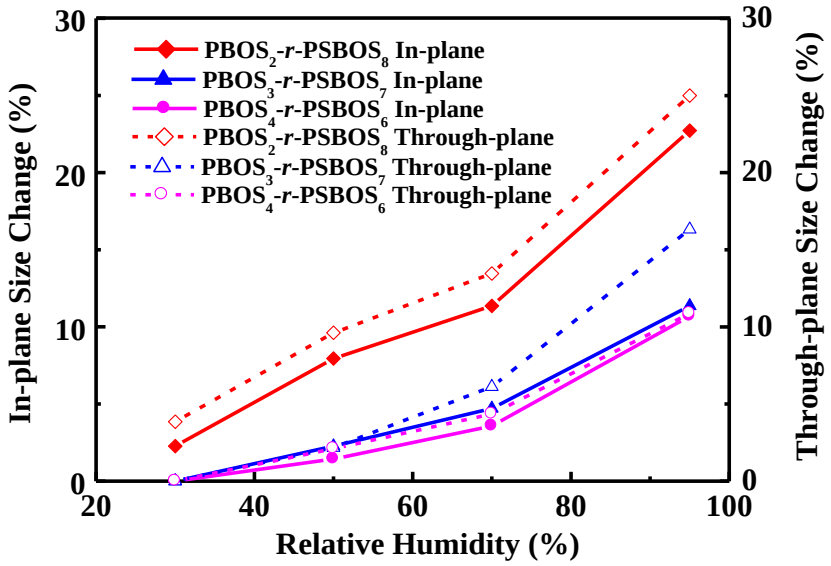

Figure 4-7. Dimensional change of cross-linked $PBOS_x$-*r*-$PSBOS_y$ membranes at different RH and 80 ^oC.

RH, and still shows comparable values to that of Nafion in the low RH range. As described above, the high water uptake of the cross-linked $PBOS_2$-*r*-$PSBOS_8$ membrane under a low RH induces a high proton conductivity at low RH. Consequently, the IEC values, which are basically related to the water uptake behavior, critically dominate the proton conduction. Furthermore, the formation of well-connected proton transportation channels derived from the flexible side chains with sulfonic acids is also expected to contribute to the high proton conductivity.

4-2-8. Transmission electron microscope (TEM) observation

The cross-sectional morphology of the cross-linked $PBOS_2$-*r*-$PSBOS_8$ membrane was investigated by TEM. In the TEM image (Figure 4-9), the dark and bright regions were assigned to the hydrophilic domains with sulfonic acid groups and the hydrophobic domains, respectively. As can be seen in Figure 4-9, a phase separation between the hydrophilic and hydrophobic domains is clearly observed. Thus, the flexible long alkyl side chains introduced in the polymer successfully induced the self-arrangement of each molecule to form such nanostructures. The interdistance of each domain averages ~ 2 nm and are well-connected to each other. These continuous hydrophilic domains in the cross-linked $PBOS_2$-*r*-$PSBOS_8$ membrane must contribute to the efficient proton

transportation and excellent proton conductivity.

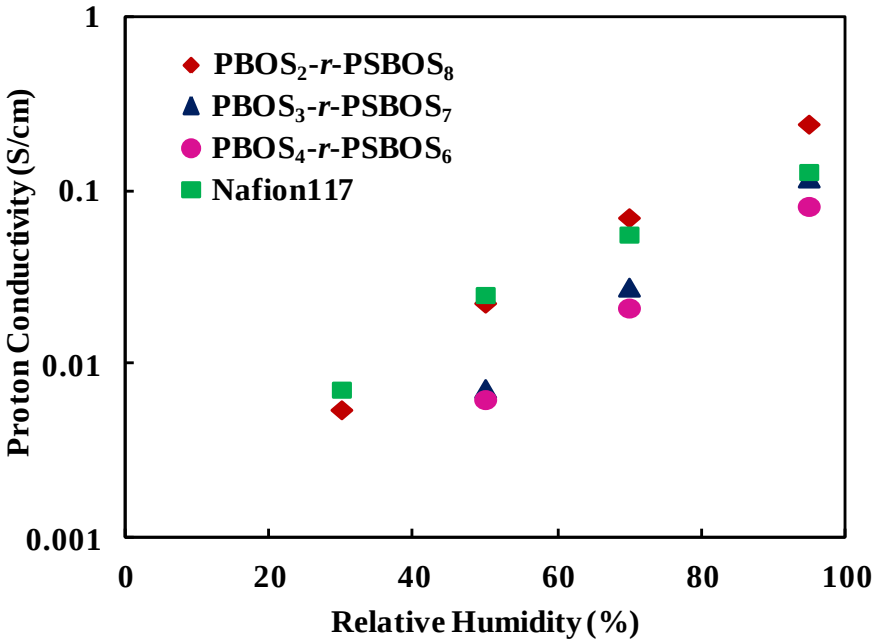

Figure 4-8. Proton conductivity of cross-linked $PBOS_x$-*r*-$PSBOS_y$ membranes at different RH and 80 ^{o}C.

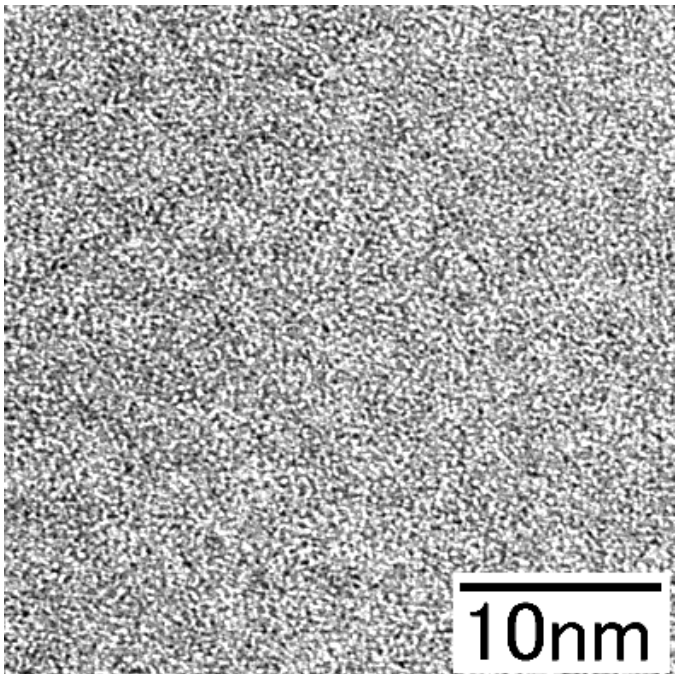

Figure 4-9. Cross-sectional TEM image of the cross-linked $PBOS_2$-*r*-$PSBOS_8$ membrane, scale bar = 10 nm.

4-3. Conclusions

Polystyrene derivatives, $PBOS_x$-*r*-$PSBOS_y$, containing flexible alkylsulfonated side chains and hydrophobic alkoxy chains were prepared by the *O*-butylation of PVP, followed by the reaction with the 1,4-butanesultone of $PBOS_x$-*r*-PVP_y. The cross-linked $PBOS_x$-*r*-$PSBOS_y$ membranes were then prepared by the reaction of $PBOS_x$-*r*-$PSBOS_y$ with MBHP as the crosslinker in the presence of methanesulfonic acid. The cross-linked $PBOS_x$-*r*-$PSBOS_y$ membranes showed a high oxidative stability against Fenton's reagent at room temperature, moderate water uptake at 95% RH, and good mechanical property in spite of the very high IEC values. The cross-linked $PBOS_2$-*r*-$PSBOS_8$ membrane exhibited a higher proton conductivity that was comparable to that of Nafion in the range of 50-95% RH. The strategy combining the introduction of flexible alkylsulfonated side chains to the polystyrene main chain and high IEC values works well when designing PEMFCs. Indeed, the oxidative stability was improved probably due to decreasing the chance of hydroxyl radical attack on the polymer main, and the proton conductivity was excellent at a low RH due to the well-developed phase separation, as confirmed by the TEM image showing the distribution of domains with an average ~2 nm size in the entire cross-linked membrane.

4-4. Experimental

Materials

4-Vinylphenyl acetate, 1,4-butanesultone, 1-bromobutane, and dimethylsulfoxide (DMSO, anhydrous) were purchased from TCI. Co. Hydrazine hydrate and 2,2'-azobis(isobutyronitrile) (AIBN) were purchased from Wako. Co. 4,4'-Methylene-bis[2,6-bis(hydroxyethyl)phenol] (MBHP) was prepared according to the previous report.[33]

Synthesis of poly(4-vinylphenyl acetate) (PVPA)

4-Vinylphenyl acetate (1.62 g, 10 mmol) and 2,2'-azobis(isobutyronitrile) (AIBN) (0.016 g, 0.1 mmol) were placed in a sealed glass tube after standard freeze-evacuate-thaw procedures. The solution was heated at 60 ^{o}C for 12 h. After cooling to the room temperature, the solid was dissolved in toluene, and poured in methanol. The precipitate was filtered off, washed with methanol and dried at 80 ^{o}C for 12 h in vacuum. The product was obtained as a white powder (1.56 g, 9.63 mmol, 96% yield). ^{1}H NMR ($CDCl_3$, ppm): δ 1.12-1.93 (d, 3H, -CH_2CH-), δ 2.08-2.47 (s, 3H, -OCOCH_3), 6.21-6.97 (m, 4H, -CH- in Ph).

Synthesis of poly(vinyl phenol) (PVP)

PVP was prepared following the procedure described in report.[28] To a 50 mL dry flask were added PVPA (1.46 g, 9.01 mmol) was dissolved in 1,4-dioxane (20 mL), hydrazine hydrate (4.4 mL) was added dropwise. The reaction mixture was magnetically stirred at room temperature under nitrogen for 5 h. The polymer precipitated during the reaction in 1,4-dioxane. The mixture was poured into 5 wt% citric acid, then washed with water several times and dried at 80 ^{o}C for 20 h in vacuum. The product was obtained as a white powder (1.03 g, 8.58 mmol, 95% yield). ^{1}H NMR (DMSO-d_6, ppm): δ 0.98-2.09 (d, 3H, -CH_2CH-), δ 6.04-6.70 (m, 4H, -CH- in Ph), δ 8.55-8.98 (s, 1H, -PhOH).

Synthesis of poly[(4-butoxystyrene)$_x$-*r*-(vinylphenol)$_y$] (PBOS$_x$-*r*-PVP$_y$) (x and y refer to the molar ratio of each unit)

To a 20 mL dry two-necked flask were added PVP (0.60 g, 5.00 mmol), sodium hydride (0.03 g, 1.20 mmol). This flask was evacuated and filled with nitrogen three times. Then anhydrous DMSO (10 mL) was added via syringe through the septum cap. The reaction mixture was magnetically stirred at 40 ^{o}C overnight, and then the

1-bromobutane (128 μL, 1.20 mmol) was added through the septum cap. The mixture was stirred at 80 ^{o}C for 24 h, and cooled to room temperature. The mixture was carefully poured into water with stirring. The resulting polymer was filtered, washed with ether, and dried at 80 ^{o}C for 20 h in vacuum. The product was obtained as a white powder (0.59 g, 4.50 mmol, 90% yield).

Synthesis of poly{(4-butoxystyrene)$_x$-*r*-[4-(4 sulfobutyleneoxy)styrene]$_y$}
(PBOS$_x$-*r*-PSBOS$_y$: x and y refer to the molar ratio of each unit)

The mixture of PBOS$_2$-*r*-PVP$_8$ (0.13 g, 1 mmol) and sodium hydride (0.03 g, 1.20 mmol), DMSO (2.5 mL) was stirred at 40 ^{o}C overnight, and then to this mixture was added 1,4-butanesultone (164 μL, 1.60 mmol) through the septum cap. The reaction mixture was heated at 100 ^{o}C for 24 h, and cooled to room temperature. The mixture was poured into ethanol with stirring, and dried at 80 ^{o}C for 10 h in vacuum. The product was obtained as a white powder (0.24 g, 0.93 mmol, 93% yield).

Cross-linked membrane formation and proton exchange

The prepared PBOS$_x$-*r*-PSBOS$_y$ in their sodium salt form and the cross-linker, MBHP (5 wt% to the polymer) were dissolved in DMSO to give a 10 w/v% solution, then one drop of methanesulfonic acid in DMSO solution was added. The solution was cast onto a glass plate, heated at 120 ℃ for 1 h, and 80 ℃ for 24 h to give a transparent membrane. The as-cast membrane was immersed in water to remove any residual solvent. Proton exchange treatment was performed by immersing the cross-linked PBOS$_x$-*r*-PSBOS$_y$ membrane in 1 M sulfuric acid solution at 45 ℃ for two days. The membrane was taken out, rinsed with deionized water till the rinsed water became neutral.

Measurements

^{1}H NMR spectrum was recorded on a Bruker DPX300S spectrometer using $CDCl_3$ or DMSO-d_6 as solvent. FT-IR spectra were recorded on a Horiba FT-120 Fourier transform spectrophotometer. Number- and weight-average molecular weights (M_n and M_w) were measured by gel permeation chromatography (GPC) on a Hitachi LC-7000 system equipped with polystyrene gel columns (TSKgel GMHHR-M) eluted with chloroform ($CHCl_3$) at a flow rate of 1.0 mL/min calibrated by standard polystyrene samples. Thermogravimetric analysis (TGA) was performed in nitrogen with a Seiko EXSTAR 6000 TG/DTA 6300 thermal instrument. Prior to measurement, all the

samples were preheated at 100 ℃ for half an hour to remove any absorbed moisture. Subsequently the samples were cooled to 50 ℃ and then reheated to 550 ℃ at a heating rate of 10 ℃/min. Dynamic mechanical analysis (DMA) was measured on a Seiko DMA 6300 apparatus in tension mode at a frequency of 1.0 Hz under nitrogen atmosphere at a heating rate of 10 ℃/min. The samples were 10 mm long, 4 mm wide and 45-55 μm thick. Thermomechanical analysis (TMA) was measured on a Seiko TMA/SS 6100 apparatus at room temperature and 60% RH. For each kind of membranes, two samples were used for measurements and the samples were 12 mm long, 3 mm wide and 47-60 μm thick. Ion exchange capacity (IEC) was measured by a titration method. The samples were immersed in saturated NaCl solution at room temperature for 3 days. After that, the samples were not taken out and the NaCl solution was directly titrated with 0.02 M NaOH until pH was 7. The oxidation stability of the membranes was determined by Fenton's test. The samples were soaked in the Fenton's reagent (3% H_2O_2 containing 20 ppm $FeSO_4$) at room temperature. The disappearance time of the samples was used to evaluate the radical oxidation stability of the membranes. Water uptake of $PBOS_x$-*r*-$PSBOS_y$ membranes was measured by placing the membrane in a thermo-controlled humid chamber. Before measurement, the membranes were placed in chamber at 80 ^oC, 30% RH for 5 h. After that, the membranes were set at desired values and kept constant for 2 h at each point. Then the membrane was taken out, and quickly weighed on a microbalance. Water uptake (WU) was calculated according to the following eqution:

$$WU = (W_s - W_d) / W_d \times 100 \text{ wt \%}$$

where W_s and W_d are the weights of wet and dried membranes, respectively. Dimensional change of a hydrated membrane was also investigated by placing the membrane in a therm-controlled humid chamber (80 °C) for 5 h, and the changes of length and thickness were calculated from

$$\Delta l = (l_s - l_d) / l_d \times 100 \text{ \%} \qquad \Delta t = (t_s - t_d) / t_d \times 100 \text{ \%}$$

where l_s and t_s are the length and thickness of the wet membrane, respectively, l_d and t_d refer to those of the dried membrane. For transmission electron microscopy (TEM) observations, the membranes were stained with lead ions by ion exchange of the sulfonic acid groups in 2 wt% $Pb(OCOCH_3)_2$ aqueous solution, rinsed with deionised water for 3 days, and dried at room temperature for 1 day. The strained membranes were embedded in an epoxy resin, sectioned to 90 nm thickness with microtome Ultracut UCT, and placed on copper grids. Images were taken on a Hitachi H7100FA TEM with an accelerating voltage of 100 kV. Proton conductivity was measured using a

two-probe electrochemical impedance spectroscopy technique over the frequency from 5 Hz to 1 MHz (Hioki 3532-80). The samples were 8 mm long, 8 mm wide and 55-60 μm thick. The cell was placed in a thermo-controlled humid chamber at 80 ^{o}C, 30% RH for 5 h before the measurement. Proton conductivity (σ) was calculated from the following equation:

$$\sigma = d/(t_s w_s R)$$

where d is the distance between the two electrodes, t_s and w_s are the thickness and width of the membrane, and R is the resistance measured.

4-5. References

(1) Jacobson, M. Z.; Colella W. G.; Golden, D. M. *Science*, **2005,** *308,* 1901.

(2) Carrette, L.; Friedich K. A.; Stimming, U. *Fuel cells* **2001,** *1,* 5-39.

(3) Costamagna, P.; Srinivasan, S. J. *J. Power Sources* **2001,** ***102***, 253-269.

(4) Hickner, M. A.; Pivovar, B. S. *Fuel cell*, **2005,** *5,* 213-229.

(5) Zawodzinski, T. A.; Neeman, M.; Sillerud, L. O.; Gottesfeld, S. *J. Phys. Chem.* **1991,** *95,* 6040-6044.

(6) Mauritz, K. A.; Moore, R. B. *Chem. Rev.* **2004,** *104,* 4535-4585.

(7) Li, E.; He, R.; Jensen J. O.; Bjerrum, N. *J. Chem. Mater.* **2003,** *15,* 4896-4915.

(8) Smitha, B.; Sridhar, S.; Khan, A. A. *J. Membr. Sci.* **2005,** *259,* 10-26.

(9) Wang, F.; Hickner, M.; Ji, Q.; Harrison, W.; Mechaam, J.; Zawodzinski, T. A.; MccGrath, J. E. *Macrol. Symp.* **2001,** *175,* 387-396.

(10) Li, N.; Shin, D. W.; Hwang, D. S.; Lee, Y. M.; Guiver, M. D. *Macromolecules* **2010,** ***43***, 9810-9820.

(11) Katzfub, A.; Krajinovic, K.; Chromik, A.; Kerres, J. *J. Polym. Sci. Part A: Polym. Chem.* **2011,** *49,* 1919-1923.

(12) Nakabayashi, K.; Matsumoto, K.; Ueda, M. *J. Polym. Sci. Part A: Polym. Chem.* **2008**, *46,* 3947-3957.

(13) Nakabayashi, K.; Matsumoto, K.; Higashihara, T.; Ueda, M. *J. Polym. Sci. Part A: Polym. Chem.* **2008,** *46,* 7332-7341.

(14) Matsumoto, K.; Nakagawa, T.; Higashihara, T.; Ueda, M. *J. Polym. Sci. Part A: Polym. Chem.* **2009,** *47,* 5827-5834.

(15) Nakabayashi, K.; Higashihara, T.; Ueda, M. *J. Polym. Sci. Part A: Polym. Chem.* **2010,** *48,* 2757-2764.

(16) Nakabayashi, K.; Higashihara, T.; Ueda, M. *Macromolecules* **2010,** *43,* 5765-5773.

(17) Nakagawa, T.; Nakabayashi, K.; Higashihara, T.; Ueda, M. *J. Mater. Chem.* **2010,** *20,* 6662-6667.

(18) Genies, C.; Mercier, R.; Sillion, B.; Cornet, N.; Gebel, G.; Pineri, M. *Polymer* **2001,** *42,* 359-373.

(19) Fang, J. H.; Guo, X. X.; Harada, S.; Watari, T.; Tanaka, K.; Kita, H.; Okamoto, K. *Macromolecules* **2002,** *35,* 9022-9028.

(20) Yin, Y.; Fang, J. H.; Watari, T.; Tanaka, K.; Kita, H.; Okamoto, K. *J. Mater. Chem.* **2004,** *14,* 1062-1070.

(21) Saito, J.; Miyatake, K.; Watanabe, M. *Macromolecules* **2008,** *41,* 2415-2420.

(22) Liu, B.; Robertson, G. P.; Kim, D.-S.; Guiver, M. D.; Hu, W.; Jiang, Z. *Macromolecules* **2007,** *40,* 1934-1944.

(23) Ghassemi, H.; McGrath, J. E. *Polymer* **2004,** *45,* 5847-5854.

(24) Wu, S.; Qiu, Z.; Zhang, S.; Yang, X.; Yang, F.; Li, Z. *Polymer* **2006,** *47,* 6993-7000.

(25) Lee, H.-C.; Lim, H.; Su, W.- F.; Chao, C.-Y. *J. Polym. Sci. Part A: Polym. Chem.* **2011,** *49,* 2325-2338.

(26) Hickner, M. A.; Ghassemi, H.; Kim, Y. S.; Einsla, B. R.; McGrath, J. E. *Chem. Rev.* **2004,** *104,* 4587-4612.

(27) Yin, Y.; Suto, Y.; Sakabe, T.; Chen, S.; Hayashi, S.; Mishima, T.; Yamada, O.; Tanaka, K.; Kita, H.; Okamoto, K. *Macromolecules* **2006,** *39,* 1189-1198.

(28) Hu, Z.; Yin, Y.; Okamoto, K.; Moriyama, Y.; Morikawa, A. *J. Membr. Sci.* **2009,** *329,* 146-152.

(29) Yin, Y.; Du, Q.; Qin, Y.; Zhou, Y.; Okamoto, K. *J. Membr. Sci.* **2011,** *367,* 211-219.

(30) Yasuda, T.; Li, Y.; Miyatake, K.; Hirai, M.; Nanasawa, M.; Watanabe, M. *J. Polym. Sci. Part A: Polym. Chem.* **2006, *44,*** 3995-4005.

(31) Miyatake, K.; Yasuda, T.; Hirai, M.; Nanasawa, M.; Watanabe, M. *J. Polym. Sci. Part A: Polym. Chem.* **2007,** *45,* 157-163.

(32) Kabasawa, A.; Saito, J.; Yano, H.; Miyatake, K.; Uchida, H.; Watanabe, M. *Electrochim. Acta*. **2009, *54,*** 1076-1082.

(33) Mitsui Petrochemical Industries, Ltd., Jpn. Kokai Tokkyo Koho JP 58,116,433 [83,116,433],**1983,** *Chem. Abstr.* **1984,** *100,* 7356n.

(34) Arshady, R.; Kenner, G. W.; Ledwith, A. *J. Polym. Sci. Polym. Chem. Edition* **1974, *12,*** 2017-2025.

(35) Ueda, M.; Nakayama, T. *Macromolecules* **1996,** *29,* 6427-6431.

(36) Lee, S. M.; Fréchet, M. J.; Willson, C. G. *Macromolecules* **1994,** *27,* 5154-5159.

(37) Nakagawa, T.; Nakabayashi, K.; Higashihara, T.; Ueda, M. *J. Mater.Chem.* **2010**, *20,* 6662-6667.

(38) Matsumoto, K.; Nakagawa, T.; Higashihara, T.; Ueda, M.; *J. Polym. Sci. Part A: Polym. Chem.* **2008,** *46,* 7560-7565.

(39) Matsumoto, K.; Nakagawa, T.; Higashihara, T.; Ueda, M. *J. Polym. Sci. Part A: Polym. Chem.* **2009,** *47,* 3444-3453.

(40) Bae, B.; Miyatake, K.; Watanabe, M. *Macromolecules* **2010,** *43,* 2684-2691.

(41) Zhang, X.; Hu, Z. X.; Okamoto, K. *J. Power Sources* **2012,** *216,* 261-268.

(42) Ishida, T.; Kasai, Y.; Urayama, K.; Takigawa, T. *J. Soc. Mater. Sci. Japan* **2007,** *56,* 1005-1008.

(43) Asano, N.; Aoki, M.; Suzuki, S.; Miyatake, K.; Uchida, H.; Watanabe, M. *J. Am. Chem. Soc.* **2006,** *128,* 1762-1769.

(44) Wang, C.; Li, N.; Shin, D. W.; Lee, S. Y.; Kang, N. R.; Lee, Y. M.; Guiver, M. D. *Macromolecules* **2011,** *44,* 7296-7306.

(45) Li, N.; Wang, C.; Lee, S. Y.; Park, C. H.; Lee, Y. M.; Guiver, M. D. *Angew. Chem. Int. Ed.* **2011,** *50,* 9158-9161.

Chapter 5

Block Copolystyrene Derivatives Containing Pendant Alkyl Sulfonic Acid for Polymer Electrolyte Membranes

ABSTRACT: A series of block copolystyrene derivatives, poly{[4-(4-sulfobutyloxy)styrene]$_x$-*block*-[4-(*n*-butoxystyrene)]$_y$} (PSBOS$_x$-*b*-P*n*BOS$_y$), containing a flexible alkylsufonated side chain and hydrophobic alkoxy chain with various ion exchange capacities (IECs) have been synthesized based on living anionic polymerization. The resulting cross-linked membranes were prepared using 4,4'-methylene-bis[2,6-bis(hydroxyethyl)phenol] (MBHP) as the cross-linker in the presence of methanesulfonic acid. The cross-linked PSBOS$_{2.2}$-*b*-P*n*BOS$_1$ membrane with IEC of 2.89 mequiv/g displayed a fairly high proton conductivity (0.01 S/cm) at a 30% relative humidity and 80 ^{o}C, which was comparable to that of Nafion. The well-developed phase separation and the continuous hydrophilic domains in the cross-linked PSBOS$_{2.2}$-*b*-P*n*BOS$_1$ membranes have been observed in a transmission electron microscope (TEM) image. Moreover, the DMA measurement and Fenton's reagent testing showed that the cross-linked PSBOS$_x$-*b*-P*n*BOS$_y$ membranes have good mechanical properties and oxidative stability. These results indicated that the introduction of flexible alkylsulfonated side chains to the polystyrene main chains positively affected both the proton conductivity and oxidative stability.

5-1. Introduction

Polymer electrolyte membrane fuel cells (PEMFCs) have received tremendous attention because of their potential to achieve higher efficiencies than current power sources using a renewable fuel at a low environmental cost.[1-3] In PEMFCs, the perfluorosulfonic acid polymers, such as Nafion® (DuPont), have been widely utilized as proton exchange membranes (PEMs), serving as both a cell separator and an electrolyte. However, the high cost, high methanol/gas diffusion and the limited operating temperature of the perfluorinated polymers have significantly prevented their widespread use.[4-6] Thus, intensive efforts have been devoted to the development of low-cost proton-conducting sulfonated hydrocarbon polymers used at elevated temperatures to reduce the impurity poisoning of the PEMFCs.[7-8]

The proton conductivity could be one of the most significant characteristics of the PEMs for use in PEMFCs. The proton conductivity of sulfonated hydrocarbon polymers is strongly dependent upon the sulfonic acid group contents, *i.e.,* the ion exchange capacity (IEC) values. These polymers show a suitable conductivity only at high IEC values. However, high IEC values would result in some negative effects on the properties of the PEMs, such as dimensional stability and mechanical strength.[9] Recently, some investigations of PEMs revealed that the proton transport properties are dependent on the polymer morphology, in particular, the nanochannel that contain the sulfonic acid groups.[10-14] The "hydrated" protons can efficiently pass through the proton nanochannels,[15-17] which should increase the proton conductivity even at a low relative humidity (RH).

The block copolymers containing perfectly alternating hydrophilic and hydrophobic segments have received increasing attention because of the enhanced conductivity when compared to the similar structured random copolymers with similar IEC values. It is well-established that block copolymers, having immiscible segments, self-assemble into a range of ordered, periodic structures through the process of microphase separation.[18-19] The morphology and properties of PEMs based on sulfonated polystyrene-containing block copolymers have been extensively studied.[20-29] However, the oxidative stability and mechanical strength have been far less investigated in these reports because polystyrene is not considered to be an ideal material for PEM application due to its poor oxidative stability of the benzylic C-H bond. On the other hand, the results of experiment in chapter 4 showed an interesting finding, the introduction of flexible alkylsulfonated side chains to the random copolystyrene main chains improved the oxidative stability probably due to prevention or reduction of the hydroxyl radical attack

on the polymer main chain, and also increased the proton conductivity at a low RH.[30] An attractive way to obtain a well-organized phase separation is to fabricate block copolymers consisting of hydrophilic and hydrophobic blocks. Some sulfonated multiblock copolymers have been reported, which form nano-size water channels for proton transportation, resulting in less dependence of the humidity on the proton conductivity, as well as improving the mechanical properties compared to the random copolymers with the same IEC.[37] In this chapter, a series of block copolystyrene derivatives having flexible alkylsulfonated side chains and hydrophobic alkoxy chains have been synthesized and the relationship between the block polymer structure and the membrane properties, such as the water uptake, oxidative stability, mechanical properties, proton conductivity, morphology, was also investigated in detail.

5-2. Results and Discussion

5-2-1. Synthesis of PHS_x-*b*-P*n*BOS_y and $PSBOS_x$-*b*-P*n*BOS_y

*n*BOS was prepared via a two-step reaction (Scheme 5-1), that is, the hydrolysis of the acetate group of 4-vinylphenyl acetate, followed by the reaction with 1-bromobutane. As shown in Scheme 5-2, a series of block copolystyrene derivatives, P*t*BOS_x-*b*-P*n*BOS_y, were prepared by the anionic polymerization of *n*BOS and *t*BOS using *sec*-BuLi as the initiator at -78 °C.

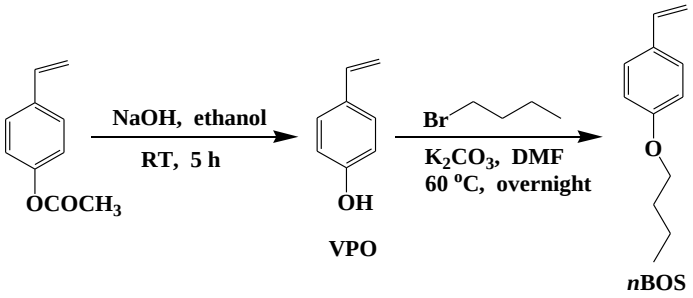

Scheme 5-1. Synthesis of *p*-(*n*-butoxy)styrene (*n*BOS).

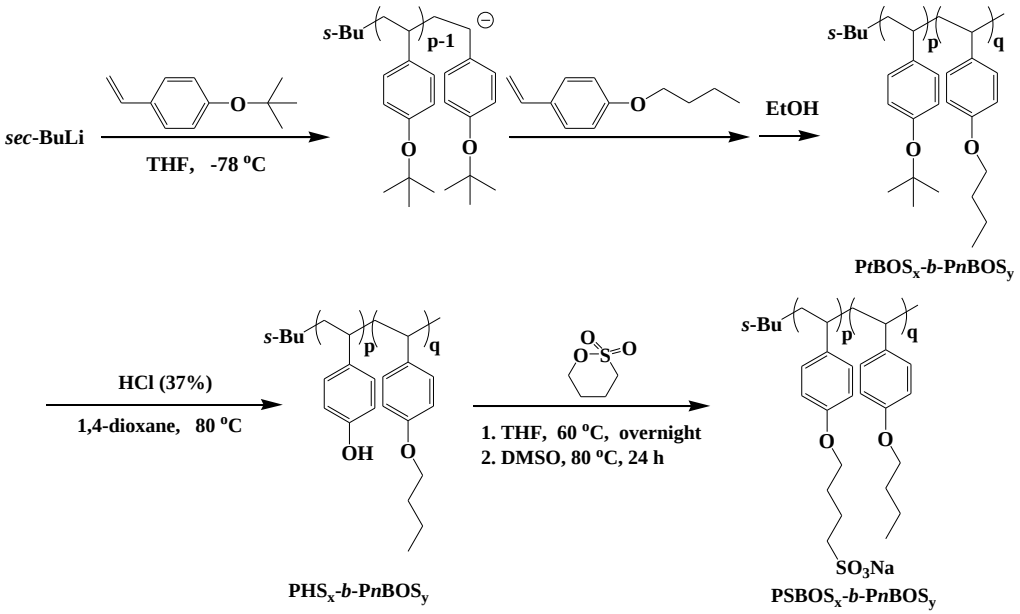

Scheme 5-2. Synthesis of PHS_x-*b*-P*n*BOS_y and $PSBOS_x$-*b*-P*n*BOS_y.

The length of each unit was adjusted by controlling the molecular weight of P*t*BOS_x and P*n*BOS_y (Table 5-1). All the prepared block polymers displayed fairly high molecular weights and a low polydispersity index (PDI). P*t*BOS_1-*b*-P*n*$BOS_{3.2}$, for example, had the number-averaged molecular weight of 1.11×10^5 and PDI of 1.06. The

P*t*BOS$_x$-*b*-P*n*BOS$_y$ was converted to PHS$_x$-*b*-P*n*BOS$_y$ by treatment with an HCl solution, and the PSBOS$_x$-*b*-P*n*BOS$_y$ was produced by the reaction of PHS$_x$-*b*-P*n*BOS$_y$ with the 1,4-butanesultone. The chemical structure of the synthesized *n*BOS was confirmed by ^{1}H NMR (Figure 5-1). The characteristic peaks of the methyl protons at 1.01 ppm and methylene protons next to the ether group at 4.04 ppm were observed. The other peaks were in good agreement with the proposed structure. Figure 5-2 shows the ^{1}H NMR spectra of the block copolymers (a) before and (b) after hydrolysis. The characteristic signal around 1.28 ppm assigned to the *tert*-butyl protons in the initial P*t*BOS$_x$-*b*-P*n*BOS$_y$ block copolymer completely disappeared in the deprotected PHS$_x$-*b*-P*n*BOS$_y$ copolymer, and a broad peak around 8.77 ppm corresponding to the phenol protons appears after the acidic cleavage, indicating that the deprotection was completed. In addition, the compositions of the P*t*BOS$_x$-*b*-P*n*BOS$_y$ block polymers were determined using the relative intensities between the aromatic protons of the phenyl rings and the methyl group of the P*n*BOS$_y$, which were similar to that determined from the GPC. The ^{1}H NMR spectrum of PSBOS$_x$-*b*-P*n*BOS$_y$ showed characteristic methylene protons next to the sodium sulfonate group at 2.73 ppm and the hydroxyl protons completely disappeared (Figure 5-3).

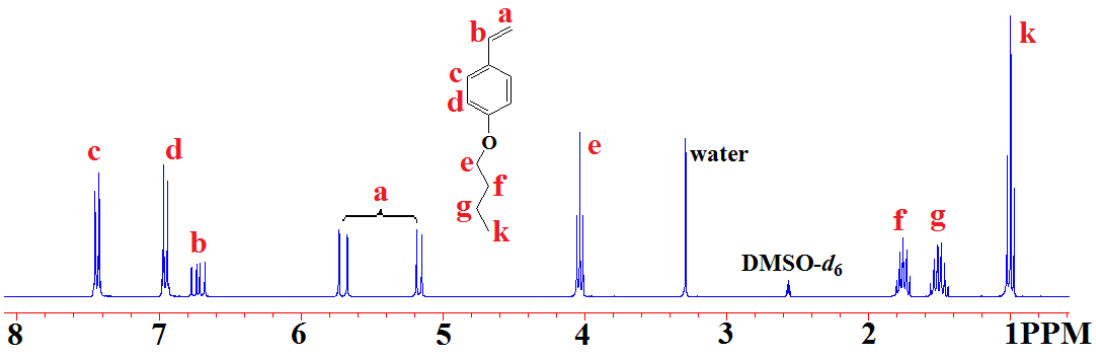

Figure 5-1. ^{1}H NMR spectrum of *n*BOS

Table 5-1. The Molecular Weights and the Compositions of P*t*BOSx-*b*-P*n*BOSy

Sample	Target M_n	M_n (PDI)[a] of P*t*BOS	Total M_n (PDI)[a]
P*t*BOS$_{2.2}$-*b*-P*n*BOS$_1$	30k-10k	27,600 (1.19)	40,300 (1.16)
P*t*BOS$_1$-*b*-P*n*BOS$_{1.3}$	20k-30k	21,600 (1.05)	49,900 (1.04)
P*t*BOS$_1$-*b*-P*n*BOS$_{3.2}$	30k-90k	26,400 (1.06)	111,000 (1.06)

[a]Determined from GPC eluated with $CHCl_3$ calibrated by stabdard polystyrene samples.

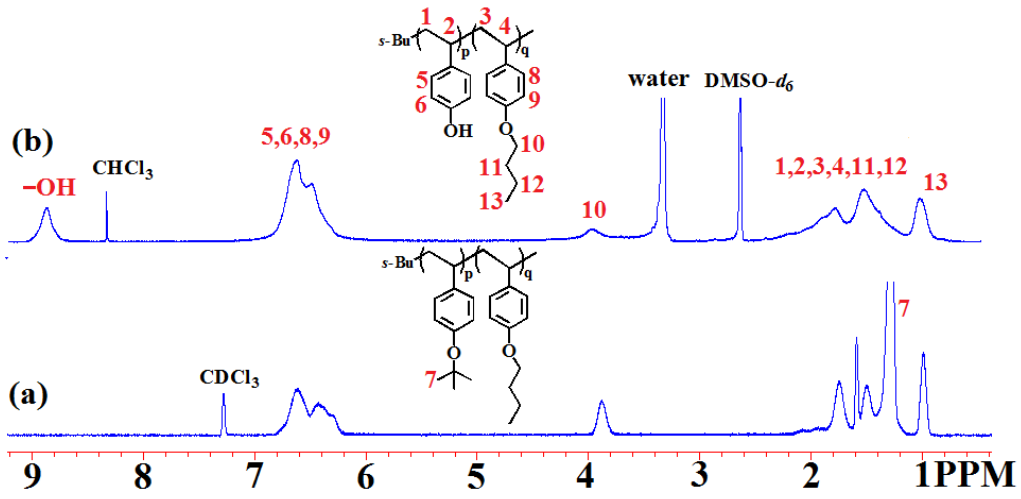

Figure 5-2. ^{1}H NMR spectra of P*t*BOS$_x$-*b*-P*n*BOS$_y$ (a) and PHS$_x$-*b*-P*n*BOS$_y$ (b).

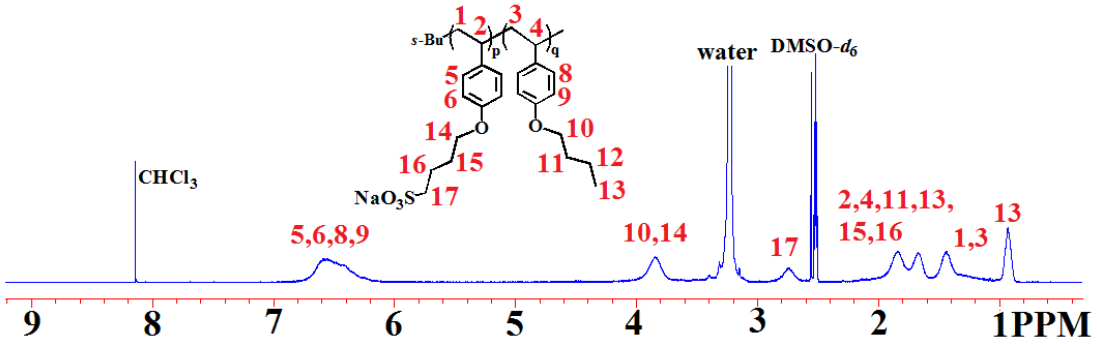

Figure 5-3. ^{1}H NMR spectrum of PSBOS$_x$-*b*-P*n*BOS$_y$.

5-2-2. Preparation of cross-linked PSBOS$_x$-*b*-P*n*BOS$_y$ membranes

The cross-linked PSBOS$_x$-*b*-P*n*BOS$_y$ membranes were prepared according to the chapter 4 with minor modification.[30] A solution of PSBOS$_x$-*b*-P*n*BOS$_y$, 3 mol% of MBHP and a catalytic amount of methanesulfonic acid in DMSO was cast on a glass plate. The film was dried at 80 ℃ for 36 h under ambient conditions, and the obtained membrane was then immersed in water. After the cross-linking reaction, the film became insoluble in water, NMP, and DMSO, which indicated that the crosslinking reaction successfully took place.

5-2-3. Thermal stability and mechanical properties

The thermal stability of the cross-linked PBOS$_x$-*b*-P*n*BOS$_y$ membranes in their proton form was evaluated by TGA under nitrogen (Figure 5-4). Prior to the

measurement, the samples were preheated at 100 ℃ for 30 min to remove any absorbed moisture. A three-step weight loss was observed from 150 °C to 200 °C, from 250 °C to 350 °C, and above 350 °C. The first stage weight loss is due to the dehydration between the sulfonic acids and desulfonation reaction.[35,36] The second and third-stage weight losses are attributed to the decomposition of the polymer side chains and main chains, respectively.

The mechanical property was characterized by the maximum storage modulus (*E'*), maximum stress (MS) and elongation at break (EB). These results are listed in Table 5-2. The *E'* and MS values increased when the decreasing IEC values of the cross-linked PSBOS$_x$-*b*-P*n*BOS$_y$ membranes. The *E'* and MS of the cross-linked PSBOS$_1$-*b*-P*n*BOS$_{1.3}$ are 371 MPa and 30 MPa, respectively. The MS value is two times higher than the cross-linked PSBOS$_{2.2}$-*b*-P*n*BOS$_1$. Moreover, the cross-linked PSBOS$_{2.2}$-*b*-P*n*BOS$_1$ and PSBOS$_1$-*b*-P*n*BOS$_{1.3}$ membranes exhibit a higher maximum stress than the sulfonated PS in spite of the higher IEC values,[32] indicating that the cross-linking reaction has successfully occurred.

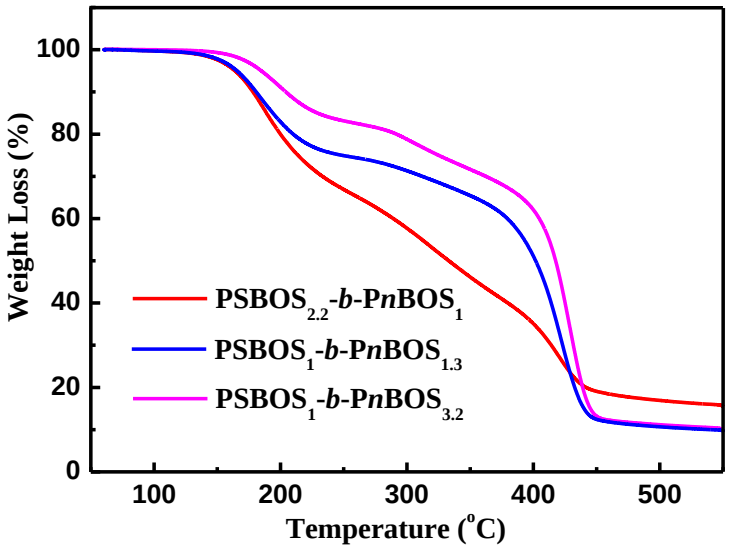

Figure 5-4. TGA curves of the cross-linked PSBOS$_x$-*b*-P*n*BOS$_y$ (in acid form) in N_2.

5-2-4. Oxidative stability

Fenton's test is a common method which has been widely used for evaluating the oxidative stability of PEMs. The membranes are generally immersed in 3% hydrogen peroxide containing 20 ppm $FeSO_4$ at room temperature or 3% hydrogen peroxide

containing 3 ppm $FeSO_4$ at elevated temperature (*e.g.*, 80 ^oC), and the oxidative stability is characterized either by the disappearance time of the membranes or by the weight loss of the membranes as a function of time. In this chapter, 3% hydrogen peroxide containing 20 ppm $FeSO_4$ was used as Fenton's reagent at room temperature. Table 5-2 shows the disappearance time of the cross-linked $PSBOS_x$-*b*-P*n*BOS_y membranes (the size of each sheet: 10 mm long, 7 mm wide and 50-60 um thick). The cross-linked $PSBOS_1$-*b*-P*n*$BOS_{3.2}$ membrane with the lowest IEC value resisted soaking in Fenton's reagent for more than 70 h. It can be seen from the Table 5-2, the oxidative stability is closely related to the IEC levels, and the higher IEC, the lower oxidative stability. However, all the prepared cross-linked membranes displayed a better oxidative stability against Fenton's reagent compared to the other sulfonated polymers with similar IEC values such as the poly(ether sulfone)[31,32] and c-SPS (in chapter 4) which indicated that the introduction of flexible side chains can effectively improve the oxidative stability. It is interesting to compare the stability of the block copolystyrene membranes to that of the random copolystyrene which we have already reported.[30] Although the cross-linked $PSBOS_{2.2}$-*b*-P*n*BOS_1 membranes had a slightly higher IEC than the cross-linked $PBOS_3$-*r*-$PSBOS_7$, the stability was much better for the former than for the latter, which indicated that the more organized morphologies may also enhance the oxidative stability.

5-2-5. IEC, water uptake and dimensional change

The IEC values of the cross-linked $PSBOS_x$-*b*-P*n*BOS_y membranes were determined by a titration method, and the measured IECs were in the range of 1.39-2.89 mequiv/g (Table 5-2). It is well known that the water uptake of most aromatic PEMs strongly affects the proton conductivity because water within the membrane acts as a carrier of the protons. The water uptakes and hydration number (λ) of the cross-linked $PSBOS_x$-*b*-P*n*BOS_y membranes and Nafion 117 are shown in Figures 5-5 (A) and (B), respectively. As shown in Figures 5-5 (A), the water uptakes of the membranes are in the following order: $PSBOS_{2.2}$-*b*-P*n*BOS_1 > $PSBOS_1$-*b*-P*n*$BOS_{1.3}$ > $PSBOS_1$-*b*-P*n*$BOS_{3.2}$, which is just consistent with the IEC order, and increases with the increasing RH. The cross-linked $PSBOS_{2.2}$-*b*-P*n*BOS_1 membrane with the highest IEC value (2.89 mequiv/g) shows the highest water uptake among these membranes. The water uptake is around 70 wt% at 95% RH, which corresponds to an absorption of 12 water molecules per sulfonic acid group. The water uptake and λ dramatically decreases when decreasing the RH, The cross-linked $PSBOS_1$-*b*-P*n*$BOS_{3.2}$ membrane with the low IEC value (1.39

mequiv/g) displays a low water uptake (<2 wt%), corresponding to ~1 water molecule per sulfonic acid group at 30% RH.

Table 5-2. Ion exchange capacities (IECs), disappeared time after Fenton's test, maximum stress (MS), elongation at break (EB) and maximum storage moduli (*E'*s) of the cross-linked $PSBOS_x$-*b*-P*n*BOS_y membranes

Polymer	IEC (mequiv/g)		Disappearance	*E'*	MS[c]	EB[c]
	Theoretical	Measured[a]	time (h)[b]	(10^8 Pa)	(MPa)	(%)
$PSBOS_{2.2}$-*b*-P*n*BOS_1	2.97	2.89	54	2.25	15	15
$PSBOS_1$-*b*-P*n*$BOS_{1.3}$	2.06	2.03	70	3.71	30	7
$PSBOS_1$-*b*-P*n*$BOS_{3.2}$	1.22	1.39	71	7.95	45	8
Sulfonated PS[d]	- [e]	1.50	-	-	2.7[f]	909
Nafion 117[g]	-	0.91	-	0.4-0.5	26	200

[a] By titration method; [b] Measured by soaking the membranes in Fenton's reagent (3% H_2O_2 containing 20 ppm $FeSO_4$) at room temperature; [c] Measured at room temperature and 60% relative humidity; [d] Cited from reference 32; [e] No data in this reference; [f] Tensile strength at break; [g] Cited from reference 30.

The dimensional change in the cross-linked membranes was measured in both the length and thickness directions (Figures 5-6). All the cross-linked membranes exhibit an isotropic swelling, and the dimensional change increases with the increasing IEC and RH. The cross-linked $PSBOS_{2.2}$-*b*-P*n*BOS_1 membrane with the highest IEC among these membranes displays a dimensional change lower than 20% even at 95% RH.

5-2-6. Proton Conductivity

Figure 5-7 shows the variation in the proton conductivity of the cross-linked $PSBOS_x$-*b*-P*n*BOS_y membranes at 80 ^oC as a function of RH, in which the datas of Nafion 117 obtained in this chapter are presented for comparison. Although the proton conductivities of the cross-linked $PSBOS_1$-*b*-P*n*$BOS_{1.3}$ and $PSBOS_1$-*b*-P*n*$BOS_{3.2}$ membranes are lower than that of Nafion 117 in the RH range below 70%, these membranes exhibit higher or comparable proton conductivities compared to Nafion 117 at 95% RH. On the other hand, the cross-linked $PSBOS_{2.2}$-*b*-P*n*BOS_1 membrane shows a fairly high proton conductivity, which is comparable to that of Nafion 117 at 30% RH and higher than that of Nafion 117 in the RH range above 50%, especially, almost 2.5

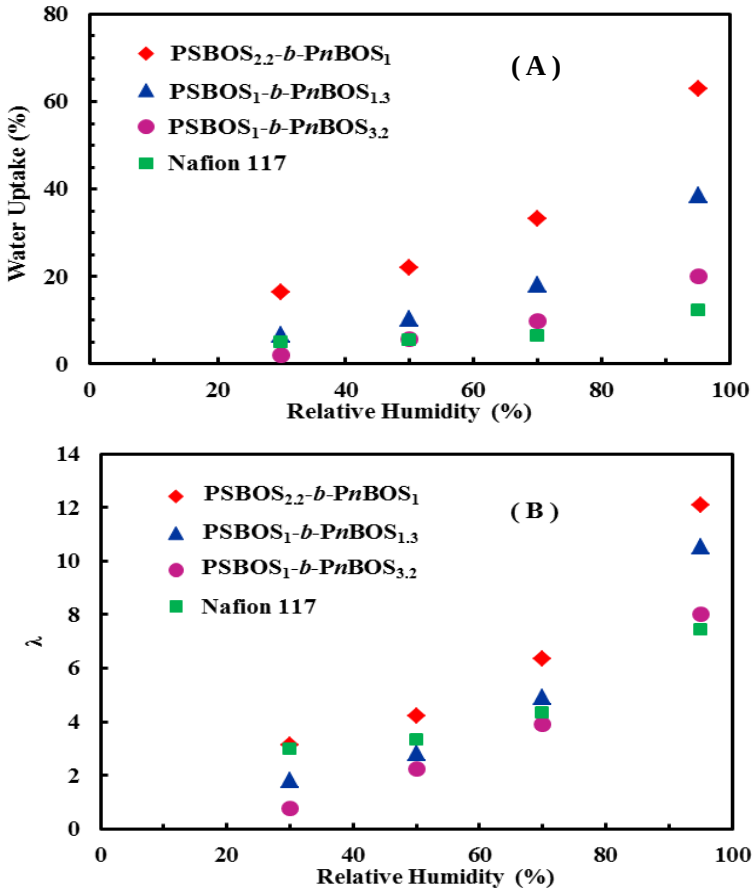

Figures 5-5. (A) Water uptake and (B) hydration number (λ) of cross-linked $PSBOS_x$-*b*-P*n*BOS_y membranes and Nafion 117 at different RH and 80 °C.

times higher at 95% RH. Furthermore, the block copolymers display higher proton conductivities than the corresponding random copolymers we recently reported,[30] despite the lower IEC values. The cross-linked $PSBOS_{2.2}$-*b*-P*n*BOS_1 membrane has the lower IEC value of 2.89 mequiv/g than, for example, that of the random copolymer $PBOS_2$-*r*-$PSBOS_8$ membrane (3.03 mequiv/g), however, the proton conductivities of the former membrane are much higher than the latter membrane over the entire RH range. The proton conductivity of the block copolymers follows the typical proton conductivity behavior of the sulfonated aromatic polymers, depending on the IEC values of the membranes, the higher IEC, the higher proton conductivity. Notably, the difference between the proton conductivity and IEC value is smaller for the $PSBOS_x$-*b*-P*n*BOS_y block copolymers than for the $PBOS_x$-*r*-$PSBOS_y$ random copolymers at a low RH.[30] This is likely related to the differences in morphology of the random and block copolymers. The $PSBOS_x$-*b*-P*n*BOS_y membranes displayed a more well-organized

microphase separation than that of the random $PBOS_2$-*r*-$PSBOS_8$. Although the cross-linked $PSBOS_1$-*b*-P*n*$BOS_{1.3}$ has a low IEC (2.03 mequiv/g), the phase separation between the hydrophilic and hydrophobic domains is clearly observed and the matrix of the hydrophilic domains is well-connected to each other.

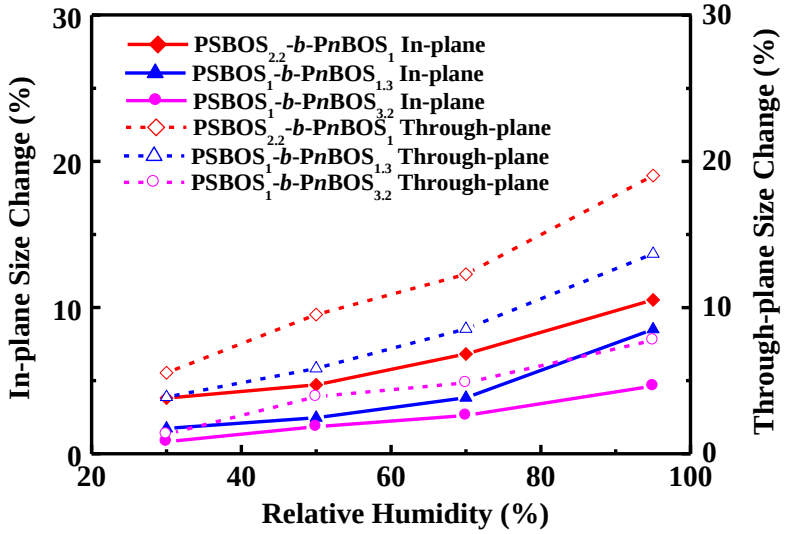

Figure 5-6. Dimensional change of cross-linked $PSBOS_x$-*b*-P*n*BOS_y membranes at different RH and 80 ^oC.

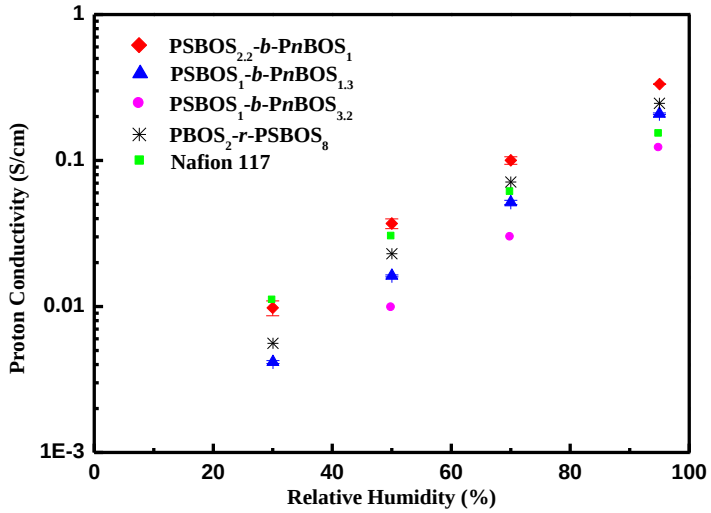

Figure 5-7. Proton conductivity of cross-linked $PSBOS_x$-*b*-P*n*BOS_y membranes and Nafion 117 at different RH and 80 ^oC.

5-2-7. TEM and small angle X-ray scattering (SAXS)

The nanostructure and morphology of the cross-linked PSBOS$_{2.2}$-*b*-P*n*BOS$_1$ and PSBOS$_1$-*b*-P*n*BOS$_{1.3}$ membranes were investigated by TEM using cross-sectional slices of dry membranes and SAXS. The membranes were stained in an aqueous lead acetate solution prior to imaging, therefore, the dark areas in the TEM correspond to the region of hydrophilic domains containing sulfonic acid groups. As can be seen in Figure 5-8, a phase separation between the hydrophilic and hydrophobic domains of both membranes is clearly observed. The interdistance of each domain averages 35 nm for the cross-linked PSBOS$_{2.2}$-*b*-P*n*BOS$_1$ membrane and 30 nm for the cross-linked PSBOS$_1$-*b*-P*n*BOS$_{1.3}$ membrane. The amphiphilic nature of PBOS$_x$-*b*-P*n*BOS$_y$ leads to an enhanced phase separation and aggregation of the ionic cluster. Moreover, the matrices of the hydrophilic domains are well-connected to each other. Figure 5-9 shows the SAXS intensity profiles for the cross-linked PSBOS$_x$-*b*-P*n*BOS$_y$ (in their proton forms) in which the membrane was solution-cast from a mixture of DMSO/THF (5/1 w/w). The SAXS profile also strongly supported the formation of a microphase-separated nanostructure in the resulting membranes. For example, the first scattering peaks of the cross-linked PSBOS$_{2.2}$-*b*-P*n*BOS$_1$ and PSBOS$_1$-*b*-P*n*BOS$_{1.3}$ membranes at 0.016 Å^{-1} and 0.019 Å^{-1} show the formation of the nanostructure with the domain spacing of approximately 39 nm and 33 nm, respectively, which are in good agreement with the averaged distance between the domains observed in the TEM images. Moreover, the SAXS line profile of the cross-linked PSBOS$_1$-*b*-P*n*BOS$_{1.3}$ membranes obviously displayed the first and second order peaks with q values of 0.019 and 0.034 Å^{-1}, thus having the q value ratio of these peaks of 1:$\sqrt{3}$. This is associated with the formation of a hexagonally packed microphase-separated structure in the membrane.

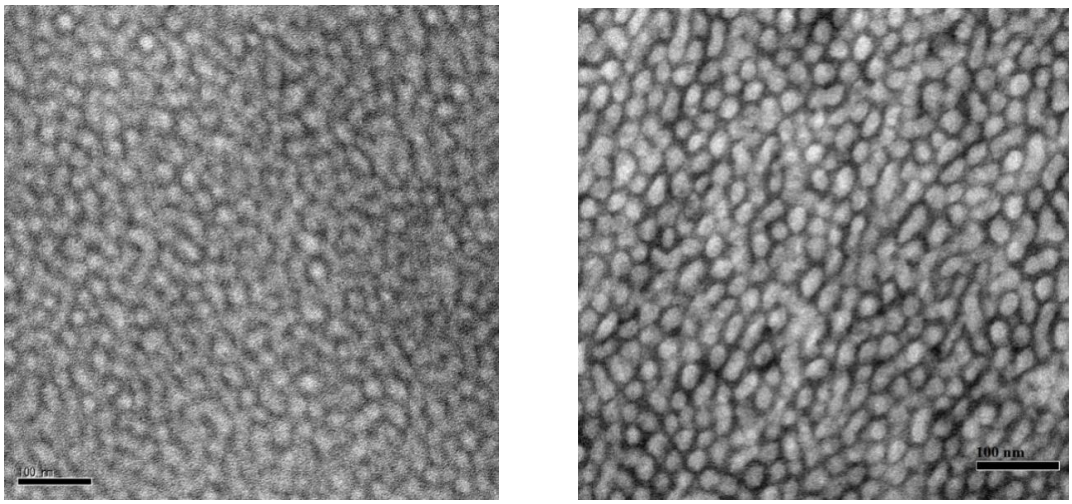

Figure 5-8. TEM image of the crosslinked PSBOS$_{2.2}$-*b*-P*n*BOS$_1$ membrane (L) and PSBOS$_1$-*b*-P*n*BOS$_{1.3}$ membrane (R), scale bar = 100 nm.

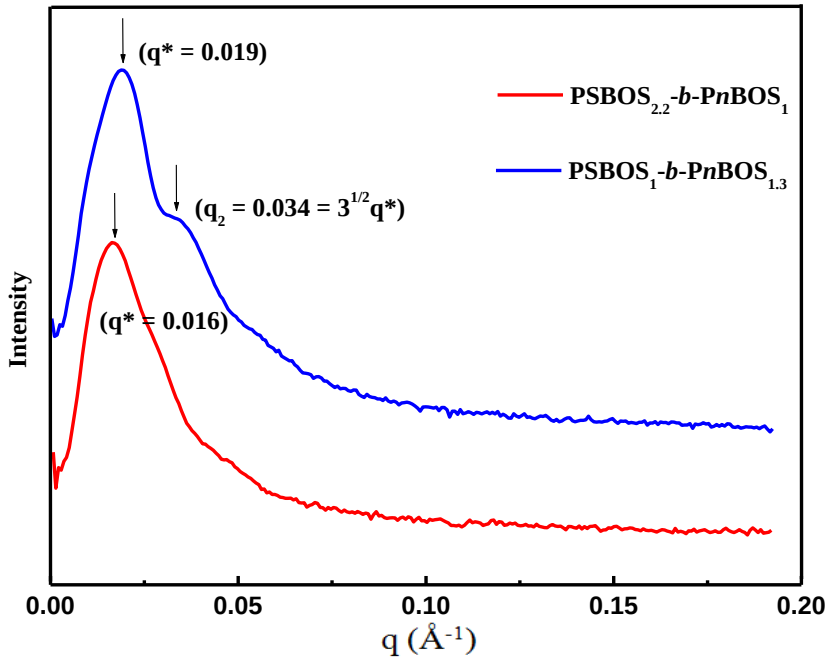

Figure 5-9. Small angle X-ray scattering profiles for cross-linked PSBOS$_{2.2}$-*b*-P*n*BOS$_1$ and PSBOS$_1$-*b*-P*n*BOS$_{1.3}$ membranes.

5-3. Conclusions

A series of PSBOS$_x$-*b*-P*n*BOS$_y$ block copolymers having flexible alkylsulfonated side chains and hydrophobic alkoxy chains were prepared by anionic polymerization of *n*BOS and *t*BOS, the deprotection of the *tert*-butyl ether group, followed by the reaction of the resulting PHS$_x$-*b*-P*n*BOS$_y$ with 1,4-butanesultone. The cross-linked PSBOS$_x$-*b*-P*n*BOS$_y$ membranes were prepared by the reaction of PSBOS$_x$-*b*-P*n*BOS$_y$ with MBHP as the cross-linker in the presence of methanesulfonic acid. The cross-linked PSBOS$_x$-*b*-P*n*BOS$_y$ membranes showed a higher oxidative stability against Fenton's reagent at room temperature, lower water uptake at 95% RH, and good mechanical property than those of the corresponding cross-linked PBOS$_2$-*r*-PSBOS$_8$ random copolymer membranes. Furthermore, the cross-linked PSBOS$_{2.2}$-*b*-P*n*BOS$_1$ membrane exhibited a higher proton conductivity than Nafion 117 over the entire relative humidity range of 30-95%. TEM images showed a well-developed phase separation of the cross-linked PSBOS$_{2.2}$-*b*-P*n*BOS$_1$ and PSBOS$_1$-*b*-P*n*BOS$_{1.3}$ membranes.

5-4. Experimental

Materials.

4-Vinylphenyl acetate, 1,4-butanesultone, 1-bromobutane, 4-*tert*-butoxystyrene (*t*BOS), 1,4-dioxane, hydrochloric acid (HCl), dimethylsulfoxide (DMSO, anhydrous) were purchased from TCI. Co. *sec*-butyllithium in cyclohexane, *n*-hexane (*s*-BuLi) and di-*n*-butylmagnesium, 1.0 M solution in heptanes were purchased from Sigma-Aldrich Co. *t*BOS was purified by washing sequentially with diluted aqueous base, water followed by drying with magnesium sulphate (dried), and distilled under reduced pressure from finely ground CaH_2 and stored in the glovebox under the purified nitrogen atmosphere. The other reagents were used as received. Hydrazine hydrate and 2,2'-azobis(isobutyronitrile) (AIBN), tetrahydrofuran (THF, super dehydrated) were purchased from Wako. Co. 4,4'-Methylene-bis[2,6-bis(hydroxyethyl)phenol] (MBHP) was prepared according to the chapter 4.[33]

Synthesis of *p*-(*n*-butoxy)styrene (*n*BOS).

4-Vinylphenol (VPO) was prepared from 4-vinylphenyl acetate according to the procedures in the literature with minor modification.[34] After stirring the ethanol/NaOH solution of 4-vinylphenyl acetate at room temperature for 5 h, the solvent was evaporated, then the residue was dissolved in ethyl acetate. The organic layer was washed with a citric acid solution and water several times, followed by drying with anhydrous magnesium sulphate. The mixture was filtered, and the solvent was evaporated under reduced pressure. The product was isolated by drying under reduced pressure at room temperature for 3 h. Yield: 85%. ^{1}H NMR (DMSO-d_6, ppm): δ 5.01-5.07 (d, 1H, -CH=CH_2), δ 5.53-5.61 (d, 1H, -CH=CH_2), δ 6.56-6.68 (q, 1H, -C*H*=CH_2), δ 6.72-6.79 (d, 2H, -C*H*- in Ph), δ 7.24-7.31 (d, 2H, -C*H*- in Ph), δ 9.37-9.45 (s, 1H, -O*H*-).

To a 250 mL dry flask were added VPO (24.0 g, 200 mmol) and K_2CO_3 (41.4 g, 300 mmol). This flask was evacuated and filled with nitrogen three times. Then anhydrous DMF (150 mL) and 1-bromobutane (32.5 mL, 300 mmol) were added via syringe through the septum cap. The reaction mixture was magnetically stirred at 60 ^{o}C under nitrogen overnight. The mixture was cooled to room temperature, and then was poured into water. After the mixture was extracted by ethyl ether, the organic layer was washed with water three times, and dried with magnesium sulphate. The mixture was filtered, and the solvent was evaporated under educed pressure. The product (BOS) was isolated by column chromatography on silica gel (hexane). Yield 31.7 g, (90%). ^{1}H NMR

(DMSO-d_6, ppm): δ 0.96-1.95 (t, 3H, -CH_2CH_3-), δ 1.44-1.58 (m, 2H, -CH_2C$H_2$$CH_3$-), δ 1.70-1.83 (m, 2H, -C$H_2$$CH_2$$CH_3$-), δ 4.00-4.09 (t, 2H, -OC$H_2$$CH_2$-),δ 5.13-5.21 (d, 1H, -CH=CH_2), δ 5.65-5.76 (d, 1H, -CH=CH_2), δ 6.65-6.79 (q, 1H, -C*H*=CH_2), δ 6.91-7.00 (d, 2H, -C*H*- in Ph), δ 7.40-7.48 (d, 2H, -C*H*- in Ph).

BOS was further purified by washing sequentially with diluted aqueous base, water followed by drying with magnesium sulfate, and distilled under reduced pressure over finely ground CaH_2 and stored in the glovebox.

Synthesis of P*t*BOS$_x$-*b*-P*n*BOS$_y$ (x and y refer to the molar ratio of each unit calculated from gel permeation chromatography (GPC))

P*t*BOS$_x$-*b*-P*n*BOS$_y$ block copolymers composed of different length blocks were synthesized through anionic polymerization in THF at -78 ^oC using *sec*-BuLi as an initiator. All the polymerizations were performed in the glovebox. A general procedure is described below using P*t*BOS$_1$-*b*-P*n*BOS$_{1.3}$, consisted of a poly(4-*tert*-butoxystyrene) (P*t*BOS) segment with the target M_n of 20,000 and a poly(*n*-butoxystyrene) (P*n*BOS) segment with an M_n of 30,000, as an example.

To a 100 mL dry one-necked flask were added anhydrous THF (10.0 mL) and *t*BOS (1.07mL). A suitable quantity of di-*n*-butylmagnesium was also added at -78 ^oC to remove residual protic sources, followed by adding the *sec*-BuLi (0.050 mL, 0.050 mmol) solution in cyclohexane to initiate the polymerization. A bright yellow-orange color appeared corresponding to the carbanion. The polymerization was allowed to perform for 1 h and some drops of polymer solution were transferred to ethanol for measuring molecular weight by GPC. The THF (10.0 mL) solution of *n*BOS (2.14 mL) and a suitable quantity of di-*n*-butylmagnesium was transferred into the above P*t*BOS anion solution at -78 ^oC. Upon the addition of *n*BOS the color changed immediately to the bright yellow. After another 2 h, ethanol was added to terminate the polymerization. The block polymer was isolated by precipitation in methanol, filtered, and dried at 40 ^oC for 20 h in vacuum.

Synthesis of PHS$_x$-*b*-P*n*BOS$_y$

The *tert*-butyl group of P*t*BOS$_1$-*b*-P*n*BOS$_{1.3}$ (2.00 g, 4.94 mmol of P*t*BOS) was deprotected by treating with hydrochloric acid (37 wt%, 3.00 mL) in 1,4-dioxane (26.0 mL) at 80 ^oC overnight, followed by cooling to room temperature. The mixture was carefully poured into water with stirring, then the polymer was washed with water several times, and dried at 80 ^oC for 24 h in vacuum. Yield 1.67 g, (97%).

Synthesis of PSBOS$_x$-*b*-P*n*BOS$_y$

The mixture of PHS$_1$-*b*-P*n*BOS$_{1.3}$ (0.872 g, 2.50 mmol), sodium hydride (0.120 g, 5.00 mmol) and 1,4-butanesultone (0.681 g, 5.00 mmol) were stirred in THF (8.00 mL) at 60 ^{o}C overnight, and then another 8 mL DMSO was added into the mixture. The mixture was stirred at 80 ^{o}C for 24 h, and was then poured into methanol. The isolated polymer was dried at 60 ^{o}C for 5 h in vacuum. Yield 1.24 g, (98%).

Crosslinked membrane formation and proton exchange

The PSBOS$_x$-*b*-P*n*BOS$_y$ in their sodium salt form and the cross-linker, MBHP (3 mol% to the polymer) were dissolved in DMSO/THF (5/1w/w) to give a 5-8 w/v% solution, then one drop of methanesulfonic acid in DMSO solution was added. The solution was cast onto a glass plate, and heated at 80 ℃ for 36 h to give a transparent membrane. The as-cast membrane was immersed in water to remove any residual solvent.

Proton exchange treatment was performed by immersing the crosslinked PSBOS$_x$-*b*-P*n*BOS$_y$ membrane in 1 M sulfuric acid solution at room temperature for three days. The membrane was taken out, and rinsed with deionized water till the rinsed water became neutral.

Measurements

^{1}H NMR spectrum was recorded on a Bruker DPX300S spectrometer using $CDCl_3$ or DMSO-d_6 as solvent. Number- and weight-average molecular weights (M_n and M_w) were measured by gel permeation chromatography (GPC) on a Hitachi LC-7000 system equipped with polystyrene gel columns (TSKgel GMHHR-M) eluted with chloroform ($CHCl_3$) at a flow rate of 1.0 mL/min calibrated by standard polystyrene samples.

Thermogravimetric analysis (TGA) was performed in nitrogen with a Seiko EXSTAR 6000 TG/DTA 6300 thermal instrument. Prior to measurement, all the samples were preheated at 100 ℃ for 30 min to remove any absorbed moisture. Subsequently the samples were cooled to 50 ℃ and then reheated to 550 ℃ at a heating rate of 10 ℃/min.

Dynamic mechanical analysis (DMA) was measured on a Seiko DMA 6300 apparatus in tension mode at a frequency of 1.0 Hz under nitrogen atmosphere at a heating rate of 2 ℃/min. The samples were 10 mm long, 4 mm wide and 35-52 μm thick.

Thermomechanical analysis (TMA) was measured on a Seiko TMA/SS 6100 apparatus at room temperature and 60% RH. For each kind of membranes, two samples

were used for measurements and the samples were 12 mm long, 3 mm wide and 35-60 μm thick.

Ion exchange capacity (IEC) was measured by a titration method. The samples were immersed in saturated NaCl solution at room temperature for 3 days. After that, the samples were not taken out and the NaCl solution was directly titrated with 0.02 M NaOH using phenolphthalein as pH indicator.

The oxidation stability of the membranes was determined by Fenton's test. The samples were soaked in the Fenton's reagent (3% H_2O_2 containing 20 ppm $FeSO_4$) at room temperature. The disappearance time of the samples was used to evaluate the radical oxidation stability of the membranes.

Water uptake of $PSBOS_x$-*b*-P*n*BOS_y membranes was measured by placing the membrane in a thermo-controlled humid chamber. The membranes were set at desired values and kept constant for 2 h at each point. Then the membrane was taken out, and quickly weighed on a microbalance. Water uptake (WU) was calculated according to the following equation:

$$WU = (W_s - W_d) / W_d \times 100 \text{ wt \%}$$

where W_s and W_d are the weights of wet and dried membranes, respectively. Water sorption was also expressed as the average number of water molecules per ion exchange site ($[H_2O]/[SO_3^-]$), often referred to as λ value, and calculated according to the following equation:

$$\lambda = [H_2O] / [SO_3^-] = \text{water uptake (\%)} \times 10 / [18 \times \text{IEC (mmol/g)}]$$

Dimensional change of a hydrated membrane was also investigated by placing the membrane in a thermo-controlled humid chamber (80 ^oC) at desired RH for 2 h, and the changes of length and thickness were calculated from

$$\Delta l = (l_s - l_d) / l_d \times 100 \text{ \%}$$

$$\Delta t = (t_s - t_d) / t_d \times 100 \text{ \%}$$

where l_s and t_s are the length and thickness of the wet membrane, respectively, l_d and t_d refer to those of the dried membrane.

Proton conductivity was measured using a two-probe electrochemical impedance spectroscopy technique over the frequency from 5 Hz to 1 MHz (Hioki 3532-80). The samples were 8 mm long, 8 mm wide and 30-55 μm thick. Proton conductivity (σ) was calculated from the following equation:

$$\sigma = d/(t_s w_s R)$$

where d is the distance between the two electrodes, t_s and w_s are the thickness and width of the membrane, and R is the resistance measured.

For TEM observations, the membranes were stained with lead ions by ion exchange of the sulfonic acid groups in a 2 wt% $Pb(NO_3)_2$ aqueous solution for 3 days, immersed into deionised water for 1 days, and dried at 60 ^oC overnight. The stained membranes were embedded in an epoxy resin, sectioned to 90 nm thickness at -50 ^oC using a microtome Ultracut UCT equipped with a cryo unit of Leica EMFCS, and placed on a copper grid. The TEM images were taken on a Hitachi H7650 with an accelerating voltage of 100 kV.

Small angle X-ray Scattering (SAXS) was performed using Bruker NanoSTAR. The scattering was recorded by charge coupled device (CCD). The intensity of scattering peaks is a function of the magnitude of scattering vector $q = 4\pi\sin\theta / \lambda$, where λ is the X-ray wavelength of 1.54 Å (Cu Kα radiation) and 2θ is scattering angle. The d spacing was calculated from Bragg's equation, $d = 2\pi / q^*$ with q^* being the position of primary scattering peak.

5-5. References

(1) Elabd, Y. A.; Napadensky, E.; Walker, C. W.; Winey, K. I. *Macromolecules* **2006**, *39*, 399-407.

(2) Costamagna, P.; Srinivasan, S. *J. Power Sources* **2001**, *102*, 253-269.

(3) Hickner, M. A.; Ghassemi, H.; Kim, Y. S.; Einsla, B. R.; McGrath, J. E. *Chem. Rev.* **2004**, *104*, 4587-4611.

(4) Roziere, J.; Jones, D. J. *Annu. Rev. Mater. Res.* **2003**, *33*, 503-555.

(5) Lakshmanan, B.; Huang, W.; Olmeijer, D.; Weidner, J. W. *Electrochem. Solid-State Lett.* **2003**, *6*, A282-A285.

(6) Schuster, M. E.; Meyer, W. H. *Annu. Rev. Mater. Res.* **2003**, *33*, 233-261.

(7) Rikukawa, M.; Sanui, K. *Prog. Polym. Sci.* **2000**, *25*, 1463-1502.

(8) Li, Q.; He, R.; Jensen, J. O.; Bjerrum, N. J. *Fuel Cells* **2004**, *4*, 147-159.

(9) Si, K.; Dong, D. Wycisk, R. Litt, M. *J. Mater. Chem.* **2012**, 22, 20907-20917.

(10) Matsumoto, K.; Higashihara, T.; Ueda, M. *Macromolecules* **2009**, 42, 1161-1166.

(11) Li, N. W.; Wang, C. Y.; Lee, S. Y.; Park, C. H.; Lee, Y. M.; Guiver, M. D. *Angew. Chem. Int. Ed.* **2011**, 50, 9158-9161.

(12) Bae, B.; Miyatake, K.; Watanabe, M. *Macromolecules* **2010**, 43, 2684-2691.

(13) Chang, Y.; Brunello, G. F.; Fuller, J.; Hawley, M.; Kim, Y. S.; Miller, M. D.; Hickner, M. A.; Jang, S. S.; Bae, C. *Macromolecules* **2011**, 44, 8458-8469.

(14) Lee, H.-C.; Lim, H.; Su, W.-F.; Chao, C.-Y. *J. Polym. Sci. Part A: Polym. Chem.* **2011**, 49, 2325-2338.

(15) Diat, O.; Gebel, G. *Nat. Mater.* **2008**, 7, 13-14.

(16) Schmidt-Rohr, K.; Chen, Q. *Nat. Mater.* **2008**, 7, 75-83.

(17) Elliott, J. A.; Hanna, S.; Elliott, A. M. S.; Cooley, G. E. *Macromolecules* **2000**, 33, 8708-8713.

(18) Bates, F. S.; Fredrickson, G. H. *Annu, Rev. Phys. Chem.* **1990**, 41, 525-557.

(19) Bates, F. S.; Schulz, M. F.; Khandpur, A. K.; Forster, S.; Rosedale, J. H.; Almdal, K.; Mortensen, K. *Faraday Discuss.* **1994**, 98, 7-18.

(20) Mokrini, A.; Acosta, J. L. *Polymer* **2001**, 42, 9-15.

(21) Mauritz, K. A.; Blackwell, R. I.; Beyer, F. L. *Polymer* **2004**, 45, 3001-3016.

(22) Weiss, R. A.; Sen, A.; Pottick, L. A.; Willis, C. L. *Polymer* **1991**, 32, 2785-2792.

(23) Lu, X.; Steckle, W. P.; Weiss, R. A. *Macromolecules* **1993**, 26, 5876-5884.

(24) Elabd, Y. A.; Napadensky, E. *Polymer* **2004**, 45, 3037-3043.

(25) Kim, B.; Kim, J.; Jung, B. *J. Membr. Sci.* **2005**, 250, 175-182.

(26) Won, J.; Choi, S. W.; Kang, Y. S.; Ha, H. Y.; Oh, I. H.; Kim, H. S.; Kim, K. T.; Jo, W. H. *J. Membr. Sci.* **2003**, 214, 245-257.

(27) Kim, J.; Kim, B.; Jung, B.; Kang, Y. S.; Ha, H. Y.; Oh, I. H.; Ihn, K.J. *Macromol. Rapid Commum.* **2002**, 23, 753-756.

(28) Kim, J.; Kim, B.; Jung, B. *J. Membr. Sci.* **2002**, 207, 129-137.

(29) Mani, S.; Weiss, R. A.; Williams, C. E.; Hahn, S. F. *Macromolecules* **1999**, 32, 3663-3670.

(30) Sheng, L.; Higashihara, T.; Nakazawa, S.; Ueda, M. *Polym. Chem.* **2012,** 3, 3289-3295.

(31) Nakagawa, T.; Nakabayashi, K.; Higashihara, T.; Ueda, M. *J. Mater.Chem.* **2010**, 20, 6662-6667.

(32) Matsumoto, K.; Nakagawa, T.; Higashihara, T.; Ueda, M. *J. Polym. Sci. Part A: Polym. Chem.* **2009,** 47, 5827-5834.

(33) Mitsui Petrochemical Industries, Ltd., Jpn. Kokai Tokkyo Koho JP 58, 116, 433 [83, 116, 433], 1983; *Chem. Abstr.* **1984**, 100, 7356n.

(34) Dale, W. J.; Hennis, H. E. *J. Am. Chem. Soc.* **1958**, 80, 3645-3649.

(35) Yasuda, T.; Li, Y.; Miyatake, K.; Hirai, M.; Nanasawa, M.; Watanabe, M. J. *Polym. Sci. Part A: Polym. Chem.* **2006,** 44, 3995-4005.

(36) Miyatake, K.; Yasuda, T.; Hirai, M.; Nanasawa, M.; Watanabe, M. *J. Polym. Sci. Part A: Polym. Chem.* **2007,** 45, 157-163.

(37) Park, C. H.; Lee, C. H.; Guiver, M. D.; Lee, Y. M. *Prog. Polym. Sci.* **2011,** 36, 1443- 149

Chapter 6

Poly(*m*-phenylene)s Containing Pendant Alkyl Sulfonic Acid for Polymer Electrolyte Membranes

ABSTRACT: Polymer electrolyte membranes (PEMs) based on the cross-linked poly(*m*-phenylene)s with sulfonic acid via long alkyl side chains (c-SPMPs) were successfully obtained by the reaction of the phenyl groups in the sulfonated poly(*m*-phenylene)s (SPMPs) and 4,4'-methylene-bis[2,6-bis(hydroxyethyl)phenol] (MBHP) as the cross-linker in the presence of methanesulfonic acid. The c-SPMPs produced transparent membranes with a relatively high mechanical property in the dry state, regardless of their high ion exchange capacity (IEC) values. The rigid main chains and the cross-linking structure suppressed the unacceptable water uptake and dimensional change of the c-SPMPs membranes even in the hydrated state. The c-SPMP8-2 membrane with IEC = 2.93 mequiv/g showed a higher proton conductivity than Nafion 117 over a wide range of relative humidities (30-95%) at 80 ^{o}C. The c-SPMP membranes might be promising alternatives of the perfluorinated PEM materials based on both advantageous features of a high proton conductive performance and straightforward synthetic method.

6-1. Introduction

Polymer electrolyte membranes (PEMs) are key materials for polymer electrolyte membrane fuel cells (PEMFCs) which are one of the clean and efficient energy sources as alternatives to limited fossil fuel resources[1-19]. Among the PEMs, sulfonated perfluoropolymers (*e.g.* Dupont's Nafion®, 3M, Aquivion® membranes) have been widely used for PEMFCs because of their high proton conductivity and high chemical stability. By chemical modifications or stabilizations, their new products (*e.g.* NRE212, PFIA, Aquivion™, etc)[5] could be used even at a high temperature of 120 ^{o}C. However, some other notable drawbacks such as harsh producing process, high cost, and environmental pollutions still restrict their practical use more or less. Hence, a number of sulfonated aromatic hydrocarbon-based polymers have been developed as alternatives to the perfluorinated PEM materials.[3-19] However, in spite of numerous efforts, the performance of hydrocarbon-based PEM materials, especially their proton conductivity at a low relative humidity (RH) even with high ion exchange capacities (IECs), is still inferior to that of the perfluorinated PEM materials, probably due to the weak phase separation between the hydrophilic and hydrophobic moieties. Consequently, further improvement in the hydrocarbon-based PEM performance is essential for realization of the PEMFCs.

Recently, sulfonated polyphenylenes (SPPs) have drawn much attention as alternatives to Nafion® for fuel cell applications.[20-29] Among them, sulfonated poly(*p*-phenylene)s (SPPPs) and their derivatives are of great interest due to their stiff and rod-like chemical structures which generally exhibit an exceptionally good mechanical toughness and chemical stability. Rikukawa and co-workers first reported the preparation of SPPPs using commercially available PPPs, followed by post-sulfonation.[22] Ohira et al. reported SPPPs with long side chains by the Ni(0) catalyzed coupling polymerization from 2,5-dichloro-4-(phenoxypropyl)benzoyl chloride, followed by sulfonation, and the membrane with the IEC value of 3.39 mequiv/g showed a high proton conductivity comparable to Nafion 112 at 80 ^{o}C and 30% RH.[8,26] More recently, to improve the solubility of the final SPPP polymers, Chen and co-workers developed a series sulfonated poly(*p*-phenylene-*co*-arylene ether ketone)s from different types of dichloro-monomers also by the Ni(0) catalyzed coupling polymerization. Their membrane with the IEC value of 2.38 mequiv/g exhibited a proton conductivity of 1.7 mS/cm at 60 ^{o}C and 30% RH, which is one-third that of Nafion 112.[28] Quite recently, Rikukawa et al. reported another hydrophilic-hydrophobic block SPPP with a narrow polydispersity index (PDI) using a

catalyst-transfer polycondensation method. Although their polymers showed a clear phase separation, the proton conductivity of the membrane with the IEC value of 2.2 mequiv/g was lower than 1 mS/cm at 80 ^{o}C and 30% RH.[30] Generally, SPPPs should have a fairly high molecular weight (MW) for good handling and mechanical stabilities. However, it is, in most cases, difficult to prepare high MW SPPPs and post-functionalize them for further molecular designs due to their low solubility in most organic solvents.

Compared to poly(*p*-phenylene)s, poly(*m*-phenylene)s with meta-linkages between the monomer units seem to be preferred based on solubility, since it increases the main chain flexibility and the conformational disorder in the solid state. Rager et al. first developed the poly(*m*-phenylene)s with phosphonic acids directly introduced into the phenyl rings as polymer electrolytes.[31] However, the MWs of the polymers were not high enough, thus more or less unsuitable for practical applications. In an earlier decade, Ueda et al. reported the facile synthesis of poly(4,6-di-*n*-butoxy-1,3-phenylene) using $FeCl_3$ as the oxidant.[32] The resulting polymer had a high regioregularity as well as a high MW. Meanwhile, in recent decades, many researchers proved that flexible pendant hydrophilic sulfonic acid groups in the side chains could effectively form the phase separations thus enhance the proton conductivities.[17,25,26,30] For example, Lee's group developed a type of poly(arylene ether sulfone) with long flexible acid side chains, and their membranes showed a 1-3 nm width of the hydrophilic clusters based on TEM photographs.[17] Ueda et al. also prepared poly(phenylene ether)s with pendant perfluoroalkyl sulfonic acids side chains. Owing to the flexibility and high acidity of the side chains, their membranes with an IEC of 1.8 mequiv/g showed proton conductivities comparable to that of Nafion even at a 30% RH.[25]

In this chapter, we used this concept to prepare cross-linked sulfonated poly(*m*-phenylene)s with long alkyl side chains (c-SPMPs) for the first time. Considering the straightforward synthetic process as well as the commercially available raw materials, this type of PEM could attract significant attention from industries compared to some other methods using high cost catalysts. It should be mentioned that the c-SPMP8-2 membrane with IEC = 2.93 mequiv/g showed a higher proton conductivity than Nafion 117 over a wide range of RH at 80 ^{o}C. Furthermore, their membrane properties, such as water uptake, dimensional change, thermal and mechanical stabilities and morphology were investigated in detail.

6-2. Results and Discussion

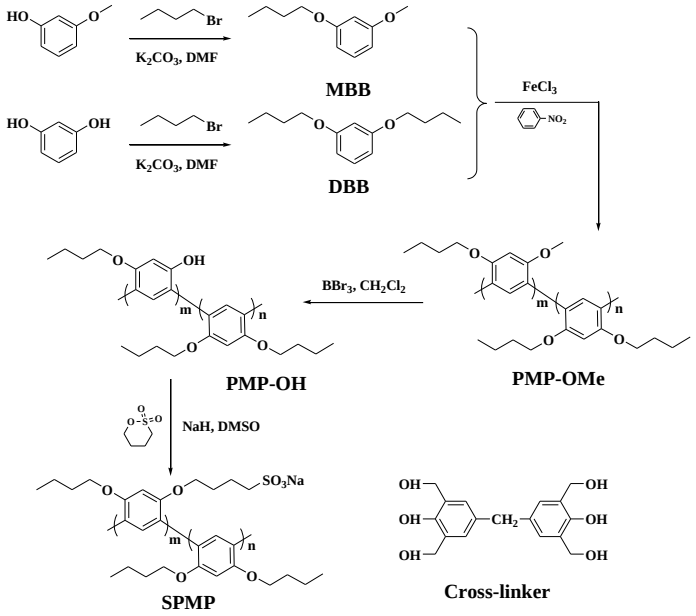

Scheme 6-1. Synthetic routes for SPMPs and the structure of cross-linker (MBHP).

Table 6-1. Polymerizations of MBB and DBB

Run	Feed Ratio		GPC		
	MBB/mol	DBB/mol	M_n(kDa)	M_w(kDa)	*PDI*
PMP-OMe-1	5	5	28	56	2.0
PMP-OMe-2	7	3	27	67	2.5
PMP-OMe-3	8	2	31	64	2.1

6-2-1. Synthesis of monomers and polymers

Scheme 6-1 shows the synthetic routes for the sulfonated poly(*m*-phenylene)s (SPMPs). Two monomers, MBB and DBB, were prepared by the Williamson reaction of *m*-methoxyphenol and resorcinol with 1-bromobutane, respectively.

For an oxidative coupling polymerization, it is very important to select monomers with a low oxidation potential in which the polymerization initiation easily occurs. The oxidation potentials (*E*) of the monomers were measured by cyclic voltammetry (CV). As shown in Figure 6-1, the *E* values could be observed at 1.26 V and 1.25 V for MBB and DBB versus SCE, respectively. The *E* value for DBB was also similar to our previous report.[32]

The oxidative coupling polymerizations of MBB and DBB by changing the molar ratios of both monomers were carried out in the presence of anhydrous $FeCl_3$ as the

oxidizing agent in nitrobenzene at room temperature, producing the corresponding PMP-OMe copolymers. As published elsewhere,[33,34] the oxidative coupling polymerization was usually processed by the slow addition of a solution of anhydrous $FeCl_3$ to the polymerization solution. However, this method always produced only oligomeric products in our case. Therefore, the monomers and anhydrous $FeCl_3$ were mixed together, followed by injecting nitrobenzene to efficiently start the polymerization. The results are summarized in Table 6-1.

The number-average molecular weight (M_n) and PDIs of PMP-OMe were around 2.7 $\times 10^4$ - 3.1$\times 10^4$ and 2.0-2.5, respectively. All of the PMP-OMes were soluble in the common organic solvents, such as CH_2Cl_2, THF, DMF, etc.

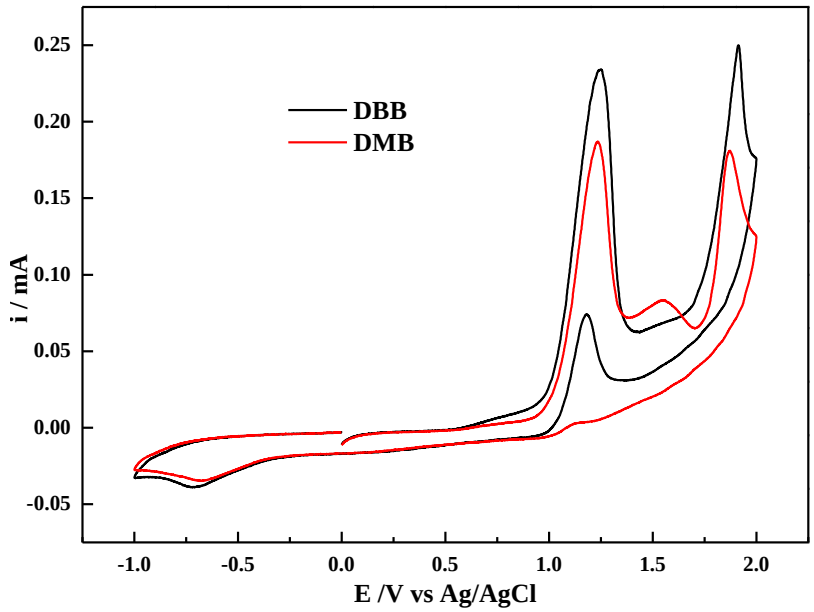

Figure 6-1. CV curves of monomers DBB and MBB.

Figure 6-2 shows the ^{1}H NMR spectrum of PMP-OMe-2. The broad signals at 0.69, 1.22, and 1.49 ppm are assigned to the methyl, γ-methylene, and β-methylene protons, respectively. Protons in the methoxy and α-methylene of the alkoxy group are overlapped and appear around 3.88 to 3.67 ppm. Meanwhile, the signals at 6.90 and 6.61 ppm are assigned to the aromatic protons. PMP-OMe was then converted to the copolymer with phenolic hydroxy groups (PMP-OH) by treatment with BBr_3. Finally, the SPMPs were obtained by the reaction of the resulting PMP-OH with 1,4-butanesultone. In this study, the nomenclature of the membranes is as follows: c-SPMPx-y, where **x-y** refers to the molar ratio of MBB to DBB. The structures of the

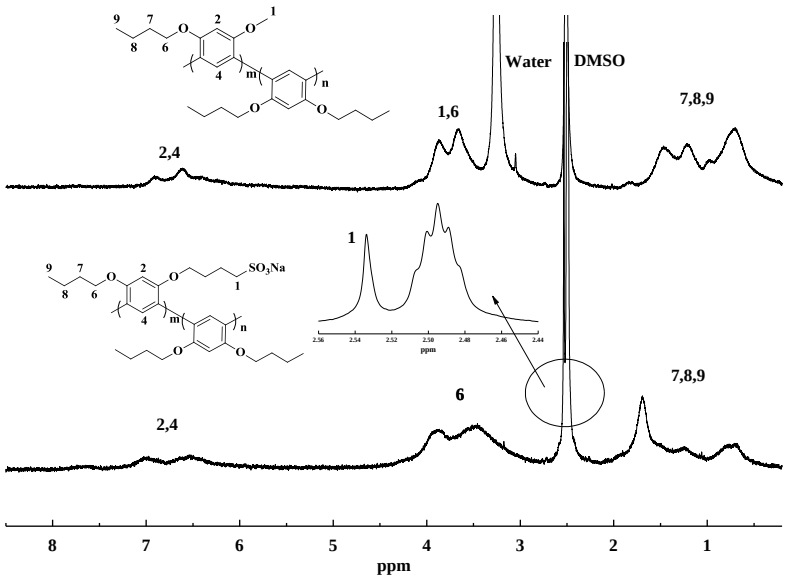

Figure 6-2. ^{1}H NMR spectra of PMP-OMe-2 and SPMP7-3 in DMSO-d_6.

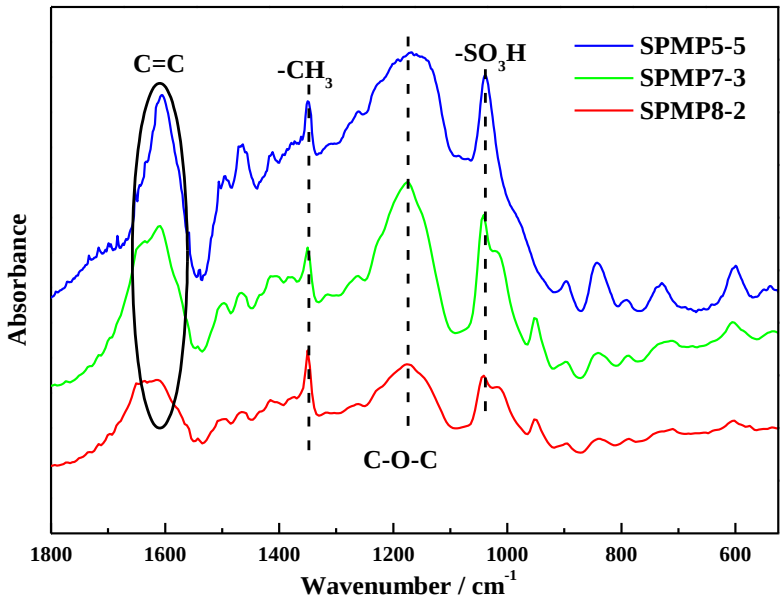

Figure 6-3. FTIR spectra of **SPMPs**.

SPMP copolymers were also confirmed by the IR and ^{1}H NMR spectroscopies. The IR spectrum of SPMPs (Figure 6-3) show characteristic absorptions corresponding to the C=C and SO_2 stretchings at 1604 and 1039 cm^{-1}, respectively. The ^{1}H NMR spectrum of SPMP7-3 is also shown in Figure 6-2. All the signals are well assigned, and the expected copolymer structure was confirmed. The integral ratio of the signals at 2.54 and 6.55 -7.01 ppm, which are assigned to the α-methylene protons next to the sulfonic

acid group and aromatic protons, respectively, was calculated to determine the composition of the MBB and DBB units in the polymer. The calculated composition from the ^{1}H NMR spectrum (7.5/2.5) agreed well with the theoretical one (7/3).

6-2-2. Cross-linked SPMPs

As SPMPs are partially soluble in hot water, the cross-linked SPMPs (c-SPMPs) were prepared. The preparation of the c-SPMPs is based on the reaction of the phenyl groups in the SPMPs and MBHP as the cross-linker in the presence of methanesulfonic acid (Scheme 6-2).[35] The c-SPMP membrane was prepared as follows: a DMSO solution of SPMPs, 3 wt% MBHP and a catalytic amount of methanesulfonic acid was cast onto a glass plate. The film was dried at 120 ^{o}C for 1 h, and at 80 ^{o}C for 20 h in ambient air, and the obtained membrane was then immersed in water. After the cross-linking reaction, the film became insoluble in hot water, NMP, and DMSO, which indicated that the cross-linking reaction had successfully occurred.

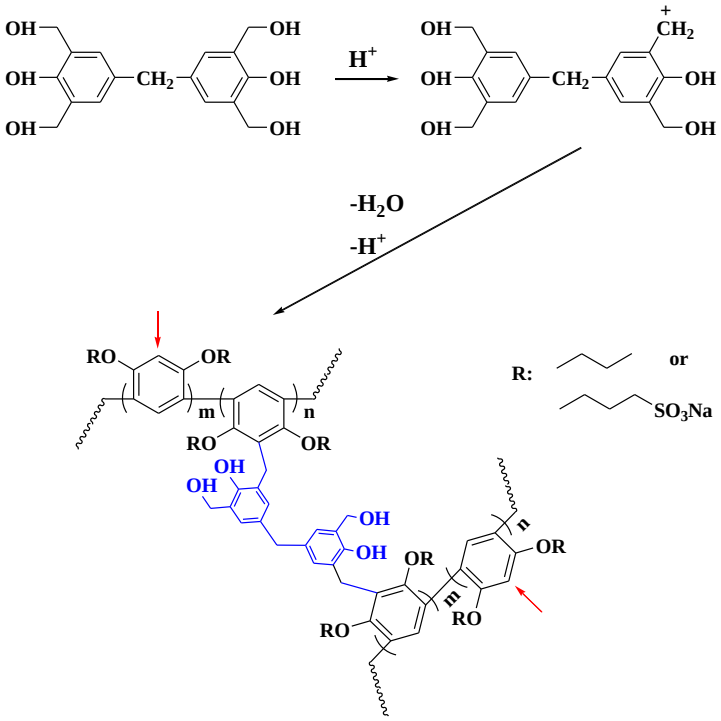

Scheme 6-2. Structures of c-SPMPs (red arrows: possible cross-linking sites).

6-2-3. Thermal stability

The thermal stability of the obtained c-SPMPs membranes was evaluated by a TG analysis. As showed in Figure 6-4, there is an apparent weight loss starting from 220 to 300 ^{o}C, which is due to the decomposition of the sulfonic acid groups in the side chains.

The next weight loss observed from 300 to 550 ^{o}C is assigned to the decomposition of the alkyl side chains. However, the clear main chain degradation is not observed until 550 ^{o}C. These results indicate the excellent thermal stability of the phenyl-phenyl bond in the c-SPMP architectures.

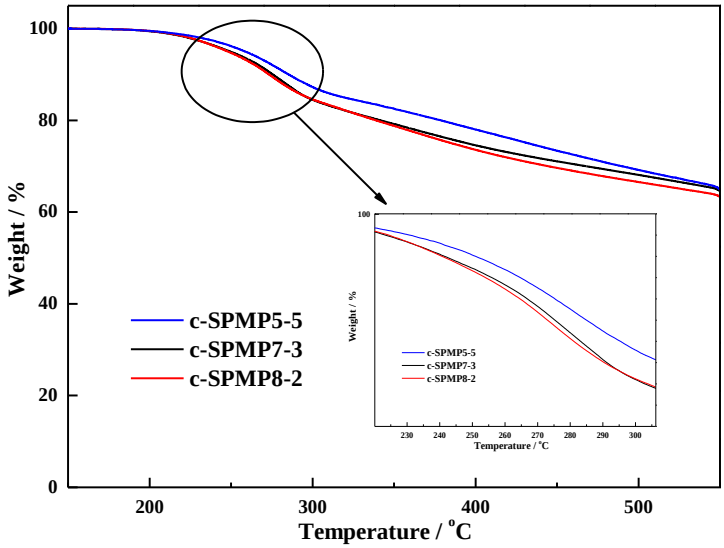

Figure 6-4. TGA curves of c-SPMP membranes (in their proton form) in N_2.

6-2-4. Oxidative stability

The oxidative stability of the c-SPMP membranes was evaluated by the remaining weight in Fenton's reagent (3% H_2O_2 aqueous solution containing 2 ppm $FeSO_4$) at 80 ^{o}C for 1 h, and the results are listed in Table 6-2. Regardless of its highest IEC values of 2.93 mequiv/g, c-SPMP8-2 still maintained 67% of the residues. Compared to some other reported multi-blocked poly(arylene ether sulfone)s[36] (*e.g.* a typical membrane X15Y4 with an IEC of 2.01 mequiv/g was completely dissolved in aqueous solution after the test under the same condition), c-SPMPs showed much higher stability. Since it is widely considered that the electron-donating groups (-O-) in the *ortho* and *para* positions to the sulfonic acid group may lead to a lower hydrolytic stability,[37,38] the sulfonated aliphatic side chains would contribute to the high oxidative stabilities of the c-SPMPs. The remaining IEC values after oxidative test were 91%, 81% and 70% of their original values, respectively, which was almost in accordance with the data of remaining weight. This result indicated that the degradation was primarily caused by the cleavage of sulfonic acid groups.

Table 6-2. Oxidative stability of c-SPMPs

Polymers	IEC/mequiv/g		After oxidative test	
	Cal.	Titr.	RW[a] / %	IEC
c-SPMP5-5	1.92	1.97	93	1.80
c-SPMP7-3	2.53	2.60	75	2.11
c-SPMP8-2	2.81	2.93	67	2.04

[a] Remaining weight; Measured by soaking the membranes in Fenton's reagent (3% H_2O_2 containing 2 ppm $FeSO_4$) at 80 ^oC for 1 h.

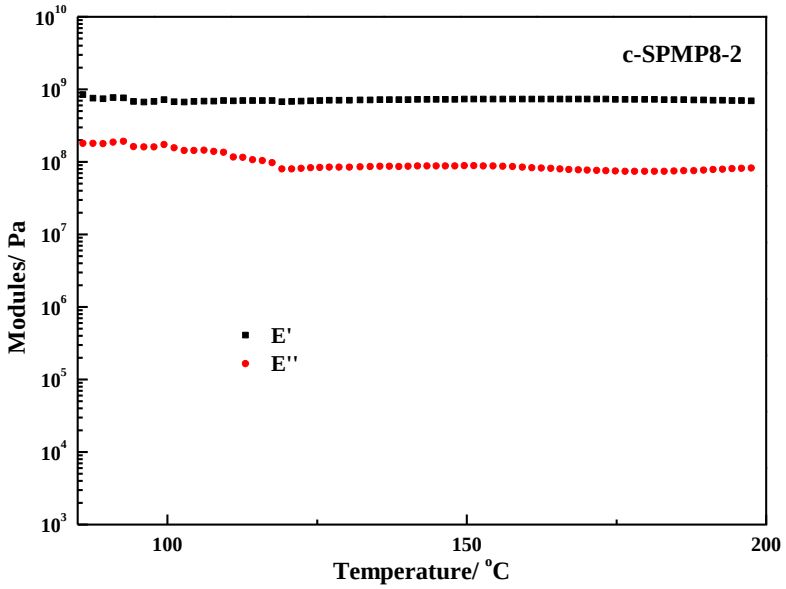

Figure 6-5. DMA curve of c-SPMP8-2.

6-2-5. Mechanical properties

The dynamic mechanical properties of the dry c-SPMP membranes were investigated by DMA measurement. Figure 6-5 shows the storage modules (*E*') and loss modules (*E*'') of c-SPMP8-2 as a function of the temperature. The *E*' and *E*'' values of 1.0 GPa and 100 MPa are maintained from 80 to 200 ^oC, respectively. Although it is widely considered that membranes with high IEC values are more or less brittle in the dry state, these results indicate that the c-SPMP8-2 membrane has a high mechanical strength despite the highest IEC value (2.93 mequiv/g).

6-2-6. IEC, water uptake and dimensional change

The titrated IEC values for all three c-SPMP membranes are slightly higher than the

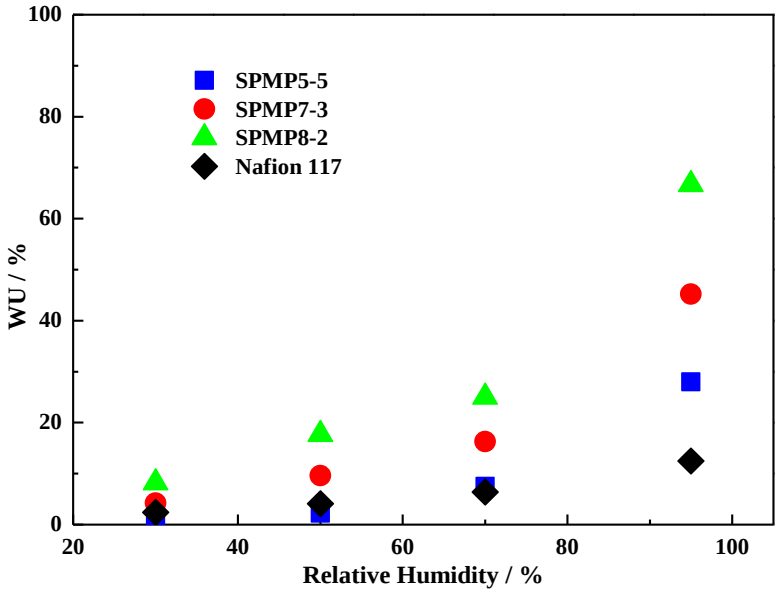

Figure 6-6. WU of c-SPMPs as a function of relative humidity.

calculated ones. Based on the ^{1}H NMR results that the calculated molar ratio for MBB and DBB was also slightly higher than the feeding ratio as already discussed, this titrated IEC values seem to be reasonable.

As is well-known, the WU and dimensional change of the PEMs have a significant effect on the membrane conductivity and mechanical properties. Water usually facilitates proton transfer. However, excessive WU inevitably leads to an undesirable membrane swelling, which might damage the mechanical stability. It is apparent that the WUs of the c-SPMPs increase with an increase in the IEC values, as showed in Figure 6-6. The c-SPMP8-2 exhibits the highest WU over the entire RH range due to its highest IEC value. Even reducing the RH condition to 30%, the c-SPMP8-2 and c-SPMP7-3 still show higher WU values than Nafion 117, indicating their better water-retention capacity. For the dimensional change, the c-SPMPs showed almost an isotropic swelling behavior with a slightly higher change in the thickness direction, as shown in Figure 6-7. The in-plane dimensional change for c-SPMP8-2 was about 0.16 at 80 ^{o}C and 95% RH. However, it seems comparable or even lower than some other well-developed poly(ether sulfone) materials at a similar IEC level.[39,40] Although there are many flexible alkyl side chains in the c-SPMPs, the rigid phenyl-phenyl main chain and the cross-linking might restrict the free volumes in the polymer matrix, resulting in the enhanced dimensional stability.

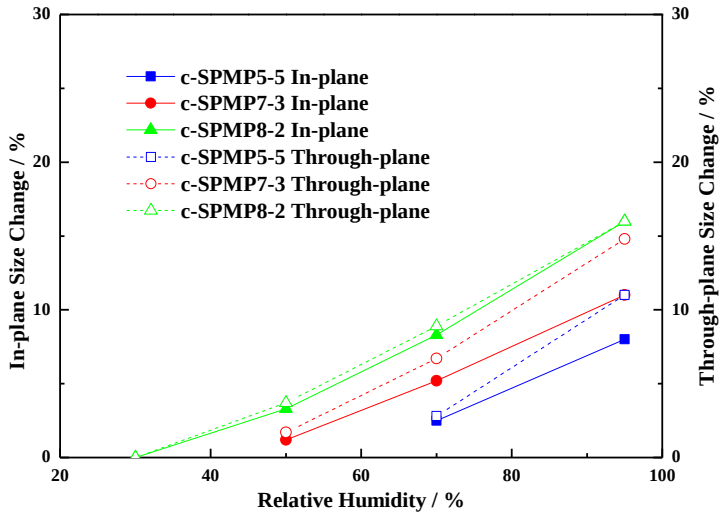

Figure 6-7. Dimensional change of c-SPMPs as a function of relative humidity.

The hydration number (λ) is the number of water molecules per a sulfonic acid unit. The relationship between λ and RH is shown in Figure 6-8. Similar to the tendency of WU, the λ values decrease with the decreasing RH. For example, c-SPMP8-2 shows about a 1.5 times higher λ than Nafion 117 at 80 ^{o}C and 95% RH, whereas almost the same value for them at 30% RH. The higher λ values of c-SPMP8-2 would contribute to the effective proton conductive performance as discussed in the following section.

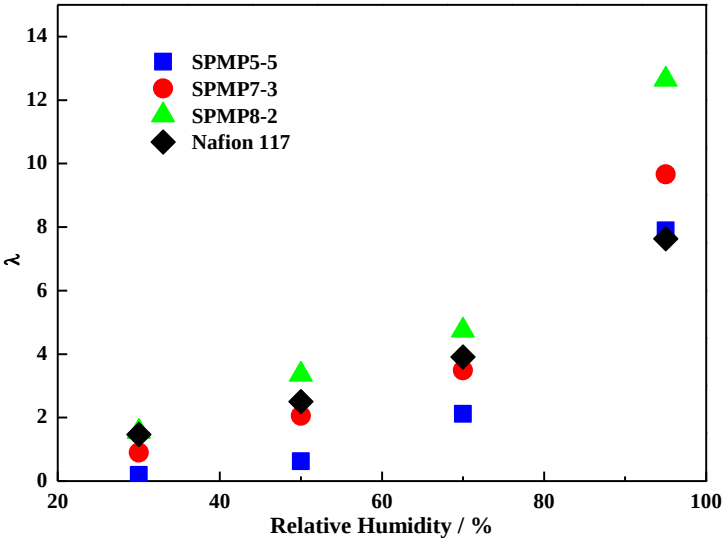

Figure 6-8. Hydration numbers of c-SPMPs as a function of relative humidity.

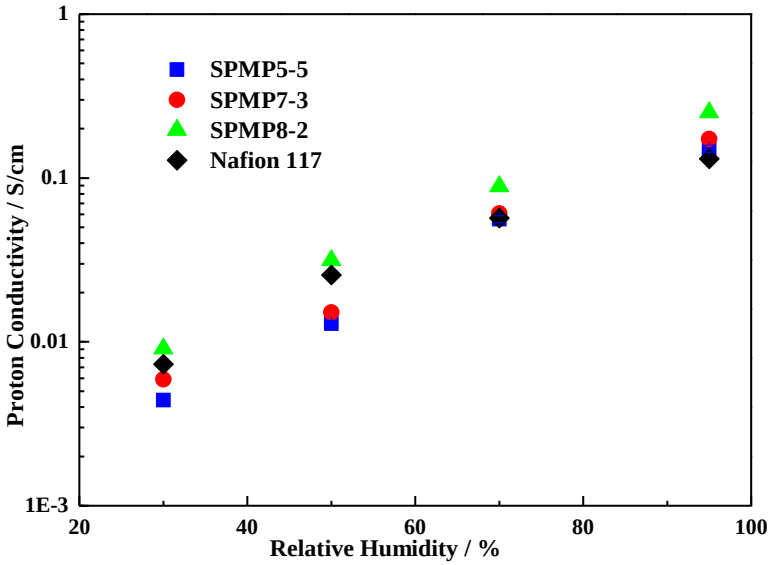

Figure 6-9. Proton conductivities c-SPMPs as a function of relative humidity.

6-2-7. Proton conductivity

Figure 6-9 shows the proton conductivities (σ) of c-SPMPs as a function of RH, together with Nafion 117 for comparison. Generally, the c-SPMPs membranes display greater RH dependence than Nafion 117, which is similar to other aromatic ionomers as reported elsewhere.[25,28,40] For example, the c-SPMP5-5 shows a σ value of 151 mS/cm at 80 ^{o}C and 95% RH, which is 15% higher than that of Nafion 117 (131 mS/cm). However, the σ value of c-SPMP5-5 decreases to 4 mS/cm at 80 ^{o}C and 30% RH, whereas Nafion 117 showed the higher value of 7.3 mS/cm. It is noted that c-SPMP8-2 exhibits higher proton conductivities than Nafion 117 over the entire RH range. On the one hand, due to its high IEC value, there would be large amount of sulfonic acid groups which could supply a sufficient numbers of protons for diffusion. On the other hand, the flexible side chains might also contribute to form the phase separations in polymer matrix and thus improve the proton conductivities.

6-3. Conclusions

A series of poly(*m*-phenylene)s with sulfonic acid via long alkyl side chains, SPMPs, were successfully obtained by the oxidative coupling polymerization of the co-monomers, MBB and DBB, utilizing $FeCl_3$ as the oxidant, followed by demethylation of PMP-OMe with BBr_3, and finally by the reaction of the resulting PMP-OH containing alkoxyphenol units with 1,4-butanesultone. The IEC values could also be easily controlled in the range of *ca*. 2.0-3.0 mequiv/g by adjusting the feed ratio of the two monomers. The c-SPMPs were prepared by the reaction of the phenyl groups in the SPMPs and MBHP in the presence of methanesulfonic acid. The c-SPMPs exhibited a high thermal stability despite the full aliphatic side chains. The DMA results showed the high storage modules of 1.0 GPa for the c-SPMP8-2 from 80-200 ^{o}C, regardless of its high IEC value of 2.93 mequiv/g, and exhibited a good oxidative stability due to their complete phenyl-phenyl linkages. The high IEC values and flexible alkyl sulfonic acid side chains contributed to the high proton conductivities of the c-SPMP membranes. The c-SPMP8-2 showed the high proton conductivity of 9.1 mS/cm compared to a σ value of 7.3 mS/cm for Nafion 117 at 80 ^{o}C and 30% RH. Consequently, the novel poly(*m*-phenylene)s with pendant alkyl sulfonated side chain, are promising candidates for fuel cell applications.

6-4. Experimental

Materials

3-Methoxyphenol, resorcinol and 1-bromobutane were purchased from TCI. $FeCl_3$ was purchased from Kanto Chem. Co, Inc. Nitrobenzene was purchased from Wako Pure Chemical Industries, Ltd. and purified by washing sequentially with diluted aqueous base, water, diluted aqueous acid, and water, followed by drying with magnesium sulfate and distillation. Other solvents and reagents were used as received. 1,3-Di-*n*-butoxybenzene (DBB) was prepared according to the reported procedure.[32]

Methoxy-3-*n*-butoxybenzene (MBB)

To a 200 mL three-necked flask equipped with a nitrogen inlet/outlet, were charged 3-methoxyphenol (6.00 g, 48.3 mmol), 1-bromobutane (9.93 g, 72.5 mmol), potassium carbonate (10.0 g, 72.5 mmol) and DMF (80 mL). The mixture was stirred at 80 ^oC for 12 h and poured into water. The solution was extracted with ether and the ether phase was dried over anhydrous sodium sulfate, filtered, and concentrated on a rotary evaporator to give the crude product. The product was purified by silica gel column chromatography using ethyl acetate/n-hexane (1:9) to afford a colorless liquid. Yield: 7.65 g (88%). ^1H NMR ($CDCl_3$, ppm): δ =7.14-7.19 (t, J = 7.8 Hz, ^1H, Ar-H), δ = 6.46-6.51 (m, 3H, Ar-H), δ = 3.92-3.97 (t, J = 6.6 Hz, 2H, -OCH_2-), δ = 3.79 (s, 3H, -OCH_3), δ = 1.71-1.81 (m, 2H, -CH_2-), δ = 1.43-1.52 (m, 2H, -CH_2-), δ = 0.95-1.00 (t, J = 7.35 Hz, 3H, -CH_3). IR (NaCl): ν 2957-2870 (C-H), 1600 (C=C), 1153 cm^{-1} (C-O-C).

Copolymer (PMP-OMe) from MBB and DBB

A typical procedure is as follows: To a 50 mL three-necked flask equipped with a nitrogen inlet/outlet, were charged MBB (0.649 g, 3.60 mmol), DBB (0.200 g, 0.900 mmol) and anhydrous $FeCl_3$ (2.91 g, 18.0 mmol). Then anhydrous nitrobenzene (18.0 mL) was added to the mixture via syringe through the septum cap. The reaction was performed at room temperature for 5 h and the resulting slurry was then poured into methanol solution containing 5% hydrochloric acid. The polymer was collected, extracted with ethanol by a Soxhlet extractor for 24 h and finally dried under vacuum at 60 ^oC. Yield: 0.486 g (58%). ^1H NMR (DMSO-d_6, ppm): δ = 6.90 (s, (m+n)H, Ar-H), δ = 6.61 (s, (m+n)H, Ar-H), δ = 3.88 (s, (2m+4n)H, -OCH_2-), δ = 3.67 (s, 3mH, -OCH_3), δ = 1.49 (s, (2m+4n)H, -CH_2-), δ=1.22 (s, (2m+4n)H, -CH_2-), δ = 0.69 (s, (3m+6n)H, -CH_3). IR (KBr): ν 2957-2871 (C-H), 1601 (C=C), 1170 cm^{-1} (C-O-C).

Copolymer (PMP-OH)

A typical procedure is as follows: To a 200 mL three-necked flask equipped with a nitrogen inlet/outlet, were charged PMP-OMe polymer (0.55 g, 0.288 mmol) and dichloromethane (45.0 mL). The solution was cooled to 0 ^{o}C with an ice bath, and a BBr_3/CH_2Cl_2 solution (4.0 mL) was added dropwise to the solution. After addition, the reaction was kept at room temperature overnight. The resulting copolymer was obtained by carefully pouring the solution into water, filtered, washed thoroughly with water, and dried under vacuum at 60 ^{o}C. Yield: 0.429 g (82%). ^{1}H NMR(DMSO-d_6, ppm): δ = 8.95 (s, -OH), δ = 7.07 (s, (m+n)H, Ar-H), δ = 6.45 (s, (m+n)H, Ar-H), δ = 3.25 (s, (2m+4n)H, -OCH_2-), δ = 1.48 (s, (2m+4n)H, -CH_2-), δ = 1.24 (s, (2m+4n)H, -CH_2-), δ = 0.80 (s, (3m+6n)H, -CH_3). IR (KBr): ν 3500-3200 (O-H), 1608 (C=C), 1161 cm^{-1} (C-O-C).

Sulfonated copolymer (SPMP)

A typical procedure is as follows. To a 20 mL three-necked flask equipped with a nitrogen inlet/outlet, were charged PMP-OH polymer (0.30 g, 0.171 mmol), sodium hydride (0.049 g, 2.05 mmol) and dimethyl sulfoxide (DMSO) (8.0 mL). The solution was heated to 100 ^{o}C, and 1,4-butanesultone (0.373 g, 2.73 mmol) was added dropwise to the mixture. After 12 h, the solution was cooled to room temperature and slowly poured into ethanol. The sulfonated copolymer was filtered and then dried in a vacuum oven at 100 ^{o}C for 10 h. Yield: 0.487 g (94%). ^{1}H NMR (DMSO-d_6, ppm): δ = 7.01 (s, (m+n)H, Ar-H), δ = 6.55 (s, (m+n)H, Ar-H), δ = 3.88-3.49 (d, (4m+4n)H, -OCH_2-), δ = 2.54 (s, 2mH, -CH_2-SO_3Na), δ = 1.69 (s, (4m+4n)H, -CH_2-), δ = 1.23 (s, (4m+4n)H, -CH_2-), δ = 0.76 (s, (3m+6n)H, -CH_3). IR (KBr): ν 2955-2870 (C-H), 1604 (C=C), 1172 (C-O-C), 1039 cm^{-1} (O=S=O).

Preparation of c-SPMP membranes

Membranes were prepared by a solution casting method. Firstly, **SPMP** polymer and 4,4'-methylene-bis[2,6-bis(hydroxyethyl)phenol] (MBHP) (3 wt%) were dissolved in DMSO with concentration of 7% (m/v). After filtration, a drop of methanesulfonic acid was added to the solution and then the solution was cast onto a clean Petri dish, dried at 120 ^{o}C for 1 h and 80 ^{o}C for 20 h, respectively. The membrane was detached from the dish by immersing into water to remove the residual solvent, followed by soaking in 2 M H_2SO_4 for 72 h for proton exchange. Then, the membrane was thoroughly washed with Milli-Q water. The thickness of the membranes was controlled to be about 50 μm.

Characterizations

^{1}H (300 MHz) spectra were recorded on a Bruker DPX300S spectrometer using $CDCl_3$ or DMSO-d_6 as the solvent and tetramethylsilane as the reference. Fourier transform-infrared (FT-IR) spectra were obtained with a Horiba FT-120 Fourier transform spectrophotometer. Number- and weight-average molecular weights (M_n and M_w) were measured by gel permeation chromatography (GPC) on a Hitachi LC-7000 system equipped with polystyrene gel columns (TSKgel GMHHR-M) eluted with *N*,*N*-dimethylformamide (DMF) containing 0.01 M LiBr at a flow rate of 1.0 mL min^{-1} calibrated by standard polystyrene samples. The cyclic voltammogram was measured at room temperature under nitrogen atomsphere in anhydrous acetonitrile solution containing 0.2 M solution of tetrabutylammonium perchlorate (TBAP) and 1.0 mM monomer with the aid of an ALS electrochemical analyzer model 612C; the scanning rate was 0.1 V/s. A typical three electrode with a working (glassy carbon), a reference (Ag/AgCl), and an auxiliary electrode (Pt wire) were used. Thermogravimetric analysis (TGA) was measured in N_2 on a Seiko EXSTAR 6000 TG/DTA 6300 thermal analyzer at a heating rate of 10 ^{o}C min^{-1}. Dynamic mechanical analysis (DMA) was performed on the film specimens (length, 30 mm; width, 10 mm; thickness, 50 μm) by using the Seiko DMS 6300 at a heating rate of 2 ^{o}C min^{-1} with a load frequency of 1 Hz under nitrogen atmosphere. Wide-angle X-ray diffraction (WAXD) measurements were performed at ambient temperature by using a Rigaku-Denki UltraX-18 X-ray generator with monochromic Cu Kα radiation (40 kV, 50 mA) from graphite crystal of monochromator and flat-plate type of imaging plate.

Water Uptake and Dimensional Change. The humidity dependence of water uptake was measured by placing the membrane in a thermo-controlled humid chamber for 4 h under each RH condition. The membrane was then taken out, and quickly weighed on a microbalance. Water uptake (WU) was calculated according to the following equation (1):

$$WU = (W_s - W_d)/W_d \times 100\ wt\% \qquad (1)$$

where, W_s and W_d are the weights of wet and dried membranes, respectively.

For dimensional change measurements, squared membrane sheets were placed in a thermo-controlled humid chamber for 4 h under each RH condition. The dimensional change in membrane thickness direction (Δt_c) and the plane direction (Δl_c) were calculated from equation (2):

$$\Delta t_c = (t-t_s)/t_s \qquad \Delta l_c = (l-l_s)/l_s \qquad (2)$$

where t_s and l_s refer to the thickness and diameter of the membrane equilibrated at about

30 ^{o}C/30% RH, respectively; *t* and *l* refer to those of the membrane under each condition.

Ion Exchange Capacity. IECs of the membranes were determined by a titration method. The proton-type samples were ion-exchanged by a 15 wt% NaCl solutions and titrated with a 0.02 M NaOH solution with phenolphthalein as the indicator. IEC was calculated from equation (3):

$$IEC = C_{NaOH} \times V_{NaOH} / W_d \quad (3)$$

where C_{NaOH} and V_{NaOH} are the concentration of NaOH solution and the consumed volume of NaOH solution, respectively.

Water Sorption (λ). The λ value was calculated from the equation (4):

$$[H_2O]/[SO_3^-] = WU \times 10/18 \times IEC \quad (4)$$

Proton Conductivity. Proton conductivity in plane direction of the membrane was determined using an electrochemical impedance spectroscopy technique over the frequency from 5 Hz to 1 MHz (Hioki 3532-80). A two-point probe conductivity cell with two platinum plate electrodes was fabricated. The cell was placed in a thermo-controlled humid chamber at 80 ^{o}C for 2 h before the measurement. Proton conductivity (σ) was calculated from the following equation (5):

$$\sigma = d/(t_s w_s R) \quad (5)$$

where *d* is the distance between the two electrodes, t_s and w_s are the thickness and width of the membrane, and *R* is the resistance measured.

6-5. References

(1) Mauritz, K. A.; Moore, R. B. *Chem. Rev.* **2004,** *104,* 4535-4586.

(2) Savadoga, O. J. *New. Mater. Electrochem. Syst.* **1998,** *1,* 47-66.

(3) Rikukawa, M.; Sanui, K. *Prog. Polym. Sci.* **2000,** *25,* 1463-1502.

(4) Hickner, A. H.; Ghassemi, H.; Kim, Y. S.; Einsla, B. R.; McGrath, J. E. *Chem. Rev.* **2004,** *104,* 4587-4611.

(5) (a) Takamuku, S.; Jannasch, P. *Adv. Energy Mater.* **2012,** *2,* 129-140;
(b) The 2011 Progress Report for US DOE Hydrogen and Fuel Cells Program.http://www.hydrogen.energy.gov/pdfs/progress11/v_c_1_hamrock_2011.pdf;
(c) Gebert, M.; Ghielmi, A.; Merlo, L.; Corasaniti, M.; Arcella, V. *ECS Trans.* **2010,** *26,* 279-283.

(6) Higashihara, T.; Matsumoto, K.; Ueda, M. *Polymer* **2009,** *50,* 5341-5357.

(7) Ghassemi, H.; McGrath, J. E. *Polymer* **2004,** *45,* 5847-5854.

(8) Seesukphronrarak, S.; Ohira, A. *Chem. Commun.* **2009,** 4744-4746.

(9) Zaidi, S. M. J.; Mikhailenko, S. D.; Robertson, G. P.; Guiver, M. D.; Kaliaguine, S. *J. Membr. Sci.* **2000,** *173,* 17-34.

(10) Liu, B.; Robertson, G. P.; Guiver, M. D.; Hu, W.; Jiang, Z. *Macromolecules* **2007,** *40,* 1934-1944.

(11) Matsumoto, K.; Higashihara, T.; Ueda, M. *Macromolecles* **2008,** *41,* 7560-7565.

(12) Miyatake, K.; Chikashige, Y.; Watanabe, M. *Macromolecles* **2003,** *36,* 9691-9693.

(13) Chikashige, Y.; Chikyu, Y.; Miyatake, K.; Watanabe, M. *Macromolecles* **2005,** *38,* 7121-7126.

(14) Miyatake, K.; Chikashige, Y.; Higuchi, E.; Watanabe, M. *J. Am. Chem. Soc.* **2007,** *129,* 3879-3887.

(15) Matsumoto, K.; Higashihara, T.; Ueda, M. *Macromolecules* **2008,** *42,* 1161-1166.

(16) Lafitte, B.; Jannasch, P. *Adv. Funct. Mater.* **2007,** *17,* 2823-2834.

(17) Wang, C.; Shin, D, W.; Lee, S, Y.; Kang, N, R.; Lee, Y, M.; Guiver, M, D. *J. membr. Sci.* **2012,** *405-406,* 68-78.

(18) Miyatake, K.; Yasuda, T.; Hirai, M.; Nanasawa, M.; Watanabe, M. *J. Polym. Sci., Part A: Polym. Chem.* **2007,** *45,* 157-163.

(19) Li, N.; Yasuda, T.; Cui, Z.; Zhang, S.; Li, S. *J. Polym. Sci., Part A: Polym. Chem.* **2008,** *46,* 2820-2832.

(20) Maier, G.; Meier, H. *J. Adv. Polym. Sci.* **2008,** *216,* 1-62.

(21) Wu, S.; Qiu, Z.; Zhang, S.; Yang, X.; Yang, F.; Li, Z. *Polymer* **2006,** *47,* 6993-7000.

(22) Bae, J.-M.; Honma, I.; Murata, M.; Yamamoto, T.; Rikukawa, M.; Ogata, N. *Solid State Ionics* **2002,** *147,* 189-194.

(23) Goto, K.; Rozhanskii, I.; Yamakawa, Y.; Otsuki, T.; Naito, Y. *Polym. J.* **2009,** *41,* 95-104.

(24) Zhang, X.; Hu, Z.; Luo, L.; Chen. S.; Liu, J.; Chen, S.; Wang, L. *Macromol. Rapid Commun.* **2011,** *32,* 1108-1113.

(25) Nakabayashi, K.; Higashihara, T.; Ueda, M. *Macromolecules* **2011,** *44,* 1603-1609.

(26) Seesukphronrarak, S.; Ohira, K.; Kidena, K.; Takimoto, N.; Kuroda, S.; Ohira, A. *Polymer* **2010,** *51,* 623-631.

(27) Miyahara, T.; Hayano, T.; Matsumo, S.; Watanabe, M.; Miyatake, K. *ACS Appl. Mat. Interfaces* **2012,** *4,* 2881-2884.

(28) Zhang, X.; Hu, Z.; Pu, Y.; Chen, S.; Ling, J.; Bi, H.; Chen, S.; Wang, L.; Okamoto, K.-i. *J. Power Sources* **2012, *216,*** 261-268.

(29) Zhang, X.; Chen, S.; Liu, J.; Hu, Z.; Chen, S.; Wang, L. *J. Membr. Sci.* **2011,** *371,* 276--285.

(30) Umezawa, K.; Oshima, T.; Yoshizawa-Fujita, M.; Takeoka, Y.; Rikukawa, M. *ACS Macro Lett.* **2012,** *1,* 969-972.

(31) Rager, T.; Schuster, M.; Steininger, H.; Kreuer, K.-D. *Adv. Mater.* **2007,** *19,* 3317-3321.

(32) Okada, T.; Fujiwara, N.; Ogata, T.; Haba, O.; Ueda, M. *J. Polym. Sci., Part A: Polym. Chem.* **1997,** *35,* 2259-2266.

(33) Percec, V.; Okita, S.; Wang, J. H. *Macromolecules* **1992,** *25,* 64-74.

(34) Abd-El-Aziz, A. S.; C. R. de Denus, E. K. Todd, S. A. Bernardin, *Macromolecules* **2010,** *33,* 5000-5005.

(35) (a) Lee, S. M.; Frechet, J. M. J.; Willsont, C. G. *Macromolecules* **1994,** *27,* 5154-5159;

(b) Ueda, M.; Nakayama, T. *Macromolecules* **1996,** *29,* 6427-6431;

(c) Mitsui Petrochemical Industries, Ltd., Jpn. Kokai Tokkyo Koho JP 58,116,433 [83,116,433], **1983,** *Chem. Abstr.* **1984,** *100,* 7356n.

(36) Bae, B.; Hoshi, T.; Miyatake, K.; Watanabe, M. *Macromolecules* **2011, *44,*** 3884-3892.

(37) Schuster, M.; Kreuer, K.-D.; Andersen, H. T.; Maier, J. *Macromolecules* **2007,** *40,* 598-607.

(38) Zhang, X.; Hu, Z.; Zhang, S.; Chen, S.; Chen, S.; Liu, J.; Wang, L. *J. Appl. Polym. Sci.* **2011,** *121,* 1707-1716.

(39) Nakabayashi, K.; Higashihara, T.; Ueda, M. *J. Polym. Sci. Part A: Polym. Chem.* **2010,** *48,* 2757-2764.

(40) Nakabayashi, K.; Matsumoto, K.; Higashihara, T.; Ueda, M. *Polym. J.* **2009,** *41*, 332-33

Chapter 7

Poly(phenylene ether)s Containing Pendant Alkyl Sulfonic Acid for Polymer Electrolyte Membranes

ABSTRACT: A series of poly(phenylene ether)s with sulfonic acid groups via long alkyl side chains, SPPEs, were successfully prepared as proton exchange membranes for fuel cells. The new monomer, bis[4-fluoro-3-(*p*-methoxylbenzoyl)]biphenyl (BFMBP), containing two pendent methoxyphenyl groups was synthesized by the Friedel-Crafts reaction of 5-chloro-2-fluorobenzoyl chloride with anisole, followed by the nickel-mediated homocoupling reaction. Poly(phenylene ether)s (PPEs) were then successfully obtained by the aromatic nucleophilic substitution polycondensation of BFMBP with dihydroxy-monomers in the presence of potassium carbonate. Sulfonated PPEs (SPPEs) (IEC: 1.96~2.45 mequiv/g) could be prepared by the reactions of PPEs containing phenol units with 1,4-butanesultone. By the solution casting method, SPPEs produced the transparent membranes with good mechanical properties, and showed good oxidative and dimensional stabilities, and high proton conductivities, *e.g.*, 8.60×10^{-3} S/cm under 30% relative humidity at 80 ^{o}C, which is higher than that of Nafion 117.

7-1. Introduction

Polymer electrolyte membrane fuel cells (PEMFCs) have drawn worldwide attention because of their potential applications in transportation, stationary and portable electronics. PEMFC technology already provides sufficient performance to be competitive with alternative technologies in energy conversion applications. Polymer electrolyte membranes (PEMs) play an important role in the PEMFC system since it serves as a proton conductive carrier as well as the separator of the anode/cathode.[1-26] Among the state-of-the-art PEMs, sulfonated perfluoropolymers, (*e.g.*, Dupont's Nafion®, 3M, Aquivion® membranes) have been widely used for PEFCs due to their high proton conductivity and high chemical stability. By chemical modifications or stabilizations, their new products (*e.g.*, NRE212, PFIA, Aquivion™, etc.) could even withstand the high temperature of 120 ^{o}C.[5] However, some other notable drawbacks, such as a harsh producing process, high cost, and fluoro-release problem still more or less restrict their practical use. Hence, a number of non-fluorinated acid ionomers, especially the sulfonated aromatic hydrocarbon polymers, have been widely studied as a branch of alternate PEMs. The typical materials used for these PEMs, such as sulfonated poly(ether ketone)s (SPEKs),[11,12] sulfonated poly(arylene ether sulfone)s (SPAESs),[16,17] sulfonated polyimides(SPIs),[18] sulfonated poly(phenylene)s (SPPs),[19-21] sulfonated poly(phenylene ether)s (SPPEs),[22-25] etc., have been well developed during the past two decades.

Typical SPPEs are prepared by the sulfonation of the precursor poly(phenylene ether)s (PPEs). The phenylene rings in the main chain provide a high electron density and could be easily functionalized by sulfuric acid, chlorosulfonic acid, etc. For instance, Xu's group reported a series of SPPEs.[24] By blending SPPEs with brominated PPE, their membranes showed a higher fuel cell performance than Nafion. However, the sulfonic acid groups were directly located onto the main chain, *ortho* to the "–O–" linkages, which might decrease the oxidative stability of these polymers. Unfortunately, no further information on their durability was presented by the authors. Watanabe's group previously prepared a series of SPPEs using the sulfonated alkoxyl side chains as the pendants.[25] Unlike the situation of SPPEs described above, the fairly low polarity of the main chain with a high polarity side chain produced problems regarding the solubility for such types of SPPEs. The as-prepared polymers became insoluble once it was recovered from the solution. Therefore, the authors treated them with tetrabutylammonium tetrafluoroborate. The resulting polymers with an ammonium-form could finally dissolve in benzyl alcohol and produce the membranes.

The polymers with flexible ether and rigid phenyl-phenyl linkages in the main chains are promising candidates for PEM designs, since they could support polymers with a good toughness as well as the high chemical stability. The issue lies in where to functionalize the sulfonic acid groups in order to satisfy the requirements for solubility and proton conductive capacity. Our previous study showed interesting results such that the introduction of flexible alkylsulfonated side chains to the random polymer main chains improved the proton conductivity at a low relative humidity (RH) due to the phase separation between the hydrophilic and hydrophobic domains, and the oxidative stability of membranes was also increased due to the location of the sulfonic acid groups far from main chains, where oxy and peroxy radicals might be preferably formed.[20,26] However, the mechanical stability of these membranes was not sufficient for fuel cell applications. Therefore, in this study, the more robust poly(phenylene ether) was selected as the polymer main chain.

In this chapter, we report a novel type of PPEs with long alkyl sulfonic acids, which were synthesized from a new monomer of bis[4-fluoro-3-(4'-methoxylbenzoyl)]biphenyl (BFMBP) and various dihydroxy-monomers via aromatic nucleophilic substitution polycondensation, demethylation, followed by the reaction of the resulting polymers having phenol groups with 1,4-butanesultone. Their properties, such as ion exchange capacity (*IEC*), water uptake (*WU*), dimensional change, mechanical properties, proton conductivities and morphology, were investigated in detail.

7-2. Results and discussion

7-2-1. Synthesis of monomers and polymers

Scheme 7-1 shows the synthetic route of the monomer **BFMBP**. **CFMB** was firstly prepared by the aluminium chloride catalyzed Friedel-Crafts acylation of anisole with 5-chloro-2-fluorobenzoyl chloride. Due to electronic and steric effects, the substitution reaction selectively occurred at the *para*-position to the methoxyl group of anisole. The chemical structure of **CFMB** was confirmed by its ^{1}H NMR, ^{13}C NMR (Figure 7-1).

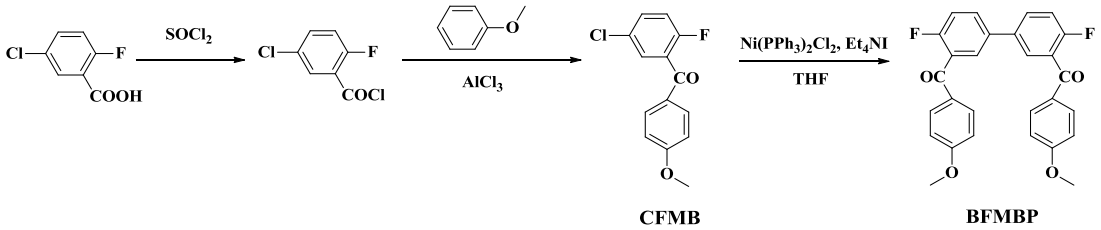

Scheme 7-1. Synthetic route of monomer BFMBP.

$NiBr_2$ and triphenylphosphine (PPh_3) were used as the catalyst and ligand for the nickel-catalyzed coupling reaction, respectively. The reaction proceeded well in DMAc, DMF and THF, however, the yield for the final product was only 10-20%, which might be due to the moisture-sensitive catalyst. Thus, a more stable catalyst of $Ni(PPh_3)_2Cl_2$ was instead investigated and the temperature was maintained at the mild condition of 50 ^{o}C. The yield was improved to about 50% after recrystallization from ethanol. Unlike many reported nickel-mediated reactions, which provided almost quantitative yields of the coupling products from various aryl halides,[27,28] the relatively negative results in this study might be attributed to the low reactivity of the precursor monomer **CFMB**. A carbonyl group was substituted at the *meta*- position toward the chloride group, which made it less reactive than some other chloride groups at the *ortho*-/*para*- positions toward the electron-withdrawing groups. The same phenomenon was also found by D. K. Taylor's group.[29] The chemical structure of **BFMBP** was confirmed by its ^{1}H NMR, ^{13}C NMR (Figure 7-2). On the one hand, the chemical shifts of the two protons *ortho*- to the chloride (H2 and H5 in Figure 7-1a, δ = 7.47-7.40 ppm) shifted to the low field (δ = 7.66-7.62 ppm) in Figure 7-2a. On the other hand, the peak assigned to the carbon atom C1 (δ = 132.25 and132.14 ppm in Figure 7-1b) also shifted to 135.78 and135.74 ppm, respectively, in Figure 7-2b. These results provide obvious evidence for the phenyl-phenyl bond formation.

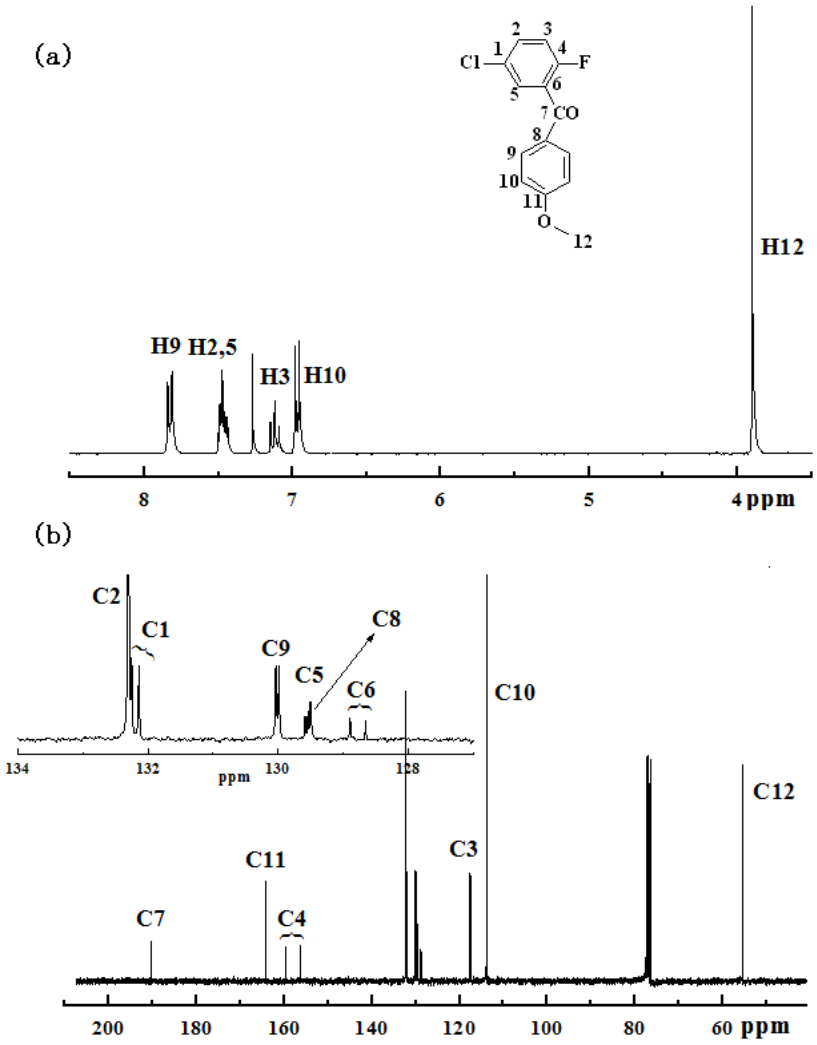

Figure 7-1. ^{1}H and ^{13}C NMR spectra of **CFMB** in $CDCl_3$.

Scheme 7-2 shows the synthetic route of the polymers **4**. The polymers **2** were first obtained by the aromatic nucleophilic substitution polycondensation in the presence of K_2CO_3. Although two of the three counterpart (dihydroxy) monomers chosen in this study have rigid rod structures (**a** and **b**), no precipitation occurred during the polymerizations. The results of the polymerizations are summarized in Table 7-1.The number-average molecular weights (M_n) and polydispersity indices (*PDI*s) of the polymers **2** were in the range of $3.1\sim4.3\times10^4$ and 2.0~2.4, respectively. The polymers **2** showed good solubilities in the common organic solvent, such as $CHCl_3$, CH_2Cl_2, DMSO, DMAc, etc. The chemical structures of the polymers **2** were confirmed by their ^{1}H NMR spectra. The relative intensities of the aromatic-H to methoxy-H were 3.09,

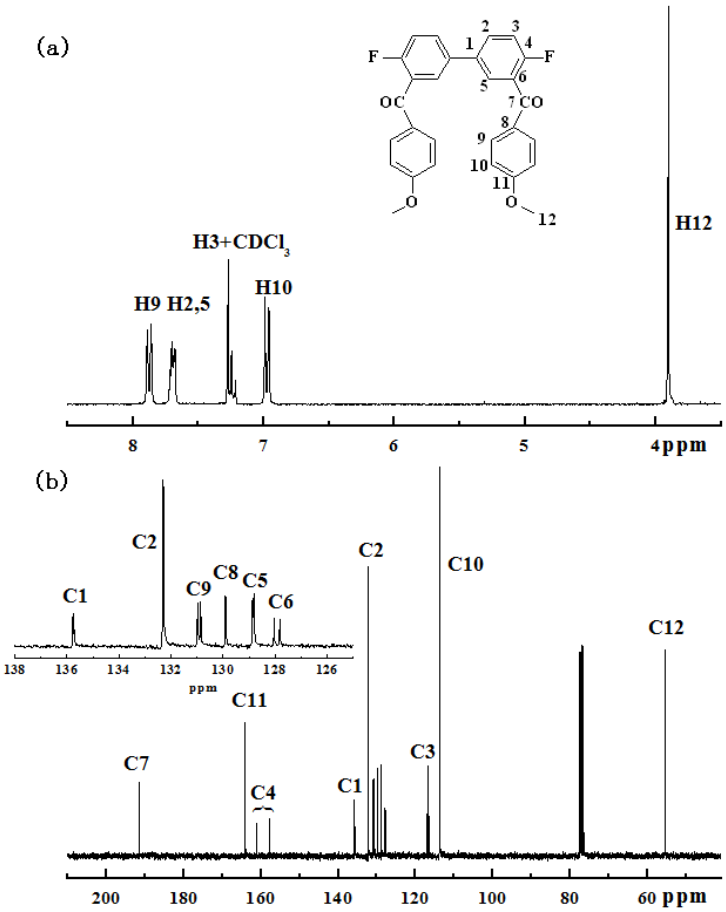

Figure 7-2. ^{1}H and ^{13}C NMR spectra of **BFMBP** in $CDCl_3$.

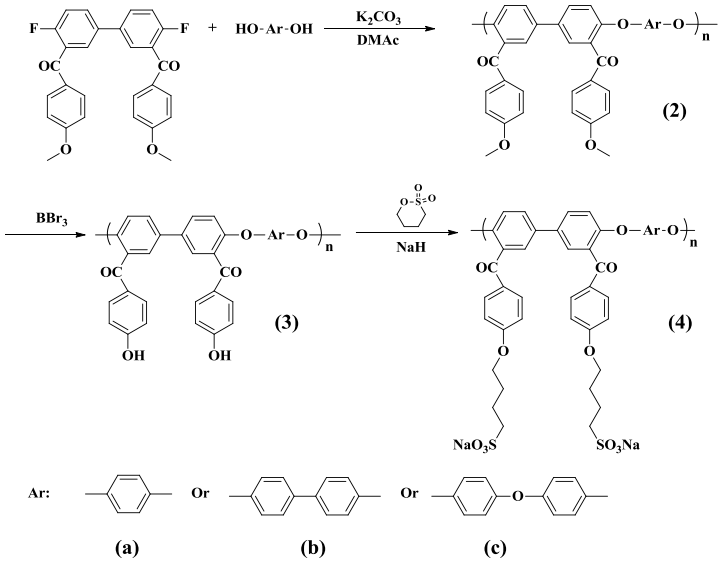

Scheme 7-2. Synthetic route of the sulfonated polymers **4**.

3.78 and 3.67 for polymers **2a**, **2b** and **2c**, respectively, close to the theoretical values of 3.00, 3.67 and 3.67, respectively. The polymers **2** were then converted to the polymers **3** by treatment with BBr_3. In the ^1H NMR spectra of the polymers **2b** and **3b**, the characteristic methoxy protons at 3.82 ppm of polymer **2b** have completely disappeared, and hydroxy proton signals appear at 10.36 ppm. Finally, the SPPEs, **4**, were obtained by the reaction of the resulting polymers **3** with 1,4-butanesultone in the presence of sodium hydride.

Table 7-1. Synthesis of polymers **2**.

Code	M_n (kDa) [a)]	M_w (kDa) [a)]	*PDI*[a)]
2a	31	74	2.4
2b	43	85	2.0
2c	35	77	2.2

a)Determined by GPC eluted with DMF using polystyrene standard.

The chemical structures of the polymers **4** were also confirmed by FTIR and ^1H NMR spectroscopies. The IR spectra of the polymers **4** showed characteristic absorptions corresponding to the C=O and C=C stretchings around 1658 and 1600 cm^{-1}, whereas the typical O=S=O stretching was observed at around 1115 and 1050 cm^{-1}.The ^1H NMR spectra of polymers **4** are shown in Figure 7-3. New peaks at around 4.01, 3.91 and 3.89 ppm were assigned to the α-methylene protons next to the phenoxy groups for **4a**, **4b** and **4c**, respectively, indicating the introduction of long sulfoalkyl side chains. Since the typical signals of the α-methylene protons next to the $-SO_3Na$ groups overlapped with the DMSO-d_6 peak, the IEC_{NMR} values were calculated by the relative intensities of the methylene protons to the aromatic protons. All the data were close to the theoretical values, which suggested the well-controlled nucleophilic reaction of the polymers **3** with 1,4-butanesultone (Table 7-2).

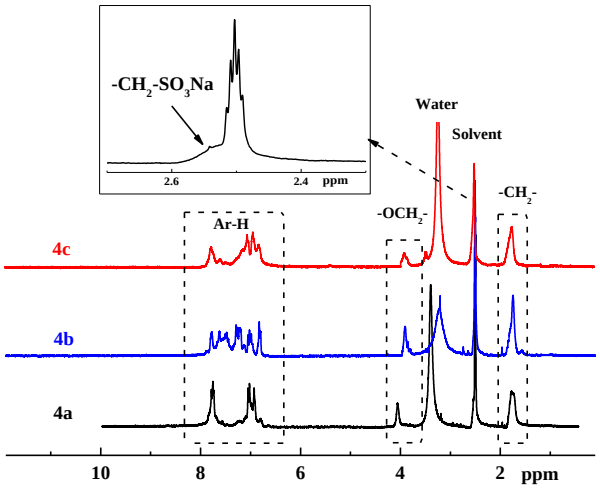

Figure 7-3. ^{1}H NMR spectra of the polymers **4a**, **4b** and **4c** in DMSO-d_6.

Table 7-2. Physical properties of polymers **4**.

	$IEC_{cal.}$/ mequiv.g^{-1}	IEC_{NMR}/ mequiv. g^{-1}	$IEC_{titr.}$/ mequiv.g^{-1}	T_d /^{o}C 5%	50% RH[a)]		70% RH [a)]		95% RH [a)]		RW [b)]
					Δl_c	Δt_c	Δl_c	Δt_c	Δl_c	Δt_c	%
4a	2.59	2.51	2.45	257.4	0.021	0.03	0.060	0.09	0.110	0.13	81
4b	2.36	2.19	2.08	244.4	0.014	0.02	0.048	0.07	0.102	0.12	90
4c	2.31	2.10	1.96	254.2	0.010	0.02	0.040	0.05	0.070	0.09	94

a) Dimensional changes of **SPPEs** at 80 ^{o}C. Δl_c and Δt_c refer to the changes in plane and through plane directions, respectively.

b) Remaining weight. Measured by soaking the membranes in Fenton's reagent (3% H_2O_2 containing 2 ppm $FeSO_4$) at 80 ^{o}C for 1 h.

7-2-2. Thermal properties and oxidative stability

The thermal properties of the polymers **4** in the acid form were evaluated by TGA and DSC. No obvious glass transition temperatures T_gs could be observed in all the polymers **4**. Figure 7-4 shows the TGA curves of the polymers **4** in N_2, and the weight loss temperatures are listed in Table 7-2. All the polymers **4** exhibited T_d5% values over 244 ^{o}C, which could satisfy the requirement for medium-temperature fuel cells. There is an apparent weight loss starting from 220 to 300 ^{o}C, which is close to the theoretical values for the decomposition of the sulfonic acid groups in the side chains. The second weight loss step is observed from 300 to 550 ^{o}C, attributable to the cleavage of the alkyl side chains.

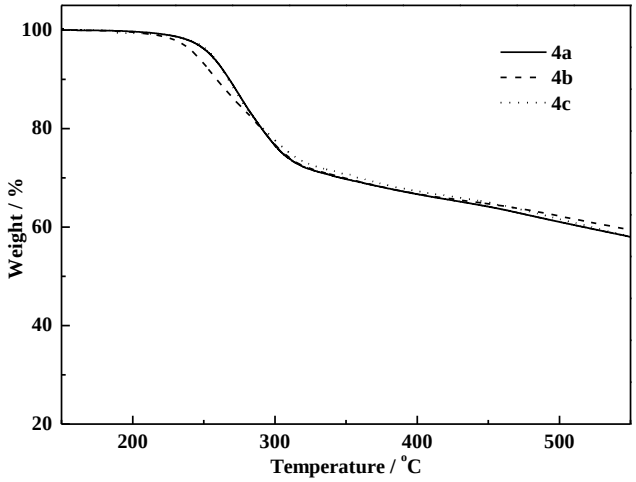

Figure 7-4. TGA curves of SPPEs.

The oxidative stability of the SPPE membranes was evaluated by the remaining weight in Fenton's reagent (3% H_2O_2 aqueous solution containing 2 ppm $FeSO_4$) at 80 ^oC for 1 h, and these results are listed in Table 7-2. All the membranes showed an excellent oxidative stability with a remaining weight greater than 81%. Since it is widely considered that the electron-donating groups (–O–) in the *ortho*- and *para*-positions to the sulfonic acid group may lead to a lower oxidative stability, the sulfonated aliphatic side chains would contribute to the high oxidative stabilities of the SPPEs.[20]

7-2-3. Mechanical property

The dynamic mechanical properties were investigated by DMA measurements. The *E*' and *E*'' values of 2.6 GPa and 300 MPa are maintained from 80 to 180 ^oC, respectively, indicating the excellent mechanical strength despite of the relatively high *IEC* value (1.96 mequiv/g).

Typical tensile stress-strain curves of all the SPPE membranes are shown in Figure 7-5. They exhibited a reasonably high mechanical strength with a Young's modulus (*M*), maximum stress (*S*) and elongation at break (E_b) values ranging from 1.01 to 1.30 GPa, 34-54 MPa and 4.4-21.2%, respectively, which indicated that the membranes could undergo a fairly large deformation or sustain a quite high external impact without breaking in practical applications. Polymer **4c** exhibited the highest values of 1.30 GPa, 54 MPa and 21.2% for the *M*, *S* and E_b, respectively, which might indicate that the appropriate level of rigidity for the polymer backbone can improve the mechanical strength for these types of PEMs. The free rotation of ether linkages between aromatic

groups of **4c** should cause the higher elasticity compared to others, and thereby its mechanical properties such as tensile strengths could also be improved.

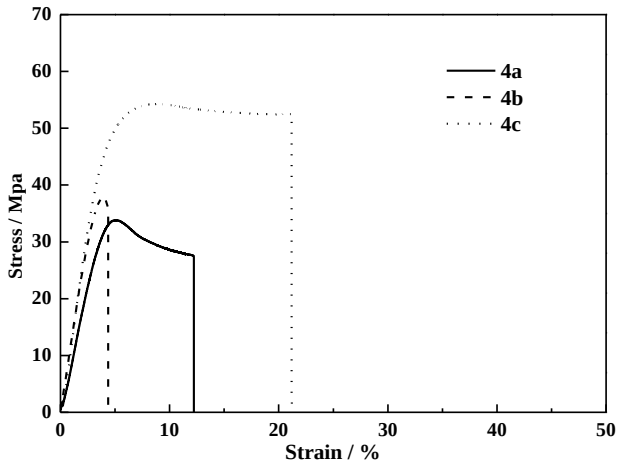

Figure 7-5. Stress-strain curves of SPPEs.

7-2-4. IEC, water uptake and dimensional change

The *IEC* values were determined by a back-titration method, and the results are listed in Table 7-2. All the titrated data were close to the calculated ones from the ^{1}H NMR spectra, indicating a complete proton exchange process.

As is well known, the water uptake (*WU*) of the PEMs has a significant effect on the membrane conductivity. Water molecules usually facilitate the proton transfer; however, an excessive *WU* would inevitably lead to an undesirable membrane swelling, resulting in a reduced mechanical strength of the membrane. Figure 7-6 shows the *WU* of the polymers **4** as a function of the relative humidity, together with that of Nafion 117 for comparison. Analogous to the common aromatic sulfonated polymers, the *WU*s of the polymers **4** showed a greater RH dependence than that of Nafion, especially under a high RH condition. Regardless of the similar *IEC* values, the *WU* of **4c** is 30% lower than **4b** over the entire RH range, which indicates the better swelling behavior of the latter.

The dimensional change data of the polymers **4** are also summarizes in Table 7-2. Compared to some other well-developed poly(phenylene)s or poly(ether sulfones)s, the polymers **4** exhibit much lower dimensional changes.[30-32] The phenyl-phenyl bond increases the rigidity of the main chain, which may suppress the excessive swelling of the membranes even under high RH conditions. For example, polymer **4a** with an *IEC* of 2.45 mequiv/g shows only 0.021 and 0.03 in-plane and through-plane directions

under 50% RH, respectively, whereas 0.110 and 0.13 in-plane and through-plane directions under 95% RH, respectively. It is expected that polymer **4c** displayed the best dimensional stability due to its lowest *IEC* values. Its Δl_c was 0.07 under 80 ^{o}C/95% RH, which would meet the requirement for a single cell test.

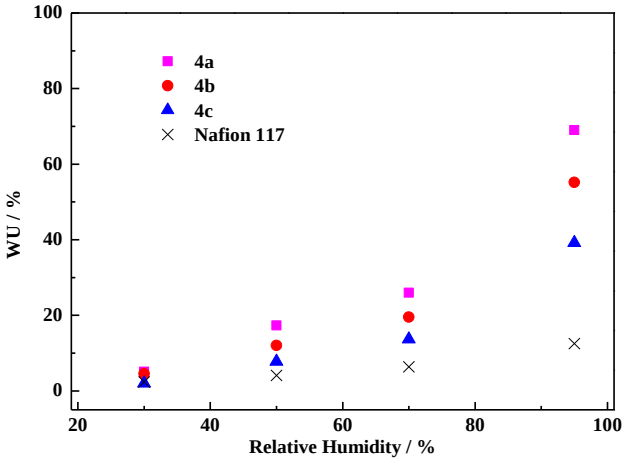

Figure 7-6. *WU* of the polymers **4** as a function of relative humidity.

7-2-5. Proton conductivity

Figure 7-7 shows the proton conductivity of the polymers **4** as a function of RH at 80 ^{o}C, together with that of Nafion 117 for comparison. All of polymers **4** exhibited a greater humidity dependence than that of Nafion. For example, polymer **4a** with the *IEC* value of 2.45 exhibited the highest σ value of 237 mS/cm under the 95% RH condition. It decreased to 8.5 mS/cm with the decreasing RH to 30%, however, it was still slightly higher than that of Nafion (7.3 mS/cm), indicating the better proton conductive capacity of the former.

The relationship between the *WU* and proton conductivity of the polymers **4** and Nafion 117 was investigated. In Figure 7-8, the σ value is plotted versus the hydration number, λ, which is the number of water molecules per a sulfonic acid unit. As could be seen, all the membranes tend to increase their proton conductivity with increasing λ values. At a similar proton conductivity level, the polymers **4** have higher λ values than Nafion, indicating that the polymers **4** require many more water molecules to facilitate proton transfer than the latter. The polymer **4a** exhibits a higher proton conductivity compared to Nafion 117 over the entire range, probably due to its highest *IEC* value and well-connected proton pathways.

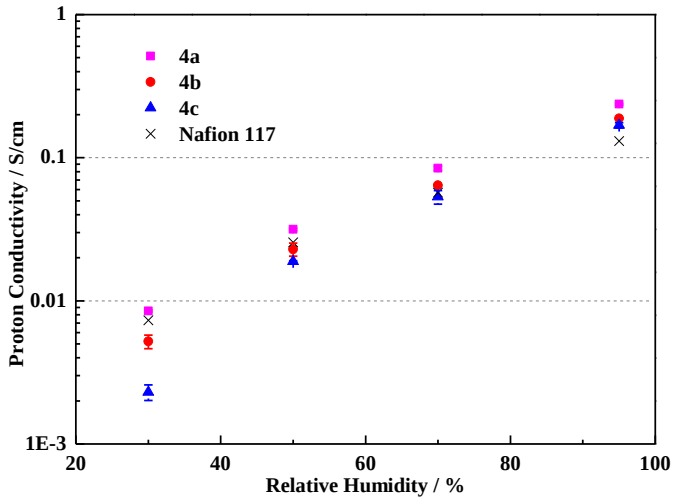

Figure 7-7. Humidity dependence of proton conductivities of the polymers **4** and Nafion 117 at 80 ^{o}C.

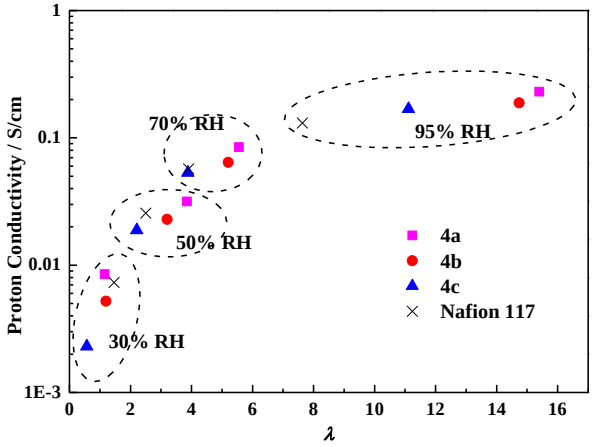

Figure 7-8. Relationship between hydration number (λ) and proton conductivity for the polymers **4** and Nafion 117 at 80 ^{o}C.

7-2-6. Morphology

The nanostructure and morphology of the polymer **4a** were studied using AFM. The AFM tapping mode phase image of the **4a** membrane was recorded under ambient conditions on an 800 $\times$ 800 nm^2 size scale to investigate its surface morphology. As can be seen in Figure 7-9, a continuous phase-separated nanostructure was found in which the sulfonic acid groups aggregate to form the nano-channels structures (dark region in Figure 7-9), although the direction of the structures is disordered. The formation of a phase-separated nanostructure, even disordered, may contribute to the efficient proton transport and excellent proton conductivity.

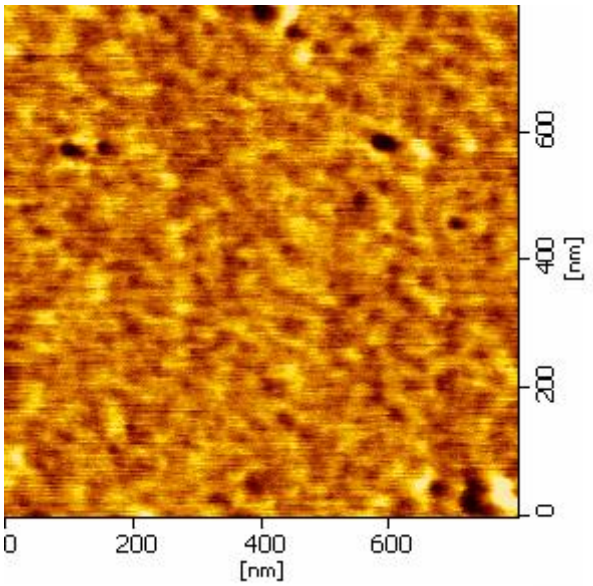

Figure 7-9. AFM tapping mode phase image of **4a** membrane: scan size is 800 × 800nm^2.

7-3. **Conclusions**

A series of PPEs with sulfonic acids via long alkyl side chains, SPPEs (polymer **4**), were successfully obtained by the polycondensation of BFMBP and various dihydroxy-monomers in the presence of K_2CO_3, followed by demethylation of the polymer **2** with BBr_3, and finally by the reaction of the resulting polymer **3** with 1,4-butanesultone. The titrated *IEC* values of the SPPEs were slightly lower than the theoretical and calculated ones from the ^{1}H NMR spectra. The SPPEs exhibited high thermal stabilities despite the fully aliphatic side chains, excellent oxidative stabilities, and reasonably high mechanical strengths with a Young's modulus (*M*), maximum stress (*S*) and elongation at break (E_b) values that ranged from 1.01 to 1.30 GPa, 34-54 MPa and 4.4-21.2%, respectively. The DMA results showed the high storage modules of 2.6 GPa for **4c** from 80-180 ^{o}C, regardless of its relatively high *IEC* value of 1.96 mequiv/g. All SPPEs exhibited a greater RH dependence than Nafion for the proton conductivities. The polymer **4a** with the *IEC* value of 2.45 mequiv/g showed the high σ value of 8.6 mS/cm under 80 ^{o}C/30% RH conditions, whereas it was 7.3 mS/cm for Nafion 117. Consequently, the novel PPEs with pendant alkyl sulfonated side chains, are promising candidates for fuel cell applications.

7-4. Experimental

Materials

5-Chloro-2-fluorobenzoic acid, anisole, $AlCl_3$ were purchased from TCI and used as received. Thionyl chloride was purchased from Wako Pure Chemical Industries, Ltd and used as received. Bis(triphenylphosphino)nickel(II) ($Ni(PPh_3)_2Cl_2$, TCI) and tetraethylammonium iodide (Et_4NI, TCI) were dried at 100 ^oC under vacuum prior to use. Zinc power was purchased from Aldrich, washed with 2.0 M hydrochloric acid, deionized water, ethanol, diethylether, successively, and dried at 100 ^oC for 6 h and at room temperature for 18 h under vacuum. Tetrahydrofuran (THF, dehydrated, stabilizer-free, 99.5%, Wako) was refluxed over sodium benzophenone under N_2 for 2 h, then distilled just before use. *N*,*N*-Dimethylacetamide (DMAc, Wako) was dried over CaH_2, distilled under reduced pressure and stored over 4 Å molecular sieves prior to use. Other solvents and reagents were used as received.

Synthesis of 5-Chloro-2-fluoro-4'-methoxylbenzophenone (CFMB)

To a 50 mL flask equipped with a magnetic stirrer, 5-chloro-2-fluorobenzoic acid (12.5 g, 71.6 mmol) and 20.0 mL of thionyl chloride was added. The solution was kept at 85 ^oC for 10 h and the excessive thionyl chloride was evaporated under atmosphere. The 5-chloro-2-fluorobenzoyl chloride (**CFBC**) was obtained by evaporating under reduced pressure to afford a colorless liquid; 12.8 g (yield: 92%). 1H NMR ($CDCl_3$, ppm): δ = 8.07-8.04 (m, 1H, Ar-H), δ = 7.62-7.57 (m, 1H, Ar-H), δ = 7.19-7.13 (t, *J* = 8.7 Hz, 1H, Ar-H).

To a fully dried 100 mL three-necked flask, $AlCl_3$ (9.12 g, 68.4mmol) and anisole (90.0 mL) were charged. After cooling to 0 ^oC by an ice-water bath, **CFBC** (12.0 g, 62.2mmol) was added dropwise to the mixture through a pressure-equilibrium drop funnel and the reaction mixture was then heated to 50 ^oC for 3 h. The solution was poured into ice water with a few drops of HCl, and the product was extracted with chloroform. After dying over $MgSO_4$, evaporation, and recrystallization from ethanol, CFMB(12.5 g) was obtained; yield: 76%. IR (KBr): *ν* 2960-2870 (C-H), 1647 (C=O), 1597 (C=C), 1180 cm^{-1} (C-O-C). ^1H NMR ($CDCl_3$, ppm): δ = 7.81-7.78 (d, *J* = 8.7 Hz, 2H, Ar-H), δ = 7.47-7.40 (m, 2H, Ar-H), δ = 7.12-7.06 (t, *J* = 8.4 Hz, 1H, Ar-H), δ= 6.95-6.92 (d, 2H, *J* = 8.7 Hz, Ar-H), δ = 3.87 (s, 3H, $-OCH_3$). ^{13}C NMR ($CDCl_3$, ppm): δ = 190.24 (1C, C7), 164.18 (1C, C11), 159.73, 156.40 (1C, C4), 132.31 (1C, C2), 132.25, 132.14 (1C, C1), 130.03, 129.99 (2C, C9), 129.59, 129.54 (1C, C5), 129.50 (1C,

C8), 128.89, 128.65 (1C, C6), 117.76, 117.45 (1C, C3), 113.86 (2C, C10), 55.53 (1C, C12). Anal. Calcd. for $C_{14}H_{10}ClFO_2$: C:63.53; H: 3.81. Found: C: 63.58; H: 3.90.

Synthesis of Bis[4-fluoro-3-(4'-methoxylbenzoyl)]biphenyl (BFMBP)

To a 50 mL two-necked flask equipped with a magnetic stirrer, were charged with **CFMB** (5.00 g, 18.9mmol), $Ni(PPh_3)_2Cl_2$ (1.24 g, 1.89mmol), Et_4NI (0.486 g, 1.89 mmol) and zinc dust (3.71 g, 56.7mmol). After being exchanged with argon three times, 38.0 mL of anhydrous THF was added. The reaction mixture underwent a color change from green to yellowish brown and finally dark red at 50 ^oC for 24 h. After filtration, the product was separated by a silica column using CH_2Cl_2 as an eluent. By recrystallization from ethanol, BFMBP (2.05 g) was obtained as white needle-like crystals; yield: 46%. IR (KBr): *v* 2960-2870 (C-H), 1647 (C=O), 1600 (C=C), 1180 cm^{-1} (C-O-C).^{1}H NMR ($CDCl_3$, ppm): δ = 7.83-7.80 (d, *J* = 9.0 Hz, 4H, Ar-H), δ = 7.66-7.62 (m, 4H, Ar-H), δ = 7.22-7.16 (t, *J* = 9.0 Hz, 2H, Ar-H), δ= 6.93-6.90 (d, *J* = 9.0 Hz, 4H, Ar-H), δ = 3.84 (s, 6H, $-OCH_3$).^{13}C NMR ($CDCl_3$, ppm): δ = 191.51 (2C, C7), 164.05 (2C, C11), 161.03, 157.69 (2C, C4), 135.78, 135.74 (2C, C1), 132.30 (2C, C2), 130.98, 130.86 (4C, C9), 129.91 (2C, C8), 128.87, 128.82 (2C, C6), 128.04, 127.82 (2C, C5), 116.90, 116.61 (2C, C3), 113.81 (4C, C10), 55.51 (2C, C12). Anal. Calcd.for $C_{28}H_{20}F_2O_4$: C: 73.36; H: 4.40. Found: C: 73.03; H:4.72.

Synthesis of Poly(phenylene ether) (2)

A typical procedure of polymer **2b** is as follows. A three-necked flask was charged with BFMBP (1.20 g, 2.62mmol), bisphenol (0.487 g, 2.62mmol), K_2CO_3 (0.416 g, 3.01mmol), DMAc (8.40 mL) and toluene (8.00 mL). The mixture was purged with nitrogen and then heated to 140 ^oC for 2 h. After toluene was fully removed, the reaction temperature was gradually risen to 165 ^oC and kept for another 6 h. The resulting viscous solution was cooled down to room temperature, diluted with 8.40 mL of DMAc, and precipitated into methanol containing a few drops of concentrated HCl. The polymer was reprecipitated from 5 wt% DMF solution into a mixture solution ($CHCl_3$/methanol = 2/8). After drying at 100 ^oC under vacuum for 12 h, the fibrous polymer was obtained (1.23 g, yield: 77%). IR (KBr): *v* 2960-2870 (C-H), 1658 (C=O), 1597 (C=C), 1169 cm^{-1} (C-O-C).^{1}H NMR (DMSO-d_6, ppm): δ = 7.87-7.77 (bm, Ar-H), δ = 7.52 (bs, Ar-H), δ = 7.14-6.96 (bm, Ar-H), δ = 3.82 (s, $-OCH_2-$).

Synthesis of Poly(phenylene ether) (3)

A typical synthetic procedure of polymer **3b** is as follows. To a 200 mL three-necked flask equipped with a nitrogen inlet/outlet, were charged polymer **2b** (1.00 g, 1.65mmol) and CH_2Cl_2 (80.0 mL). The solution was cooled to 0 ^oC in an ice bath, and a BBr_3/CH_2Cl_2 solution (12.0 mL) was added dropwise to the solution. After addition, the reaction was kept at room temperature overnight. The resulting copolymer was obtained by carefully pouring the solution into water, filtered, washed thoroughly with water, methanol, successively, and dried under vacuum at 80 ^oC for 12 h. Yield: 0.912 g (96%). IR (KBr): *v* 3500-3200 (-OH), 2960-2870 (C-H), 1643 (C=O), 1597 (C=C), 1169 cm^{-1} (C-O-C).^1H NMR (DMSO-d_6, ppm): 10.36 (s, -OH), δ = 7.87-7.67 (bm, Ar-H), δ = 7.34-7.26 (bm, Ar-H), δ = 7.10-6.99 (bm, Ar-H), δ = 6.86-6.64 (bm, Ar-H).

Synthesis of Sulfonated Poly(phenylene ether) (4)

A typical synthetic procedure of polymer **4b** is as follows. To a 20 mL three-necked flask equipped with a nitrogen inlet/outlet, were charged polymer **3b** (0.80 g, 1.39 mmol), sodium hydride (0.050 g, 2.08mmol) and dimethyl sulfoxide (DMSO) (15.0 mL). The solution was heated to 100 ^oC, and 1,4-butanesultone (0.756 g, 5.45mmol) was added dropwise to the mixture. After 12 h, the solution was cooled to room temperature and slowly poured into ethanol. The sulfonated copolymer was filtered and then dried in a vacuum oven at 100 ^oC for 12 h. Yield: 1.14 g (97%). IR (KBr): *v* 2960-2870 (C-H), 1658 (C=O), 1600 (C=C), 1176 cm^{-1} (C-O-C), 1119, 1049 cm-1 (O=S=O). ^1H NMR (DMSO-d_6, ppm): δ = 7.77-6.80 (bm, Ar-H), δ = 3.91 (s, -OCH_2-), δ = 2.54 (s, -CH_2-SO_3Na), δ = 1.84-1.74 (m, -CH_2-).

Preparation of Polymers 4 Membranes

Membranes were prepared by a solution casting method. Polymer 4 was dissolved in DMSO with concentration of 5% (m/v). After filtration, the solution was cast onto a clean Petri dish, dried at 80 ^oC for 20 h under atmosphere. The membrane was detached from the dish by immersing into water to remove the residual solvent, followed by soaking in 2 M H_2SO_4 at 50 ^oC for 72 h for proton exchange. Then, the membrane was thoroughly washed with Milli-Q water. The thickness of the membranes was controlled to be about 50 μm.

Characterizations

^1H (300 MHz) and ^{13}C (75 MHz) NMR spectra were recorded on a Bruker DPX300S

spectrometer using $CDCl_3$ or DMSO-d_6 as the solvent and tetramethylsilane as the reference. Fourier transform-infrared (FT-IR) spectra were obtained with a Horiba FT-120 Fourier transform spectrophotometer. Number- and weight-average molecular weights (M_n and M_w) were measured by gel permeation chromatography (GPC) on a Hitachi LC-7000 system equipped with polystyrene gel columns (TSKgel GMHHR-M) eluted with *N*,*N*-dimethylformamide (DMF) containing 0.01 M LiBr at a flow rate of 1.0 mL min^{-1} calibrated by standard polystyrene samples. Thermogravimetric analysis (TGA) was measured in N_2 on a Seiko EXSTAR 6000 TG/DTA 6300 thermal analyzer at a heating rate of 10 ^oC min^{-1}. Dynamic mechanical analysis (DMA) was performed on the film specimens (length, 30 mm; width, 10 mm; thickness, 50 μm) by using the Seiko DMS 6300 at a heating rate of 2 ^oC min^{-1} with a load frequency of 1 Hz under nitrogen atmosphere. The mechanical properties of SPPE membranes were also analyzed by tensile measurement, which was performed with a universal testing instrument (AGS-X 349-05489A, Shimadzu, Japan) at 20^oC and around 50% RH at a crosshead speed of 2 mm/min. Tapping mode atomic force microscope (AFM) images were taken by using Seiko InstrumentsSPA-400 with a stiff cantilever of Seiko Instruments DF-20.

Water Uptake and Dimensional Change

The humidity dependence of water uptake was measured by placing the membrane in a thermo-controlled humid chamber for 4 h under each RH condition. The membrane was then taken out, and quickly weighed on a microbalance. Water uptake (*WU*) was calculated according to the following equation (1):

$$WU = (W_s - W_d)/W_d \times 100 \text{ wt\%} \qquad (1)$$

where W_s and W_d are the weights of wet and dried membranes, respectively.

For dimensional change measurements, squared membrane sheets were placed in a thermo-controlled humid chamber for 2 h under each RH condition. The dimensional change in membrane thickness direction (Δt_c) and the plane direction (Δl_c) were calculated from equation (2):

$$\Delta t_c = (t - t_s)/t_s \qquad \Delta l_c = (l - l_s)/l_s \qquad (2)$$

where t_s and l_s refer to the thickness and diameter of the membrane equilibrated at about 80 ^oC/30% RH, respectively; t and l refer to those of the dry membrane under each condition.

Ion Exchange Capacity

*IEC*s of the membranes were determined by a titration method. The proton-type samples were ion-exchanged by a 15 wt% NaCl solutions and titrated with a 0.02 M NaOH solution with phenolphthalein as the indicator. IEC was calculated from equation (3):

$$IEC = C_{NaOH} \times V_{NaOH} / W_d \quad (3)$$

where C_{NaOH} and V_{NaOH} are the concentration of NaOH solution and the consumed volume of NaOH solution, respectively.

Water Sorption (λ)

The λ value was calculated from the equation (4):

$$[H_2O]/[SO_3^-] = WU \times 10/18 \times IEC \quad (4)$$

Proton Conductivity

Proton conductivity in plane direction of the membrane was determined using an electrochemical impedance spectroscopy technique over the frequency from 5 Hz to 1 MHz (Hioki 3532-80). A two-point probe conductivity cell with two platinum plate electrodes was fabricated. The cell was placed in a thermo-controlled humid chamber at 80 ^oC for 2 h before the measurement. Proton conductivity (σ) was calculated from the following equation (5):

$$\sigma = d/(t_s w_s R) \quad (5)$$

where d is the distance between the two electrodes, t_s and w_s are the thickness and width of the membrane, and R is the resistance measured.

Oxidative stability

Oxidative stability was determined by soakinga membrane sample (10 × 10 mm^2) in 50 mL of Fenton's reagent (3% H_2O_2 containing 2 ppm$FeSO_4$) at 80 ^oC for 1 h. The residue was then taken out, washed with water, and dried under vacuum at 100 ^oC until a constant weight (remaining weight).

7-5. References

(1) Mauritz, K. A.; Moore, R. B. *Chem. Rev.* **2004**, *104*, 4535-4586.

(2) Savadoga, O. J. *New.Mater.Electrochem. Syst.* **1998**, *1*, 47-66.

(3) Rikukawa, M.; Sanui, K. *Prog. Polym. Sci.* **2000**, *25*, 1463-1502.

(4) Hickner, A. H.; Ghassemi, H.; Kim, Y. S.; Einsla, B. R.; McGrath, J. E. *Chem. Rev.* **2004**, *104*, 4587- 4612.

(5) (a) Takamuku, S.; Jannasch, P. *Adv. Energy Mater.* **2012**, *2*, 129-140; (b) The 2011 Progress Report for US DOE Hydrogen andFuel Cells Program. http://www.hydrogen.energy.gov/pdfs/progress11/v_c_1_hamrock_2011.pdf; (c) Gebert, M.; Ghielmi, A.; Merlo, L.; Corasaniti, M.; Arcella, V. *ECSTrans*. **2010**, 279- 283.

(6) Higashihara, T.; Matsumoto, K.; Ueda, M. *Polymer* **2009**, *50*, 5341- 5357.

(7) Park, C. H.; Lee, C. H.; Guiver, M. D.; Lee, Y. M. *Prog.Polym. Sci*. **2011**, *36*, 1443-1498.

(8) Liu, Y. L. *Polym. Chem.* **2012**, *3*, 1373-1383.

(9) Zhang, H.; Shen, P. K. *Chem. Rev.* **2012**, *112*, 2780-2832.

(10) Zhang, H.; Shen, P. K. *Chem. Soc. Rev.* **2012**, *41*, 2382-2394.

(11) Matsumoto, K.; Higashihara, T.; Ueda, M. *Macromolecles* **2008**, *41*, 7560-7565.

(12) Zhang, X.; Hu, Z.; Luo, L.; Chen, S.; Liu, J.; Chen, S.; Wang, L. *Macromol. Rapid Commun.* **2011**, *32*, 1108-1113.

(13) Zhang, X.; Chen, S.; Liu, J.; Hu, Z.; Chen, S.; Wang, L. *J.Membr. Sci.* **2011**, *371*, 276-285.

(14) Miyatake, K.; Chikashige, Y.; Higuchi, E.; Watanabe, M. *J. Am. Chem. Soc.* **2007**, *129*, 3879- 3887.

(15) Matsumoto, K.; Higashihara, T.; Ueda, M. *Macromolecules* **2008**, *42*, 1161-1166.

(16) Lafitte, B.; Jannasch, P. *Adv. Funct. Mater.* **2007,** *17*, 2823-2834.

(17) Wang, C.; Shin, D. W.; Lee, S. Y.; Kang, N. R.; Lee, Y. M.; Guiver, M. D. *J. Membr. Sci.* **2012,** *405-406*, 68-78.

(18) Hu, Z.; Yin, Y.; Okamoto, K-I.; Moriyama, Y.; Morikawa, A. *J.Membr. Sci*. **2009,** *329*, 146-152.

(19) Seesukphronrarak, S.; Ohira, A. *Chem. Commun*. **2009,** 4744-4746.

(20) Zhang, X.; Sheng, L.; Higashihara, T.; Ueda, M. *Polym. Chem*. **2013, *4,*** 1235-1242.

(21) Zhang, X.; Hu, Z.; Pu, Y.; Chen, S.; Ling, J.; Bi, H.; Chen, S.; Wang, L.; Okamoto, K.-I. *J. Power Sources* **2012,** *216*, 261-268.

(22) Xu, T.; Wu, D.; Wu, L. *Prog.Polym. Sci*. **2008,** *33,* 894-915.

(23) Zhang, Z.; Wu, L.; Xu, T. *J.Membr. Sci*. **2011,** *373,* 160-166.

(24) Xu, T.; Wu, D.; Seo, S.-J.; Woo, J.-J.; Wu, L.; Moon, S.-H. *J. Appl.Polym. Sci*. **2012,** *124,* 3511-3519.

(25) Miyatake, K.; Zhou, H.; Watanabe, M. *J.Polym. Sci.: Part A: Polym. Chem.* **2005,** *43,* 1741-1744.

(26) Sheng, L.; Higashihara, T.; Nakazawa, S.; Ueda, M. *Polym. Chem.* **2012,** *3,* 3289-3295.

(27) Iyoda, M.; Otsuka, H.; Sato, K.; Nisato, N.; Oda, M. *Bull. Chem. Soc. Jpn.* **1990,** *63,* 80-87.

(28) Colon, I.; Kelsey, D. R. *J. Org. Chem*. **1986,** *51,* 2627-2637.

(29) Koepnick, B. D.; Lipscomb, J. S.; Taylor, D. K. *J. Phys. Chem. A.* **2010,** *114,* 13228-13233.

(30) Zhang, X.; Hu, Z.; Zhang, S.; Chen, S.; Chen, S.; Liu, J.; Wang, L. *J. Appl. Polym. Sci*. **2011,** *121,* 1707-1716.

(31) Nakabayashi, K.; Higashihara, T.; Ueda, M. *J. Polym. Sci., Part A: Polym. Chem.* **2010,** *48,* 2757-2764.

(32) Nakabayashi, K.; Matsumoto, K.; Higashihara, T.; Ueda, M. *Polym. J.* **2009,** *41,* 332-337.

Chapter 8

Poly(arylene ether ether nitrile)s Containing Different Length of Pendant Alkyl Sulfonic Acid for Polymer Electrolyte Membranes

ABSTRACT: A series of poly(arylene ether ether nitrile)s with different chain lengths of the alkylsulfonates (SPAEEN-x : x refers the number of the methylene units) were successfully synthesized for fuel cell application. The polymers produced flexible and transparent membranes by solvent casting. The resulting membranes displayed a high thermal stability, oxidative stability and higher proton conductivity than that of Nafion 117 at 80 ^{o}C and 95% relative humidity (RH). Furthermore, the SPAEEN-12 with the longest alkylsulfonated side chain exhibited a higher proton conductivity at 30% RH than that of SPAEEN-6 despite the lower IEC value, which indicated that the introduction of longer alkylsufonated side chains to the polymer main chain induced efficient proton conduction by the formation of a well-developed phase-separated morphology.

8-1. Introduction

Polymer electrolyte membrane fuel cell (PEMFC) has been actively developed worldwide as an efficient and clean energy sources as alternatives to limited fossil fuel resources.[1] The polymer electrolyte membrane (PEM) is the key component of PEMFC because it serves as the separator of the electrodes and transports protons from anode to cathode. PEMs that have received the most attention in recent years are fully fluorinated polymers with acid-functionalized side chains, such as Dupont's Nafion®, Dow Chemical's Aquivion® due to their good proton conductivity, excellent chemical stability and long-term durability. However, they suffer from some drawbacks such as a high production cost, poor thermomechanical properties above 80 ^{o}C, environmental incompatibility and high permeability of fuels and oxygen. To date, numerous sulfonated aromatic hydrocarbon-based polymers, which contain sulfonic acid groups on the polymer main chain, have been already reported as alternative membranes.[2-15] The low-cost productivity is an attracting advantage for hydrocarbon-based polymers in comparison to the perfluoropolymers. However, most of them have failed to meet the requirements of a high conductivity under a low relative humidity (RH) and durability under fuel cell operating conditions. To improve the proton conductivity at a low RH, increasing the content of the sulfonic acid groups in the polymer main chain, that is, the higher ion exchange capacity (IEC) values, is an effective way. Litt *et al*.,[16] for example, reported the synthesis of poly(*para*-phenylene disulfonic acid) with the IEC higher than 8.0 mequiv/g. The proton conductivity value was about 11 times higher than that of Nafion® NR-212 even at 30% RH and 80 ^{o}C, which has never been reported so far. However, this membrane absorbed a large amount of water, significantly swelled, and the conductivity could not be measured above 65% RH. Therefore, to prepare high performance PEMs for using under fuel cell conditions cannot only focus on increasing IEC. Recently, the Okamoto and Watanabe groups reported a series side chain type sulfonated polyimide (SPIs) including both the short side chains (sulfopropoxy and sulfobutoxy groups) and long side chains.[17-22] The resulting membranes showed a higher hydrolytic stability compared to the main chain type SPIs, because the sulfonic acid groups were located on flexible side chains separated from the main chains, which reduced the chances of nucleophilic attack by water on the imide linkage, and also displayed some improvement of proton conductivity by forming a well-dispersed hydrophilic domains compared with the main chain type ones.[2] However, the proton conductivity of SPIs could not be improved even the number of aliphatic carbons were extended to 12,[20,21] probably due to the bulky imide ring in the main chain, which

increases the distance between the sulfonic acid groups of the SPI. On the other hand, appropriate high IEC, which is required for high proton transport, is difficult to obtain for increasing the length of side chain on SPIs.[20] Zhang group also reported side chain type polymers for PEM,[27] they chose the cardo poly(arylene ether sulfone)s as main chain and introduced long side chains with the number of alkyl carbon of 10. However, the proton conductivity was lower than that of Nafion even in water due to the low density of the alkylsulfonic acid groups in the polymers.

In this chapter, the aromatic poly(arylene ether ether nitrile)s (SPAEEN-x) with high density of the alkylsulfonic acid groups were successfully prepared. The nitrile groups were introduced into the polymer main chain to suppress the water uptake according to the previous reports.[29] Furthermore, the effect of chain lengths of alkylsulfonic acid groups on the membrane properties, such as thermal stability, oxidative stability, mechanical strength, water uptake, and proton conductivity was investigated. We found that the membrane SPAEEN-12 with the lower IEC value of 1.89 mequiv/g showed higher proton conductivity than the membrane SPAEEN-6 with the higher Iec value of 2.32 mequiv/g at low RH by the formation of well-developed nanophase-separated morphology, which was supported by atomic force microscope (AFM) image.

8-2. **Results and discussion**

8-2-1. **Synthesis of sodium bromoalkylsulfonates and polymers.**

As shown in Scheme 8-1, various sodium bromoalkylsulfonates were prepared according to a previous paper.[25] The chemical structure of sodium 6-bromohexylsulfonate, sodium 10-bromodecylsulfonate and sodium 12-bromododecylsulfonate were confirmed by ^{1}H NMR spectroscopy (Figure 8-1). New peaks at 2.36-2.46 ppm corresponding to the methylene protons next to the –SO_3Na groups are clearly observed. All the other peaks are also well assigned to the corresponding structures.

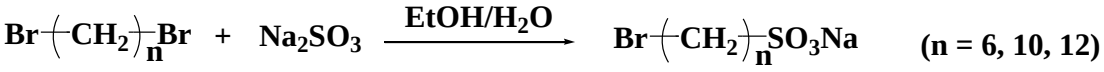

Scheme 8-1. Synthesis of sodium bromoalkylsulfonates.

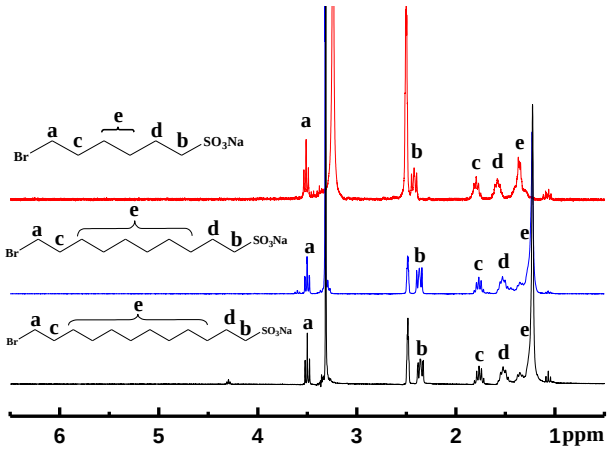

Figure 8-1. ^{1}H NMR spectra of sodium bromoalkylsulfonates.

Poly(arylene ether ether nitrile)s with pendant alkylsufonic acid groups (SPAEEN-x, x refers the number of the methylene unit) were prepared via a three-step reaction as shown in Scheme 8-2. First, the polycondensation of DFBN with MRS was conducted at 160 ^oC, leading to low molecular weight polymer because of premature precipitation of the polymer. Then, MHQ in place of MRS was employed to improve the solubility of the resulting polymer. Although the high molecular weight polymer could be easily prepared from DFBN and MHQ, the resulting polymer showed limited solubility in halogenated hydrocarbons which are suitable solvents for demethylation of methoxy groups using BBr_3. Finally, MPAEEN (M_n = 41,000, M_w = 116,000) was prepared by nucleophilic substitution polycondensation of DFBN with MHQ and MRS in DMAc at

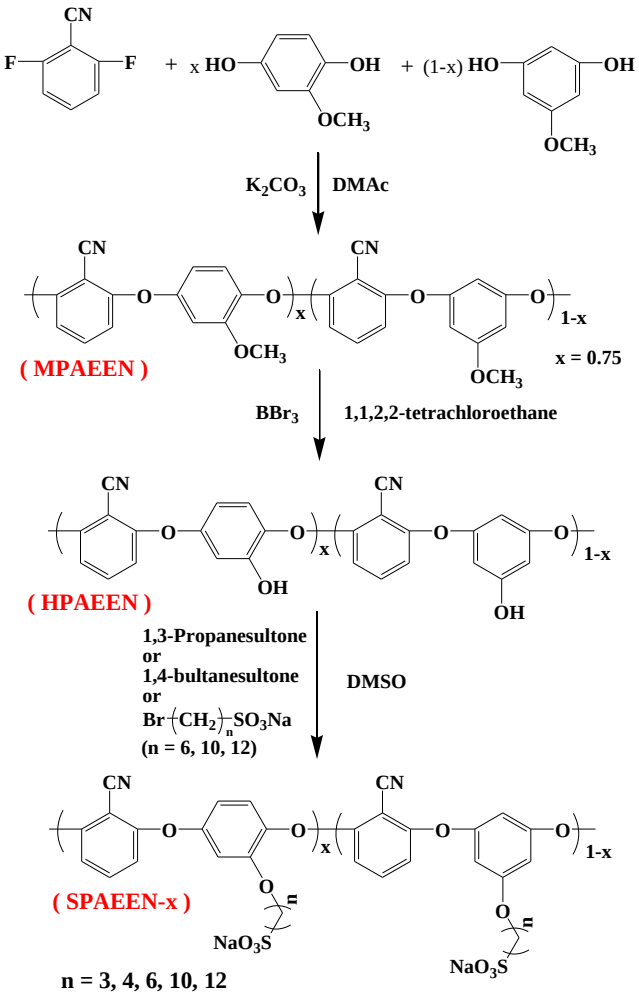

Scheme 8-2. Synthesis of poly(arylene ether ether nitrile) with pendant alkylsufonic acid groups (SPAEEN-x).

160 ^{o}C. The demethylation of methoxy groups was conducted using BBr_3 in 1,1,2,2-tetrachloroethane. HPAEEN was precipitated during the reaction due to the polar nature of the phenol groups. Figure 8-2 shows the ^{1}H NMR spectra of MPAEEN and HPAEEN. The characteristic methoxy protons at 3.79 ppm in the initial MPAEEN disappear in the HPAEEN, and the peak around 10.35 ppm corresponding to the phenol protons appears, indicating that the deprotection is successfully proceeded. Finally, SPAEEN-x were obtained by the reaction of alkanesultones or sodium bromoalkylsulfonates with HPAEEN in the presence of NaOH as a base. Before adding alkanesultones or sodium bromoalkylsulfonates, the water in the reaction mixture was removed by azeotropic distillation with cyclohexane. The structures of the SPAEEN-x were also confirmed by the FT-IR and ^{1}H NMR spectroscopy. The FT-IR spectra of the SPAEEN-x in their sodium form are shown in Figure 8-3. SPAEEN-x show a

characteristic band at 1047 and 1128 cm^{-1} assigned to O=S=O stretching vibration of sulfonated groups. The band at 2230 cm^{-1} corresponding to the stretching vibrations of nitrile group is also observed. The ^{1}H NMR spectra of SPAEEN-x are also shown in Figure 8-4, exhibiting characteristic methylene protons next to the sodium sulfonate group at 2.37 ppm and no hydroxyl protons are observed.

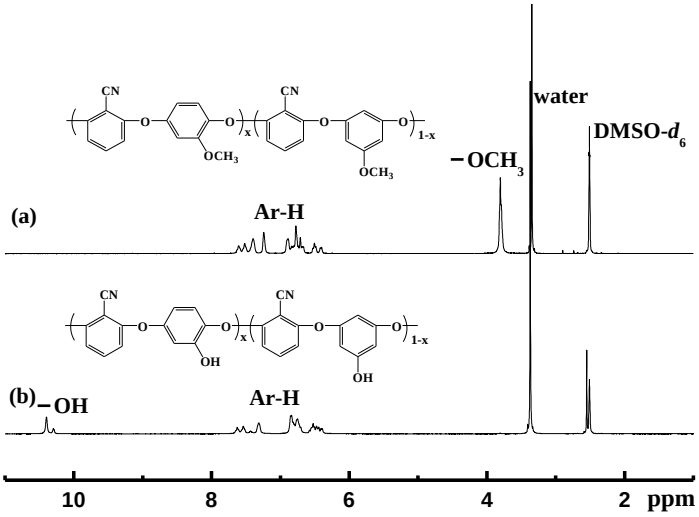

Figure 8-2. ^{1}H NMR spectra of (a) MPAEEN and (b) HPAEEN.

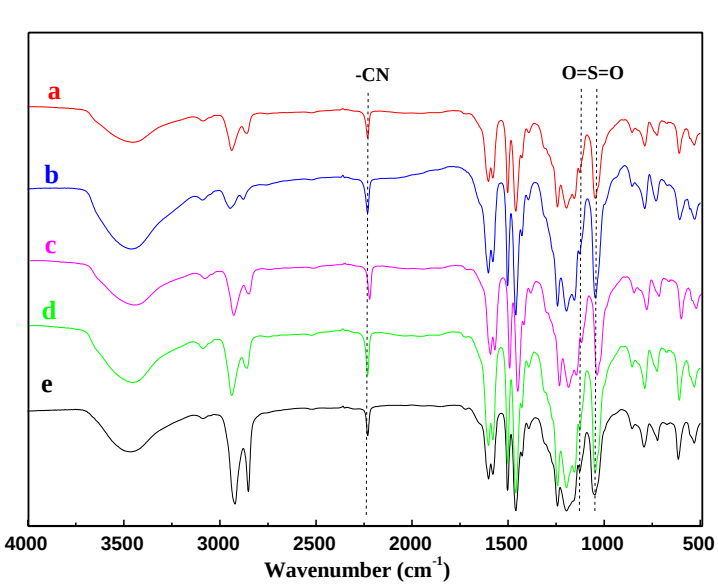

Figure 8-3. FT-IR spectra of SPAEEN-x in sodium form (a: SPAEEN-3; b: SPAEEN-4; c: SPAEEN-6; d: SPAEEN-10; e: SPAEEN-12).

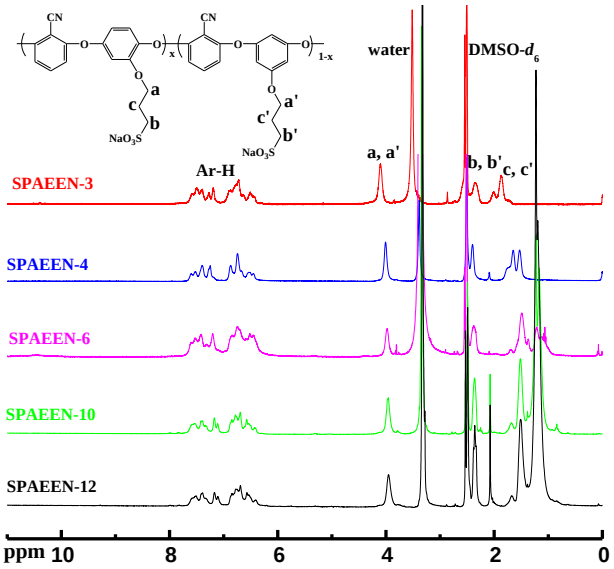

Figure 8-4. ^{1}H NMR spectra of SPAEEN-x.

8-2-2. Thermal stability.

Thermal stability of the polymer SPAEEN-x in acid forms was investigated by TGA analysis under nitrogen (Figure 8-5). All the samples were pre-heated at 150 ^{o}C for 30 min in the TGA furnace to remove moisture. For comparison, the crosslinked sulfonated random ($PBOS_4$-*r*-$PSBOS_6$)[23] and block copolystyrene derivatives ($PSBOS_1$-*b*-P*n*$BOS_{3.2}$) [24] having flexible alkylsulfonated side chains and hydrophobic alkoxy chains are also shown in Figure 8-5. All the SPAEEN-x membranes showed two-stage weight loss behavior. The first stage weight loss temperature start from 220 ^{o}C is possibly associated with the loss of bound water and degradation of sulfonic acid groups, which is much higher than that of the $PBOS_4$-*r*-$PSBOS_6$ (150 ^{o}C)[23] and $PSBOS_1$-*b*-P*n*$BOS_{3.2}$ (150 ^{o}C)[24]. The second stage weight loss temperature at around 350 ^{o}C is likely related to the degradation of alkyl side chain and polymer main chain. The 5wt% weight loss temperatures ($T_{d\ 5\%}$) of all SPAEEN membranes summarized in Table 8-1 are higher than 270 ^{o}C. The TGA results indicate that the SPAEEN-x has high thermal stability, which is high enough for the applications in medium temperature (100-180 ^{o}C) fuel cells.

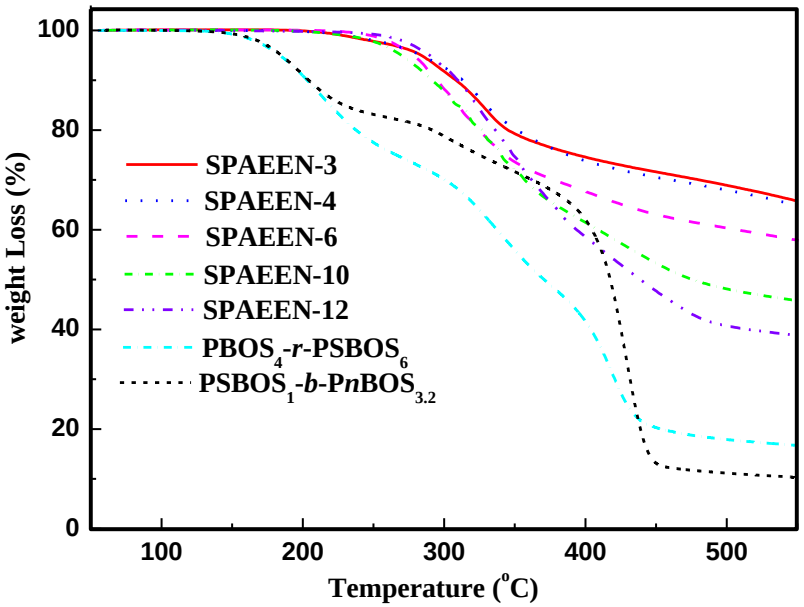

Figure 8-5. TGA curves of the SPAEEN-x membranes, crosslinked sulfonated random ($PBOS_4$-*r*-$PSBOS_6$)[23] and block copolystyrene derivatives ($PSBOS_1$-*b*-P*n*$BOS_{3.2}$) [24] in acid form under N_2.

8-2-3. IEC, water uptake and dimensional change.

The IEC values were determined by a titration method, and the measured IEC values of the SPAEEN-x membranes were in the range of 1.89-2.69 mequiv/g (Table 8-2). The water uptake (WU) and swelling ratio of PEMs are very important properties that significantly related to the proton conductivity and mechanical strength. As other sulfonated aromatic polymers, the IEC values of the membranes generally dominate the WU. The WU and hydration number (λ) of SPAEEN-3 are the highest among the studied membranes due to its high IEC (Figure 8-6). However, the WU of SPAEEN-3 at 80 ^{o}C under 95% RH is lower than 60%, which corresponds to the absorption of less than 12 water molecules per sulfonic acid group. One plausible explanation is the presence of nitrile-nitrile dipole interactions that combine to limit WU. In addition, the nitrile-sulfonic acid group may be important as nitrile groups have been found to associate with sulfonic acid groups through bridging water molecules bridged in specific spectroscopic studies.[26] On the other hand, the WU and λ dramatically decreased at 95% RH when the length of the alkyl side chains is increased. The SPAEEN-3 membrane, for example, has a WU around 57%, which is two times higher than that of the SPAEE-12 membrane (25%).

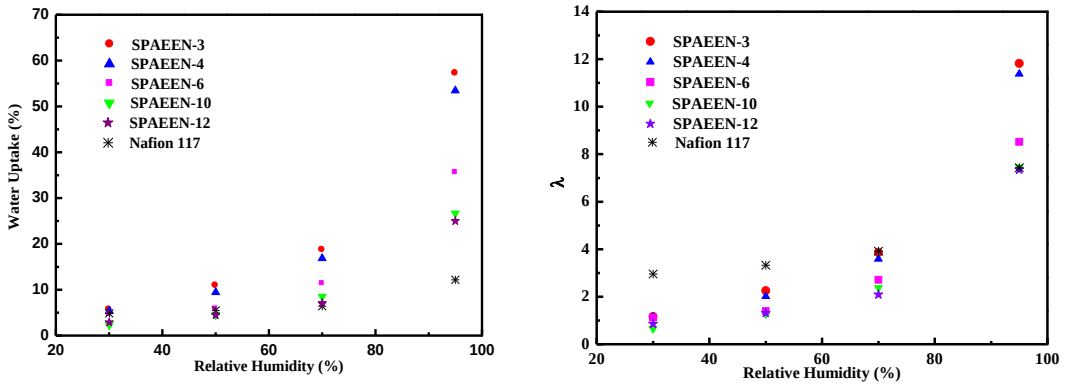

Figure 8-6. Water uptake (L) and hydration number (λ) (R) of SPAEEN-x and Nafion 117 under different RH at 80 ^{o}C.

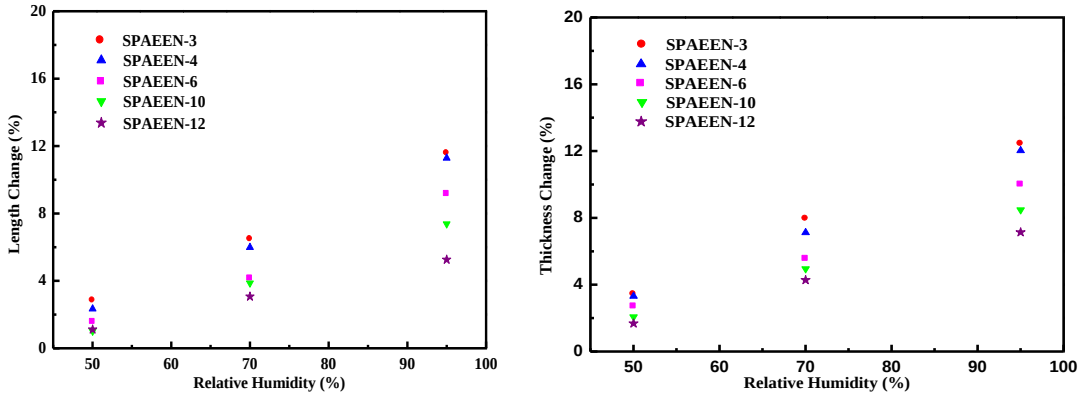

Figure 8-7. Dimensional change of SPAEEN-x: length change (L) and thickness change (R) under different RH at 80 ^{o}C.

The dimensional change in all the SPAEEN-x membranes was also measured at different RHs (50-95%) and 80 ^{o}C (Figure 8-7). The SPAEEN-x membranes show an anisotropic swelling behavior with a slightly higher change in thickness direction. The SPAEEN-3 membrane with the highest IEC among these membranes displays a dimensional change lower than 13% even at 95% RH. This result indicates that the introduction of –CN group and long alkylsulfonated side chains could effectively suppress the swelling ratio of the membrane.

8-2-4. Oxidative stability and mechanical properties.

It is well known that poor oxidative stability of the membranes may cause failure during long-term fuel cell operation. All the prepared membranes were performed to the

Table 8-1. Thermal, mechanical properties and oxidative stability of SPAEEN-x membranes

samples	$T_{d\ 5\%}$ (^oC)	maximum stress(MPa)[b]	Young's modulus(MPa)[b]	Elongation at break(%)[b]	disappearance time (h)[c]
SPAEEN-3	285	-[a]	-	-	43
SPAEEN-4	284	19	714	25	44
SPAEEN-6	278	22	522	15	62
SPAEEN-10	270	18	435	25	>80
SPAEEN-12	289	-	-	-	>80

-: has not measured

[b]Measured at 20 ^oC under 50% RH.

[c]Measured by soaking the membranes in Fenton's reagent (3% H_2O_2 containing 20 ppm $FeSO_4$) at room temperature.

oxidative stability test by immersing the samples in Fenton's reagent (3% H_2O_2, 20 ppm $FeSO_4$) at room temperature. The resistance to oxidation of the membranes was evaluated by observing the dissolving behavior, and their results are summarized in Table 8-1. The SPAEEN-3 membrane with the highest IEC value resisted soaking in Fenton's reagent for more than 40 h. On the other hand, the membranes with longer alkylsulfonated side chains shows better oxidative stability than those with the shorter side chains. The SPAEEN-12 membrane, for example, does not disappear for up to 80 h. Furthermore, the remaining weight of SPAEEN-10 after soaking in Fenton's reagent (3% H_2O_2, 2 ppm $FeSO_4$) at 80 ^oC for 1 h, is still more than 95 wt%, which indicates that the introduction of flexible alkylsufonic acids side chains can improve the oxidative stability. Because the sulfonic acid group is an electro-withdrawing group, when it is directly attached to the aromatic ring of the polymer main chain, it can reduce the electron density of the neighboring aromatic groups by a resonance effect and facilitate the nucleophilic displacement reaction. It would be reasonable to assume that the oxidative degradation of sulfonated poly(arylene ether)s commences at *ortho*-carbons to the ether linkages by attack of hydroxyl radicals. For the side chain type polymers, the longer alkyl side chains could more effectively separate the polymer main chain apart from sulfonic acid groups to keep the main chain in hydrophobic atmosphere that prevent or reduce the chance of radical attack, and introduction of the –CN group, which decreases the water uptake and swelling ratio, could also retard the entrance of the oxidative agent into membrane.[27]

The tensile properties of the SPAEEC-x membranes were measured and the results are listed in Table 8-1. It can be seen that these membranes (except SPAEEN-3 and SPAEEN-12) showed maximum stress in the range of 18-22 MPa, which is similar to that of crosslinked sulfonated polystyrene with flexible alkylsulfonated side chains,[23,24] while the Young's modulus and elongation at break of the SPAEEN-x membranes are much higher than those of the latter probably due to the introduction of the ether linkage in the polymer main chains.

8-2-5. Proton Conductivity.

The proton conductivities of the SPAEEN-x membranes were measured at 80 ^{o}C under different RH (30-95%) and the results are shown in Figure 8-8, in comparison with that of Nafion 117 membrane. It can be seen that for all the SPAEEN-x membranes the proton conductivities increases with increasing RH. They show higher proton conductivities (0.137-0.212 S/cm) than that of Nafion 117 (0.118 S/cm) at 95% RH. It is well know that the proton conductivity of the sulfonated aromatic hydrocarbon-based polymers is mainly dependent on the IEC values and the higher IEC, the higher proton conductivity. The morphology of the membrane is another factor which also affects the proton conductivity. The longer flexible side chains were supposed to favor well-connected phase separation, which is expected to contribute to the high proton conductivity. In this study, the side chain type SPAEEN-x exhibits higher proton conductivity than that of other sulfonated poly(ether sulfone)s (BNSH-67),[10] which contains sulfonic acid groups on the main chain. For example, the proton conductivity of the SPAEEN-10 (IEC=1.99 mequiv g^{-1}) was 8.0 × 10^{-3} S/cm, which was higher than that of the BNSH-67 (IEC=2.18 mequiv g^{-1}) (10^{-5} S/cm) at 80 ^{o}C and 50% RH. Probably, the hydrophilic sulfonic acid groups attached directly to the main chains of BNSH-67 would reduce the hydrophobicity of the main chain, resulting in poor phase separation. Compared with other side chain type polymers, the conductivity of SPAEEN-12 was much higher than that of sulfonated polyimide with long side chain 12(12)[20] due to the high density of the alkylsulfonic acids. All these results indicated that introduction of flexible side chain and increasing the density if the alkylsulfonic acids in the polymer could effectively improve the proton conductivity.

As described above, the proton conductivity of the sulfonated aromatic hydrocarbon-based polymers is mainly dependent on the IEC values. However, in this chapter, the SPAEEN-6, SPAEEN-10 and SPAEEN-12 containing the alkyl carbon more than 4 displayed an interesting phenomenon, their proton conductivities are

independent on the IEC values at 30% RH (Table 8-2). The results can be explained by proton conduction mechanism. The decrease of RH would cause the disconnection of SO_3^- clusters and proton transfer by water molecular motion between clusters became dominant for Nafion and other sulfonated membranes,[28] therefore, the conductivity of these membranes mainly depended on water uptake, which is affected by IEC. For the membranes which maintain the connectivity of ion channel even at low RH, their proton transportation may follow the grotthuss mechanism or structure diffusion mechanism.[28] The SPAEEN-12 membrane contains the longest flexible aliphatic side chain, which was expected to form ion channel and easier transport protons by diffusion mechanism.

Table 8-2. Ion exchange capacities (IEC), water uptake (WU) and proton conductivity (σ) of the SPAEEN-x membranes

Samples	IEC (mequiv g^{-1})		WU^b (wt%)		σ^b (mS/cm)	
	Theoretical	Measured[a]	30% RH	95% RH	30%RH	95%RH
SPAEEN-3	2.87	2.69	5.65	57.3	1.71	212
SPAEEN-4	2.76	2.61	5.37	53.5	1.06	226
SPAEEN-6	2.57	2.32	4.67	35.6	0.416	175
SPAEEN-10	2.24	1.99	2.31	26.7	0.750	150
SPAEEN-12	2.11	1.89	2.89	25.0	0.877	137

[a] By titration method; [b] Measured at 80 °C.

8-2-6. Morphology.

The microstructure of the SPAEEN-x membranes was investigated by AFM. As shown in Figure 8-9, both of SPAEEN-6 and SPAEEN-12 membranes display the formation of phase-separated structures, in which the alkylated sulfonic acids would aggregate into hydrophilic clusters. In the AFM images, more organized phase-separated morphology can be observed for the SPAEEN-12 membrane (the domain spacing is approximately 12 nm) than that of SPAEEN-6. This indicates that the longer alkyl chain induces the formation of well-organized nanodomains. The formation of the domains in a series of SPAEEN membranes would be to improve proton conductivity and oxidative stability. The aggregation of sulfonic acids supported by longer flexible alkyl chains generates the well-developed nanochannel liked morphology, which could improve the proton conduction at low RH and also prevent from oxidizing the polymer main chain by hydroxyl radical attack.

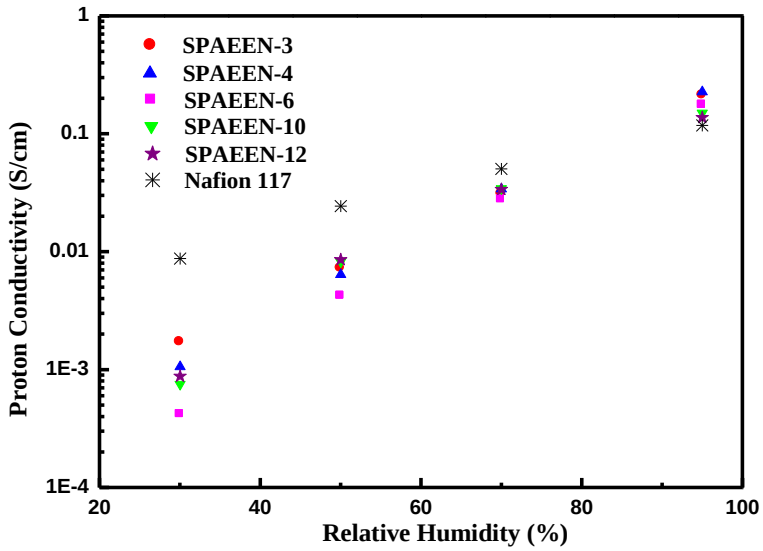

Figure 8-8. Variation of proton conductivity of the SPAEEN-x and Nafion 117 as a function of RH at 80 ^{o}C.

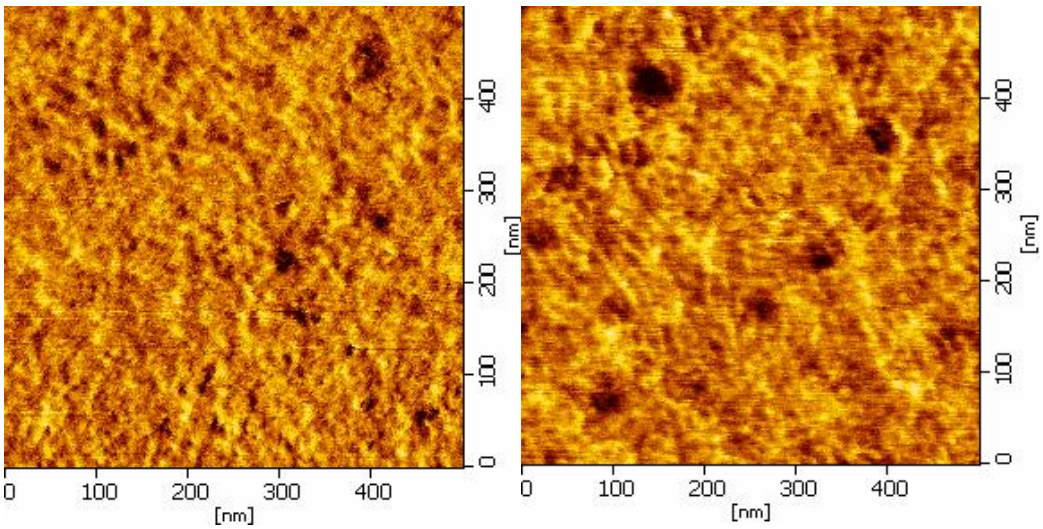

Figure 8-9. AFM image of SPAEEN-6 membrane (L) and SPAEEN-12 membrane (R).

8-3. Conclusions

A series of SPAEEN-x copolymers having different length of flexible alkylsulfonated side chains have been prepared by three-step reaction: that is, polycondension of DFBN containing strongly polar –CN group with MRS and MHQ, followed by demethylation and the reaction with alkanesultones or sodium bromoalkylsulfonates. The resulting membranes exhibited high thermal stability despite the full aliphatic side chains, high oxidative stability against Fenton's reagent at room temperature, low water uptake and dimensional change even at 95% RH. The SPAEEN-3 membrane with the IEC of 2.69 mequiv/g displayed higher proton conductivity among these prepared membranes over the whole range of RH from 30% to 95%. On the other hand, the SPAEEN-12 membrane with the longer side chain displayed lower water uptake and higher proton conductivity (at 30% RH) than those with the shorter side chain membrane SPAEEN-6 in spite of its lower IEC value. The introduction of aliphatic carbon more than 6 as the side chain may improve the proton conductivity especially at low RH by forming the well-developed phase separation.

8-4. Experimental

Materials

5-Methoxyresorcinol (MRS) was purchased from Aldrich. 2,6-Difluorobenzonitrile (DFBN), methoxyhydroquinone (MHQ), boron tribromide (17% in dichloromethane, *ca*. 1 mol/L), 1,1,2,2-tetrachloroethane, 1,3-propanesultone, 1,4-butanesultone, 1,6-dibromohexane, 1,10-dibromodecane and 1,12-dibromododecane were purchased from TCI. 1,1,2,2-Tetrachloroethane was distilled under reduced pressure from finely ground $CaCl_2$. The other reagents were used as received.

Synthesis of sodium 6-bromohexylsulfonate, sodium 10-bromodecylsulfonate and sodium 12-bromododecylsulfonate

Sodium 6-bromohexylsulfonate, sodium 10-bromodecylsulfonate and sodium 12-bromododecylsulfonate were synthesized following the procedure described in a report.[25] A typical example for the synthesis of sodium 6-bromhexylsulfonate is as follows:

To a 50 mL flask with a reflux condenser and a nitrogen inlet were added *1*,6-dibromohexane (4.88 g, 20.0 mmol), ethanol (10.0 mL) and deionized water (4.00 mL). The mixture was heated to boiling temperature, and a solution of sodium sulfite (0.756 g, 6.00 mmol) in deionized water (2.70 mL) was added dropwise, after refluxing for 2 h, most of solvent was removed by evaporation. The remaining mixture was washed with acetone. Then the solid product was then extracted from the sodium bromide and unreacted sodium sulfite with boiling 95% ethanol, thoroughly washed with acetone and then dried at 110 ^{o}C for 24 h in vacuum.

Yield: 77%. ^{1}H NMR (300 MHz, DMSO-d_6, δ): 1.21-1.46 (4H, -CH_2-CH_2-), 1.50-1.65 (2H, -CH_2-CH_2SO_3Na), 1.72-1.86 (2H, $BrCH_2$-CH_2-), 2.37-2.46 (2H, -CH_2-SO_3Na), 3.47-3.56 (2H, Br-CH_2-).

Synthesis of poly(arylene ether ether nitrile) containing methoxy groups (MPAEEN)

The MPAEEN was synthesized by nucleophilic substitution reaction. DFBN (1.67 g, 12.0 mmol), MHQ (1.26 g, 9.00 mmol), MRS (0.420 g, 3.00 mmol), K_2CO_3 (2.00 g, 14.4 mmol), DMAc (15.0 mL) and toluene (15.0 mL) were added into a dry 100 mL three-neck flask equipped with a nitrogen inlet and a Dean-Stark trap. The reaction mixture was heated to 140 ^{o}C for 3 h. After dehydration and removal of toluene, the reaction temperature was increased to 160 ^{o}C. When the solution viscosity had

apparently increased, the mixture was cooled to 120 ^{o}C, then slowly poured into a large excess of deionized water. The fiber-like precipitate was filtered off, washed with deionized water. The polymer was re-precipitated from 2 wt% DMAc solution into ethanol, and dried in vacuo at 100 ^{o}C for 24 h. Yield: 98%.

FT-IR (membrane): ν2943-2835 (C-H), 2230 (C≡N), 1602 (C＝C), 1192, 1240 (Ar-O-Ar), 1130 cm^{-1} (O-C)

Synthesis of poly(arylene ether ether nitrile) containing hydroxyl groups (HPAEEN)

Demethylation reaction was described as follow: MPAEEN (3.20 g) was dissolved into 200 mL anhydrous 1,1,2,2-tetrachloroethane in a 500 mL three-neck flask with a nitrogen inlet. The solution was cooled down to 0 ^{o}C (ice bath) and 1 M solution of BBr_3 in CH_2Cl_2 was added dropwise. After 12 h, the resulting polymer was filtered, washed with ethanol and deionized water several times, and then dried under vacuum at 100 ^{o}C for 24 h. Yield: 97%.

FT-IR (membrane): ν3525-3260 (-OH), 2230 (C≡N), 1602 (C＝C), 1192, 1240cm^{-1} (Ar-O-Ar).

Synthesis of poly(arylene ether ether nitrile) with pendant alkylsufonic acid groups (SPAEEN-x)

A typical synthetic procedure for SPAEEN-6 is described as follows: HPAEEN (0.450 g, 2.00 mmol) was added into a 50 mL dry two-necked flask equipped with a Dean-Stark trap, a condenser and a nitrogen inlet. Anhydrous DMSO (8.00 mL) was then added via a syringe through a septum cap. After HPAEEN was completely dissolved in DMSO at 100 ^{o}C, NaOH (0.160 g, 4.00 mmol) and cyclohexane (8.00 mL) were added. The mixture was heated at 100 ^{o}C for 2 h to remove water. After removal of cyclohexane and water, sodium 6-bromo hexylsulfonate (1.07 g 4.00 mmol) and a suitable quantity of KI were added into the mixture, and the reaction was kept at 100 ^{o}C for 24 h. The resulting polymer was obtained by carefully pouring the solution into water, filtered, washed thoroughly with water and ethanol, and dried under vacuum at 80 ^{o}C for 10 h. Yield: 95%.

FT-IR (membrane): ν2230 (C≡N), 1602 (C＝C), 1192, 1240 (Ar-O-Ar), 1128, 1047 (O＝S＝O).

Film formation and proton exchange

Films were prepared by casting the SPAEEN-x (in their sodium form) solution in DMSO onto glass plates and dried at 80 ^{o}C for 24 h. Proton exchange was performed by immersing the films in 2.0 M H_2SO_4 at 40 ^{o}C for three days. The proton exchanged films were washed with deionized water for one day.

Measurements

^{1}H NMR spectrum was recorded on a Varian MERCURY 300 NMR spectrometer using DMSO-d_6 as solvent and tetramethylsilane (TMS) as an internal standard. Number- and weight-average molecular weights (M_n and M_w) were measured by gel permeation chromatography (GPC) on a Hitachi LC-7000 system equipped with polystyrene gel columns (TSKgel GMHHR-M) eluted with *N*,*N*-dimethylformamide (DMF) at a flow rate of 1.0 mL min^{-1} calibrated by standard polystyrene samples. Thermogravimetric analysis (TGA) was performed on a TA Instruments Q500 in nitrogen. Prior to measurement, all the samples were preheated at 150 ℃ for 30 min to remove any absorbed moisture. Subsequently the samples were cooled to 50 ℃ and then heated to 550 ℃ at a heating rate of 10 ℃ min^{-1}. Ion exchange capacity (IEC) was measured by a titration method. The samples were immersed in saturated NaCl solution at room temperature for 3 days. After that, the NaCl solution was directly titrated with 0.02 M NaOH using phenolphthalein as pH indicator. Tensile measurements were performed with a universal testing instrument (AGS-X 349-05489A, Shimadzu, Japan) at 20 ^{o}C and around 50% RH at a crosshead speed of 2 mm/min. The oxidation stability of the membranes was determined by Fenton's test. The samples were soaked in the Fenton's reagent (3% H_2O_2 containing 20 ppm $FeSO_4$) at room temperature (RT). The disappearance time of the samples was used to evaluate the radical oxidation stability of the membranes. Water uptake of the membranes was measured by placing the membrane in a thermo-controlled humid chamber. The membranes were set at desired values and kept constant for 2 h at each point. Then the membrane was taken out, and quickly weighed on a microbalance. Water uptake (WU) was calculated according to the following equation:

$$WU = (W_s - W_d) / W_d \times 100 \text{ wt\%} \quad (1)$$

where W_s and W_d are the weights of wet and dried membranes, respectively. Water sorption was also expressed as the average number of water molecules per ion exchange site ($[H_2O]/[SO_3^-]$), often referred to as λ value, and calculated according to the following equation:

$$\lambda = [H_2O] / [SO_3^-] = \text{water uptake (\%)} \times 10 / [18 \times \text{IEC (mmol/g)}] \quad (2)$$

Dimensional change of a hydrated membrane was also investigated by placing the membrane in a thermo-controlled humid chamber (80 ^oC) at desired RH for 2 h, and the changes of length and thickness were calculated from

$$\Delta l = (l_s - l_d) / l_d \times 100\% \quad (3)$$

$$\Delta t = (t_s - t_d) / t_d \times 100\% \quad (4)$$

where l_s and t_s are the length and thickness of the wet membrane, respectively, l_d and t_d refer to those of the dried membrane. Proton conductivity was measured using a two-probe electrochemical impedance spectroscopy technique over the frequency from 5 Hz to 1 MHz (Hioki 3532-80). The samples were 8 mm long, 8 mm wide and 68-109 μm thick. Proton conductivity (σ) was calculated from the following equation:

$$\sigma = d/(t_s w_s R) \quad (5)$$

where d is the distance between the two electrodes, t_s and w_s are the thickness and width of the membrane, and R is the resistance measured. Tapping mode atomic force microscope (AFM) images were taken by using Seiko Instruments SPA-400 with a stiff cantilever of Seiko Instruments DF-20.

8-5. References

(1) Savadogo, O. J. *New Mater. Electrochem. Syst.* **1998,** *1,* 47.

(2) Asano, N.; Aoki, M.; Suzuki, S.; Miyatake, K.; Uchida, H.; Watanabe, M. *J. Am. Chem. Soc.* **2006,** *128,* 1762.

(3) Besse, S.; Capron, P.; Gebel, G.; Jousse, F.; Marsacq, D.; Pineri, M.; Marestin, C.; Mercier, R. *J. New Mater Electrochem Systems* **2002,** *5,* 109.

(4) Genies, C.; Mercier, R.; Sillion, B.; Cornet, N.; Gebel, G.; Pineri, M. *Polymer* **2001,** *42,* 359.

(5) Higashihara, T.; Matsumoto, K.; Ueda, M. *Polymer* **2009,** *50,* 5341.

(6) Bae, J. M.; Honma, I.; Merata, M.; Yamamoto, T.; Rikukawa, M.; Ogata, N. *Solid State Ionics,* **2002,** *147,* 189.

(7) Kerres, J. A. *J. Membr. Sci.* **2001,** *185,* 3.

(8) Mehta, V.; Cooper, J. S. *J. Power Sources* **2003,** *114,* 32.

(9) Nakabayashi, K.; Matsumoto, K.; Ueda, M. *J. Polym. Sci., Part A: Polym. Chem.* **2008,** *46,* 3947.

(10) Matsumoto, K.; Nakagawa, T.; Higashihara, T.; Ueda, M. *J. Polym. Sci., Part A: Polym. Chem.***2009,** *47,* 5827.

(11) Nakabayashi, K.; Higashihara, T.; Ueda, M. *J. Polym. Sci., Part A: Polym. Chem.* **2010,** *48,* 2757.

(12) Nakabayashi, K.; Higashihara, T.; Ueda, M. *Macromolecules* **2010,** *43,* 5756.

(13) Guo, X.; Fang, J.; Watari, T.; Tanaka, K.; Kita, H.; Okamoto, K. *Macromolecules* **2002,** *35,* 6707.

(14) Fang, J.; Guo, X.; Harada, S.; Watari, T.; Tanaka, K.; Kita, H.; Okamoto, K. *Macromolecules* **2002,** *35,* 9022.

(15) Yin, Y.; Fang, J.; Kita, H.; Okamoto, K. *Chem. Lett.* **2003,** *32,* 328.

(16) Si, K.; Dong, D.; Wycisk, R.; Litt, M. J. Mater. Chem. 2012, 22, 20907.

(17) Yin, Y.; Suto, Y.; Sakabe, T.; Chen, S.; Hayashi, S.; Mishima, T.; Yamada, O.; Tanaka, K.; Kita, H.; Okamoto, K. Macromolecules 2006, 39, 1189.

(18) Hu, Z.; Yin, Y.; Okamoto, K.; Moriyama, Y.; Morikawa, A. J. Membr. Sci. 2009, 329, 146.

(19) Yin, Y.; Du, Q.; Qin, Y.; Zhou, Y.; Okamoto, K. J. Membr. Sci. 2011, 367, 211.

(20) Yasuda, T.; Li, Y.; Miyatake, K.; Hirai, M.; Nanasawa, M.; Watanabe, M. J. Polym. Sci., Part A: Polym. Chem. 2006, 44, 3995.

(21) Miyatake, K.; Yasuda, T.; Hirai, M.; Nanasawa, M.; Watanabe, M. J. Polym. Sci., Part A: Polym. Chem. 2007, 45, 157.

(22) Kabasawa, A.; Saito, J.; Yano, H.; Miyatake, K.; Uchida, H.; Watanabe, M. Electrochem. Acta 2009, 54, 1076.
(23) Sheng, L.; Higashihara, T.; Nakazawa, S.; Ueda, M. Polym. Chem. 2012, 3, 3289.
(24) Sheng, L.; Higashihara, T.; Maeda, R.; Hayakawa, T.; Ueda, M. J. Polym. Sci., Part A: Polym. Chem. 2013, 51, 2216.
(25) Marvel, C.S.; Bailey, C.F.; Sparburg, M.S. J. Am.Chem.Soc. 1927, 49, 1833.
(26) Kim, Y. S.; Kim, D. S.; Liu, B.; Guiver, M. D.; Pivovar, B. S. J. Electrochem. Soc. 2008, 155, B21.
(27) Gao, N.; Zhang, F.; Zhang, S. B.; Liu, J. J. Membr. Sci. 2011, 372, 49.
(28) Hase, K.; Nakano, T.; Koiwai, A. ECS Transactions 2007, 11, 159.
(29) Kim, D. S.; Kim, Y. S.; Guiver, M. D.; Pivovar, B. S. J. Membr. Sci. 2008, 321, 199.

Chapter 9

General Conclusion

In this study, hydrocarbon-based PEMs were prepared by two approaches. The low cost productivity is an attracting advantage for these hydrocarbon-based polymers in comparison with perfluoropolymers. In this chapter, conclusions of each chapter and the future perspective were summarized as follws:

In chapter 1, the general introduction about the background of this study is described.

In chapter 2, the first section, the ether containing PBI, poly[2,2'-(*p*-oxydiphenylene)-5,5'-bibenzimidazole] (OPBI) was synthesized to improve the solubility of PBI. The phosphoric acid (PA)-doped OPBI was prepared for PEM and the moderate molecular weight poly[2,2'-(m-phenylene)-5,5'-bibenzimidazole] (*m*PBI) was synthesized and used as the binder in catalyst layers. The OPBI with the PA doping level (defined as the molar ratio of the PA per PBI repeat unit) of 6.5 showed output power density of 366 mW/cm^2 at 160 ^{o}C with H_2-O_2 under ambient pressure without any external humidification. In the second section, for further improve the fuel cell performance, sulfonated copolybenzimidazoles (SPBIs) were synthesized by random condensation copolymerization of 4,4-dicarboxydiphenyl ether, 3,3'-diaminobenzidine and a new sulfonated dicarboxylic acid monomer 4,6-bis(4-carboxyphenoxy)benzene-1,3-disulfonate, which contains two sulphonic groups per molecule, in PPMA (phosphorus pentoxide dissolved in methanesulfonic acid at a weight ratio of 1:10). The SPBI-11 membrane with the PA doping level of 13, which was higher than that of OPBI, still maintained high mechanical strength. The membrane displayed fairly high proton conductivity of 37.3 mS/cm at 170 ^{o}C and 0% relative humidity (RH). The result of fuel cell performance showed high output power density of 580 mW/cm^2 at 170 ^{o}C with H_2-O_2 under ambient pressure without any external humidification.

In chapter 3, a series of polystyrenes with phosphonic acid via long alkyl side chains

(4, 6, and 8 methylene units) were prepared by the radical polymerization of the corresponding diethyl-(4-vinylphenoxy)alkylphosphonates, followed by the hydrolysis with trimethylsilyl bromide. The resulting phosphonated polystyrene membranes had a high oxidative stability against Fenton's reagent at room temperature. These membranes with the IEC value of 3.0-3.8 also exhibited a very low water uptake, similar to that of Nafion 117 over the wide range of 30-80% RH. And the proton conductivity comparable or higher than those of the reported phosphonated polymers with much higher IEC values, such as the phosphonated poly(*N*-phenylacrylamide) (PDPAA, IEC: 6.72 mequiv/g) and fluorinated polymers with pendant phosphonic acids (M47, IEC: 8.5 mequiv/g), at low RH conditions..

In chapter 4, the cross-linked membranes of random copolystyrene derivatives based on a hydrophobic alkoxystyrene unit and a hydrophilic styrene unit containing a pendant alkyl sulfonic acid with the ion exchange capacity (IEC) of 2.57-3.03 mequiv/g were prepared by using 4,4'-methylene-bis[2,6-bis(hydroxyethyl)phenol] as the crosslinker in the presence of acid agent. The crosslinked membrane (IEC=3.03 mequiv/g) showed a high proton conductivity compared to that of Nafion 117 over the entire range of 50-95% RH. Furthermore, the cross-linked membranes had a high oxidative stability against Fenton's reagent regardless of their high IECs. The introduction of flexible alkylsulfonated side chain to the polystyrene main chains improved the oxidative stability probably due to preventing or reducing the hydroxyl radical attack on the polymer main chain.

In chapter 5, for further improvement of the proton conductivity at low RH, especially at 30% RH, the cross-linked block copolystyrene derivatives, which have the similar structure with the random copolysytene (chapter 4), were synthesized by the living anionic polymerization. The cross-linked membrane (IEC=2.89 mequiv/g) displayed high proton conductivity (0.01 S/cm) at a 30% RH and 80 ^{o}C, which was comparable to that of Nafion 117, and 2.5 times higher at 95% RH. On the other hand, the block copolymers show a more well-organized microphase separation than that of the random copolymers, therefore, the proton conductivities of the former membranes are much higher than the latter membranes over the entire RH range despite the lower IEC values. Moreover, the block copolymers show higher mechanical strength and oxidative stability, lower water uptake when decreasing the IEC values.

Furthermore, to improve the thermal and mechanical properties, the polymer aromatic main chain was chosen in place of polystyrene. The poly(*m*-phenylene)s and poly(phenylene ether)s with sulfonic acid via alkyl side chains were prepared in chapter

6 and 7, respectively. In chapter 6, the c-SPMPs produced transparent membranes with a relatively high mechanical property in the dry state, regardless of their high ion exchange capacity (IEC) values. The rigid main chains and the cross-linking structure improve the thermal stability and suppressed the unacceptable water uptake and dimensional change of the c-SPMPs membranes even in the hydrated state. The c-SPMP8-2 membrane with IEC = 2.93 mequiv/g showed a higher proton conductivity than Nafion 117 over a wide range of relative humidities (30-95%) at 80 ^{o}C. To prepare more flexible membrane, which is required for fabricating MEA, the poly(phenylene ether)s (SPPE) with ether group on the main chain have been synthesized by Nickel-mediated homocoupling reaction in chapter 7. SPPE shows high mechanical properties, good oxidative stability and high proton conductivity, *e.g.*, 8.6 $\times$ 10^{-3} S/cm under 30% RH at 80 ^{o}C which is higher than that of Nafion 117.

In chapter 8, to synthesize polymer by sample method and the study on clarifying the detailed structure-property relationship for the design of future PEMs, the poly(arylene ether ether nitrile)s with ether group on the main chain and different length of alkylsulfonated side chains was synthesized. The introduction of ether linkages and longer flexible alkylsulfonated side chains improved the elongation property and induced better well-organized nanodomains, respectively. The membrane containing longer alkylsulfonated side chain (SPAEEN-12) displayed higher proton conductivity than that of the short akylsulfonated side chain membrane (SPAEEN-6) at 30% RH even its IEC value is lower than that of the latter membrane.

Phosphoric acid (PA)-doped PBIs and phosphonated, sulfonated polystyrene derivatives, poly(*m*-phenylene)s and poly(arylene ether ether nitrile)s with sulfonic acid via long alkl side chains were synthesized for PEMs. One of the advantages of PA-doped PBIs is higher proton conductivity even at anhydrous conditions. However, the proton conductivities and fuel cell performance of PA-doped PBIs were strongly depended on the PA doping level, and the higher doping levels, the higher performance. On the other hand, the higher PA uptake would decrease the mechanical strength of membranes. The PA-doped sulfonated PBIs have been prepared for the first time (chapter 2), the membrane with higher degree of sulfonation displayed higher PA uptake and higher mechanical strength after PA doping, because the sulfonic acid groups should preferentially react with the basic benzimidazole groups to form ionic crosslinking due to the sulfonic acid is more acidic than phosphonic acid.

For sulfonated hydrocarbon-based polymers used as PEMs, the polymer morphology, in particular, the nanochannel that contain the sulfonic acid groups plays an important

role to increase proton conductivity at low relative humidity (RH< 50%) due to the “hydrated” protons can efficiently pass through the proton nanochannels. The introduction of pendant alkylsulfonated side chain may distribute in well-organized domains and thus improve the proton conductivity at a low RH. Moreover, it improved oxidative stability due to prevention or reduction of the hydroxyl radical attack on the main chain (chapter 4). The block polymers containing perfectly alternating hydrophilic and hydrophobic segments is one of the method to obtain a better-organized domain (chapter 5), and random copolymer contains much longer flexible side chains is another method (chapter 7, chapter 8).

From the results of this study, we found that the aromatic random polymer with longer side chain show both the membrane mechanical property and proton condutvitiy at low RH (the polymer should have appropriate high IEC) by form well-orgainzed phase-separated structure. For future study, an ideal morphology we have pursued is the gyroid structure, that is a biscontinuous phase-separated morphology. The continous hydrophilic sulfonated polymer segments form an interconnected three-dimensional network responsible for efficient proton transport, while the continous of hydrophobic non-sulfonated segments imparts a reinforcing effect, preventing excessive swelling in water and enhancing the mechanical properties. However, the challenge is we should precisely control the volumn ratio between the hydrophilic and hydrophobic segment in random polymer to form the gyroid structure.

Appendix

List of publications

(1) "Fuel Cell Characteristics of the Membrane Electrode Assemblies Using Phosphoric Acid-doped Poly[2,2'-(p-oxydiphenylene)-5,5'-bibenzimidazole] membranes" Fang, L.; Sheng, L.; Guo, X.; Fang, J.; Ma, Z.-F. *J. New Mater. Electrochem. Systems.* **2011,** *14,* 159-165.

(2) "Synthesis and Properties of Novel Sulfonated Polybenzimidazoles From Disodium 4,6-bis(4-carboxyphenoxy)benzene-1,3-disulfonate" Sheng, L.; Xu, H.; Guo, X.; Fang, J.; Yin. J. *J. Power Sources.* **2011,** *196,* 3039-3047.

(3) "Polymer Electrolyte Membranes Based on Polystyrenes with Phosphonic Acid via Long Alkyl Side Chains" Tamura, Y.; Sheng, L.; Nakazawa, S.; Higashihara, T.; Ueda, M. *J. Polym. Sci., Part A: Polym. Chem.* **2012**, *50,* 4334-4340.

(4) "Polystyrenes Containing Flexible Alkylsulfonated Side Chains as a Proton Exchange Membrane for Fuel Cell Application" Sheng, L.; Higashihara, T.; Nakazawa, S.; Ueda, M. *Polym.Chem.* **2012,** *3,* 3289-3295

(5) "Polymer Electrolyte Membranes Based on Poly(*m*-phenylene)s with Sulfonic Acid via Long Alkyl Side Chains" Zhang, X.; Sheng, L.; Higashihara, T.; Ueda, M. *Polym.Chem.* **2013,** *4,* 1235-1242

(6) "Block Copolystyrene Derivatives Having Flexible Alkylsulfonated Side Chains and Hydrophobic Alkoxy Chains as a Proton Exchange Membrane for Fuel Cell Application" Sheng, L.; Higashihara, T.; Maeda, R.; Hayakawa, T.; Ueda, M. *J. Polym. Sci., Part A: Polym. Chem.* **2013,** *51,* 2216-2224.

(7) "Polymer Electrolyte Membranes Based on Poly(phenylene ether)s with Sulfonic Acid via Long Alkyl Side Chains" Zhang, X.; Sheng, L.; Hayakawa, T.; Ueda, M.; Higashihara, T. *J. Mater. Chem.A* **2013, Accepted.**

(8) "Sulfonated poly(arylene ether ether nitrile)s containing flexible alkylsulfonated side chains for PEM application" Sheng, L.; Higashihara, T.; Ueda, M.; Hayakawa, T. *J. Polym. Sci., Part A: Polym. Chem.* **Submitted**.

List of presentations

(1) "Phosphoric Acid doped Sulfonated Polybenzimidazoles as Proton Exchange Membrane for High Temperature Fuel Cell Application" Sheng, L.; Xu, H.; Fang, J.; Yin, J. The *2nd International Fuel Cell Summer Seminar (IFCSS)* Nagano (Japan), August **2011** (poster).

(2) "Polystyrene Containing Flexible Alkylsulfonated Side Chain as a Proton Exchange Membrane for Fuel Cell Application" Sheng, L.; Higashihara, T.; Ueda, M. *61st SPSJ Annual Meeting* Yokohama (Japan), May **2012** (poster).

(3) "Polystyrene Containing Flexible Alkylsulfonated Side Chain as a Proton Exchange Membrane for Fuel Cell Application" Sheng, L.; Higashihara, T.; Ueda, M. *Polycondensation 2012* San Francisco (USA), September **2012** (poster).

(4) "Sulfonated Block Copolymer Containing Flexible Alkylsulfonated Side Chains as a Proton Exchange Membrane for Fuel Cell Application" Sheng, L.; Higashihara, T.; Ueda, M. The *9th SPSJ International Polymer Conference (IPC 2012)* Kobe (Japan), December **2012** (poster).

(5) "Polymer Electrolyte Membranes Based on Poly(phenylene ether ether)s with Sulfonic Acid via Long Alkyl Side Chains" Sheng, L.; Zhang, X.; Hayakawa, T.; Ueda, M.; Higashihara, T. *62st SPSJ Annual Meeting* Kyoto (Japan), May **2013** (oral presentation).

Acknowledgements

The studies described in this dissertation supervised by Professor Mitsuru Ueda and Associated Professor Teruaki Hayakawa at Department of Organic and Polymeric Materials, Graduate School of Science and Engineering, Tokyo Institute of Technology during 2011/4 to 2013/9. The studies are concerned with development of sulfonated hydrocarbon-based polymer electrolyte membranes for fuel cell applications.

I appreciate the opportunity to learn at Ueda Lab in Tokyo Institute of Technology of last two years. I really want to express my sincere appreciation to Professor Mitsuru Ueda, who is a knowledgeable, kind and patient professor. I would like to thank Professor Ueda for his interesting discussion with me which I have found very informative and useful.

I am grateful to Associate professor Teruaki Hayakawa, who accepts me and give me the chance to continue my PhD research work. I would also like to thank Associate professor Hayakawa for his help and helpful advices during this half an year.

I am grateful to Associate professor Tomoya Higashihara, who is the assistant professor in Ueda lab before. Thanks for his kind help.

I am grateful to Mr. Ryohei Kikuchi in Materal Analysis O-okayama Center, Mr. Satoshi Nakazawa in Higashifuji Technical Center of Toyota Motor Corporation and Mr. Higami Makoto in JSR company for their technical support to measure morphology of the membranes, and all the members in Ueda lab before and Hayakawa lab.

I also want to thank my parents and all my friends for their kindness.